THE UNIVERSITY of EDINBURGH

DEVELOPMENT OF ANTIBODY THERAPEUTIC APPROACHES FOR POULTRY DISEASES USING AVIAN INFLUENZA AS A DISEASE MODEL

Deimante Lukosaityte

THE UNIVERSITY *of* EDINBURGH

Submitted for the degree of Doctor of Philosophy

The University of Edinburgh

[2021]

Declaration

I declare that this thesis was composed by myself and the work contained within is my own, with the exception or where it is explicitly stated in the text, and that the work has not be submitted for any other degree or professional qualification.

29 September 2021

Deimante Lukosaityte

Abstract

One of the main threats to poultry is avian influenza virus (AIV), causing significant economic losses worldwide and threatening human populations due to its zoonotic potential. To reduce disease impact, vaccination of poultry is carried out; however, most of the vaccines are insufficient to induce sterile immunity, leading to enzootic disease prevalence worldwide. In addition, due to virus evolution, new virus variants continuously arise, further compromising vaccine effectiveness. The aim of this study was to assess if monoclonal antibodies could be used as prophylactic treatment to reduce avian influenza disease impact as an alternative to vaccination in emergency situations, and to investigate approaches which could be employed for delivery of antibodies as antiviral therapeutics for poultry.

A panel of monoclonal antibodies, specific to the AIV H9N2 subtype (A/chicken/Pakistan/UDL-01/2008) (UDL-1/08) major antigenic surface glycoprotein hemagglutinin (HA), generated from mouse hybridomas, were gene sequenced for their variable domains that were subsequently used for recombinant antibody production in cultured cell supernatants. Functional activities (HA binding affinity and AIV neutralizing activity) of the recombinant antibodies were evaluated against homologous and heterologous viruses. Three antibodies retained functional activity matching that of the natural antibody isotype after conversion to single chain variable fragment (scFv) format, suggesting the antibody fragment crystallizable (Fc) region did not mediate function for these antibodies, but that function was dependent on direct antigen recognition.

Next, scFv antibodies were chosen for passive immunization purposes *in vivo* due to their small molecule size and potentially reduced immunogenicity. scFvs were administered to birds intranasally 24 h before challenge with H9N2 AIV representative UDL-1/08 and treatment was continued for seven days post-infection. Results indicated reduced morbidity and virus shedding in treated birds. Moreover, compared to non-treated birds, treated chickens also produced lower levels of IL-6, a known pro-inflammatory cytokine induced in

response to virus infection. This data suggests treated birds experienced overall reduced impact of disease. Nevertheless, like *in vivo* vaccine induced antibodies, the antibody treatment also provoked the virus to generate HA antibody escape mutants likely to overcome the neutralizing activity of therapeutic antibodies.

Finally, this study investigated if herpesvirus of turkeys (HVT), which is used as a viral vaccine vector in poultry, could act as a vector for therapeutic antibody delivery to poultry. A recombinant virus encoding a transgene of a broadly AIV-neutralizing antibody was generated using a CRISPR/Cas9 approach. It was found that antibody gene insertion into HVT altered recombinant virus growth kinetics, resulting in reduced replication when compared to a wildtype virus control. Antibody levels secreted in rHVT infected cell culture supernatant were retained after 20 virus passages. Next, to investigate antibody expression and tolerability *in vivo*, rHVT was administered to day-old birds; however, no detectable systemic antibody circulation was identified throughout 42-days post rHVT delivery. Instead, an anti-antibody response was generated, suggesting only a low level of expression occurred that was sufficient to act as an antigen.

Taken together, this work has built a proof-of-concept suggesting that passive immunization for poultry can reduce weight loss in infected birds and overall disease burden, but selection of antibodies targeting different antigens and epitopes is crucial to avoid virus escape mutant formation. For the first time it was also demonstrated that HVT can act as an efficient vector for antigen but not antibody delivery. This information can be relevant not only to AIV but also other pathogens affecting poultry.

Lay Summary

Ever growing demand in livestock products has resulted in expansion of the poultry sector, with the estimated number of birds culled annually reaching 60 billion. In the UK alone, this translates to £3 billion market value. One of the main threats to the poultry industry is avian influenza virus (AIV), which causes significant economic losses worldwide and puts the human population at risk due to the virus's ability to cause sporadic human infections that might result in a pandemic situation. To control virus circulation, vaccination regimes are carried out in poultry; however, continuous virus changes compromise vaccine efficiency. The aim of this study is to assess if monoclonal antibodies can be used in a therapeutic and prophylactic context during AIV infection of poultry and to investigate approaches that could serve for delivery of therapeutic antibodies.

A panel of monoclonal antibodies, specific to the AIV A/chicken/Pakistan/UDL-01/2008 (UDL-1/08) H9N2 subtype major antigenic surface glycoprotein haemagglutinin (HA) were generated after mice immunization, allowing subsequent harvesting and immortalization of the antibody producing cells, by previous lab members. During this project, commercial sequencing services were used to determine the nucleic acid sequences that encoded the antibody variable domains. Sequences retrieved were used for gene synthesis, inserted into expression vectors and used for antibody production in cultured cell supernatants. Functional activities (HA binding affinity and AIV neutralizing activity) of six recombinantly generated antibodies were evaluated against an array of different H9N2 AIV strains prevalent in poultry. Importantly, three antibodies retained functional activity when converted to smallest functional antibody fragment – a single chain variable fragment (scFv) composed of variable heavy and variable light chains (responsible for antigen recognition) but lacking a constant domain. This indicated antibody activity depended on direct interaction with virus.

Next, the efficacy of scFv antibodies against H9N2 (UDL-1/08) virus was tested in birds following virus infection. The scFv antibodies were administered

to birds intranasally 24 hours before challenge and treatment was continued for seven days post-infection. Results indicated no reduced weight loss or release of virus progeny in treated, infected birds. However, treated chickens produced lower levels of IL-6, a known pro-inflammatory cytokine induced in response to virus infection. These data suggest treated birds experienced an overall reduced impact of disease. Sequencing of viruses from the treated chickens identified virus variants carrying three mutations in the HA protein located near predicted antibody binding sites. These changes in HA sequence were likely escape mutations that could have arisen due to the pressure from the antibodies used for therapy.

Finally, this study investigated if herpesvirus of turkeys (HVT), which is used as a viral vaccine vector in poultry for delivery of various antigens, could act as a vector for therapeutic antibodies. Using a virus genome editing approach known as CRISPR-Cas9, a recombinant HVT virus (rHVT) encoding a transgene for a broadly AIV-neutralizing antibody was generated. rHVT infection of cells produced soluble antibodies in the culture supernatants. The rHVT vector also retained stable antibody expression after 20 virus passages. However, it was found that antibody gene insertion into HVT led to reduced virus replication when compared to a wildtype control virus. To investigate antibody expression and tolerability in chickens, rHVT was administered to day-old birds; however, no detectable systemic antibody circulation was identified at any point throughout 42-days post rHVT delivery. Instead, an anti-antibody response was generated, suggesting an immune response was elicited against the therapeutic antibody could result in destruction of therapeutic antibody or that low levels of expression beyond the limit of detection were occurring initially.

Taken together, this work has built a proof-of-concept suggesting that therapeutic antibodies for poultry can reduce morbidity in infected birds and their overall disease burden, but thorough selection of antibodies is crucial to avoid virus escape mutant formation. For the first time it was also demonstrated that HVT cannot act as an efficient vector for antibody delivery

or that further evaluation would be required. This information can be relevant not only to AIV, but also other pathogens affecting poultry.

Acknowledgements

First and foremost, I would like to thank both of my supervisors who have given me their trust for this PhD and immense support throughout. I am grateful for Professor Munir Iqbal always being available and having thousands of ideas on how to come around a problem and Professor Paul Digard who would accept last minute meetings and help to choose the most rational decisions. Both of their guidance and advice were invaluable in helping to set a basis for my working ethics and personal development. I would also like to thank my Master's degree supervisors Dr Michael Skinner and Dr Efstathios Giotis who encouraged me to pursue a PhD.

I am grateful to everyone who I met along my way during the four years I had at The Pirbright Institute, especially AIV lab members Pengxiang, Sushant and Josh who helped me during my very first months and continued with advises until the completion of my thesis. I would like to also give my thanks to Jean-Remy for his efforts in managing the whole lab. I am grateful for Angita who I could share experiences with daily. I would also like to thank all students and visitors who joined lab for a great company and help in performing experiments. I would like to directly thank Dr Dagmara Bialy who I can call my mentor for helping me not only with scientific questions but also in making career decisions. An additional acknowledgement should be made for everyone in the influenza viruses' group, Angila and Archana for listening about all unsuccessful experiments and having enjoyable lunch breaks.

I am much obliged to animal services with their help for taking care of the birds during animal studies.

I am thankful for my family, my mum, my fiancé Bien and his family and my best friend Neringa who were there 24/7 during high and low times, listening to how difficult PhD can be and how exhausting and never-ending thesis writing is. Finally, thanks to The Pirbright Institute and The University of Edinburgh for funding and support in getting me onto my next step.

Contents

List of figures and tables

Chapter 1 INTRODUCTION

Chapter 2 CAN ENGINEERED ANTIBODIES RETAIN FUNCTION OF MONOCLONAL ANTIBODIES PRODUCED FROM HYBRIDOMAS?

Abbreviations

A	adenine
aa	amino acid
AAV	adeno associated virus
ADCC	antibody-dependent cell-mediated cytotoxicity
AD	antibody dependent cellular phagocytosis
ADE	antibody dependent enhancement
AID	activation-induced cytidine deaminase
AIV	avian influenza virus
ANOVA	analysis of variance
ASC	antibody secreting cell
BAC	bacterial artificial chromosome
Bcl-xL	B-cell lymphoma-extra large
Bcl-2	B-cell lymphoma 2 protein
Bcl-6	B-cell lymphoma 6 protein
BCR	B cell receptor
BiTE	bispecific T cell engager
bnAb	broadly cross-reactive neutralizing antibody
bsAb	bispecific antibody
C	constant gene segment
C (Cys)	cysteine
Cas9	CRISPR associated protein 9
CCL28	chemokine ligand 28
CDC	complement dependent cellular cytotoxicity **CDR**

CDR	complementarity determining region
CD3	cluster of differentiation 3
CD4	cluster of differentiation 4
CD19	cluster of differentiation 19
CD40L	cluster of differentiation 40 ligand
CEF	chicken embryo fibroblasts
C_H	constant heavy chain
ch-mAb	chimeric antibody
C_H1	constant heavy chain domain 1
C_H2	constant heavy chain domain 2
C_H3	constant heavy chain domain 3
C_L	constant light chain
CMV	cytomegalovirus
COBRA	computational optimisation of broadly reactive antigens
CPE	cytopathic effect
CpG	5'—C—phosphate—G—3'
CRIPR	clustered regularly interspaced short palindromic repeats
cRNA	complementary RNA
CRM1	chromosomal maintenance 1 protein, also known as exportin 1
D	
DAB	diversity gene segment
DEV	3,3'Diaminobenzidine
DIV	duck enteritis virus
DIVA	differentiation between infected and vaccinated

DIVA	differentiation between infected and vaccinated animals
DNA	deoxyribonucleic acid
E (Glu)	glutamic acid
ED	embryonic day
ELISA	enzyme-linked immunosorbent assay
EBV	Epstein-Barr virus
eNP	elongated NP
ER	endoplasmic reticulum
Fab	antigen-binding fragment
FACS	fluorescence activated cell sorting
FAdV	fowl adenovirus vector
Fc	crystallizable region
FcR	Fc receptor
FP	fowlpox
FR	framework region
Fuc	fucose
Fv	variable fragment
G	guanine
G (Gly)	glycine
Gal	galactose
GalNAc	N-acetyl-D-galactosamine
GFP	green fluorescent protein
GlcNAc	N-acetyl-D-glucosamine
gp41	glycoprotein 41

gp120	glycoprotein 120
gRNA	guide RNA
G2	growth 2 phase
H (His)	histidine
HA	haemagglutinin
HAI	HA inhibition assay
hcIg	heavy chain only immunoglobulin
HDR	homology directed repair
HIV-1	human immunodeficiency virus-1
HPAI	high pathogenicity AIV
HRP	horseradish peroxidase
HVT	herpesvirus of turkeys
IAV	influenza A virus
IBV	infectious bronchitis virus
IBDV	infectious bursal disease virus
IFNγ	interferon gamma
Ig	immunoglobulin
IL-4	interleukin 4
IL-6	interleukin 6
IL-21	interleukin 21
IM	intramuscular injection
IMGT	ImMunoGeneTics
IRF3	interferon regulatory factor 3
IV	intravenous injection
J	joining chain
K (Lys)	lysine

kDa	fragment crystallizable region
LPAI	low pathogenicity avian influenza
mAb	monoclonal antibody
MACS	magnetic activated cell sorting
Man	mannose
MDV	Marek’s disease virus
MERS	Middle East Respiratory Syndrome
MNT	virus microneutralization assay
MOI	multiplicity of infection
mRNA	messenger RNA
M1	matrix 1 protein
M2	matrix 2 protein
N	asparagine
NA	neuraminidase
NCBI	National Center for Biotechnology Information
NDV	newcastle disease virus
NeuAc	N-acetylneuraminic acid
NHEJ	non-homologous end joining
NK	natural killer cells
nonNbAb	broadly cross-reactive non-neutralizing antibodies
NP	nucleoprotein
NS1	non-structural protein 1
NS2	non-structural protein 2
NS3	non-structural protein 3
OD	optical density
ORF	open reading frame

P (Pro)	proline
PA	polymerase acidic
PBMC	peripheral blood mononuclear cells
PB1	polymerase basic 1
PB2	polymerase basic 2
PCR	polymerase chain reaction
PEG	polyethylene glycol
PFU	plaque forming units
pI	isoelectric point
PTM	post-translational modification
qRT-PCR	Real-Time Quantitative Reverse Transcription PCR
RdRp	RNA dependent RNA polymerase
rHVT	recombinant HVT
RIR	Rhode Island Red
RNA	ribonucleic acid
RSV	respiratory syncytial virus
(RT)-PCR	reverse transcription PCR
tp	tail piece
S (Ser)	serine
S	synthesis phase
SC	subcutaneous injection
SD	standard deviation
SDS –	sodium dodecyl sulphate–polyacrylamide gel
PAGE	electrophoresis
SEED	strand-exchange engineered domain
scFv	single chain variable fragment

sgRNA	single gRNA
SPF	specific - pathogen free
SV40 polyA	simian virus 40 polyadenylic acidic tail
T (Thr)	threonine
TK	thymidine kinase
UL	unique long
US	unique short
UTR	untranslated region
V	variable gene segment
VEE	Venezuelan equine encephalitis
V_H	variable heavy chain
VHH	heavy chain of the heavy chain only antibody
VIP	vectored immunoprophylaxis
V_L	variable light chain
VLP	virus like particle
vRNA	virus RNA
vRNP	virus ribonucleoprotein
V1V2	variable regions 1 and 2 of HIV-1 gp120 envelope
W (Trp)	tryptophan
WT	wildtype

Chapter 1 INTRODUCTION

A plethora of viral and bacterial pathogens able to infect both humans and animals is continuously growing and threatening the entire earth ecosystem. The emergence of SARS Cov-2 illustrates an extreme example of the necessity to have appropriate control measures and approaches for disease mitigation. With regards to viral pathogens, this can be particularly ambiguous due to rapidly occurring changes within target antigens leading to vaccine and antiviral drug failure. A somewhat more recent approach focuses on the humoral immune response via employment of antibodies for disease control. Herein, naturally occurring antibodies, recombinant antibodies and antibody therapeutics in the context of influenza virus will be discussed.

1.1 Antibody structure and function relationship

Antibodies, also known as immunoglobulins (Ig), are antigen-binding proteins that function in pathogen elimination. Antibodies are one of the main serum constituents that mark the development of an immune response against an antigen. The first indication of a protective component present in serum was gained in 1890; however, it took another 50 years to attribute it to gamma globulins, - a class of globular proteins, generally serving as messengers, enzymes, transporters, or that carry out regulatory and structural roles (1, 2).

Specificity of antibodies is generated during B-cell maturation when a fully mature immunocompetent B-cell commits to secretion of a single monoclonal antibody (mAb) that recognizes a single epitope within an antigen; a process prior to which every B-cell carries up to 10^5 different membrane bound antibodies (3). Overall reactivity to infection is generated by a global population of B-cells, resulting in a polyclonal humoral response. Interaction between antigen and antibody molecule works in a ‘lock and key’ principle and is based on a vast array of non-covalent bonds including hydrogen bonds, ionic bonds, hydrophobic interactions and van der Waals interactions (4, 5).

Antibodies are classified according to the constant region of heavy chain isotype, determining the molecular properties and biological activities of immunoglobulin molecule. Five antibody classes: IgG, IgM, IgA, IgE and IgD are found in mammals including humans and mice, whilst birds carry only IgY, IgM and IgA class antibodies (6-8). Amongst many others, the main antibody effector functions include neutralization, agglutination, precipitation, opsonization, complement activation and antibody-dependent cell-mediated cytotoxicity (ADCC) (9). Valency, specificity, affinity and avidity defines the functional strength of immunoglobulin molecules (10-12). However, selection of the most potent antibodies might be counterintuitive, as in many instances lower affinity antibodies perform better than the ones having higher binding profile; a phenomenon mediated by the affinity threshold which, otherwise, might interfere with dissociation from the first antigen encountered (13). An ever-growing understanding of antibody organization and expression, their structure and function, and their interaction with antigens has allowed antibody harnessing as research tools as well as in diagnostic and therapeutic applications.

1.1.1 Antibody structure

Traditionally, antibody structure is represented by a Y-shaped heterodimer molecule containing identical heavy and light chains (50 kilodaltons (kDa) and 25 kDa each, respectively) aligned vertically and joined by disulphide bridges to form a bivalent four-chain antibody molecule (Figure 1.1a).

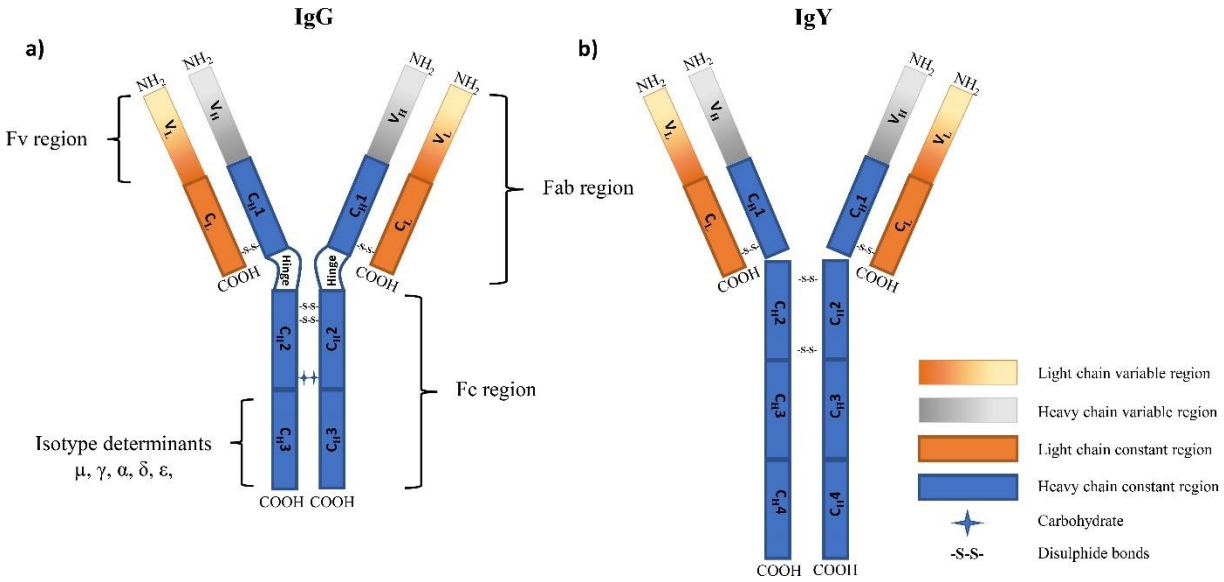

Figure 1.1. Schematic diagram representative for a) IgG mammalian and **b)** IgY birds immunoglobulin molecules structures. The antibody molecule is made up of two identical heavy chains and two identical light chains bound by disulphide bonds. The amino terminal domain of the antibody recognizes antigen and is known as the Fv region, containing the most variable regions termed V_H and V_L for heavy and light chains, respectively. Variable regions are linked to more constant (C) domains C_H1 and C_L for heavy and light chains respectively, that together with the Fv region, constitute the Fab domain. Additional C regions constitute the Fc part of the antibody, which is responsible for engagement with cellular receptors, ensuring longer half-life and defining antibody isotype.

Each of the heavy chains is further composed of three constant (C_H) and one variable region (V_H) whilst the light chain contains a single constant (C_L) and single variable (V_L) region. Each region is made up of 110-130 amino acids (aa), with molecular mass varying from 12 to 13 kDa, forming 7 (constant region) or 9 (variable region) antiparallel β-strands joined by loops and arranged in two β-sheets resulting in β sandwich with a hydrophobic core (Figure 1.2a) and Figure 1.2b).

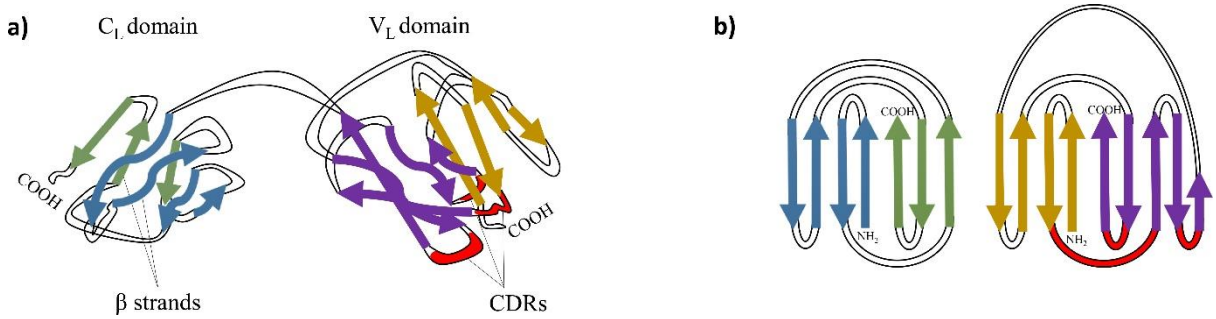

Figure 1.2. Schematic diagram of antibody's light chain fold. a) Cartoon representation of light chain variable and constant domains fold. β-strands of different colours comprise distinct β-sheets. Two β-sheets for each domain are joined by a disulphide bond and hydrophobic interactions. CDRs present within variable domain are depicted in red. **b)** opened out β-sheets demonstrating relationship between β-strands within each of the domains.

The combination of V_H and C_H1 with V_L and C_L regions is known as the antigen binding domain (Fab); a region of ~ 50 kDa that can be separated by papain hydrolysis from another Fab and a fragment crystallizable region (Fc) containing two to three C_H regions (14). Some antibodies contain a hinge region between C_H1 and C_H2 while others incorporate an additional C_H region (15).

Different antibody regions serve distinct biological functions. The C_H1 and C_L regions ensure variable domains are held in place, play a role in Fab arm rotation and contribute to overall immunoglobulin diversity (16). The hinge regions, rich in proline (P) and cysteine (C) residues, are present only in IgA, IgD and IgG (also IgY in birds (Figure 1.1b)) antibodies and provide an additional flexibility that facilitates interaction with antigen. The same role is substituted by the C_H2 region of IgM and IgE antibodies (15). Unlike other domains, C_H2s (in IgA, IgD and IgG but C_H3s in IgM and IgE) cannot interact directly but instead engage oligosaccharide side chains positioned between them leading to facilitated complement activation (17). In addition, C_H2 sequences are responsible for the charge of the immunoglobulin molecule that can support higher affinity towards the antigen. The last C_H region determines whether antibody is to be secreted or membrane bound, contributes to general

antibody structure and accommodates 18 aa C-terminal tail piece (tp) in IgA and IgM molecules that leads to their multimerization (18, 19).

On the other hand, variable regions are composed of hypervariable parts termed as complementarity determining regions (CDR). CDRs define antigen specificity while the remaining residues in the variable region serve as a framework region (FR) (20-22). The ability of an antibody to access hidden, often well conserved, epitopes is thought to depend on the length of CDR loops. In particular,, CDR3 is known to be able to exhibit exceptional length in immunoglobulin molecules derived from cattle, camelids and cartilaginous fishes (23, 24). A proportion of chicken-derived antibodies also carry CDR3 sequences longer than those present in humans or mice. In addition, CDRs derived from poultry antibodies are mainly composed of small amino acids, with cysteines also important in formation of noncanonical disulphide bonds and enhancement of antibody repertoire complexity (25).

Immune system co-evolution with the host has led to the rise of antibodies that do not necessarily follow typical immunoglobulin molecule conformation. Representatives of such ‘unconventional’ antibodies are heavy chain immunoglobulin molecules (hcIg), ~70kDa in size, produced by camelids (alpacas, lamas) and immunoglobulin new antigen receptor (IgNAR) antibodies, ~150kDa in size, produced by cartilaginous fishes (sharks, rays) (Figure 1.3a), Figure 1.3b) (26-28).

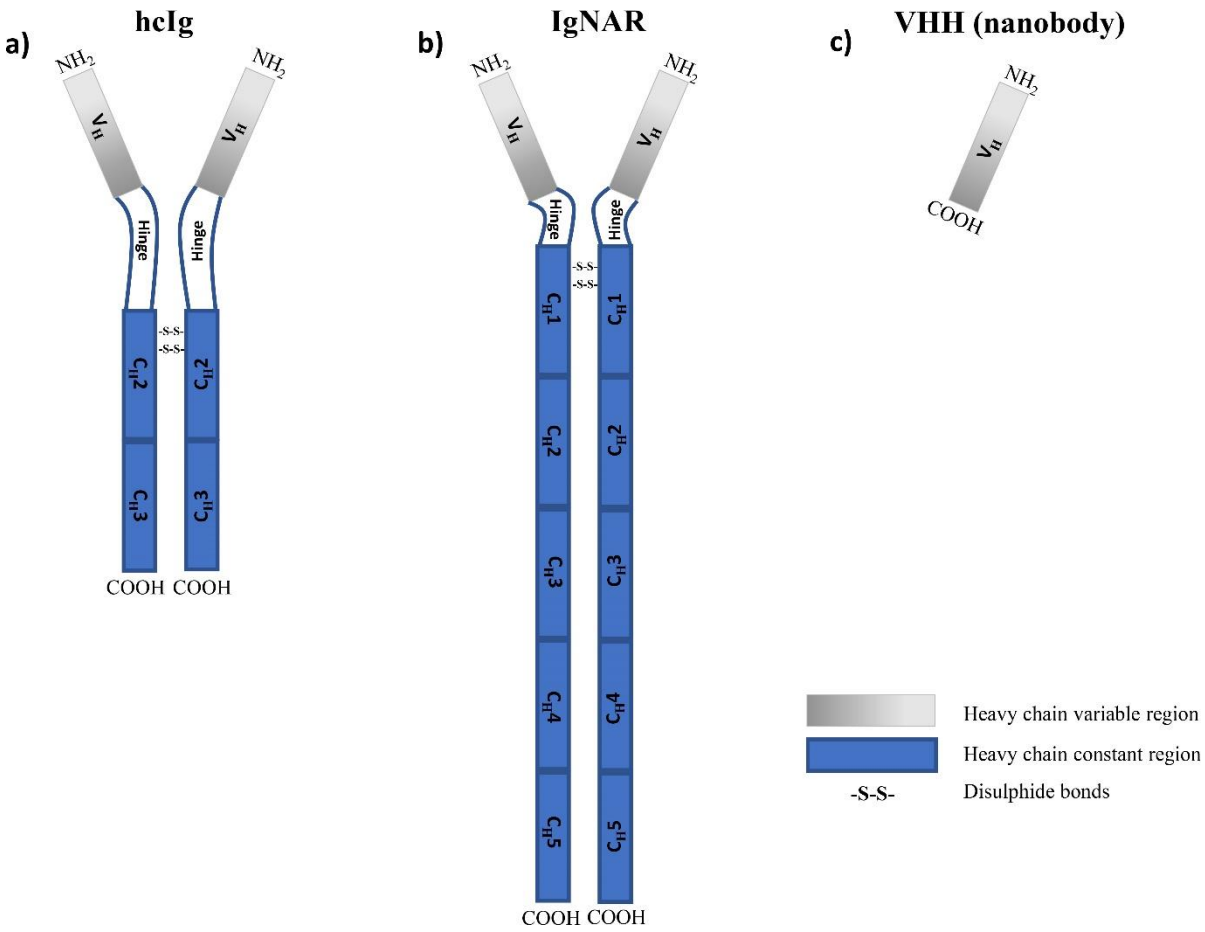

Figure 1.3. Schematic diagram representative for heavy chain immunoglobulin molecules. a) hcIg is a representative of antibodies of ~70 kDa in size derived from camelids. hcIg is naturally devoid of light chains and a C_H1 domain. **b)** IgNAR is an antibody molecule derived from cartilaginous fishes that lacks light chains but has five constant domains resulting in an ~150 kDa molecule. **c) a** recombinant VHH antibody of ~15 kDa in size consisting of only the variable heavy chain of the heavy chain only immunoglobulin molecule.

Such antibodies, although they form Y-shaped structures, have completely abrogated light chains resulting from deletion of the C_H1 domain taking place during mRNA splicing, due to a single guanine (G) to adenine (A) substitution in the immunoglobulin gene and other modifications in V_H region (29). Recognition of antigen is mediated by the V_H domain; something that has lately been harnessed for generation of recombinant heavy chain only (VHH) antibodies (otherwise, known as single domain antibody or nanobody) (Figure

1.3c). A few nucleotide changes upstream of the CDRH1, with respect to a traditional immunoglobulin gene, makes the motifs more permissible for somatic hypermutation and affinity maturation that facilitate remarkable antibody affinity and avidity (29). VHH antibodies also display high solubility leading to low aggregation, which is mediated by the VHH tetrad consisting of four residues at positions 37, 44, 45 and 47 (30, 31). Overall, a Y-shaped structure ensures the antibody's ability to recognize antigen via variable regions and interact with receptors displayed on the surface of host immune cells via constant domains.

1.1.2 Antibody classes

Isotypic determinants are constant region determinants that define heavy chain class and subclass and light chain class. In humans, there are five heavy chain isotypes encoded by α, δ, γ, ε and μ genes giving rise to IgA, IgD, IgG, IgE and IgM antibodies respectively, while only two types (lambda (λ) and kappa (κ)) of light chain exist (7, 8) (Figure 1.4). Alternatively, in birds, the υ gene encodes for IgY antibodies. Overall, the heavy chain isotype dictates the class of the whole antibody molecule.

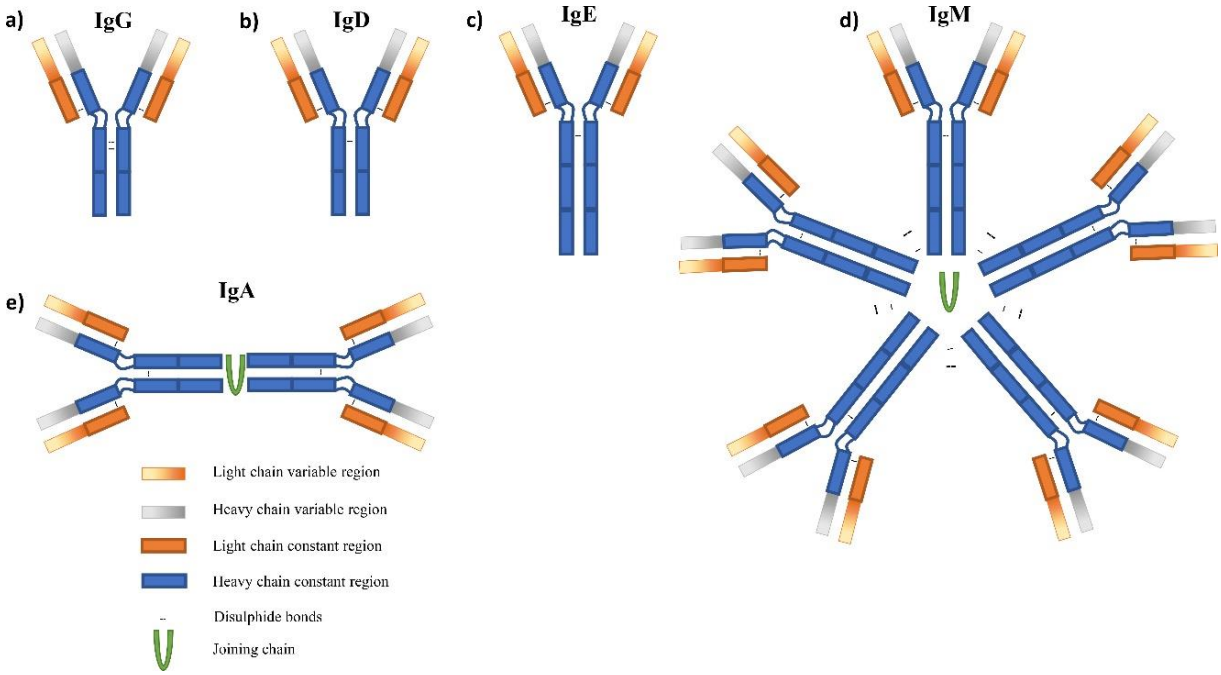

Figure 1.4. Schematic diagram of five main immunoglobulin classes. a) IgG is an ~150k Da molecule encoded by the γ gene. IgG contains two antigen binding sites and is the main antibody isotype found in serum. **b)** IgD isotype antibody resembles the IgG molecule in containing two antigen binding sites. It is an ~180 kDa molecule encoded by the δ gene with only ~1% of IgD present in serum. **c)** IgE is another monomer of ~200kDa in size encoded by the ε gene that carries two antigen binding sites. **d)** IgM is a pentameric molecule of ~900 kDa carrying ten antigen binding sites, encoded by the μ gene. **e)** IgA antibody usually forms dimers containing four antigen binding sites. IgA is encoded by the α gene.

IgA antibodies constitute three quarters of daily immunoglobulin production. The monomeric form of this antibody is exclusively found in serum, while dimeric and more rarely tetrameric IgA is secretory and often resides on mucosal surfaces (32). An additional joining (J) chain is present in multimers inducing polymerisation of the immunoglobulin molecules (33).Two IgA subclasses (IgA1 and IgA2) exist that differ in hinge region length and, therefore, their ability to interact with two antigens simultaneously (34).

The secondary immune response is mediated by more refined IgG molecules that form the largest proportion (80%) of antibody isotype found in serum. Human IgGs can be classified into further subclasses of IgG1, IgG2, IgG3 and

IgG4, depending on the size of the hinge region and position of disulphide bonds between heavy chains (35). Different subclasses might be crucial for foetal development (IgG1, IgG3, IgG4), complement activation during infection (IgG1) or opsonization (IgG1, IgG3) (35). Differences in Fc regions lead to interaction with distinct Fc receptors (FcR) displayed on the host cell surface that can be either activating (FcγR) or inhibiting (FcγRIIB) (35).

IgM antibodies are mostly pentameric and hexameric molecules that serve during a primary immune response, as they lack specificity but display rather strong affinity towards the antigen (36). As with IgA antibodies, IgM polymerisation is induced by J-chain molecules (33). In addition, proximity of the Fc regions in IgM antibodies enhances their complement activation potential (36).

IgE and IgD antibodies are involved in allergies and homeostasis, respectively, and mostly form monomers (37, 38).

IgY is found in birds, reptiles and lungfish and is homologous to mammalian IgG (39). Unlike IgG, IgY contains an additional C_H region and displays a unique oligosaccharide structure. IgY also mediates anaphylactic reactions characteristic of mammalian IgE, suggesting it is the ancestral molecule to both IgG and IgE class antibodies (39).

1.1.3 Antibody gene organization and expression

In mammals such as humans or mice, antibody chains are encoded by several gene segments separated by non-coding regions (known as multigene families) that can rearrange during B-cell maturation to form a functional immunoglobulin gene (40-42). The antibody light chain gene is produced after recombination between variable (V) and joining (J) segments, whilst the heavy chain gene requires an additional diversity (D) segment (42, 43) (Figure 1.5).

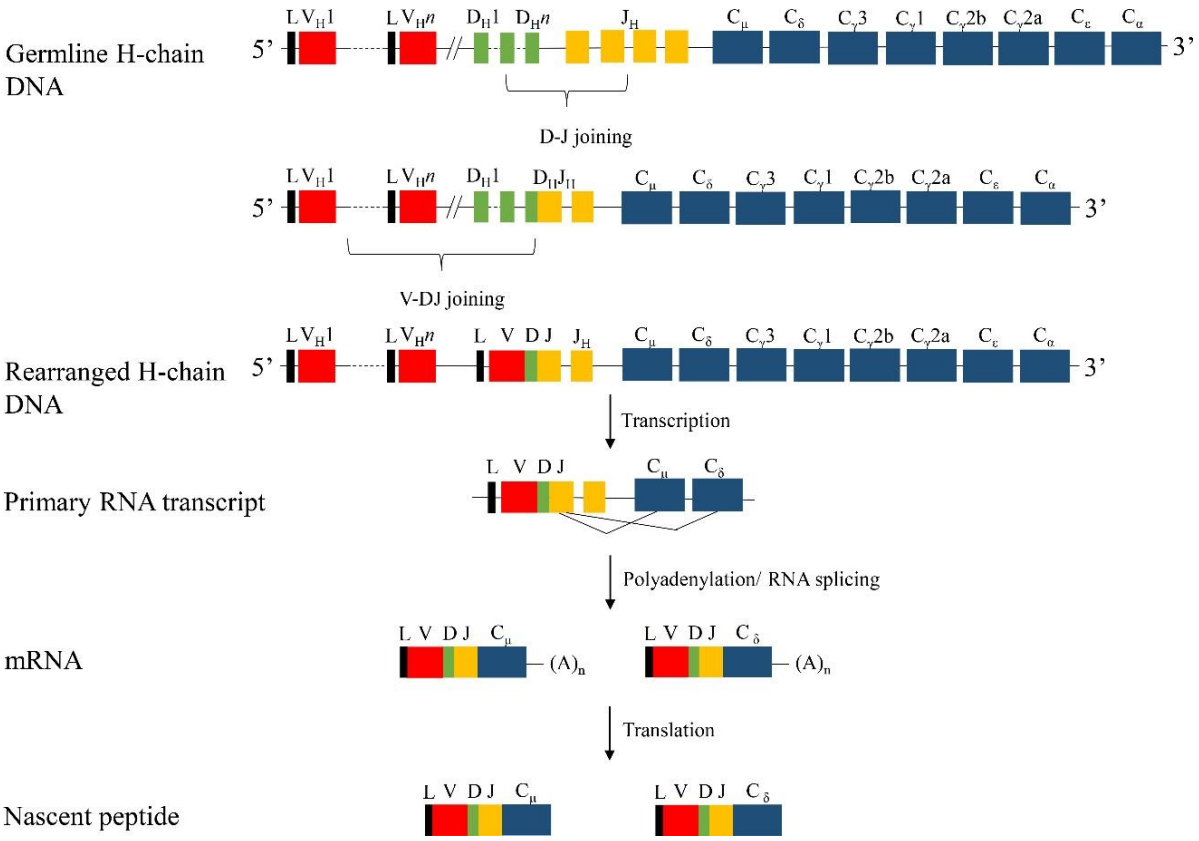

Figure 1.5. Schematic representation of heavy chain gene rearrangement and mRNA processing mechanism. Joining of D_H with J_H joining is the first step during gene rearrangement followed by V_H joining with D_HJ_H. The rearranged heavy chain gene is then transcribed and further processed to form a mature mRNA which can be translated into a nascent peptide. The light chain undergoes slightly different processing involving only V_L to J_L rearrangements to form fully functional light chain gene.

After VJ or VDJ rearrangement, a constant (C) gene segment is added, determining antibody isotype (42). This process also enables class switching whereupon VDJ recombination with new C segment, a new isotype antibody can be produced (42). VDJ rearrangement together with junctional flexibility, somatic hypermutation, and indel addition forms the basis of antibody diversity in many species (44, 45). On the other hand, rabbits, sheep, cattle, pigs, horses and birds have a very distinct mechanism for immunoglobulin diversification due to their limited number of functional V, D and J gene segments (46). In such instances, the antibody repertoire is expanded during

somatic gene conversion events dependent on pseudo V_L and V_H genes and mediated by the activation-induced cytidine deaminase (AID) enzyme (47).

Translation of mature heavy chain and light chain mRNAs takes place at the rough endoplasmic reticulum (ER) on separate polyribosomes (48). Newly synthesised chains translocate to the ER lumen where signal peptides are cleaved off and the antibody assembles in cisternae before moving to the Golgi apparatus for further post-translational modifications (48).

The most frequently encountered post-translational modification (PTM) for an antibody molecule is N-linked glycosylation where sugars are attached via asparagine residues; however, O-linked glycosylation via serine (S) or threonine (T) can also occur (49, 50). Around 10% of N-linked glycans within IgG1 and more than 90% of IgA1 N-linked glycans contain sialic acid, contributing not only to longer serum retention times but also suggesting a possible antiviral role (51). For instance, the conserved N459 sialylated glycosylation site, conserved amongst IgG molecules, is recognised as a critical position involved in interference with attachment of sialic acid binding viruses, such as influenza virus or Newcastle disease virus (NDV) (51). Whilst glycosylation at position N297, ubiquitous to IgG Fc regions, functions in triggering complement activation (49, 52).

Finally, once all PTMs are completed, secretory vesicles enclose antibody for transport and release outside the cell (53). Immunoglobulin molecules containing a transmembrane domain remain anchored to the plasma membrane during vesicle and cell membrane fusion and serve as membrane-bound antibodies (53).

1.2 Recombinant antibodies

Recombinant antibodies are antibodies produced from synthetic DNA via the use of expression vectors that support mRNA translation and transcription. Both prokaryotic and eukaryotic systems can be employed for recombinant

antibody production. Although recombinant antibodies are considered to be animal-free, their gene recovery often requires *in vivo* based methods (see 1.4.1 Antibody gene recovery platforms). Nevertheless, synthesis of expression cassettes encoding for recombinant antibodies allows application-dependent adjustments for the preferred antibody format for research, diagnostics, or therapeutics.

1.2.1 Antibody gene recovery platforms

Several strategies exist for isolation of antigen-specific antibody genes. These include hybridoma technology, *in vitro* display technologies and isolation of antibody genes directly from primary cells.

1.2.1.1 Hybridoma technology

The development of hybridoma technology in 1975 significantly accelerated research in the mAb field with the hope for production of immunoglobulins specific for desired antigens (54). Briefly, the process is based on mouse (or more rarely, other laboratory animals like rats, rabbits, etc.) immunization with antigen(s) of interest followed by isolation of the B cells from splenocytes and their co-culture with myeloma cells triggering two cell type fusion generating hybridomas (54) (Figure 1.6). Single immortalized cells producing distinct antibodies can then be chosen for further characterization and large-scale immunoglobulin generation.

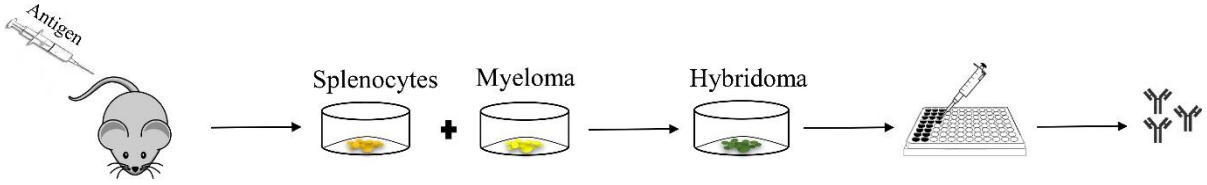

Figure 1.6. Workflow of hybridoma technology. Briefly, mice are immunized with an antigen of choice, after which splenocytes are harvested in order to fuse them with immortalized myeloma cells and to produce hybridomas. Each hybridoma generates unique monoclonal antibodies which are screened for specificity and functionality. Hybridomas can be expanded to obtain large amounts of the antibody of interest.

One of the main disadvantages for hybridoma technology is off-target binding of mAbs that results from heterogeneity in heavy and light chains encoded by a single hybridoma cell which results in expression of several different antibodies instead of the expected single mAb. Indeed, datasets from seven independent laboratories working on mAb generation found ~30% of the hybridomas to contain additional productive variable chain genes (55). Some of the reasons for the introduction of additional alleles in the hybridomas include simultaneous fusion of a myeloma partner to more than one spleen cell, the ability of a single splenocyte to encode multiple productive gene rearrangements, or post fusion modifications (55-57).

Although hybridoma-derived antibodies are crucial for research and diagnostics, the main obstacle for their application in the therapeutic field comes from high antibody immunogenicity when used in different species. This requires more refined techniques to produce therapeutically relevant antibodies.

1.2.1.2 In vitro display technology

Yeast, bacteria, ribosome, mRNA and phage display formats are the main representatives of the *in vitro* display systems; all of which offer an advantage of defined selection conditions whilst screening a huge number of antibodies from naïve, immunized, semi-synthetic or synthetic repertoires (58). These technologies aid generation of an antibody library which is then used for panning against an immobilized target. Non-bound antibodies are washed off while recovered antibodies undergo another round of selection or are propagated for further characterization (Figure 1.7).

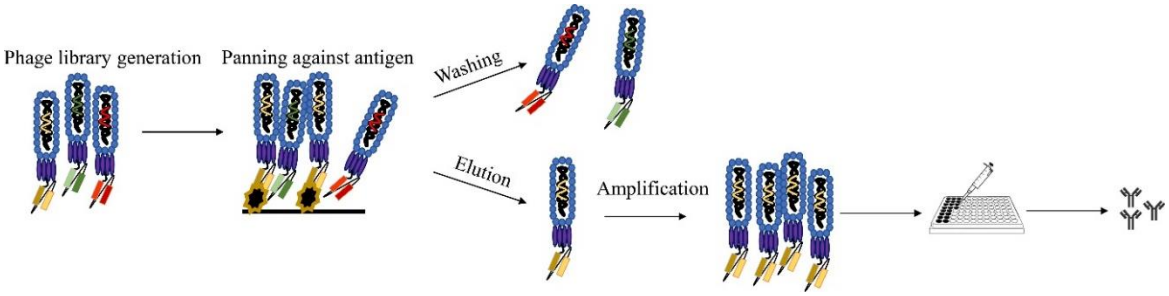

Figure 1.7. Workflow of antibody recovery using phage display. Firstly, an antibody library displayed on the surface of bacteriophage needs to be generated which then is incubated with immobilized antigen. Washing steps are performed to remove unbound material followed by the elution of phages carrying specific antibody fragments. Eluted phages are amplified in *Escherichia coli* with the workflow repeated until an enriched population of antibodies is obtained. Subsequently, antibodies can be screened for specificity and functionality and the ones meeting expected requirements can be generated in larger quantities for further characterization.

The first *in vitro* display technology was developed in bacteriophage M13, belonging to the Ff filamentous phage family, allowing the protein of interest to be displayed on the virion surface after insertion of the gene of interest into the phage's coat protein gene (59). As it is a powerful tool to study protein-protein, protein-peptide or protein-DNA interactions, phage display remains the most commonly used technology for recovery of antibodies (60). Yeast display technology creates somewhat smaller libraries but has the convenience of employing fluorescence or magnetic activated cell sorting (FACS/MACS) and is preferred for selection of antibody fragments (61). FACS is also used for bacterial display engaging gram-negative bacteria, due to the ease of transformation and relatively straightforward translocation of fusion proteins (62, 63). Mammalian cell display offers the advantages of accurate PTMs and is mostly utilised for recombinant antibody isolation and maturation (64, 65). In addition, several cell free display systems exist, including ribosome display which is employed for the selection of antibodies when secondary libraries need to be generated by error prone polymerase chain reaction (PCR), as each selection step requires PCR amplification (66). Another totally *in vitro*

display technology is based on mRNA display, creating slightly more stable complexes than those formed by ribosome display (67).

In vitro display technologies can be combined to further increase efficacy in protein recovery. Several cross-reactive single domain antibodies specific for influenza B antigen have been recovered by employment of phage display, providing a panel of antigen-specific, high affinity antibodies, followed by yeast display enabling mutational screening (68). In addition, *in vitro* display technology can allow the generation of recombinant renewable polyclonal antibodies from naïve repertoires, thereby serving as a viable alternative to the traditional immunization and affinity purification techniques (69). This approach is based on isolation of a population of antigen-specific antibodies by several rounds of phage and yeast display selection in which renewability is achieved by growing the secretory yeast pool to saturation multiple times (69).

Although *in vitro* display selects for the best affinity antibodies, it cannot ensure satisfactory expression levels in cell culture and does not necessarily represent the natural antibody repertoire. Nevertheless, advantages are self-evident due to the ability to rapidly obtain selected antibody sequences that can be further altered to induce the desired characteristics. Importantly, *in vitro* display allows high-throughput selection of antibodies recognizing epitopes containing subtle differences of PTMs or proteins of different conformations.

1.2.1.3 Isolation of antibodies and their genes from primary cells

Donor-derived antibody recovery can be based either on isolation of memory B-cells or antibody secreting cells (ASC). The first approach allows evaluation of the total immune response formed over the years, whilst the latter technique relies on activated plasmablasts that are only available at the peak of the immune response.

One of the first techniques developed enabling the isolation of an antibody of interest from peripheral B-cells is based on memory B-cell immortalisation using Epstein-Barr virus (EBV)(70). Transformed cells can be used for stable B-cell line generation and subsequent recovery of immunoglobulin gene sequences by reverse transcription (RT)-PCR. However, low immortalisation efficiency and low levels of antibodies recovered has led to optimisation of conditions, including the fusion of EBV immortalised cells with mouse myeloma cells, infection with a retrovirus encoding *ras* oncogene and the addition of CpGs, ensuring more successful formation of clonal cell lines (71-73). Alternatively, similar results can be achieved by peripheral B-cell cultivation with irradiated thymoma cells (74). In addition, a strategy of genetic B-cell reprogramming by retroviral encoded antiapoptotic factors B-cell lymphoma 6 protein (Bcl-6) and B-cell lymphoma-extra large (Bcl-x_L) can increase the recovery of antibody secreting cells (ASCs) even further (75). Apart from retroviral transduction, this approach also requires the presence of stimulants such as recombinant interleukin 21 (IL-21) and CD40 ligand (CD40L) to activate B-cell expansion into longed lived ASCs (75). Single cell cloning by limiting dilution can also be performed to allow the assessment of single cells secreting the desired antibody. Yet another approach, applicable for ASCs, is based on single cell RT-PCR without the necessity to obtain single B-cell clones (76). Based on this approach, IgG secreting cells are isolated from whole blood by flow cytometry or antigen coated magnetic beads, prior to RT-PCR featuring a cocktail of primers covering as many families of variable genes as possible (76). The heavy and light chain sequences from each cell are then cloned into appropriate vectors for transformation, sequencing and transfection of cell culture for antibody characterisation. Importantly, a similar workflow can be adapted to multiple species that are, otherwise, subject to poorly defined cellular markers or a need to establish sterile single cell cultures from non-sterile tissues (77).

1.2.2 Recombinant antibody formats

Besides higher reproducibility between batches and shorter production times than those of mAbs, recombinant antibodies can also be formatted in a way such that only certain immunoglobulin molecule fragments are used. In addition, several antibody genes can be joined together to obtain a multispecific antibody format targeting several epitopes or /and antigens by a single molecule. Antibody formatting also allows changing of isotypes and adjustment for species specificity.

1.2.2.1 Antibody fragments and unconventional antibodies

The three main types of functional antibody fragments include Fab molecules (F(ab) and F(ab')$_2$), single chain variable fragment (scFv) antibodies derived from conventional antibodies and VHH molecules obtained from 'unconventional' antibodies (Figure 1.3c). The smaller VHH format offers advantages including better tissue penetration, faster clearance, lower immunogenicity, ensures correct folding and ease during production stages, but comes with the lack of an Fc region which translates to an absence of effector functions (78).

F(ab) and F(ab')$_2$ fragments are monovalent and bivalent molecules, respectively, produced by enzymatic (papain or pepsin) digestion of the whole immunoglobulin while scFvs are made upon linkage of V_H and V_L regions (Figure 1.8) (14, 78, 79).

Figure 1.8 Schematic diagram of antibody fragments. a) F(ab')2 resembles a whole immunoglobulin molecule with two antigen binding sites. F(ab')2 is ~110 kDa in size and can be generated recombinantly or after whole antibody digestion with pepsin**. b)** A Fab fragment is ~50 kDa in size and can be produced after antibody digestion by papain or in a recombinant

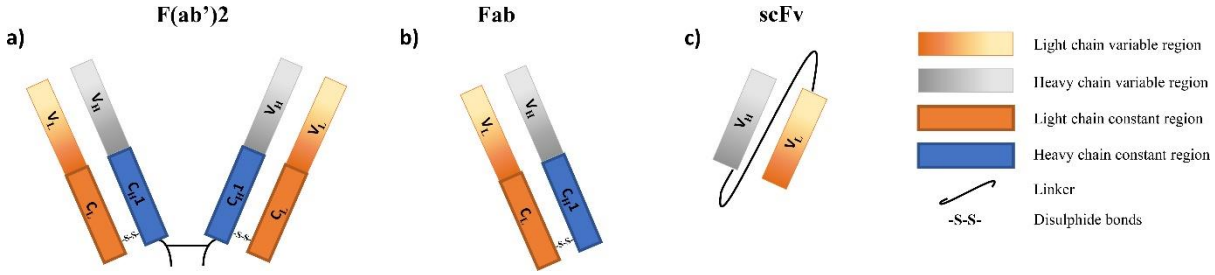

format. A Fab is a monovalent antibody fragment lacking Fc part. **c)** The scFv is the smallest antibody fragment that can retain antigen binding activity. An scFv is ~27 kDa recombinant antibody format made up of VH and VL chains linked by a short linker.

A commonly used strategy for scFv joining is based on introduction of a flexible peptide sequence resistant to endopeptidases which can separate two domains by 35 angstroms, ensuring correct antibody fragment folding (80). Such linkers usually contain small non-polar or polar amino acids such as glycine (G), S, or T to ensure flexibility, whereas introduction of glutamic acid (E) and lysine (K) residues contributes to enhanced solubility (81). The most common linker used for scFvs formation is $(G_4S)_n$, but others such as KESGSVSSEQLAQFRSLD and EGKSSGSGSESKST are also used (81-83). Small antibody fragments including Fabs and scFvs are commonly used for diagnostic purposes or cancer therapeutics.

A VHH antibody derived from the V_H region of hcIg is 15 kDa in size and displays superior access to hidden targets within the antigen and a larger antigen-antibody interaction surface due to unusually long CDR loops (28, 29). In addition, VHH antibodies do not trigger an anti-antibody response when introduced into different species (28, 29). The small nanobody format also provides an advantage by allowing the multiplexing of several VHH molecules, leading to increased antibody potency and cross-reactivity. For example, the MD2407 molecule is a multidomain antibody generated by fusing four VHHs derived from a llama immunised with an influenza antigen (84). Such a multidomain approach can induce not only greater breadth of reactivity than

that of any single VHH antibody but also carries higher neutralization activity and ability to cross link adjacent haemagglutinin (HA) trimers (84).

Stability of antibody fragments is essential in order to retain functionality and prevent aggregation which can increase protein immunogenicity. Multiple strategies have been revised to ensure antibody stability. Nevertheless, if unfolding at the variable interface occurs, interaction of complementary immunoglobulin domains from adjacent molecules is likely to induce oligomerisation or formation of dimeric antibodies that can retain their original functionality in antigen recognition but have altered pharmacokinetic traits (85).

1.2.2.2 Diabodies and bispecific antibodies

The main difference between dimeric antibodies or diabodies and bispecific antibodies (bsAbs) is the ability of bsAbs to recognize distinct epitopes located either within the same or on different antigens, while diabodies are only able to recognize single antigenic determinants (Figure 1.9) (86, 87). Both types of recombinant antibodies benefit in immunotherapeutics with bsAbs being a potential alternative to combination therapy requiring a mAb cocktail.

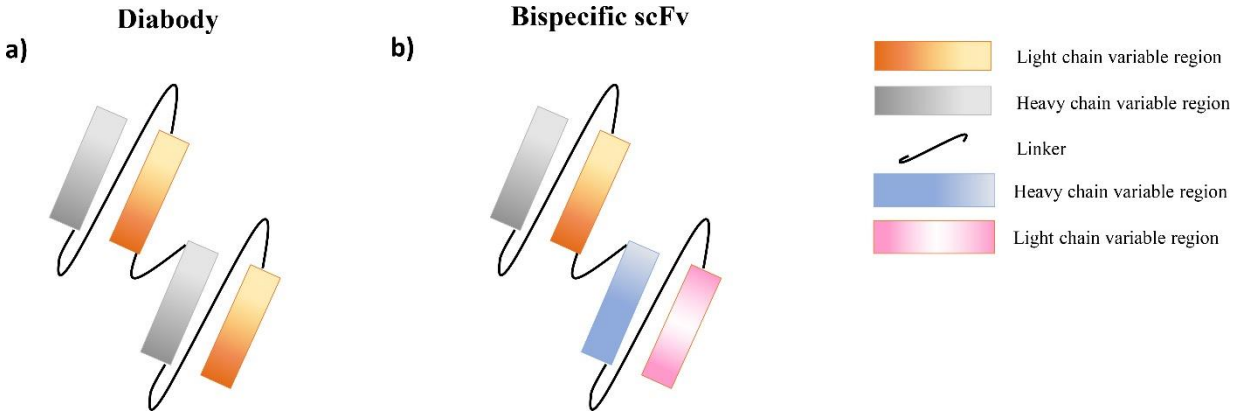

Figure 1.9. Schematic diagram of a) diabodies and b) bispecific scFvs. Diabodies are formed after a 3-10 residue linker introduction between V_H and V_L domains during generation of the scFv fragment, or by linking two identical scFv with an additional linker sequence. Bispecific scFvs are generated upon linkage of two scFvs carrying distinct specificities.

Diabodies are monospecific immunoglobulin molecules, derived from heterogeneous single-chain antibodies, which can act via cross linking multiple antigens. Diabodies are formed upon introduction of a 3-10 residue linker between the V_H and V_L domains; a process equivalent to scFv generation, with the short linker size forcing scFvs to form dimeric structures (88). In order to increase diabody stability, an interdomain disulphide bond might also be added (89, 90). Such immunoglobulin fragment structures are preferred due to their larger size than scFvs, ensuring a longer half-life and circulation *in vivo* (86).

On the other hand, bsAbs exhibit increased valency by containing multiple binding sites for the antigen or for a host cell receptor and can be generated using scFvs, Fabs and whole immunoglobulin molecules. Minimalistic bsAbs are produced upon direct linkage of two scFv molecules carrying different antigen specificities, or by linkage of the V_L region of one antibody with the V_H domain of another immunoglobulin and vice versa, inducing the formation of more stable structures (86). The greatest advancements in the development of bsAbs from scFvs have been made in cancer research. Huge success has been brought by generation of bispecific T cell engagers (BiTEs) combining anti-CD19 and anti-CD3 scFvs into a single molecule, enabling formation of a link between tumour and cytotoxic T cells (91, 92).

Dual targeting can also be facilitated by incorporation of Fab domains into the building blocks. For instance, two scFvs fused to the Fab molecule forms a F(ab)-$scFv_2$ tribody, whereas introduction of the hinge region into the Fab molecule results in a fusion protein forming a tetravalent F(ab')2-$scFv_2$ antibody (93, 94) (Figure 1.10).

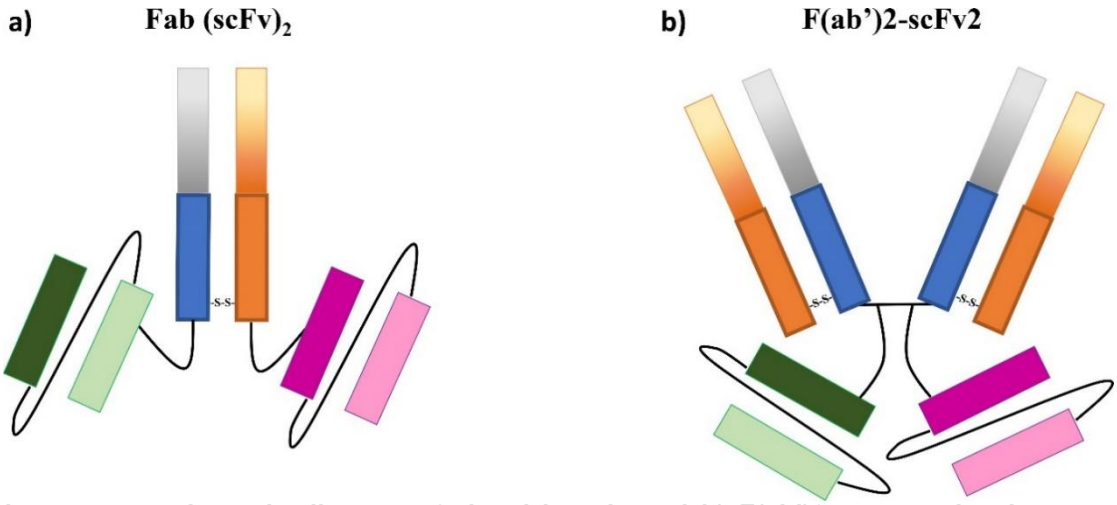

Figure 1.10. Schematic diagram of a) Fab(scFv)$_2$ and b) F(ab')2-scFv$_2$ molecules. A Fab(scFv)$_2$ is a trimeric antibody of ~105 kDa in size generated upon fusion of two scFv molecules with different specificity to the Fab fragment. A F(ab')2-scFv$_2$ is an ~180 kDa molecule requiring fusion of two scFv molecules carrying different specificities with a F(ab')2 antibody fragment. A F(ab')2-scFv$_2$ can bind three antigens: two monovalently and one bivalently.

Fusion of two Fab arms to an asymmetric Fab-like moiety at their C-termini via a $(G_4S)_n$ linker instead of a hinge region induces formation of a TriFab with the overall structure featuring IgG, able to engage two antigens: one bivalently and another monovalently (95). CrossMab is another technology for bsAb generation by the exchange of different domains (Fab domains, V_H and V_L domains or C_H1 and C_L domains) within a Fab fragment (96).

With regards to bsAbs containing Fc domains, several strategies have been implemented as well. Firstly, production of bispecific IgG molecules, with the potential to combine antibodies belonging to different isotypes or even those derived from different species, can be achieved by fusion of two hybridomas (97, 98). Alternatively, bispecific IgG formation can be driven by heavy chain heteromerization based on a 'knobs-into-holes' approach. This requires replacement of the small side chains in the C_H3 part of the Fc region from the first antibody into larger ones representing the knob, along with contrary adjustments in the C_H3 domain from the second antibody following the hole

pattern (99). An example of key substitutions triggering the intended interactions are T366Y in C_H3 domain 1 and Y407T in C_H3 domain 2 (99). Similarly, substitution of certain residues in the first C_H3 domain with positively charged lysines and introduction of negatively charged glutamic or aspartic acid residues in the second C_H3 domain results in electrostatic steering effects that trigger IgG heterodimerization (100). Other strategies for bsAb generation using whole immunoglobulin molecules are based on the natural IgG4 ability to exchange Fab arms, strand-exchange engineered domain (SEED) heterodimers design, as well as other variations (101, 102).

Out of many approaches, the 'knobs-into-holes' technique works well not only with whole antibody molecules but is also applicable for scFv engineering into the Fc region. For instance, an $scFv_2$-Fc antibody targeting human immunodeficiency virus (HIV) proteins gp41 and gp120 was generated by fusing two different specificity scFvs to human immunoglobulin C_H domains (103). Another trispecific molecule targeting the HIV CD4 binding site, the membrane proximal external region and V1V2 glycan site was engineered based on the same approach (104).

Although engineered bsAbs have remarkable improvements in functionality, it can also cause problems during production, resulting in low yields. Overall, the variety of antibody formats allows optimization of the desired functions and specificity with optimal expression levels driving the field towards generation of more therapeutically relevant antibodies.

1.2.2.3 Chimeric antibodies and antibody species adaptation

The availability of hybridoma technology to generate fully murine antibodies and a desire to use them for therapeutic purposes has led to the development of chimeric antibodies (ch-mAb) displaying reduced immunogenicity (105). One approach is based on variable regions, derived from hybridomas, fused with the constant region of an antibody matching the species of interest (106).

Such ch-mAbs can retain their original efficacy, as demonstrated after generation of a human-like antibody via substitution of a mouse Fc domain to the human Fc region in H5N1 neutralizing antibodies (107). The previously mentioned multidomain antibody approach composed of multiple VHHs (section 1.5.2.1) has also been taken forwards for species matching by introduction of a human IgG1 Fc region (84).

However, the most commonly encountered antibody species matching approach is based on CDR grafting, with in some cases, transfer of one or more framework regions to enhance the overall binding affinity of the antibody. Several strategies for CDR grafting have been implemented based on FR homology, CDR homology, frequency of gene usage and structural stability, along with usage of germline genes as the FR source or replacement of uncommon FR residues (108-111). The 8A8 – H5 HA-specific antibody is one of the examples of how CDR grafting can ensure preservation of correct antigen specificity and dual activity (recognition of conformational and linear epitopes) while introducing human T cell epitopes onto a murine immunoglobulin molecule (112). CDR grafting has also been performed to give the mouse-derived 3D8 mAb, with ability to bind to and induce RNA/DNA hydrolysis, specificity of the chicken antibody framework (113). This “chickenized” antibody displayed similar structure and functional activity to that of the original mAb and was later used for generation of a transgenic chicken line (114, 115).

Another strategy to obtain fully humanized antibodies derives from generation of transgenic animals (mainly rodents and bovines). Mouse strains encoding different isotypes of human immunoglobulin genes and carrying disrupted mouse immunoglobulin loci can produce antibodies suitable for use in humans, as illustrated by the epidermal growth factor receptor antibody panitumumab (116-118). In addition, genetically engineered cows can also successfully produce polyclonal neutralizing antibodies adapted for human use against

various antigens, including Ebola, Venezuelan equine encephalitis (VEE), Hanta and Middle East Respiratory Syndrome (MERS) viruses (119-122). Overall, implementation of antibody species adaptation has had a major impact on development of immunotherapeutics relevant for use in different species.

1.2.3 Recombinant therapeutic antibodies

Therapeutic antiviral antibodies can function either via direct antigen recognition and neutralization by their antigen binding domain, or secondarily via Fc-domain interaction with Fc-binding molecules. Depending on the pathogen and its ability to arms race, monoclonal vs polyclonal antibody therapeutics must be considered. In addition, broadly reactive immunoglobulins are of the essence when multiple quasispecies of the same pathogen are prevalent. Nevertheless, timing (pre- or post-exposure) and delivery strategy, whether the antibody would be in a form of nucleic acid or purified protein, is of an equal importance for effective passive immunization.

1.2.3.1 Polyclonal and monoclonal therapeutic antibodies

An initial idea behind immunotherapeutics was based on a transfer of blood, plasma, serum or in some cases purified immunoglobulin containing polyclonal antibodies from immune donor into recipient (1, 123). Passive blood product transfer has been used during various outbreaks, including MERS, Ebola virus and even the coronavirus pandemic in 2020 (124-126).

Generally, polyclonal antibody preparations consist of an immunoglobulin mixture carrying both neutralizing and non-neutralizing antibodies which are often of limited specificity (127, 128). However, a polyclonal response targets a broad range of epitopes; something that is crucial if therapeutics are used against rapidly evolving pathogens such as HIV, influenza or Lassa viruses, as it reduces the chances for escape mutant generation (129). In addition, the minimal production costs and technical skills required advocates the use of

polyclonal antisera (129-131). The most commonly encountered approach for polyclonal antibody preparation involves donor vaccination or natural exposure to the antigen followed by immunoglobulin recovery (131). However, such a method of antisera generation carries a risk of blood-borne disease transmission, batch-to-batch variability, and scalability issues (132, 133). Some of these concerns can be overcome if the immunoglobulin produced is not intended to be used in humans. For instance, a polyclonal response against multiple pathogens can be achieved by chicken layer flocks hyperimmunization with multiple antigens (134). Subsequently, IgY is harvested from newly laid eggs and can be used for passive transfer into 1-day-old chicks, resulting in antibody persistence in blood that overcomes the period of susceptibility in birds when maternal antibodies vanish but their own immunity is not yet formed (134). While high yields of IgY antibodies can be derived from a single egg, only few reports have shown its actual applicability, even in poultry.

Low purity and lack of specificity in polyclonal immunoglobulin preparations has triggered a shift towards use of mAbs for immunotherapeutics. The development of recombinant antibody recovery platforms (discussed in section 1.5.1) allows selection of mAbs with the highest specificity, while the ability to retain antibody sequences abolishes the need for repeated immunizations in order to produce new immunoglobulin batches (129). The change in approach is illustrated particularly well by the shift of therapeutics against respiratory syncytial virus (RSV). Use of the therapeutic hyperimmune globulin RespiGam has been overtaken by the mAb palivizumab, which targets the fusion protein of RSV with 50-100 times stronger potency (135, 136).

As mAbs can only recognize a single epitope, limiting their therapeutic potential, an alternative solution combining the advantages of a polyclonal response and mAbs has been developed. The approach is based on pre-selection of several mAbs which are combined during expression in stable cell

lines carrying single light and multiple heavy chains, or a mixture of multiple stable cell lines expressing single high quality antibodies, in essence resulting in recombinant polyclonal immunoglobulins (129). One such example is Rozrolimupab (Sym001), which contains a mixture of twenty-five mAbs and is undergoing phase 2 clinical trials to test its efficacy against haematological disorders (137, 138). A move towards generation of 'universal' antibodies with high cross reactivity and high potency seems to require either mAb cocktails or antibody formats that allow multiple specificity.

1.2.3.2 Broadly cross-reactive neutralizing antibodies

Broadly cross-reactive neutralizing antibodies (bnAbs) are a class of antibodies particularly important for immunotherapeutics against rapidly evolving viral pathogens such as influenza virus or HIV. Discovery of bnAbs for influenza virus was significantly accelerated by development of techniques allowing immunoglobulin recovery from circulating B cells, as well as the 2009 influenza pandemic that revealed HA stem-reactive antibodies (139). bnAbs typically target well conserved antigenic determinants, allowing recognition of diverse viral subtypes. For instance, bnAbs targeting influenza virus locate to the HA stem, which has lower immunogenicity than the HA head but is more conserved across viral subtypes, consequently with generation of escape mutants often costing viral fitness. A lack of appreciation for bnAbs is illustrated by the controversy surrounding the interpretation of classical influenza vaccine success based on the haemagglutination inhibition assay (HAI), which can only pick up antibodies binding to the HA head and misses ones specific for the stem (140, 141). A lot of effort has been put in to increase understanding of how such stem-binding antibodies can contribute to protection against the development of disease and what to identify the characteristic features that define bnAbs.

The mechanism of action of bnAbs targeting the HA stem is based on interference with viral and endosomal membrane fusion; however, to achieve

protection against disease, very high concentrations of bnAbs are required (>10mg/kg) (142). Usually, antibody binding to the HA stem is mediated via the V_H domain which gains access just below the trimeric head upon the formation of hydrophobic pockets within the antigen during HA0 cleavage (143). Even though the V_L chain might not be directly involved in epitope-paratope interaction, it plays a significant role by supporting overall antibody structure. The majority of bnAbs can only bind to group 1 (H1, H5, H9) but not group 2 (H3, H7) influenza virus HAs; something explained by structural epitope discrepancy. A critical residue abolishing binding to group 2 viruses is histidine (H) 111 which can induce a 90° rearrangement of the Tryptophan (W) 21 side-chain, disrupting the antigen-antibody interface (144). In addition, group 2 viruses tend to display glycosylation patterns that can also interfere with antibody binding. Although a rather small array of antibodies exist that bind exclusively to group 2 influenza viruses, their light chains are involved in the binding process by inducing conformational changes in the CDRH3 loop within the V_H chain (145). One example is CR8020, which binds to the base of the HA stem which is inaccessible on group 1 viruses due to N21 and a tendency for bulkier residues at position 34 on HA1 (146). Nevertheless, some bnAbs can bind both group 1 and 2 viruses, possibly resulting from unique angles of antibody approach as exemplified by 27F3 and CR9114 (147). Binding sites for CR9114 seem to be nearly identical with other bnAbs (CR6261 and F16); however, a slightly different conformation within the W21 loop allows displacement of HA glycans and therefore increased cross-reactivity (147).

Another antibody effector function lying within the Fc part of the immunoglobulin molecule facilitates ADCC activity and supports the ‘SOS theory’ behind cross-reactive antibodies. Recovery of bnAb libraries from ‘non-immune’ individuals has provoked a school of thought suggesting it to be a ‘SOS’ component of the immune response (143, 148). In addition, a combination of distinct immunoglobulin isotypes with variable regions derived

from bnAbs, specific for influenza virus, shows the necessity of Fc-FcR interactions to ensure protection against a challenge virus through a compensatory mechanism activated if the original FcR becomes unavailable (149). The importance of Fc-FcR compatibility is also suggested by a complete loss of protective potential of bnAb F16, recovered from mouse, when used in a swine model of infection (150). Most bnAbs are encoded by the V_H1-69 germline, undergoing very minimal affinity maturation. Nine out of ten H5 HA-specific antibodies were found to be able to bind the HA stem by a single tyrosine residue located on CDRH3, indicating the presence of a predetermined immune response when antibodies are readily accessible at the onset of infection (143, 151).

1.2.3.2.1 V_H1-69 and other germline derived broadly cross-reactive neutralizing antibodies

The main features of antibodies encoded by the V_H1-69 germline are a hydrophobic FR region and residues 53, 54 located at the tip of CDRH3 occupied by Isoleucine (I) and P, respectively (151, 152). Ten out of seventeen alleles of germline V_H1-69 encode P54 with the remaining seven encoding leucine (L) that leads to generation of weak or non-neutralizing antibodies, depicting the conservation level of critical residues (151). Antibodies produced from the V_H1-69 germline require only minimal affinity maturation, with an average of 14 amino acid changes in the heavy chain which mediates interaction with antigen (152). Importantly, V_H1-69 derived bnAbs can only bind antigen when expressed on the cell surface but not when in solution; suggesting the main antibody function to be recognition of antigen that triggers B-cell receptor stimulation and higher affinity antibody maturation rather than direct virus cycle blockage (152). However, only a fraction of individuals mount V_H1-69 germline antibodies, indicating not everyone can fully establish the ‘SOS immune response’.

Other commonly used germline genes in humans encoding bnAbs against influenza virus include V_H6-1 and V_H1-18. bnAbs generated by both these germlines, in contrast to V_H1-69 germline-generated immunoglobulin molecules, employ both V_H and V_L chains for antigen binding. However, similarly to previously described antibodies, the main contact is mediated by CDRH3. MEDI8851 is a representative V_H6-1 germline-derived antibody that has entered clinical trials for use against influenza virus (153). Activity of this antibody is mediated by ADCC as well as by antibody-dependent cellular phagocytosis (ADCP) and complement-dependent cellular cytotoxicity (CDC) (153). Superior cross-reactivity of MEDI8851 is achieved by recognition of epitopes within a hydrophobic pocket in HA2 (for group 1 viruses) as well as the fusion peptide (for group 2 viruses) (153). Overall, stem-binding bnAbs can neutralise virus and avoid escape mutant formation by targeting highly conserved residues but their activity often depends on effector functions.

1.2.3.3 Broadly cross-reactive non-neutralizing antibodies

Broadly cross-reactive non-neutralizing antibodies (non-NbAbs) have significantly lower affinity to the antigen compared to bnAbs but play an important role in induction of a protective inflammatory response. Current insights into the field suggests activity of non-NbAbs to be solely dependent on Fc-FcR interactions which can mediate complete protection against disease development (154). In addition, non-NbAbs display unique binding profiles as suggested by competition assays, as well as antigen exposure to low pH environments abrogating interaction with bnAbs but not non-NbAbs (155). During respiratory infections, like influenza, non-NbAbs have been shown to activate alveolar macrophages, natural killer cells or neutrophils that infiltrate lungs and cause an increase in cytokine and chemokine profiles (155). Subsequently, as a part of the immune response, enhanced cytokine levels trigger alveolar macrophages to shift into the phagocytic state (155). In addition, the protective profile and faster endogenous response is mediated by

the ability of non-NbAbs to form immune complexes (156). All in all, non-NAbs appear to have an improved ability to selectively recruit effector cells, which is particularly important for antigens that drive a poor humoral response.

Traditional vaccination approaches elicit very limited if any at all cross-reactive bnAbs and non-NbAbs due to the accessibility and immunodominance of epitopes located in the HA head that overwhelm the humoral immune response. Alternative strategies have been trialled including vaccination with a head-stem chimeric HA protein, headless HA or hyperglycosylated HA head with limited success up to date (157-160). A complete understanding of the mechanism of action of bnAbs will facilitate more stringent antibody selection for therapeutic purposes; however, non-NAbs able to provide durable protection are of equal importance and must also be considered when developing immunotherapeutics.

1.2.3.4 Therapeutic antibody delivery methods

Sustained antibody release at the target site is one of the major limitations for antibody therapeutics. For instance, systemic antibody administration is highly disadvantageous for respiratory diseases, with the mAb concentration in target organs, including the lungs, being 500 – 10 000 times less than that available in the systemic circulation (161, 162).

Several clinical trials have been started to test efficacy of intranasal and oral mAb administration (for example Foralumab), suggesting a shift towards less invasive, non-systemic administration methods (163, 164). Intranasal administration is particularly attractive due to an eliminated risk of fluid overload and reduced toxicity, as well as a lower anti-antibody response resulting from the lack of a systemically circulating foreign immunoglobulin molecule and constant exposure of the mucosa to foreign antigens (165, 166). Formulating mAbs into small particle aerosols can ensure substance bioavailability in the lungs; something particularly useful for treatment of

respiratory tract infections (165). Nevertheless, nasal administration might suffer from a short half-life due to the ciliary clearance of mucosal surfaces. thus requiring more frequent administration (167).

In addition, intranasal and oral drug delivery methods are also applicable when mass administration is required. For instance, farmed animals, such as poultry present in large numbers, can greatly benefit from approaches based on sprays or incorporation of therapeutics and vaccines into water or feed (168). Formulating mAbs or other therapeutics into the spray enables droplet size adjustment, allowing better control of the aerosol trajectory as well as ensuring an extended uptake period after spray sedimentation onto the animals' bodies due to natural behaviour (i.e. the tendency of birds to clean feathers). Furthermore, the therapeutic cargo can be formulated into liposomes, nanoparticles, microspheres, or dendrimers, allowing formation of the desired size of particles ranging from 10-1000 nm, to ensure sustained therapeutic agent release and increased exposure time as demonstrated with the scFv 3D8 antibody in chickens (167, 169, 170). Alternatively, mAb administration via feed can be achieved by the generation of transgenic plants. Feed containing pea flour made from transgenic peas expressing anti-Eimeria scFv antibody has been shown to be an efficacious and cost-effective therapeutic antibody delivery strategy in chickens (171). Although the latter strategy cannot ensure uniform coverage and an exact dosage that each animal receives, it can provide the required levels of protection for a vast number of individuals.

Gene expression *in situ* is yet another model gaining interest as an alternative route for therapeutic mAb administration. The approach is based on direct nucleic acid delivery into the host, ensuring continuous and sustained antibody expression. It overcomes the disadvantages of short serum half-life, high cost and supports the notion of targeted molecule delivery (172). This approach has been successfully tried in small rodents and human primates using adeno-

associated viral vectors, whilst herpes virus of turkeys (HVT), NDV, duck enteritis virus (DEV) and fowlpox (FP) virus are being evaluated as an alternative vectors for poultry and other livestock (173-179). Furthermore, non-viral vector nucleic acid delivery platforms, able to avoid long persistence and viral DNA integration, have been assessed, including lipid encapsulated nucleoside-modified mRNAs or DNA plasmids (180-185). Nucleic acid delivery without additional cargo seems as the most sensible approach, but the currently used electroporation technique requires immense improvements in order to be considered for scale up in animal models and humans.

1.3 Influenza viruses

Influenza A, B, C, D viruses together with Thogotovirus, Isavirus and Quaranjavirus are representatives of the Orthomyxoviridae family, causing infections in wide range of host species. Influenza A virus (IAV) is the only member of the family that is known to have led to several pandemics. IAV and influenza B virus still cause annual outbreaks in the human population during the cold season (186). In addition, several members of the IAV genus are extremely well adapted to domesticated animals, especially birds, resulting in endemic avian influenza virus (AIV) status in several countries around the world (187).

IAV subtypes are defined by the major antigenic determinants HA and neuraminidase (NA) expressed on the surface of the virion at an approximate ratio of 10:1 (188, 189). 16 HA and 9 NA types are known that can in theory exist in any combination (e.g. H1N1, H3N2, H7N9). H17, H18, N10 and N11 subtypes are unconventional and to date, have only been isolated from bat species (190, 191). However, not all combinations have been found in nature, suggesting that not every HA and NA match can result in viable and fit virus. The major reservoir of influenza A viruses is wild aquatic birds, where it infects and replicates in epithelial cells of the intestinal tract, facilitating spread of disease onto other species by the faecal-oral route (190, 192). Further

intraspecies spread is mostly dependent on aerosol transmission. Sustained IAV persistence in the human population is associated with, but not limited to H1N1, H2N2 and H3N2 subtypes with H1 and H3 viruses also endemic in swine. Three AIV subtypes circulating in poultry are H5, H7 and H9 viruses (190). IAV, especially H5 and H7 AIVs are further classified into low or high pathogenicity viruses (LPAI) and (HPAI) determined by HA susceptibility to cellular proteases; the difference arises by the insertion of a multi-basic cleavage site (for example PSIQSR/GLF vs PQRERRRKKR/GLF) into HA (193, 194). Although most H5 and H7 AIVs containing an HA polybasic cleavage site have an HPAIV phenotype in poultry, some retain a low pathogenicity profile and vice versa, showing that other markers affecting disease outcome also exist (195).

IAV is an enveloped virus that predominantly forms spherical particles (80-120nm in diameter) but filaments of several microns in length can also be encountered in clinical isolates (196, 197). Virus particles are shelled by a lipid bilayer derived from the host membrane with three proteins, HA, NA and the ion channel matrix 2 (M2) displayed on the surface of the virion (198). Matrix 1 (M1) protein is found underneath the membrane and is the most abundant viral protein (198). The centre of the virion is occupied by the polymerase complex and virus genome; the latter consisting of eight negative sense single stranded RNA segments encapsulated by nucleoprotein (NP) (199) (Figure 1.11).

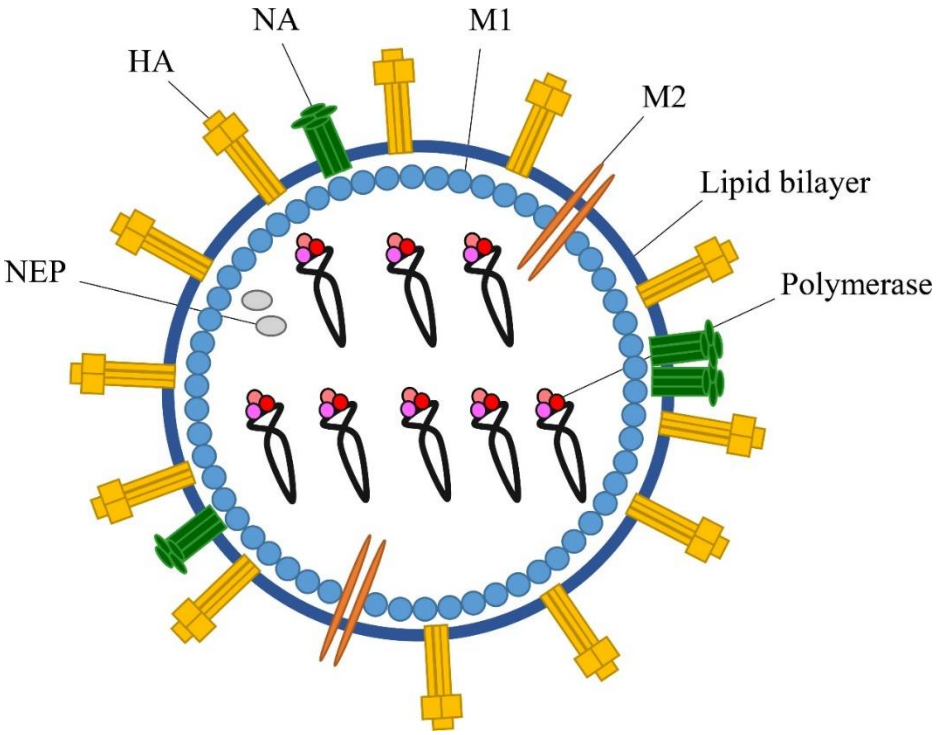

Figure 1.11. Schematic diagram of influenza A virus virion. A typical influenza A virus particle contains 8 RNA segments encapsidated by NP and forming panhandle like structure for polymerase complex association. On the surface of the virion HA and NA glycoproteins and M2 ion channel are displayed embedded within lipid bilayer derived from the host cell. M1 protein is based beneath lipid bilayer.

1.3.1 IAV genome and proteome

Eight RNA segments within IAV encode ten core proteins and a varying number of accessory proteins. The mechanism behind multiple protein production from a limited number of segments depends on translation from alternative reading frames (PB1-F2 or PA-X) and mRNA splicing (producing M1 and M2 or non-structural proteins 1 and 2 (NS1 and NS2) (200). In addition, each of the segments contain untranslated regions (UTR) at their 3' and 5' ends that serve to form panhandle-like structures that allow viral polymerase association (201). Furthermore, multiple segments serve as one of the ways to increase virus diversity via reassortment, which occurs upon co-infection of a single cell with two or more distinct viruses.

The first segment of ~2300 bases encodes the polymerase basic 2 (PB2) protein, responsible for transcription initiation. PB2 is associated with recognition of 5'-cap structures on host mRNA which are used for viral mRNA transcription (202, 203). An additional accessory protein PB2-S1 is also encoded by segment 1 but its significance remains unclear (204).

The second segment encodes gene for the polymerase basic 1 (PB1) protein, which carries RNA-dependent RNA polymerase (RdRp) function and is central to the virus ribonucleoprotein (vRNP) complex (203). The N-terminal region of PB1 is biased towards interaction with the polymerase acidic (PA) protein, whilst the C-terminal domain carries a propensity towards the PB2 protein (203). PB1 is responsible for elongation of primed nascent viral mRNAs (203). The non-essential proteins (PB1-F2 and PB1-N40), depending on viral strain are also encoded by segment 2, and are involved in altering viral virulence (205, 206).

PA protein is encoded by the third segment. PA carries endonuclease activity and is involved in the generation of capped primers recognized by PB2 (203). An accessory protein PA-X is also expressed after a ribosomal frameshift on segment three and is implicated in degradation of host mRNAs (207). PA-N155 and PA-N182 are translated from the 11^{th} and 13^{th} AUG codons respectively in the segment and are known to interact with an array of host proteins but their precise role during virus life cycle is to be determined (208).

The fourth segment encodes HA – a trimeric protein consisting of a globular head (HA1) containing the receptor binding site (RBS) and a stem (HA2). Overall, HA is the most antigenic viral protein (209). HA is involved in initial virus particle attachment to the cell and fusion with the host endosomal membrane (209). Although conserved residues and structure are retained within the HA2 domain, the remaining part of the protein is susceptible to rapid mutation, accounting for enormous structural plasticity. HA diversity is

represented by up to 9% sequence variation within a subtype and 20% - 74% divergence between subtypes, allowing partial escape from the humoral immune response and neutralizing antibodies (210).

Nucleoprotein (NP) is encoded by the fifth segment and serves in vRNA encapsidation with one subunit of NP required per 24 bases of vRNA (211). It is also thought to be involved in regulating the switch from mRNA synthesis to complementary (c) RNA and vRNA production (212). An elongated form of NP NP (eNP) can be generated if a mutation in the 5'-UTR occurs that introduces an upstream AUG codon, which can affect viral pathogenicity (213).

Segment six encodes the tetrameric glycoprotein NA, which forms patches and aggregates on the surface of virus particles (189). Like HA, NA also consists of a globular head and stalk. The enzymatic activity mediated by the NA head is involved in virus particle release from host cell receptors during newly formed virion release and spread (214). The length of the NA stalk is correlated with virus replication ability, possibly due to a reduced potential to cleave tethered substrates and penetrate through mucus barriers when the stalk domain is short (215). An accessory protein NA43 is thought to be a result of a ribosomal leaky scanning mechanism, but its function remains undefined (216).

Segment seven encodes the M1 and M2 proteins which play a role in virion structure and serve as a proton channel during uncoating, respectively (217). Part of the M2 protein protrudes from the surface of the virion, forming extracellular domain (M2e) (217). In addition, alternative splicing of segment 7 mRNA can produce an accessory protein M42 which can compensate for loss of M2 expression if required (218).

The last segment, number eight, encodes the so called non-structural proteins NS1 and NS2 (also known as NEP). NS1 protein plays a part in defence against the host immune response as an interferon antagonist, while NS2 has

a role in viral replication and nuclear vRNP transport (219, 220). A truncated version of NS1 can be generated - tNS1, which contributes to interferon regulatory factor 3 (IRF3) inhibition (221). In addition, a rare splicing event on segment eight can produce NS3, a protein derived from NS1 and lacking a larger than normal intron (222). NS3 might be involved in the process of adaptation to a new host (222).

1.3.2 IAV life cycle and species barrier

The influenza virus life cycle begins with HA attachment to host cells via sialic acid residues. The affinity ratio of HA for α2,6 relative to α2,3 sialylated glycan receptors define the receptor binding preference. Mammalian-tropic viruses have a tendency for receptors terminated with α2,6-linked sialic acids found in upper respiratory tract (URT) of humans and other mammals (223, 224). On the other hand, receptors terminated with α2,3-linked sialic acids are prevalent in the avian gut or deeply in mammalian lungs and are preferred by AIVs (223, 224). HA-binding preference is associated in part with hallmark sequence polymorphisms in the protein that identify avian-tropic viruses, including E190, Q226, G228, which reflect the different receptor conformations in the host; trans – avian, cis – mammalian known as ‘cone’ and ‘umbrella’ topologies, respectively (225-228).

Following initial attachment, virus particles are internalized by clathrin-dependent receptor-mediated endocytosis or macropinocytosis. Fusion of viral and endosomal membrane is the next step, mediated by low pH triggering a conformational change in HA (previously cleaved into HA1 (324aa) and HA2 (222aa) domains by trypsin- or furin-like proteases) that inserts the fusion domain into the endosomal membrane (209). The optimal environment for HA conformational change for mammalian tropic IAV ranges between pH 5.0 - 5.5 but is higher for avian viruses, especially HPAI (229-231). Therefore, even upon mildly acidic conditions, which can often be encountered outside of the host or outside of the host cell, AIVs are more likely to undergo irreversible

conformational changes causing an abortive viral life cycle. Contrarily, some HA molecules show extreme pH stability, resulting in virion progression into lysosomes where it gets gradually inactivated by proteases (209). A wide range of mutations, located in both HA1 and HA2 subunits, have been attributed to set HA stability in an acidic environment (232, 233).

As the pH drop triggers the conformational change within HA, the proton channel M2 also gets activated, leading to virus particle acidification which promotes vRNP dissociation and release into cytoplasm. NP and the whole polymerase complex translocate to the nucleus where primary mRNA transcription begins. Transcription of the vRNA template is mediated by the RdRp after 'cap-snatching' and priming by the PB2 and PA subunits, and continues until the 5' UTR is reached and a poly(A) tail is added, halting polymerase activity (203, 234, 235). Following nuclear export and translation of the viral mRNAs, the accumulation of several components including soluble fractions of NP and/or the RdRp, short vRNA transcripts and nucleotide levels promote a switch from mRNA to vRNA synthesis (212, 236). Production of vRNA is a primer-independent process but requires an intermediate cRNA template (vRNA → cRNA → vRNA) (237, 238). Once nascent vRNPs are assembled in the nucleus, a CRM1-NS2-M1-vRNP complex is formed mediating nuclear export with CRM1 being responsible for exportin activity and NS2 with M1 blocking re-entry (239).

The major limiting factor for AIVs entering a new host species is a polymerase requirement to overcome temperature differences within hosts, with avian virus polymerases accustomed to 41°C and mammalian ones to 33°C. Adaptations within the PB2 protein play a role in the initiation of the whole process, appearing to be more important than changes in other polymerase complex components. The identity of residues at PB2 positions 627, 271, 526, 590 and 591 as well as 701, 702 and 714 variously regulate binding to the viral nucleoprotein, evasion of the RIG-I pathway, alter the surface charge of PB2

or influence nuclear export have been proposed to be determinants of viral adaptation success (240-245). Most importantly of all, IAV polymerase must be compatible with host proteins as has been demonstrated with ANP32A, lack of which might prevent virus replication when crossing species barriers(246, 247). In addition, positions 85, 186 and 336 within PA can also increase AIV polymerase activity in human cells, while a PB1 signature position resides with residue 375 (248-250). Introduction of NP into a different virus background does not generally induce significant changes in viral replication capacity; however, NP phosphorylation patterns can act as a host range determinant to some extent (251). In addition, concurrent mutations in multiple polymerase subunits (i.e. PB2-E627K and PB1-H99Y) can further enhance replicase enzyme activity (252).

Finally, new virion assembly and release follows. Upon translation surface glycoproteins (HA and NA) and matrix 2 protein are shuttled through the Golgi apparatus onto the cell surface sending a signal for the remaining protein and vRNP recruitment (253). Packaging signals carried by each segment ensure genome integration into the virion; however, due to imprecision in the packaging mechanism it is postulated that some of the virions remain defective due to an incorrectly packaged genome. Virion budding is highly co-dependent on the ability of M2 to induce membrane curvature and scission (254, 255). This process can also lead to virus like particle (VLP) production when initiated by HA (253). Nevertheless, exclusively spherical VLPs suggest the mechanism of infectious virus formation, able to produce filaments, might be different (253). At last, NA serves to cleave sialic acids on the cell surface, allowing virion release (253, 256). The final virus maturation is designated by cleavage of HA0 into HA1 and HA2 taking place extracellularly in LPAI and intracellularly for HPAI viruses.

An NA role in host adaptation (especially for viruses jumping from wild birds into chickens) often results from deletions within the NA stalk coinciding with

the evolution of reduced HA affinity for cellular receptors (257-261). The non-structural and matrix proteins seem to have a minimal role in host range determination; however, M16I in NS2 of the H5N1 virus has been shown to increase adaptation to mammalian cells by allowing vRNA amplification (262). Understanding the mechanisms behind the virus life cycle and host range can allow virus evolution prediction if species barriers are crossed.

1.3.3 IAV evolution

The two major mechanisms of antigenic drift and shift drive IAV evolution, with the latter in particular contributing to zoonotic virus potential and both playing a role in the virus' ability to readily adapt to and avoid the host immune response. Antigenic drift results from small changes in the influenza virus genome that are generated by the error prone RdRp activity in conjunction with selective pressure (263). Two types of mutations can be selected for under immune pressure; changing the overall virus antigenicity or impacting only certain antigenic subregions. The first route leads to the acquisition of mutations introducing positively charged residues across HA at the same time as enhancing avidity towards negatively charged cellular receptors (264). Such mutations are also known as adsorptive amino acid substitutions that can decrease neutralizing efficacy of the whole serum (265, 266). However, inoculation of escape viruses, formed by this mechanism, into naïve animals promotes the re-emergence of new mutants with lower receptor binding preference, illustrating exceptional virus plasticity. Another type of mutation leading to antigenic drift are ones focused towards mAb escape virus formation via point mutations (267). This latter route introduces antigenic changes more gradually and requires longer times to bypass whole antiserum response.

On the other hand, antigenic shift represents a major change to the virus genome that occur after a single cell becomes infected with at least two strains of viruses which can swap their segments during replication (268). Such big changes often lead to emergence of new viruses with pandemic potential as

illustrated by 2009/H1N1 (combination of swine, avian, and human influenza virus genes) (269, 270). Nevertheless, in some cases detection of such major changes is less obvious and might require sophisticated sequence analysis. Only maximum likelihood tree generation from more than 3000 H1N1 sequences indicated the possible emergence of a new virus clade in Iran carrying an HA1 identical to the one which circulated in the 1930s and an HA2 closely associated with 2009 pandemic virus (271). Alternatively, it is possible that the apparent recombination event is a laboratory artefact rather than a real world event. Overall, understanding of virus evolution is crucial for development of effective control measures for influenza virus.

1.3.4 H9N2 viruses

Amongst other influenza virus subtypes, the major H9N2 clade of AIVs does not cause typical HPAI; it therefore, often remains unappreciated as an important pathogen. Although H9 viruses do not contain a polybasic cleavage site in their HAs and, therefore, do not cause classical HPAI, some of the H9N2 HAs possess di- or tri- basic cleavage sites (272). Additional residues allow HA cleavage by unconventional proteases (i.e. matriptase) but is not sufficient for the initiation of systemic infection (272). H9N2 infection can result in loss of egg production and high levels of morbidity and mortality, associated with mucus build-up leading to severe respiratory disease or increased susceptibility for secondary infections (273, 274). Although, a limited number of human infection cases have been recorded throughout the years, poultry workers from various parts of the world are known to carry H9N2-specific antibodies (275, 276).

The first recorded case of H9N2 virus in poultry in China was in the 1960s, with the disease becoming widespread throughout the country by the late 1990s (277, 278). Currently, virus is enzootic in parts of Asia, the Middle East, and Africa. Historically, H9 viruses can be divided into several sublineages including American and Eurasian lineages. Ty/Wisconsin/1/66 is the main

representative of the North American viruses while the Eurasian lineage is divided into further three groups: G1, Y439 and G9, represented by Qa/HK/G1/97 and Dk/HK/Y439/97 for G1 and Y439 viruses, respectively (279). Three prototype viruses represent the G9 lineage, including Ck/HK/G9/97 (G9-like), Dk/HK/Y280/97 (Y280-like) and Ck/BJ/1/94 (BJ94-like) (279). In addition, the lineages of internal genes for all of the viruses contain even greater diversity, suggesting frequent reassortment events (280, 281).

An important H9N2 virus characteristic is a proven record of its ability to donate and acquire new genes during reassortment events. For instance, the internal genes in the H7N9 and H10N8 viruses that emerged in China during 2013 were found to originate from an H9N2 virus (282). This indicates an enhanced potential to contribute to new virus strain generation during reassortment that can cause difficult-to-control disease.

1.3.5 Influenza virus control

1.3.5.1 Vaccination

Three main strategies of vaccination against AIV exist, with routine vaccination employed in countries with an enzootic situation (China, Israel, Egypt, Iran, Pakistan), preventative immunizations applied upon discovery of a probable risk and emergency vaccinations taking place after an outbreak has started (283-287). Most of the currently used vaccines for AIV contain inactivated, oil adjuvanted whole virus. Antigen propagation in eggs or cell culture followed by inactivation by formaldehyde makes the manufacturing step relatively easy (288). Nevertheless, administration of such vaccines requires IM or SC injections, making the process laborious. In addition, current vaccines do not provide the capacity for the differentiation between infected and vaccinated

animals (DIVA). Viral vectored vaccines carrying HA antigen are another form of vaccine that have been licensed in several countries. Administration of such vaccines can be automated; however, it often comes with the requirement of a cold chain supply. Stringent vaccination policies are followed for HPAI, however, only a few countries follow routine vaccination protocols for LPAI. In addition, broiler chickens with a lifespan of 5-7 weeks barely have enough time to build-up immunity and overcome a mandatory withdrawal time after vaccination before slaughter; therefore, these birds are often left without any protection. Importantly, H9N2 vaccines are not regularly assessed against drifted viruses, contributing to a lack of vaccination efficacy.

The aim of achieving more broadly cross-reactive protection against AIV after immunization has led to the development and evaluation of novel vaccination approaches. Multiple strategies are being tested for immune response refocusing towards conserved parts of HA antigen. These include vaccination with heterologous strain viruses, removal of glycan masking on the HA head and computational optimisation of broadly reactive antigens (COBRA), with several strategies inducing protective immunity against subsequent virus challenge (157-160). Nevertheless, some evidence from porcine models suggests that vaccines inducing immunity against the HA stalk and M2e antigens can lead to enhancement of disease pathology (289). On the other hand, vaccination with VLPs in the presence of certain cargos can increase immune response efficacy. For instance, chemokines like CCL28 prompt antibody secreting cell migration to the mucosal tissues, ensuring prolonged circulation of high levels of IgA antibodies (290). Alternatively, delivery of antigens to antigen-presenting cells or vaccination with immune complexes can induce a heightened immune response. An example of the latter includes HA complexation with antibodies containing sialylated Fc regions that alter the threshold of BCR affinity and, therefore, replace lower affinity complexes (156). The notion of immune-complex vaccine improvement of the humoral response has also been supported by *in silico* modelling (291). Advancements in

understanding the generation of an immune response upon vaccination, the importance of Fc-FcR interactions and recognition of conserved epitopes leads to the design of not only improved vaccines but also other therapeutics that can provide more universal protection.

1.3.5.2 Antivirals and defective interfering genes

Three families of antiviral drugs against IAV are (or have been) approved for use in humans, but with none accepted for utilization against AIV in farmed animals. However, lack of effective control measures against AIV prevalence in poultry leads to misuse of widely accessible drugs, limiting their therapeutic potential (292-294). The first drug family are derivatives of adamantanes with representatives rimantadine and amantadine targeting the M2 mediated ion channel activity and interfering with vRNP entry into cytoplasm (295). Importantly, multiple virus strains resistant to this class of drugs have been found, making adamantanes irredeemable for therapeutic use (296, 297). The second family are neuraminidase inhibitors (NAIs) including oseltamivir, zanamivir, laninamivir and peramivir, all aiming to interfere with nascent virion release from infected cells (298-301). The most recent viral polymerase inhibitors undergoing clinical trials or approved only in certain countries (pimodivir, favipiravir and baloxavir acid) modulate viral RNA synthesis. For example, Pimodivir is a non-nucleoside influenza virus PB2 inhibitor while T-705 acts a nucleotide analogue terminating viral replication (302, 303). Other antivirals being evaluated target host rather than viral proteins. DAS-181-F03/F04 has sialidase activity which can interfere with virus attachment to the cells while Nitazoxanide produces active metabolites following deacetylation which can inhibit HA maturation (304, 305). Alternative compounds tested for antiviral activity include short-hairpin RNAs mimicking the conserved 3’- and 5’- terminal sequences of virus genome that act as a binding site for the viral polymerase (306, 307). Similarly, defective interfering genes (DIG-3) can result in the formation of defective interfering virions (DIV) leading to abortive infection (308). Constant virus evolution and inappropriate use of drugs drives

rapid resistance to many of the currently available measures, showing a regular need for a new class of antivirals or new therapeutic approaches.

1.3.5.3 Antibody therapeutics

The main goals of passive immunotherapy, just like vaccination, include protection against disease development and mortality, a decreased duration of viral infection and amount of virus shed into the environment, and an increase in the virus dose required to successfully enable infection. The ability to retrieve mAbs carrying explicit specificity for the desired HA antigens via *in vitro* display technologies (see subsection 1.5.1.2.) and then discovery of broadly cross-reactive antibodies has had a major impact in re-evaluating immunotherapeutic antibodies as a means to control infectious diseases.

The majority of the mAbs considered for passive immunization are ones targeting the most antigenic part of the protein - HA1 - and that are able to neutralize virus by interference with its binding to cellular receptors. Antibodies against the HA head domain are of particularly high specificity but limited cross reactivity. Mab 62 is one of the antibodies targeting HA1 which was tested as a therapeutic immunoglobulin and demonstrated efficacy in reducing virus load and morbidity symptoms in mice (309). mAbs targeting conserved residues within the HA head are relatively rare, but examples of H3v-47, D1-8, 9F4 and others indicate that such immunoglobulins with broad antigen reactivity and neutralization potential do exist (310-312). On the other hand, antibodies displaying particularly high cross reactivity usually target the HA2 domain and can hinder virus fusion with the endosomal membrane. An important feature of broadly cross-reactive antibodies is the ability to mediate protection via Fc-FcR interactions, but limited accessibility to the antigen results in relatively low levels of broadly cross-reactive antibodies arising post vaccination or natural infection (see subsections 1.5.3.2. and 1.5.3.3.) The second most immunogenic IAV protein – NA - also elicits a range of neutralizing antibodies that can be used for passive immunization. For example, 3c10-3 binding near

the NA active site and likely reducing new virion egress has shown protective potential in mice (166, 313). 1G04, 1E01, and 1G01 are also NA-targeting broadly protective antibodies capable of protecting against virus challenge, by direct inhibition of NA activity as well as via effector functions displayed by Fc-FcR interactions (314). The third most immunogenic IAV protein eliciting an antibody response is the M2 protein. Bivalent immunoglobulins binding to this protein can alter the orientation or mobility of the cytoplasmic amphipathic alpha helix and interfere with virus filament formation; however, the major antiviral mechanism *in vivo* is driven by Fc-FcR interactions (315). In addition, nonNAbs against anti-M2e can shift alveolar macrophages to become phagocytic cells or induce ADCC and cytokine secretion via NK cells (316, 317). Anti-M2e antibodies (TCN-032) have also been demonstrated to play a protective role in human infections (318). Whether mAbs against internal influenza proteins (NP, M1 and others) can provide protection remains elusive, with evidence present on both sides, but more studies are required to draw a definite conclusion (319, 320).

Importantly not all the antibodies considered for therapeutic purposes against viral diseases are those targeting viral proteins. One such example is the nucleic acid-hydrolyzing antibody 3D8 (321-323). Formulated into an scFv fragment, 3D8 retained its activity to cleave the viral genome and/or transcripts within the cytosol (114). In addition, when scFv 3D8 was introduced into a transgenic chicken line, directly infected animals were not able to efficiently transmit a challenge H9N2 virus onto contact birds (114). Such an approach represents a built-in resistance concept and is yet another way of how antibodies and their fragments could successfully reduce disease burden.

Nevertheless, current control measures available for AIV are not sufficient to protect poultry and farmers from the disease, and the global economy from constant financial losses. Therefore, there is a real need for i) evaluation of the ability of neutralizing antibody fragments to fight AIV, ii) assessment whether

neutralizing antibody fragments can serve as a therapeutic approach for poultry and iii) determination of efficacy of viral vectored mediated expression of antibody fragments.

Chapter 2 CAN ENGINEERED ANTIBODIES RETAIN FUNCTION OF MONOCLONAL ANTIBODIES PRODUCED FROM HYBRIDOMAS?

Natural immunity components including antibodies raised during infection or vaccination have been attracting attention as a therapeutic means for chronic and infectious disease control (324-326). Antibodies able to prevent the influenza virus life cycle have also been explored and multiple studies have been performed to test their efficacy in animal models and even human populations (142, 327-329). However, limited information is available on the neutralizing antibody potency, when used in therapeutic context against avian influenza virus circulating in birds. Multiple approaches exist for antigen specific antibody gene sequence retrieval from infected/vaccinated donors (described in more detail in Chapter 1, section 1.4). Sequence information is crucial for the ability to produce recombinant antibodies in large scale which then can be used for further characterisation including but not limited to affinity, avidity, and activity parameters. In – depth analysis enables selection of most potent neutralizers that can be considered for therapeutic purposes.

Previous work has generated mouse hybridomas providing a panel of monoclonal antibodies against UDL-1/08 HA from which six antibodies with virus neutralizing activity were chosen for this study. (330). In this study variable domain sequences for selected antibodies were obtained and antibody diversity was explored assigning mature antibodies to their germline genes and assessing degree of divergence. It was found that specific substitutions and codons targeted differed between germlines. Following sequence analysis, recombinant antibodies were generated and their ability to bind and to inhibit growth of homologous and heterologous H9N2 viruses was tested. This work has shown that at least three out of six recombinant

antibodies when converted to different formats, including scFv, retain their binding affinity towards homologous and heterologous HA protein and could effectively neutralize live virus *in vitro*. Lack of Fc region did not abolish functional antibody activity suggesting virus neutralization being mediated by direct antibody-antigen interaction during early infection stages.

2.1 Introduction

2.1.1. Influenza virus specific antibodies

Avian influenza virus persists as a threat to the global poultry industry and worldwide economy. In addition, it carries a zoonotic risk for human population. Current AIV control measures do not provide sterile immunity and in case of epizootic pandemic 'stamping out' of entire farms is required to avoid further virus spread. Recent years has brought attention to antibody therapeutics as an alternative virus control measure. It is widely accepted that most of the functionally important antibodies elicited after exposure to influenza virus either by natural infection or vaccination target the major virus surface glycoprotein HA. Anti-HA antibodies with virus neutralization activity can be divided into three major sub-groups including: i) antibodies that bind to the HA head and are subtype and class specific, ii) antibodies that bind to the HA head and are cross-reactive amongst homologous viruses of the same subtype and iii) antibodies that bind to the HA stem and are broadly cross-neutralizing (331-334). Such antibodies can prevent virus infection by direct interference of virus attachment to the host cell via hindering virus interactions with sialic acid, or by blocking structural HA changes needed to mediate viral-cell fusion (142, 335, 336). In addition, non-neutralizing antibodies exist which activity is associated Fc-FcR interactions and downstream effector functions (154). Several monoclonal antibodies targeting IAV HA have been characterised and trialled for therapeutic use in humans (142, 337), however, studies suggesting

therapeutic antibody potency against AIV in avian hosts, especially endemic H9N2 strains are lacking.

2.1.2. Antibody maturation contributes to antigen recognition

Antibody maturation is a crucial determinant of immunoglobulin specificity, affinity, and avidity towards antigen. The whole process relies on changes within V(D)J gene segments encoding variable regions of the B-cell receptor (BCR) described in more detail in Chapter 1, section 1.3 (41, 42). Initial combination of V(D)J segments dictates antibody germline which affinity matures after a series of events resulting from V(D)J recombination and somatic hypermutation (42, 44). This leads to formation of distinct antibody lineages and later class switching to memory or plasma cells. It has been demonstrated that B-cells that have been in circulation for long periods of time experience a higher degree of somatic hypermutation that result in greater affinity maturation (338, 339). Such mutations play an important role in determining the tertiary structures of CDR loops that are involved in fine tuning of antibody affinity towards the antigen. Due to high level of diversity the CDR3 of the immunoglobulin heavy chain has been shown to be one of the main (340) mediators of interaction with antigen in many antibodies; such specificity is also generated during affinity maturation as whole CDR3 derives from the V(D)J junctional region which is one of the main contributors to repertoire generation (341). Furthermore, antibody diversity is greatly enhanced by a range of precursor genes present for each V, D, J segment, with the mouse IgH locus containing 100s of $V_{Hs,}$ 13 D_{Hs} and 4 J_{Hs} followed by C_H exons, while IgL can be made by any one of 100s of $V_{\kappa s}$, 5 $J_{\kappa s}$ and additional $V_{\lambda s}$ exons followed by C_L, allowing more than 10^{13} BCR combinations (Chapter 1, Figure 1.5) (342). A general tendency for more profound IgHV1-69, IgHV3-30, IgHV6-1 germ-line lineage involvement in generation of HA-stem broadly cross-neutralizing antibodies from human population has been observed (152, 153,

334, 343). However, analysis and antibodies available are insufficient to draw comparative conclusions for mice generated antibodies.

2.1.3. Antibody format contribution to its function

Antibody class and recombinant antibody format (described in more detail in Chapter 1 sections 1.2. and 1.4.2, respectively) is a significant contributor to overall antibody function and protection against disease. Three main antibody classes or isotypes induced after infection or vaccination with viral antigens are IgM, IgA and IgG in both humans and mice. IgM antibodies generally appear as the first class of immunoglobulins entering systemic circulation in high levels and have high potency due to their pentameric structure (36). IgAs are typically found in mucosal tissues whilst IgGs are circulating systemically and are further classified into subclasses (IgG1, IgG2, IgG3, IgG4 in humans and IgG1, IgG2a, IgG2b, IgG2c, IgG3 in mice) (32, 35). The Fc region that determines the isotype of antibodies also regulates preference for activating or inhibitory FcRs which play crucial roles in downstream effects, including the induction of ADCC, ADCP and CDC functions. The most potent isotypes for activating Fc-domain dependent functions are IgG1 and IgG2a, for human and mouse, respectively, whilst human IgG4 and mouse IgG1 are poor inducers of effector functions and therefore are less preferable in a therapeutic context (344, 345).

Multiple factors such as a form of an antigen (purified protein vs whole virus), delivery routes, adjuvants, previous infections can contribute to the antibody class induced and prevailing in circulation. For instance, in mice IgG2a has been shown to be the main antibody subclass and isotype found upon exposure to virus, followed by moderate levels of IgG2b and low levels of IgG1 and IgG3 (346-348). Alternatively, immunization with purified protein preparations can induce high levels of IgG1 but not IgG2a, IgG2b or IgG3 (348). Such antibody class distribution remains unchanged if secondary

exposure is to the same antigen delivered in the same format, however, it can change if prime and boost forms differ (348). In addition, different parts of an antigen can also drive differences in antibody response, as demonstrated with whole HA antigen inducing IgG1, IgG2 and IgG3 antibodies but only IgG1 and IgG3 responding to the HA stalk in humans (349).

Recombinant antibodies are often made to tailor effector functions depending on the species of interest or an end-goal of antibody to be used. For example, removal of the Fc part might be beneficial if antibodies are to be used in different species, or if antibody function is mainly mediated by variable domains. The smallest format of an antibody that retains epitope-binding activity is scFv, which offers easier production due to the small size or allows generation of new antibody formats, exploiting combination of multiple antibody (91, 92) domains to generate ‘polyclonal’ molecules targeting multiple antigens and epitopes.

2.1.1. Chapter objectives

- Antibody sequence analysis and identification of potential residues involved in antigen recognition.
- Generation of recombinant antibodies from sequences derived from hybridomas in mouse IgG1, mouse IgG2a and scFv formats
- Characterisation and comparison of the ability of recombinant antibodies in various formats to bind to antigen
- Evaluation of recombinant antibody ability to neutralize homologous and heterologous H9N2 viruses

2.2. Results

2.2.1. Bioinformatic analysis of monoclonal antibody variable domain sequences and representative influenza viruses

2.1.1.1 Analysis of monoclonal antibodies CDR domains reveals variation in antibody germline repertoire

Monoclonal antibodies used in this study (ID2, JF7, EC12, HA9, CG12, JF8) were isolated from mouse hybridomas, checked for their specificity for H9N2 UDL-1/08 virus and their variable domains were sequenced as discussed in section 6.2.1.1. Sequences retrieved were used for further analysis of CDR domains and assignment of allelic germlines for each heavy and light chain of all antibodies, using the publicly available NCBI IgBLAST tool (350). All sequences were numbered using ImMunoGeneTics (IMGT) numbering system.

Analysis of the heavy chains of chosen antibodies revealed the majority of diversifications occurring in the framework or CDRH3 region (Table 2.1.)

Table 2.1 CDRH amino acid sequence analysis. All antibody sequences were analysed using NCBI IgBLAST tool. IMGT numbering was used to locate each of CDRs and to predict IGHV germline.

ANTIBODY	VH GERMLINE	VH CDR1	VH CDR2	VH CDR3
ID2	1-39	GYSFTDHN	INPNYGTT	ARDYGSAMDY
JF7	1-53	GNTFTSYW	INPSNGGI	EETNDYDGFYYGMDY
EC12	5-16	GFTFSDYY	INYDGSNT	DHWGFDY
HA9	5-16	GFTFSDYY	INYDGSST	TRDHWGFDY
CG12	5-16	GFTFSDYY	INYDGSST	TRDHWGFDY
JF8	1-39	GYSFNDYN	INPNYGTT	AGGGYYGNSFDFW

Out of six antibodies, three (EC12, HA9 and CG12) were found to carry identical CDRH1 and CDRH2 regions with only two amino acid differences; additional Thr and Arg residues, present in the CDRH3 domain of HA9 and CG12 antibodies but absent in CDRH3 of EC12. The CDRH2 sequences of ID2 and JF8 antibodies were also found to be identical. In general, all CDRH1s and CDRH2s were constituted of eight amino acids, while CDRH3s ranged between 7 to 15 amino acids in length. JF7 had the longest CDRH3 region belonging to the IGHV1-53 germline, constituted of 15 residues. The IGHV1-39 germline was assigned to ID2 and JF8, with the remaining three antibodies belonging to IGHV5-16 germline.

Similarly, light chain CDRL regions were analysed, revealing antibodies falling into four different germlines for their IGKL chains (Table 2.2.). Generally, CDRL1s for all the antibodies (apart HA9) were found to be composed of six amino acids, CDRL2s made of three amino acids and CDRL3s of nine amino acids. EC12, HA9 and CG12 antibodies were found to belong to the same IGKL10-94 germline, informing on overall similarity for three antibodies. Interestingly, HA9 was identified to have only partial framework 1 and CDRL1 regions, but was otherwise identical to EC12 and CG12 in CDRL2, and EC12 in CDRL3 sequences. CG12 differed from the remaining two antibodies by a single amino acid substitution (Lys to Met) in its CDRL3 domain. The other three antibodies, ID2, JF7 and JF8, were determined to belong to IGKV12-41, IGKV6-20, and IGHV6-c germlines respectively, with minimal differences present in all three CDRLs.

Table 2.2 CDRL amino acid sequence analysis. All antibody sequences were analysed using NCBI IgBLAST tool. IMGT numbering was used to locate each of CDRs and to predict IGKV germline.

ANTIBODY	VL GERMLINE	VL CDR1	VL CDR2	VL CDR3
ID2	12-41	GNIHNY	HAK	LHYYSTPWT
JF7	6-20	ENVGTY	GAS	GQSYSYPYT
EC12	10-94	QDINNY	FTS	QQYSKRPPT
HA9	10-94	-	FTS	QQYSKRPPT
CG12	10-94	QDINNY	FTS	QQYSMRPPT
JF8	6-c	QSVSNE	YAS	QQHYSSPFT

In addition, some observations were made on general composition and amino acid prevalence in the antibody complementarity determining sequences. These included a noticeable preference for Gly and Ser residues, which constituted ≥ 13% of variable domain sequences. The next most common residues included Thr, Tyr, Leu and Lys, ranging from 5% to 9% amongst which Thr was the most ubiquitous residue (7% - 9%) in all sequences. Amino acids present at ≤ 2% incidence in all six antibodies included His, Cys, Met and Trp. Interestingly, antibodies derived from the IGHV5-16 germline had a higher overall preference for Leu, but a lower percentage of Val residues. To further assess if the same profiles were retained for heavy and light chains separately, additional analyses were performed. The light chains showed a similar pattern to overall antibody sequence, with only a slight increase in Ile incidence (≥ 6% vs ≤ 5%) in IGKL10-94 germline antibodies. Heavy chain analyses revealed a higher usage of Gln residues (≥ 6%) in all antibodies except HA9 (2%), as well as Val (≥ 5%) again except for HA9 (2%), and Ala (≥ 5%) in all antibodies. A preference for Leu and Asp was also observed in IGHV5-16 germline derived antibodies.

Overall, CDR sequence analysis informs that three antibodies (EC12, HA9, CG12) used in this study are derived from the same germline gene subgroups

for both variable chains, two of the antibodies (ID2, JF8) share the same germline for heavy but not light chain and one antibody (JF7) is unique in its heavy and light chain germline. In addition, a preference for specific amino acids in the variable regions of the antibody genes was found, as illustrated by a high incidence of Gly and Ser but low occurrence of His or Cys residues. Furthermore, analysis revealed some commonalities amongst antibodies derived from the same germlines; however, to confirm this, larger datasets should be analysed.

2.1.1.2 Antibody diversification from germline occurs in both framework and complementarity determining regions

To assess the degree of antibody diversification and somatic hypermutations, germline and mature antibody variable domain sequences were compared. The IMGT database was used for germline sequence retrieval and MEGA7 for subsequent alignment with corresponding antibodies, prior to sequence logo creation. Diversifications varied for each of the antibodies with mutations occurring in both framework and complementarity determining regions. Only three amino acid differences from IGHV1-53 germline were found in JF7 VH sequence, randomly distributed across the CDRH1, CDRH2 and FR3 regions, positions 27, 58 and 84 (Figure2.1a). With regards to IGHV5-16 and respective antibodies belonging to this germline different substitutions were distributed across FR and CDRH regions with the least changes observed in the EC12 antibody, which had only two substitutions in the FR2 and CDRH2 regions at positions 8 and 50, respectively (Figure2.1b). On the other hand, both HA9 and CG12 had six substitutions, three of which were found to reside in the FR3 region (at positions 59, 75 and 89 for CG12, positions 74, 84 and 95 for HA9). Further two substitutions were found in FR2 region for CG12 (positions 48 and 50), one of which corresponded with that located in EC12 (position 50; Asn to Thr). Position 50 was also found to be mutated in the HA9 sequence (Asn to

Ser). In addition, CG12 and HA9 were carrying an extra substitution (Ala to Thr) at the very beginning of CDRH3 (position 97). The HA9 antibody had an additional change in the FR1 region (position 16). Four substitutions were found in antibodies ID2 and JF8 when compared to germline sequences (Figure2.1c). Three out of four changes were located across framework regions for both antibodies, and one was attributed to CDRH1 at differential positions. This resulted in a 2-6% frequency of substitutions for variable heavy chains.

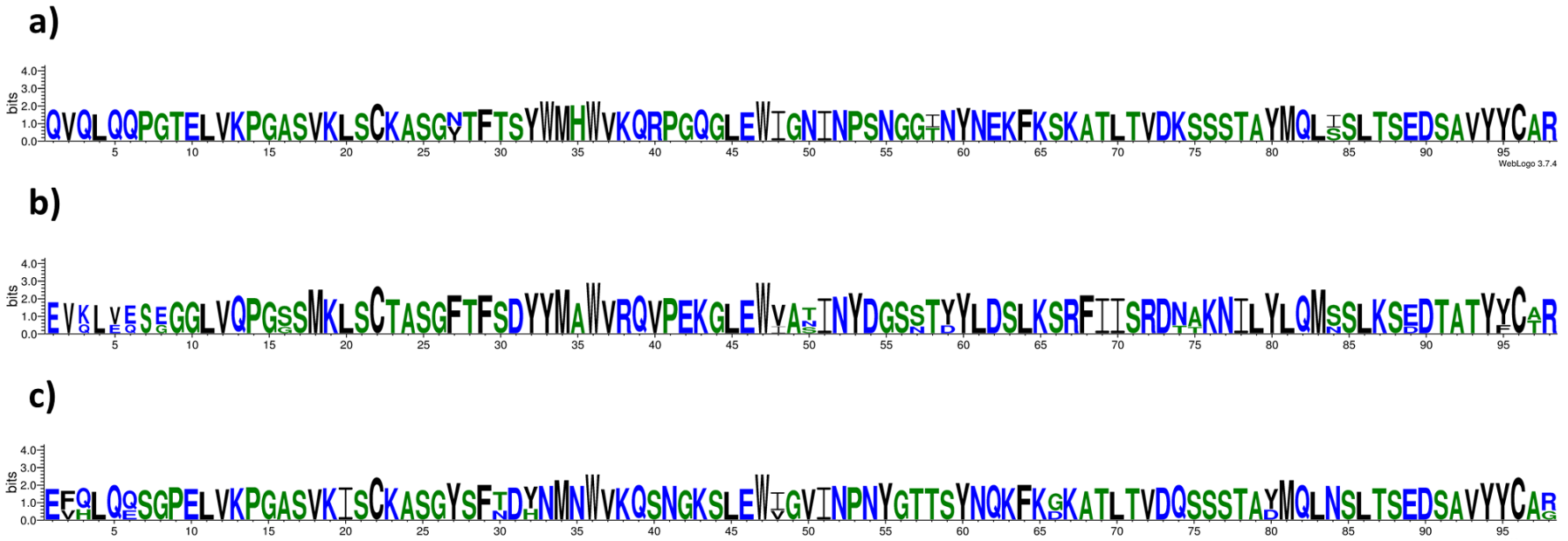

Figure 2.1. Comparison of germline and H9N2 specific antibody variable heavy sequences. Germline sequences were retrieved from the IMGT website and aligned with variable heavy domains of antibodies belonging to respective germlines **a)** IGHV1-53 and VH of JF7; **b)** IGHV5-16 and VH of EC12, HA9, CG12; **c)** IGHV1-39 and VH of ID2 and JF8. Logo plots were generated using the WebLogo online application. Amino acids were coloured depending on hydrophobicity. Only the first two amino acids of CDRH3 (Ala, Arg) were included in the analysis due to heterogeneity in CDRH3 lengths.

Nevertheless, IGKV chains were found to contain more substitutions ranging between 2 to 11% with the least mutations found in JF7 which had only two amino acid changes at FR2 and FR3 regions (positions 34 and 74, respectively) (Figure 2.2.b). IGKV of ID2 was found to have four amino acid differences distributed in FR2, CDRL2 and FR3 regions while JF8 had five substitutions across FR1 and FR3 regions (Figure 2.2.a and Figure 2.2.b). HA9 IGKV was exceptional amongst the antibodies as it had a completely abrogated CDR1 domain with truncated FR1 and FR2 regions, also carrying a single substitution in each of them. In addition, HA9 had a Tyr to Phe substitution at CDRL2 (position 50), Ser to Arg in FR3 (position 53) as well as Lys to Arg and Val to Pro substitutions at the base of CDRL3 (positions 94 and 96) (Figure 2.2.c). The aforementioned mutations in CDRL2, FR3 and CDRL3 regions (positions 50, 53, 94 and 96) were carried by all three antibodies encoded by the IGKL10-94 germline (Figure 2.2.c). Additional substitutions in EC12 included mutations in FR1 and FR2 regions (positions 1 and 43, respectively). Amongst the three IGKL10-94 antibodies, CG12 was the most diversified with a total of eleven amino acid changes. Overall, out of all six antibodies analysed most of the mutations were found to have arisen in framework regions for both heavy and light chains, in 75% and 60% of cases, respectively, with higher number of mutations harboured in light chains.

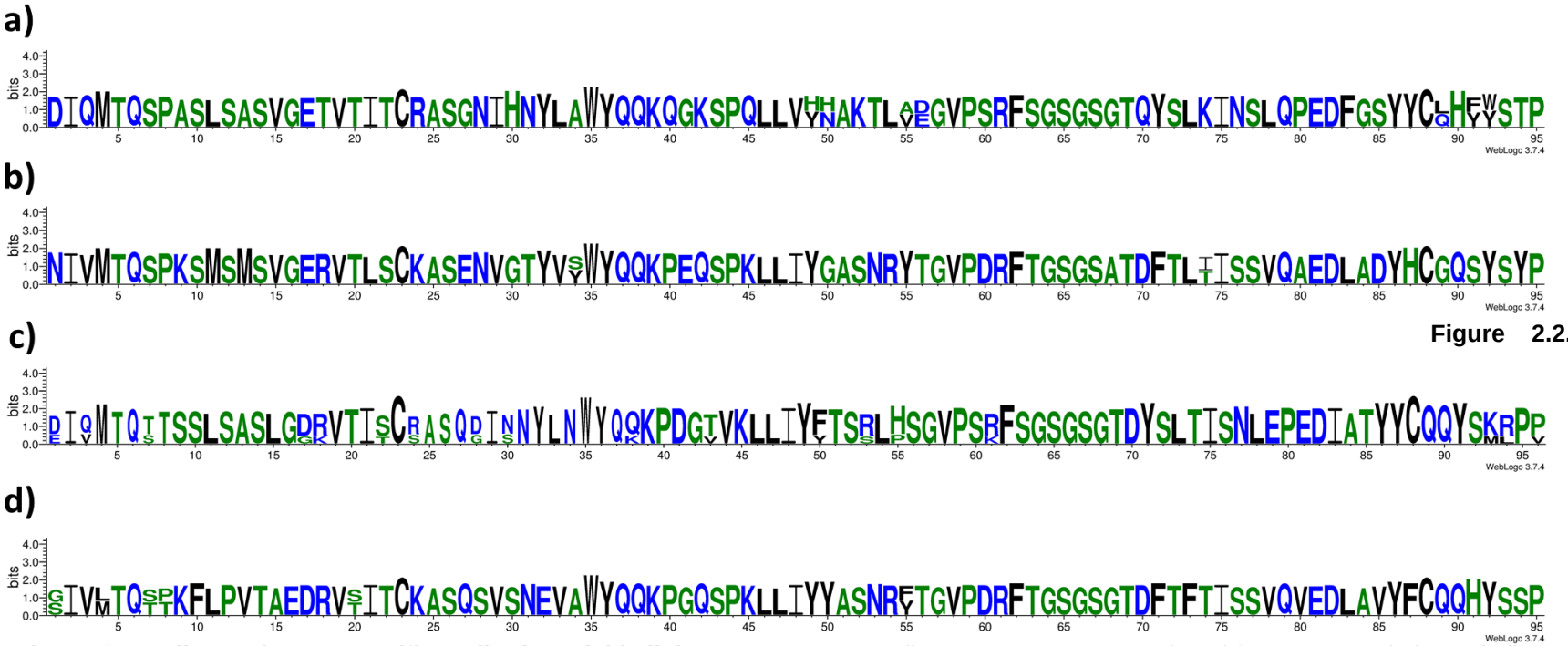

Figure 2.2. **Comparison of germline and H9N2 specific antibody variable light sequences.** Germline sequences were retrieved from IMGT website and aligned with variable light domains of antibodies belonging to respective germlines **a)** IGKV12-41 and VL of ID2; **b)** IGKV6-20 and VL of JF7 **c)** IGKV10-94 and VL of EC12, HA9, CG12 **d)** IGHV6-c and VL of JF8. Logo plots were generated using WebLogo online application. Amino acids were coloured depending on hydrophobicity. Only first seven amino acids of CDRH3 starting at position 89 were included into analysis due to heterogeneity in CDRH3 lengths.

To further analyse the evolutionary relationship of the six antibodies, a phylogenetic tree was generated using their variable region sequences (Figure 2.3). This confirmed that the antibodies fell into two main clusters; one made up of HA9, EC12 and CG12 and another of remaining three antibodies (JF7, JF8, ID2).

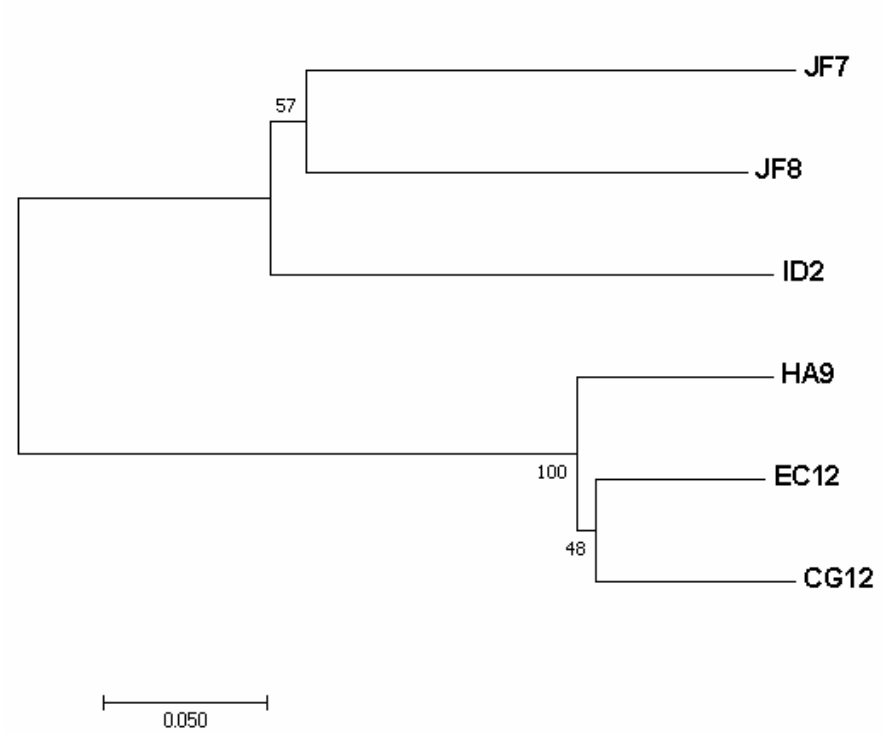

Figure 2.3. Evolutionary relationship of single chain variable fragment antibodies used in this study. The evolutionary history was inferred using the Neighbor-Joining method (351). The optimal tree with a sum of branch length = 0.87387387 is shown. The percentage of replicate trees in which the associated taxa clustered together in the bootstrap test (1000 replicates) are shown next to the branches (352). The tree is drawn to scale, with branch lengths in the same units as those of the evolutionary distances used to infer the phylogenetic tree. The evolutionary distances were computed using the p-distance method (353) and are in the units of the number of amino acid differences per site. The analysis involved 6 amino acid sequences. All positions containing gaps and missing data were eliminated. There was a total of 222 positions in the final dataset. Evolutionary analyses were conducted in MEGA7 (354).

Overall, these results indicate compilation of multiple substitutions in the variable regions of the antibodies, located throughout the FR and CDR domains. In addition, the antibody set analysed has shown that germline alleles can bias mutation rates, positions, and specificity.

2.1.1.3 Antibody structure prediction shows overall similarity for the antibodies analysed

To visualise the conformation of the antibody variable regions, framework regions and loops that might contribute towards epitope binding, modelling of the variable antibody domains was carried out using the publicly available abYmod tool (355). The deletions in FR1 and CDR1 of HA9 resulted in insufficient data for model prediction for this antibody. Model prediction of the remaining five antibodies revealed no major observable differences in the light chain framework structures (Figure 2.4).

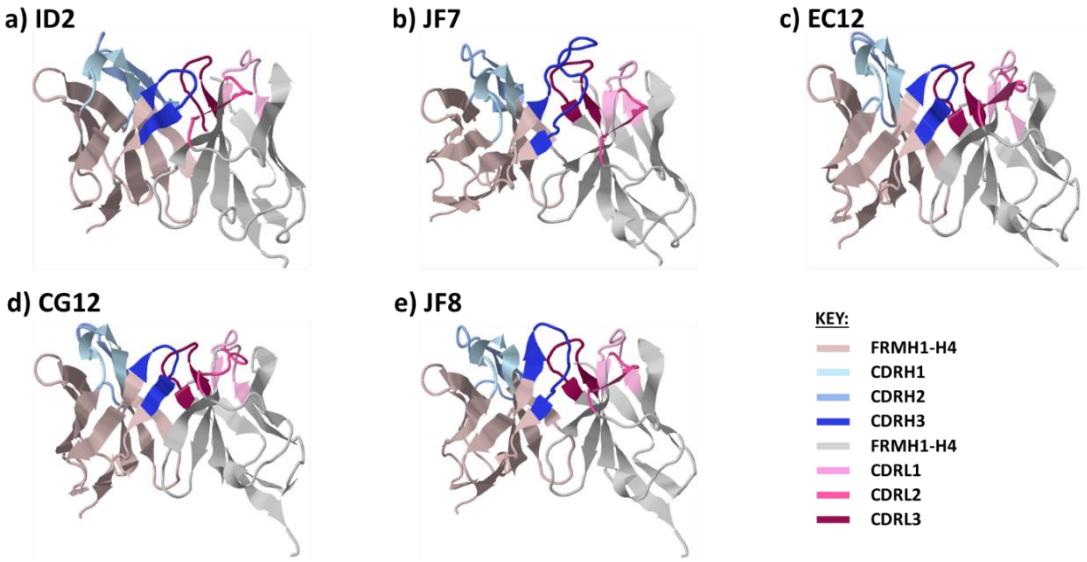

Figure 2.4. scFv antibody structure modelling. Antibody structures were predicted using sequence data and the publicly available abYmod tool. **a)** ID2; **b)** JF7; **c)** EC12; **d)** CG12; **e)** JF8. Heavy chain framework regions 1-4 are annotated by black shadows; heavy chain CDRs depicted in different shades of blue (CDR1 – blizzard blue; CDR2 – blue grey; CDR3 – blue (pantone), light chain framework regions 1-4 are annotated by grey; heavy chain CDRs depicted in different shades of pink (CDR1 – schauss pink; CDR2 – barbie pink; CDR3 – pansy purple.

With regards to the framework region of the variable heavy chain, overall similarity was retained for all but the JF7 antibody which had slightly adjusted positions for each of the regions (Figure 2.4. b). The same antibody had an observably longer loop formed by CDRH3 than those of ID2, EC12 and CG12, with an intermediate size CDRH3 of JF8. In addition, both JF7 and JF8 antibodies were predicted to form a ‘kinked’ loop structure for the CDHR3 region (Figure 2.4. b, f). Loops formed by the variable light chain appeared similar in all antibody structures, with the only difference in proximity to CDRH3 mediated by the length of the latter region. Overall, *in silico* simulations allowed visualization of antibody structures which were found to be fairly conserved amongst five molecules.

2.1.1.4 2.2.1.4. Representative influenza A viruses selected for the study are antigenically diverse

To assess the ability of antibody to recognize antigen and interfere with the virus life cycle, appropriate AIVs had to be chosen. The test viruses had to be i) antigenically similar to H9N2 UDL-1/08; ii) antigenically distant from H9N2 UDL-1/08; iii) representatives of circulating strains in poultry. For this purpose, eight viruses previously rescued in the lab and fitting the aforementioned criteria were chosen with the majority of them belonging to the G1 lineage and a single virus from BJ94. Viruses chosen from the G1 lineage represented both the main phylogenetic 'Western' and 'Eastern' groups known to be antigenically different from each other (356). Sequences of representative viruses were downloaded from NCBI Influenza database and used for evolutionary analysis (Figure 2.5).

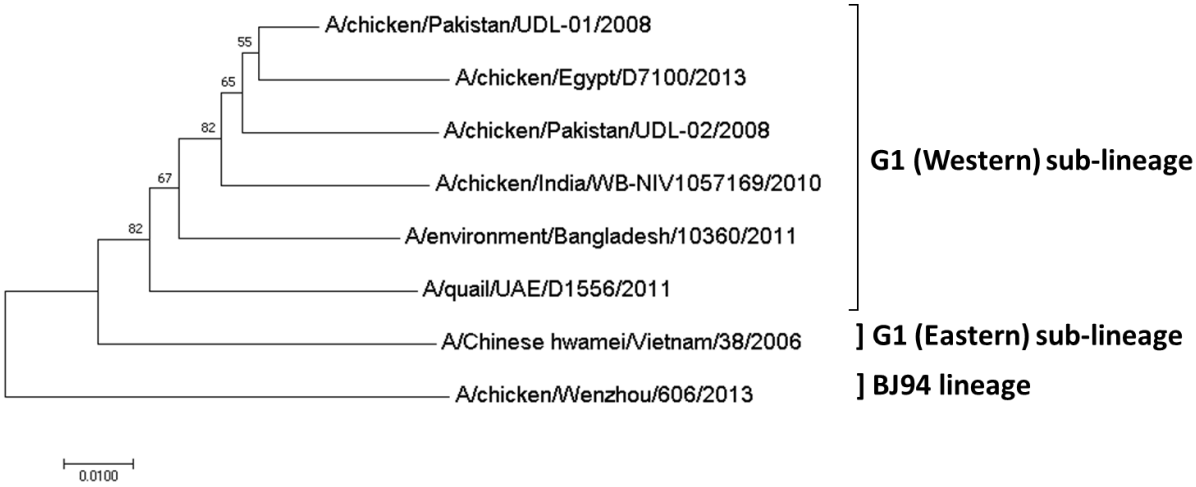

Figure 2.5. Evolutionary relationship of H9N2 viruses used in this study. The evolutionary history was inferred using the Neighbor-Joining method (351). The optimal tree with a sum of branch length = 0.3109654 is shown. The percentage of replicate trees in which the associated taxa clustered together in the bootstrap test (1000 replicates) are shown next to the branches (352). The tree is drawn to scale, with branch lengths in the same units as those of the evolutionary distances used to infer the phylogenetic tree. The evolutionary distances were computed using the p-distance method (353) and are in the units of the number of amino acid differences per site. The analysis involved 8 amino acid sequences. All positions containing gaps and missing data were eliminated. There was a total of 560 positions in the final dataset. Evolutionary analyses were conducted in MEGA7 (354).

Altogether, the eight viruses chosen had ≥ 89 % similarity with UDL-1/08 in their HA gene sequences. The closest viruses were determined to carry ≥ 95% amino acid identity and included Egy/D7100 (97%), UDL-2/08 (96%) and Env/BD (95%) while India/WB had 94%, UAE/D1556 - 93%, VN/38 - 92% and WZ/606 - 89% similarity with UDL-1/08 HA. In addition, variations within the receptor binding domain (amino acids 98 – 229; inclusive) of HA were 4% for India/WB, 5% for UDL-2/08, 6% for Egy/D7100 and Env/BD. Antigenically distant viruses included UAE/D1556 with 89% amino acid conservation, VN/38 - 83% and WZ/606 - 82% identity within the receptor binding site. All viruses chosen were rescued by previous lab members using reverse genetics systems and for the purposes of this study were propagated in eggs.

2.1.2 Antibody generation and evaluation of functional activity

2.1.2.1 Antibody purification from cell culture supernatants

To evaluate the antibodies' functional characteristics, immunoglobulin molecules and their fragments had to be produced and purified from cell culture supernatants. The variable antibody fragments characterised in section 2.2.1. were used for subcloning into vectors containing constant domains of mice IgG1 and IgG2a antibodies or for conversion into scFv molecules. ExpiCHO cells were transiently transfected with plasmids encoding full-size antibody genes and supernatants were harvested 10-days post transfection. Harvested supernatants were used for antibody purification via Protein A. scFv antibody genes were transfected into *Drosophila melanogaster* S2 cells, which were used for stable single cell line establishment after a 6-week selection with zeocin. Supernatants from stable cell lines were harvested and affinity purified via C-tag matrix. The purity of obtained proteins was evaluated via SDS - PAGE (Figure 2.6) after overnight dialysis in PBS. Two bands of ~25 kDa and ~50 kDa molecular weight corresponding to light and heavy chain, respectively, were found in all antibodies carrying mouse IgG1 (Figure 2.6a) and mouse IgG2a (Figure 2.6b) Fc regions.

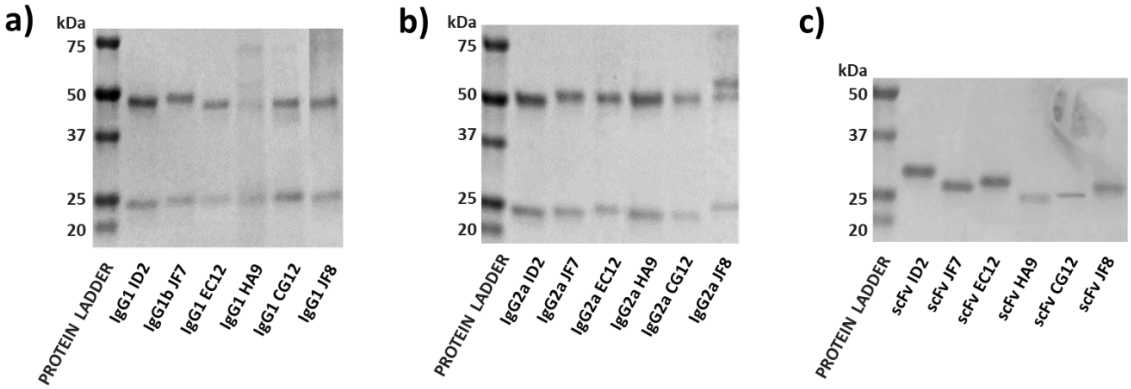

Figure 2.6. SDS-PAGE of recombinant antibodies produced in this study. a) antibodies purified from ExpiCHO cell supernatants converted to mouse IgG1 isotype; **b)** antibodies purified from ExpiCHO cell supernatants converted to mouse IgG2a isotype; **c)** antibodies purified from S2 cell supernatants converted to scFv format. All antibodies were dialysed into PBS pH 7.4 after purification. For SDS-PAGE analysis all antibodies were diluted to 5 μg, mixed with protein loading buffer, and denatured. When full length antibody samples were prepared 2% BME was added prior to boiling to ensure heavy (~50 kDa) and light (~25 kDa) chain separation. Proteins were run on either 8%, 10% or 12% Bis – Tris polyacrylamide resolving gel and visualised by Coomassie blue staining.

Some impurities were found in IgG1 HA9 and JF8 antibodies appearing as a 'smudge' at a higher molecular weight. Interestingly, IgG2a JF8 was found to have a clear additional band of ~55 kDa. Generally, the migration patterns for EC12, HA9 and CG12 antibodies were similar whilst the other three antibodies migrated at unique positions.

On the other hand, all scFvs were found to form single polypeptide bands that migrated at the expected size of ~27 - 30 kDa, with the three antibodies (HA9, CG12, JF8) that contained a 5 amino acid shorter linker $((Gly_4Ser)_3$ instead of $(Gly_4Ser)_4)$ being observably smaller (Figure 2.6c). The protein concentration after purification varied depending on the method of production, with ExpiCHO cells showing substantially variable yields ranging from 1 mg to 200 mg of full-length antibodies per litre of cell culture supernatant and S2 cells producing more uniform amounts averaging around 10 mg of protein per litre of cell culture supernatant. Thus, the recombinant antibodies and antibody fragments

were successfully produced in either mammalian or insect cell cultures using variable domain sequences and purified to high enough concentrations to perform functional assays.

2.1.2.2 Recombinant antibodies bind to H9N2 viruses with differing affinity

To investigate if recombinantly produced antibodies retained their ability to bind to virus antigens, a series of ELISAs were performed using the chosen H9N2 viruses (section 2.2.1.4) as targets. Experiments were done using 2-fold serially diluted live viruses at a starting concentration of 32 HAU to obtain plateauing binding curves. Viruses adsorbed to plates were probed with a constant concentration of either purified full length or scFv antibodies. A negative control of wR1a-28 VHH antibody (gifted from Dr Simon E. Hufton, NIBSC) specific to H7 HA but not UDL-1/08 HA was used. This negative control antibody showed no detectable binding to any of the viruses used in these experiments (Figure 2.7.). In general, the IgG1 antibodies were found to retain affinity towards UDL-1/08 and antigenically related viruses. A trend of IgG1 ID2 binding with highest affinity to most of the viral antigens was observed.

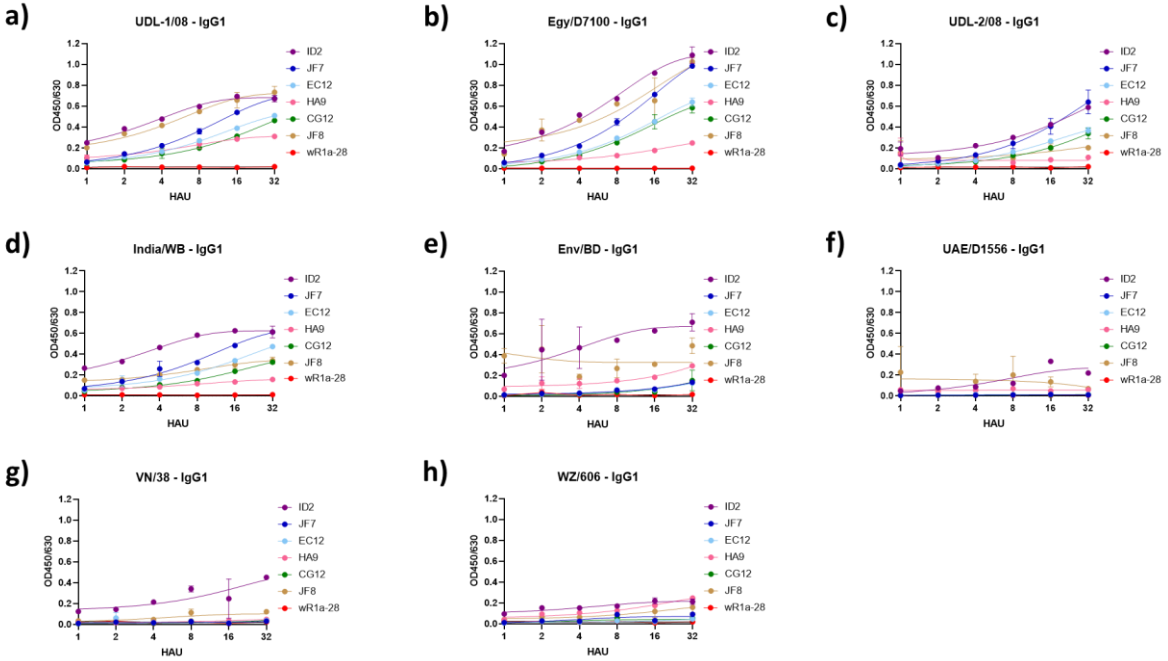

Figure 2.7. ELISA assessing monoclonal antibody carrying mouse IgG1 isotype binding to H9N2 viruses. a) UDL-1/08; **b)** Egy/D7100; **c)** UDL-2/08; **d)** India/WB; **e)** Env/BD; **f)** UAE/1556; **g)** VN/38; **h)** WZ/606. 32 HAU units and subsequent 2-fold dilutions of each virus were used for plate coating. Purified antibodies were used at 1 µg mL^{-1} and detected by rabbit anti-mouse immunoglobulins conjugated with HRP. The variable heavy chain of the heavy chain only antibody wR1a-28 specific to H7 HA was used as a negative control. Binding was measured in technical duplicate and the average OD 450/630 nm values were plotted with error bars representing ±SD. Curve fitting was performed following a nonlinear regression model.

In addition, this antibody retained binding to more antigenically distinct viruses such as UAE/D1556 and VN/38, to which the other antibodies showed no or very limited binding (Figure 2.7.f, g). Another high affinity antibody binding UDL-1/08 and Egy/D7100 to a similar extent to that of ID2 was IgG1 JF8; however, this antibody's specificity decreased with more distant viruses (Figure 2.7.a, b). Regardless of this, IgG1 JF8 maintained affinity towards Env/BD and to a certain extent, UEA/D1556 (Figure 2.7.e, f). IgG1 JF7 was specific to UDL-1/08 and the three genetically closest H9N2 viruses from the panel tested. A similar trend was observed with the remaining three antibodies (EC12, CG12, HA9), with HA9 being the weakest binder for all viruses while EC12 and CG12 retained almost identical specificity. Interestingly, all antibodies showed higher affinity towards Egy/D7100 than UDL-1/08 to which the mouse hybridomas were generated in the first place (Figure 2.6.b, a). In addition, no distinguishable binding was detected for any of the antibodies with the BJ94 lineage virus, WZ/606 (Figure 2.7.h).

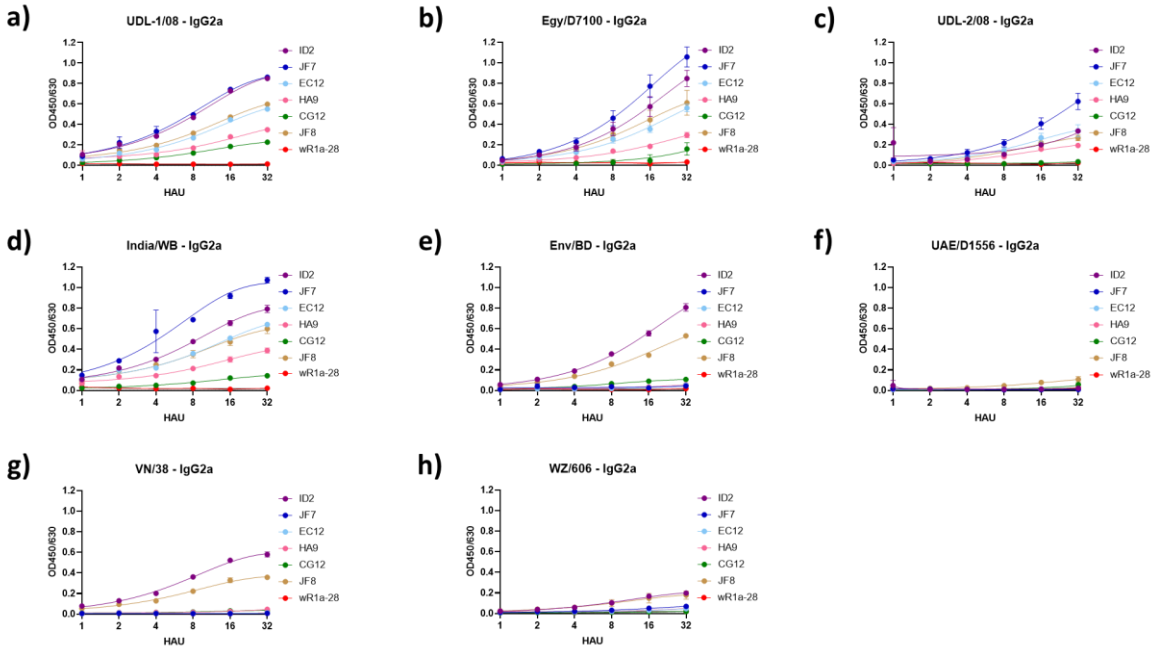

Figure 2.8. ELISA assessing monoclonal antibody carrying mouse IgG2a isotype binding to H9N2 viruses. a) UDL-1/08; **b)** Egy/D7100; **c)** UDL-2/08; **d)** India/WB; **e)** Env/BD; **f)** UAE/1556; **g)** VN/38; **h)** WZ/606. 32 HAU units of each virus was used for coating and 2-fold dilutions. Purified antibodies were used at 1 µg mL^{-1} and probed by anti C-tag antibody conjugated to biotin which was detected using HRP-conjugated streptavidin. The variable heavy chain of the heavy chain only antibody wR1a-28 specific to H7 HA non-binding UDL-1/08 was used as a negative control. Binding was measured in technical duplicate and the average OD450/630 nM was plotted with error bar representing ±SD, curve fitting was performed following nonlinear regression model.

Antibody reformatting into mouse IgG2a isotype resulted in some relative affinity changes (Figure 2.8). Unexpectedly, IgG2a JF7 was found to have the highest binding capacity on ELISA surpassing that of IgG2a ID2. In addition, the overall affinity for all antibodies was exceptionally high towards India/WB becoming almost identical, and even surpassing that seen with UDL-1/08; the antigen against which antibodies were originally raised. (Figure 2.8d, a). IgG2a JF8 specificity for UDL-1/08 and Egy/D7100 decreased compared to its IgG1 counterpart and was similar to that observed with the IgG2a EC12 antibody. Similarly to previous observations, IgG2a JF8 and ID2 retained specificity towards Env/BD and VN/38 (Figure 2.8e, g). Both UAE/D1556 and WZ/606 gave a barely detectable signal for binding by IgG2a JF8 or IgG2a JF8 and ID2, respectively with OD 450/630 nm values ≤0.2 at even the highest virus concentrations (Figure 2.8f, h). In addition, the lowest binder for genetically closest viruses was IgG2a CG12, unlike IgG1 format where HA9 gave the poorest recognition.

Next, scFv antibody ability to recognise the diverse viral antigens was explored. The data obtained had overall similarities with that from the antibodies in mouse IgG2a isotype, although the binding strength as determined by OD 450/630 nm values were lower for all antibodies and all viruses (Figure 2.9). Overall, scFv ID2 and scFv JF7 had the highest affinities, followed by scFv EC12 for UDL-1/08 and Egy/D7100, India/WB (Figure 2.9a, b, d). Binding of scFv EC12 was identical to that of scFv ID2 for UDL-2/08 (Figure 2.9c), while only scFv ID2 and scFv JF7 retained binding to Env/BD (Figure 2.9e). The binding to VN/38 was maintained by scFv ID2 (Figure 2.9g), while none of the antibodies recognised UAE/D1556 or WZ/606 above the levels of the negative control antibody (Figure 2.9f, h). An additional negative control of H5N1 VN/OIE/2202 was also tested with the scFvs, indicating no affinity towards another subtype virus from the same group 1 influenza viruses (Figure 2.9i). In addition, conversion of JF8 into scFv format was found to have a negative impact on antigen recognition as illustrated with all eight viruses.

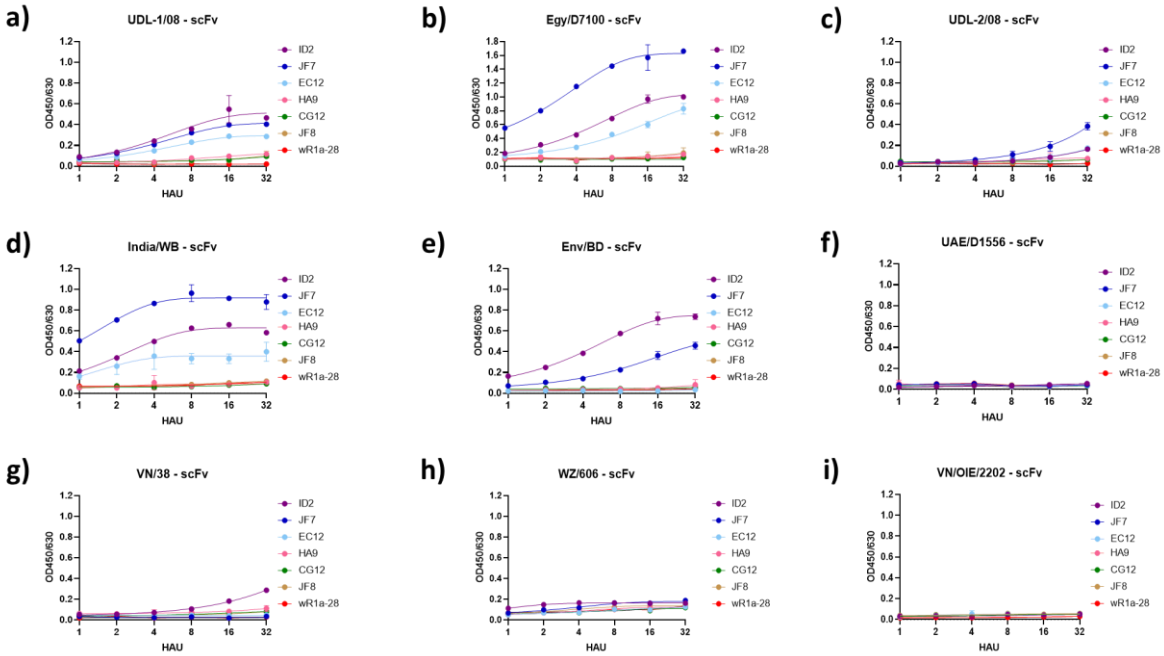

Figure 2.9. ELISA assessing scFv antibody binding to H9N2 viruses. a) UDL-1/08; **b)** Egy/D7100; **c)** UDL-2/08; **d)** India/WB; **e)** Env/BD; **f)** UAE/1556; **g)** VN/38; **h)** WZ/606; **i)** VN/OIE/2202. 32 HAU units of each virus was used for coating and 2-fold dilutions. Purified antibodies were used at 1 µg mL^{-1} and probed by rabbit anti-mouse immunoglobulins conjugated with HRP. The variable heavy chain of the heavy chain only antibody wR1a-28 specific to H7 HA non-binding UDL-1/08 was used as a negative control. Binding was measured in technical duplicate and the average OD450/630 nM was plotted with error bar representing ±SD, curve fitting was performed following nonlinear regression model.

Overall, antibodies in all formats retained appreciable binding to viruses with HAs that were ≥ 94% amino acid similar to the UDL-1/08 HA. Only one antibody in all formats (ID2) was able to interact with more diverse viruses such as Env/BD, UAE/D1556, VN/38 and WZ/606. Interestingly, JF8 ability to interact with antigen was found to be dependent on antibody format.

2.1.2.3 Recombinant antibodies can neutralize antigenically related H9N2 viruses

Having tested antibody binding to live viruses in ELISA, their ability to interfere with the virus life cycle was determined. Microneutralization assays were performed with a starting concentration of 100 µg mL^{-1} of each antibody regardless of recombinant protein format and 150 $TCID_{50}$ of virus. A negative control of the wR1a-28 VHH antibody always resulted in complete cell death, while serum raised against UDL-1/08 virus gave cell survival with homologous viruses and was used as a positive control (data not shown).

The best neutralizers in IgG1 format were JF7, EC12 and CG12 antibodies followed by ID2 (Table 2.3, Figure 2.10).

Table 2.3. IgG1 antibody activity in virus microneutralization assay. To assess antibody functional activity assay was performed in technical and biological triplicates in MDCK cells. Values represented show antibody concentration required for complete virus neutralization. Average data are shown ± SD where applicable. - indicates no activity found with the maximum antibody dose of 100 µg mL^{-1}.

Virus / Antibody	ID2 µg mL^{-1}	JF7 µg mL^{-1}	EC12 µg mL^{-1}	HA9 µg mL^{-1}	CG12 µg mL^{-1}	JF8 µg mL^{-1}
A/chicken/Pakistan/UDL-01/2008	0.65±0.81	0.09±0.09	0.20±0.19	1.17±0.55	0.32±0.12	7.56±6.28
A/chicken/Egypt/D7100/2013	0.45±0.30	0.16±0.06	0.26±0.12	0.49±0.42	0.10±0.08	4.17±1.80
A/chicken/Pakistan/UDL-02/2008	8.33±3.61	0.45±0.3	0.39	1.17±0.55	0.45±0.3	-
A/chicken/India/WB-NIV1057169/2010	3.21±2.87	0.13±0.1	0.26±0.12	0.59±0.28	0.26±0.12	3.13
A/environment/Bangladesh/10360/2011	7.29±4.77	12.5	12.5	-	6.25	-
A/quail/UAE/D1556/2011	-	-	-	-	-	-
A/Chinese hwamei/Vietnam/38/2006	-	-	-	-	-	-
A/chicken/Wenzhou/606/2013	-	-	-	-	-	-

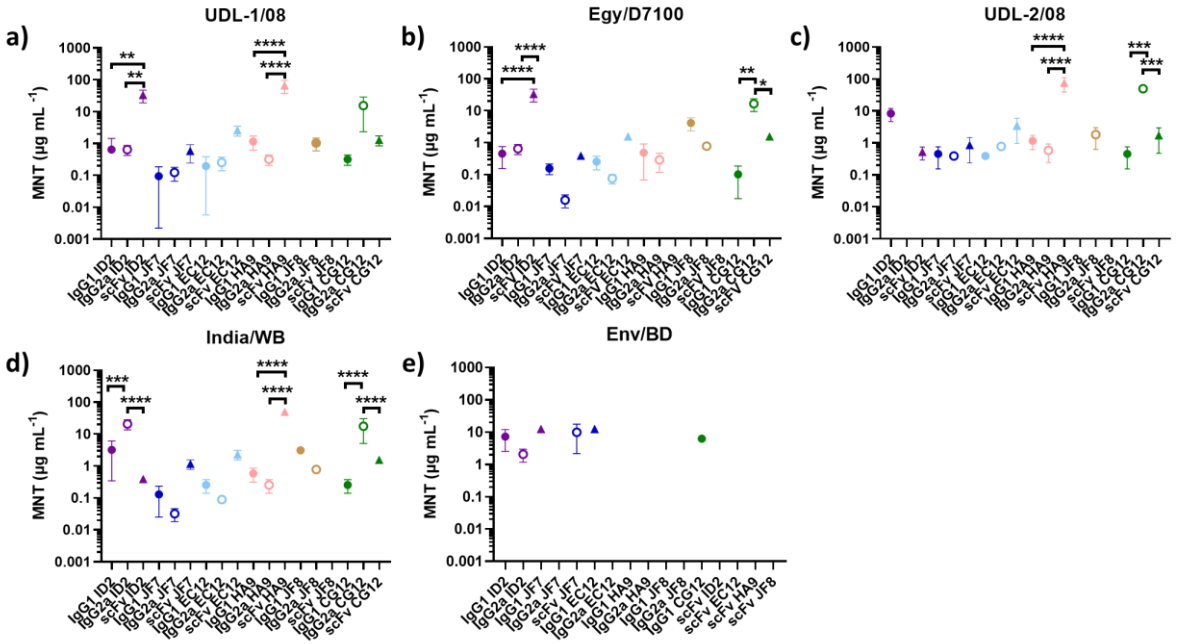

Figure 2.10. Microneutralization assay assessing functional recombinant antibody activity against H9N2 viruses in MDCK cells. a) UDL-1/08; **b)** Egy/D7100; **c)** UDL-2/08; **d)** India/WB; **e)** Env/BD. IgG1 antibodies are depicted as full circles; IgG2a antibodies are depicted as empty circles; scFv antibodies are depicted with triangles. Missing data indicates no functional activity found with the detection limit of 100 µg mL^{-1} per antibody. Data are presented as mean ± SD. A one-way ordinary ANOVA test was run for statistical analysis. *p*-values of $P < 0.05$ were considered significant (Nonsignificant (Ns) = $p > 0.05$; * = $p \leq 0.05$; ** = $p \leq 0.01$; *** = $p \leq 0.001$; **** = $p \leq 0.0001$.

All four antibodies were functional against five out of eight viruses, but with no activity detected against UAE/D1556, VN/38 and WZ/606. Both IgG1 HA9 and JF8 were not able to neutralize Env/BD, while JF8 also lacked functional activity against UDL-2/08. Interestingly, although IgG1 JF8 was shown to have good affinity towards multiple viruses including those more antigenically diverse, this antibody was not able to efficiently inhibit the virus life cycle. In agreement with the binding data, ID2, HA9 and CG12 neutralized Egy/D7100 at lower concentrations than those required for UDL-1/08, while HA9, CG12 and JF8 were better at neutralizing India/WB than the homologous UDL-1/08 (Table 2.3). The antibody concentration required for complete virus neutralization did not depend on the overall HA similarity to UDL-1/08, but rather corresponded to receptor binding site sequence; with more divergent regions requiring higher concentrations of antibodies discussed in sub-section 2.2.1.4. (Egy/D7100 was an exception).

The same microneutralization assay was performed with IgG2a antibodies, which are generally expected to have higher activity than IgG1 due to their Fc domain binding activating Fc receptors *in vivo* or *in vitro* when using cell lines expressing Fc receptors (345, 357) . This was true for HA9 and JF8 antibodies against all viruses, JF7 and EC12 antibodies with seven out of eight viruses (Table 2.4, Figure 2.10).

Table 2.4. IgG2a antibody activity in virus microneutralization assay. To assess antibody functional activity, assays were performed in technical and biological triplicates in MDCK cells. Serum samples raised against UDL-1/08 were used as a positive control and non-binder wR1a-28 was used as a negative control alongside MOCK infected cells. Values represented show antibody concentration required for complete virus neutralization. Average data is shown with ± SD where applicable. - indicates no activity found with detection limit 100 μg mL^{-1}.

Virus / Antibody	ID2 μg mL^{-1}	JF7 μg mL^{-1}	EC12 μg mL^{-1}	HA9 μg mL^{-1}	CG12 μg mL^{-1}	JF8 μg mL^{-1}
A/chicken/Pakistan/UDL-01/2008	0.65±0.23	0.12±0.06	0.26±0.12	0.32±0.12	15.63±13.26	1.04±0.45
A/chicken/Egypt/D7100/2013	0.65±0.23	0.02±0.01	0.08±0.02	0.29±0.17	16.67±7.22	0.78
A/chicken/Pakistan/UDL-02/2008	-	0.39	0.78	0.58±0.34	50	1.82±1.19
A/chicken/India/WB-NIV1057169/2010	20.83±7.22	0.03±0.01	0.09	0.26±0.12	17.71±12.63	0.78
A/environment/Bangladesh/10360/2011	2.08±0.9	-	-	-	-	-
A/quail/UAE/D1556/2011	-	-	-	-	-	-
A/Chinese hwamei/Vietnam/38/2006	-	-	-	-	-	-
A/chicken/Wenzhou/606/2013	-	-	-	-	-	-

Only IgG2a ID2 was effective against Env/BD; however, the same antibody was not able to neutralize UDL-2/08. Another outlier was found with India/WB, which required substantially higher concentrations of IgG2a ID2 than IgG1 for neutralisation. JF7 and EC12 remained the best neutralizers followed by HA9 and JF8 in this instance, corresponding to what was seen in ELISAs. Also reflecting the binding data, IgG2a CG12 was not able to neutralize any of the viruses efficiently, with concentrations as high as 15 - 50 μg mL^{-1} needed. Higher specificity to Egy/D7100 and India/WB than UDL-1/08 was observed with most of IgG2a antibodies.

Lastly, scFv ability to neutralize each virus was assessed. A general trend of 10-fold increases in the required antibody concentrations compared with full length antibodies was observed (Table 2.5, Figure 2.7); however significant differences as assessed by one-way ANOVA were found only between scFv HA9 and its full-length counterparts ($p \leq 0.0001$) for UDL-1/08, UDL-2/08 and India/WB. On the other hand, when converted from a full-length antibody into scFv HA9 lost activity against Egy/D7100. Conversion to scFv format

completely abolished JF8 activity even against the homologous UDL-1/08 (Table 2.5). Interestingly, ID2 when converted to scFv format was also required at substantially higher concentrations than full-length antibodies against UDL-1/08 and Egy/D7100 viruses, but the opposite was noted with India/WB, suggesting changes in antibody structure might lead to differences in function.

Table 2.5. scFv antibody activity in virus microneutralization assay. To assess antibody functional activity assay was performed in technical and biological triplicates in MDCK cells. Serum samples raised against UDL-1/08 were used as a positive control and non-binder wR1a-28 was used as a negative control alongside MOCK infected cells. Values represented show antibody concentration required for complete virus neutralization. Average data is shown with ± SD where applicable. - indicates no activity found with detection limit 100 µg mL^{-1}.

Virus / Antibody	ID2 µg mL^{-1}	JF7 µg mL^{-1}	EC12 µg mL^{-1}	HA9 µg mL^{-1}	CG12 µg mL^{-1}	JF8 µg mL^{-1}
A/chicken/Pakistan/UDL-01/2008	33.34±14.43	0.58±0.34	2.60±0.9	66.67±28.87	1.30±0.0.45	-
A/chicken/Egypt/D7100/2013	33.34±14.43	0.29±0.17	1.17±0.0.68	-	1.30±0.45	-
A/chicken/Pakistan/UDL-02/2008	0.52±0.23	0.78±0.68	3.65±0.2.39	50	1.82±1.19	-
A/chicken/India/WB-NIV1057169/2010	0.39	0.91±0.6	2.08±0.9	50	1.56	-
A/environment/Bangladesh/10360/2011	-	5.21±1.80	-	-	-	-
A/quail/UAE/D1556/2011	-	-	-	-	-	-
A/Chinese hwamei/Vietnam/38/2006	-	-	-	-	-	-
A/chicken/Wenzhou/606/2013	-	-	-	-	-	-

Only three antibodies in scFv form (JF7, CG12 and EC12) were able to efficiently neutralize antigenically similar viruses, agreeing with what was observed in IgG1 format and (except for CG12) in IgG2a format. Additionally, scFv JF7 was found to inhibit Env/BD, which suggested an enhanced antibody breadth not seen in the full-length form (Figure 2.7e). In general, comparison of scFv activity revealed no significant differences in JF7, EC12 and CG12 activity with UDL-1/08, Egy/D7100, UDL-2/08 and India/WB. On the other hand, to neutralize UDL-1/08, both scFv ID2 and HA9 were required at higher concentrations than remaining antibodies, with the same profile retained for scFv ID2 and Egy/D7100 (scFv HA9 did not neutralize this virus), scFv HA9

and UDL-2/08 or India/WB. In addition, by observation scFvs were more effective against Egy/D7100 than any other virus, corresponding to data observed with other full-length antibodies in MNT assay as well as the ELISA results.

To sum up, a trend of IgG2a antibodies requiring lower concentrations for neutralisation than IgG1 format ones was observed, with the exception of CG12. However, differences in antibody concentrations required were marginal, with no statistical significance. Conversion of the antibodies into scFv format retained their functional activity, apart from scFv JF8 which was not able to inhibit the virus life cycle at the concentrations tested. With the exception of HA9, most antibodies required marginally higher concentrations for neutralisation that were not statistically different from full length antibodies. None of the antibodies had identical neutralization titers, indicative of binding towards slightly different epitopes.

2.1.2.4 scFvs retain functional activity when exposed to elevated temperatures for prolonged periods

To evaluate if scFv molecules would remain stable and retain functional activity at elevated temperatures, resembling the environment that is likely to be found in nasal passages of birds, the MNT assay using UDL-1/08 as a representative virus was repeated with purified antibody fragments pre-incubated at 37 °C for 96 h. All scFvs retained identical neutralization profiles to those reported in Table2.5 with UDL-1/08. This indicated thermal scFv stability and suggested no loss of activity should occur if purified antibodies were to be delivered to birds for therapeutic purposes.

2.3 Discussion

The focus of this chapter was H9 HA-specific antibody characterization *in silico* followed by recombinant antibody production in a form of full-length antibodies

and antibody fragments, allowing the testing of their functional activity and the evaluation of neutralisation efficacy against virus *in vitro*. Antibody genes were obtained from previously generated mouse hybridomas and their variable domains were sequenced. Analysis of variable domain sequences and CDR identification was based on IMGT numbering system. This revealed homogeneity in CDRH1, CDRH2, CDRL1, CDRL2 and CDRL3 lengths, with only CDRH3s presenting variability amongst the panel of six antibodies. It should be noted that the CDR definition used throughout this study is only indicative of approximate paratope location, as different numbering systems could potentially impact results and subsequent analyses. IMGT numbering was chosen on the basis of the system being standardized for multiple proteins within the immunoglobulin superfamily (358). Other commonly used antibody numbering systems include the Kabat scheme, - the initial method developed for antibody sequence annotation based on multiple sequence alignment, the Chothia scheme that takes into consideration not only sequence, but also structural antibody configuration and some other schemes developed more recently (20, 359, 360).

Analysis of amino acid composition within the variable domains of the six antibodies used in this study revealed preference for Gly, Ser and Thr residues. Small amino acids such as Gly and Ser are commonly found within antibody sequences and are thought to provide structural flexibility that allows more efficient antigen binding (361). Other abundant residues within antibody variable regions reported in the literature include Thr, Tyr and Ala residues, which are especially prevalent within CDRH3 regions with some evidence suggesting they and in particular the Tyr side chains (in ~25% of the cases) mediate molecular recognition and antigen binding (362-364). In addition, evidence suggests that hydrophobic amino acids such as Ile, Tyr or Phe located at the tip of CDRs often mimic interactions formed between

The HA RBS and sialic acid receptor via aromatic rings (365). Other common residues mimicking the same interaction include Asp or an Asp-hydrophobic

amino acid motif as demonstrated by several studies (336, 366). Most of these amino acids could also be found in the CDRH3 sequences of the antibodies analysed here; however, to determine if they are involved in mediating interaction with antigen, crystal structures would need to be resolved.

Next, antibody diversification was assessed, focusing on individual germline genes. Three out of six antibodies were found to belong to the same germline for heavy and light chain and two antibodies shared the same germline for heavy chain only. In general, antibody diversification and affinity maturation was found to have occurred with all antibody sequences but to varying levels. Interestingly, some of the positions that were found to contain substitutions were shared between different germlines (*i.e*. positions 48 and 84 for heavy chain and positions 50, 55 for light chain). In addition, when two or more antibodies were found to belong to the same germline, substituted positions often matched between antibodies, indicating a certain degree of preference for those events. Different germline gene origins predisposing antibodies to obtain specific diversifications at a discrete rate has been described previously (367). Such phenomena can be explained by 'hot-spot' motifs, biased for mutation introduction encoded by some germlines (367, 368).

In the panel of sequences analysed, mutations were otherwise randomly distributed across framework and complementarity determining regions, with a slightly higher incidence in framework regions agreeing with previous findings (369). Mutations harboured in framework regions are thought to contribute to the biophysical characteristics, the enhancement of paratope stability or even an increase in functional profile and neutralizing breadth, as illustrated with HIV-specific antibodies (339, 370). Due to the IMGT database lacking germline CDRH3 sequence data, this study could only consider deviations within the CDRH3 region amongst the six antibody sequences generated by this study, but not their original germline genes. Generally, CDRH3 loops are the most variable parts of antibody sequence, thought to be the main mediators for antigen binding with longer CDRH3 sequences often

forming more extended loops and, therefore, gaining access to more hidden and in many cases more conserved epitopes (21). The average CDRH3 length in mice has been reported to be ~12 amino acids in length but ranging anywhere between 4 to 26 residues (369). The antibodies in this study were no exception, with CDRH3 domains varying between 7 and 15 residues.

Interestingly, one antibody (HA9) was found to carry partially missing FR1 and FR2 regions with a completely deficient CDR1 sequence within the light chain. Occasional deletions and insertions are yet another way to increase antibody repertoire, with multiple studies observing such changes to be common within CDR sites and in some cases leading to multiple codon elimination (371, 372). 22 residues identified missing from HA9 VL chain when compared to the germline sequence suggested by IMGT database were later identified to support a functional antibody profile. Importantly, some of the conclusions made herein on sequence variability match with literature reports, although having a limited dataset of only six antibodies compared at one time might not be representative for the whole population of antibodies which could be generated using mouse hybridoma technology.

Furthermore, to visualize differences between this study's six antibodies, abYmod software was used to model possible protein structures. The overall antibody backbone confirmation was predicted to be similar amongst five antibodies, but the lack of CDR1 and parts of FR1 and FR2 resulted in insufficient data for HA9 structure prediction. Only the JF7 structure generated a well protruding loop from the CDRH3 region. A kinked CDRH3 loop structures were found for two antibodies, with the other three carrying an extended version forming a strand-turn-strand conformation. A C-terminal kink is thought to be an additional means for antibody diversification, allowing β-strand disruption at the base of CDRH3 (373). The proximity of CDRH3 and CDRL3 loops was observed for all antibodies in the predicted models, suggesting all have canonical antibody structures. Understanding of antibody structural confirmation can be indicative of antigen binding sites, informing how

interactions are made, which epitopes are targeted, and how to obtain more specific, higher affinity interactions. Nevertheless, antibody structure modelling has limitations in its accuracy, as models are based on the most similar structures solved and minute, but important differences might not be reflected in the prediction. In addition, it has been demonstrated that antibody conformation might change upon interaction with antigen; something which cannot be predicted by currently available tools to best of this author's knowledge (145, 153). Experimental immunoglobulin molecule structure determination in a complex with antigen would need to be obtained to identify residues involved in paratope and epitope formation, which was not in the scope of this project. In general, the sequence data collected and analysed suggests all six antibodies binding to the HA antigen slightly differently and, therefore, functional activity for antibodies was expected to vary.

To test this hypothesis, antibodies were expressed as recombinant proteins carrying Fc regions from mouse IgG1 or IgG2a isotypes. Worth noting, most of the antibodies derived from hybridomas were originally of IgG2a isotype apart from ID2 which was carried an IgG2b Fc region (330). In addition, scFv molecules were generated, representing the smallest immunoglobulin format known to retain the specificity of the original antibodies.

Multiple aspects, including the end goal of antibody administration to poultry, a preference for smaller structures allowing easier insertion into viral vectors, or even generation of 'polyclonal antibodies' through combining multiple scFvs targeting distinct epitopes were the main factors driving a preference for an antibody fragment missing its Fc part. Herein, V_L-V_H chain orientation was used for scFv generation. Various studies investigating efficacy of scFvs depending on variable chain direction have reported a preference for a V_L-V_H orientation not only for optimal activity but also for protein expression efficiency (374, 375). Nevertheless, some contradictory data, suggesting better function in scFvs formatted following V_H-V_L orientation, can also be found, with an additional set of studies indicating no difference in antibody activity based on

variable chain direction (376, 377). If future projects are to follow this work's concept, it is highly suggested to design scFvs in both orientations and compare their functional activity; especially for antibodies which did not retain specificity after scFv reformatting, as it is likely to be case - to - case dependent. Another important factor in scFv design is the choice of linker, with linkers composed of 15 - 20 amino acids used in this study. Three of the antibodies whose open reading frame was synthesised commercially had $(Gly_4Ser)_4$ linkers, while the other three which were subcloned via PCR contained a shorter $(Gly_4Ser)_3$ linker. This was reflected by SDS-PAGE showing a slightly lower molecular weight of antibodies containing shorter linkers estimated relying on the size of protein markers. Typically, Gly, Ser linkers are used for scFv as well as other fusion proteins because they provide flexibility for different domains and thus an advantage of correct folding, with linkers ≤ 15 residues long inducing multimerization and formation of higher order structures (375).

Comparing functional activity and antibody binding to homologous and heterologous viruses, it was found that both binding and virus neutralization were isotype-dependent. Interestingly, the ELISA results in this study suggested altered relative affinities towards antigen when the antibody isotypes were changed. Although the exact reasons are not well understood, such differences are likely to occur due to changes in variable domain structure when constant regions are alternated, as observed in some previous studies (378, 379). Additionally, possibility of errors in antibody concentrations should be considered. In general, binding efficacy decreased with more antigenically distinct viruses for both full length and scFv antibodies. Both WZ/606 and VN/38 were known to have limited cross reactivity with UDL-1/08 antisera while viruses such as Egy/D7100 and UDL-2/08 were known to have high cross reactivity from previous work (330), which was re-established herein. This work also noted that antibodies in all formats were highly specific to India/WB HA which carried overall 94% similarity with UDL-1/08 HA.

Conversion of antibodies to scFv format did seem to affect their ability to bind viruses, as OD 450/630 nm values were markedly lower in ELISA results. However, different secondary antibodies used for detection could also introduce additional variability, so the two different formats cannot necessarily be compared directly. Altogether, the dataset from the ELISA results categorized antibodies into two main groups: one of which were the better binders consisting of ID2, JF7 and JF8 antibodies, and a second group showing lower affinity which included the remaining antibodies (EC12, HA9 and CG12). This corresponded to information obtained by a phylogenetic tree generation analysing the evolutionary relationship of antibodies (Figure 2.3).

Furthermore, evaluation of antibody functional activity in MNT assays showed that affinity towards the antigen is not the sole contributor towards neutralization efficacy. This was evidenced by ID2 antibody which showed superior affinity in different formats towards a multitude of antigens but did not maintain the ability to neutralize virus as efficiently as JF7 or EC12 antibodies which were weaker binders in ELISA. Nevertheless, some binding is essential to retain any functional activity, as evidenced by tests against more diverged viruses such as WZ/606 and VN/38 to which antibodies were neither able to bind nor to neutralize.

A slight preference for IgG2a and not IgG1 format was found, but the differences were not big enough to provide statistical significance, with the exception of IgG2a CG12 that for unknown reasons displayed reduced binding and neutralizing activity. In addition, it was observed that antibody reformatting into scFv significantly affected functional activity of HA9 and JF8 antibodies, with the remaining four antibodies requiring noticeably but non-significantly higher concentrations of scFv vs full-length immunoglobulin molecules for virus neutralization. This could be explained by lost bivalency and other structural changes within the scFvs. Importantly, this work has established that for at least four antibodies tested herein, function is not mediated by Fc-Fc receptor interactions inducing effector functions such as ADCC, ADCP, CDC, such as

has been observed for several broadly cross-reactive neutralizing antibodies (150, 153, 380). In addition, in combination with previous knowledge, it is expected that the set of antibodies analysed herein function via binding near the receptor binding site of HA and preventing virion attachment to the host cell surface (330).

Overall, analysis of antibody sequences revealed a degree of diversification from original germline genes. Interestingly, antibodies with the least diversifications from original germline genes (JF7, EC12) were found to be most efficient against multiple H9 viruses when converted to different formats. Although binding avidity of scFvs, especially scFv JF7, to the antigen might have been impacted by lost antibody bivalence or other structural changes, scFv JF7 maintained superior neutralizing activity. Importantly, this study has established that antibody conversion to scFv format does retain functional activity, indicating antibody fragments could potentially be used for therapeutic purposes and hopefully achieving comparable effects to those obtained when using full length antibodies. In addition, the small size and lack of Fc region implies reduced immunogenicity, and overall, established a strong basis for future work and testing of scFv activity *in vivo*.

Chapter 3 CAN scFv ANTIBODIES PROVIDE PROTECTION AGAINST INFLUENZA VIRUS CHALLANEGE?

Adapted and expanded from “Engineered Recombinant Single Chain Variable Fragment of Monoclonal Antibody Provides Protection to Chickens Infected with H9N2 Avian Influenza” Lukosaityte et al., 2020 (381).

Avian influenza virus (AIV) poses a global health threat and a significant economic burden for poultry industry worldwide. Lack of effective control measures for avian influenza virus circulating in poultry requires the development of novel approaches that could limit virus spread in case of outbreaks or in animals whose lifespan is not long enough to gain protection after vaccinations. Chapter 2 has investigated a panel of monoclonal antibodies which were found to retain neutralizing activity *in vitro* when converted to scFv format. To test therapeutic scFv efficacy *in vivo,* two of the recombinantly produced scFv antibodies were chosen for prophylaxis and treatment of chickens infected with H9N2 UDL-1/08 virus. Birds treated with scFv antibody (200-300 µg/dose) showed reduced buccal shedding as opposed to non-treated controls during the peak of infection, indicating antibody therapy could be beneficial for controlling disease burden in some situations. Nevertheless, use of single antibody therapeutics led to changes in virus HA sequence due to potential escape mutant generation, indicating multiple antibodies targeting conserved epitopes should be combined for therapeutic purposes.

3.1 Introduction

3.1.1 Poultry pathogens, prevalence, and control of avian influenza virus

Viral and bacterial pathogens bring significant losses to the poultry industry and worldwide economy. Whilst the majority of the causative pathogens are restricted to avian hosts (e.g. infectious bursal disease virus (IBDV) and infectious bronchitis virus (IBV), others such as avian influenza virus, *Salmonella* or *Campylobacter* carry an additional risk of zoonosis (382-388). Further complications arise due to some of the pathogens, especially AIV, efficiently infecting migratory wild birds, facilitating virus spread across the globe (389, 390). Due to the low pathogenicity profile of H9N2 AIV, only causing signs of ruffled feathers and isolated behavioural changes, symptoms are often overlooked contributing to further virus spread (391). This has led to the H9N2 subtype becoming enzootic across Asia, Middle East, and Africa with an increasing threat of incursion into Europe (392, 393). In addition, occasional reports with a recent rise in cases indicate H9N2 AIV being able to infect humans leading to seroconversion; however, symptomatic disease manifestation remains unlikely (394). On the other hand, H7 and H5 AIVs with an intrinsic propensity for HPAI profile acquisition can infect both poultry and humans, resulting in a wide spectrum of symptoms and up to 100% or 40% mortality in these respective hosts (395). HPAI viruses like H5N1, H5N2 and H5N5, H5N6, H5N8 are also enzootic in parts of Asia, including Taiwan, China, the Middle East, and Africa, suggesting existing countermeasures are inadequate for both LPAI and HPAI viruses (396-398).

The current approaches used to tackle AIV are based on mass vaccination programs with whole inactivated virus vaccines, and, in some instances when sporadic disease outbreaks occur, a stamping out of poultry is implemented. One of the most successful preventative vaccination regimes to control AIV is

exemplified by H7N9 virus control in China (395). On the other hand, emergency vaccination against H5N1 in Hong Kong has also led to enhanced biosecurity and outbreak control (399). Unfortunately, regardless of the aforementioned examples, most of the vaccines for poultry are suboptimal, offering protection from clinical disease but not interfering with virus transmission and thus resulting in endemic AIV prevalence. Continuous virus evolution due to antigenic shifts and drifts results in vaccine strains becoming less antigenically relevant, requiring regular updates (400, 401). In addition, current use of whole virus vaccines grown in eggs does not allow easy differentiation between infected and vaccinated animals. It is also starting to raise ethical concerns and food supply reliability issues in panzootic and pandemic scenarios; hence, novel production systems, vaccine and therapeutic designs are being tested. Some of the main novel vaccine platform aims are: i) induction of the most broadly cross-reactive immune response that can be achieved by focusing on antigenicity of more conserved epitopes such as the HA stalk region, ii) induction of potent responses mediated not only by humoral but also by cellular immunity that could be harnessed by antigen delivery to antigen presenting cells, iii) induction of immune responses by the most antigenically relevant epitopes versus whole virus particles using recombinant protein vaccines or virus like particles that can incorporate multiple HA strains, iv) vaccines that allow differentiation between infected and vaccinated animals (DIVA) (159, 402-406). To further improve vaccine efficacy, novel delivery systems such as nanoparticles or virus vectored vaccines produced from cultured cells are considered (407, 408). Although well-matched and formulated vaccines remain superior control measures for preventative reasons, they have a major drawback of having a long immune response generation time, especially if vaccines need to be administered in case of outbreaks or in broiler flocks with a relatively short lifespan, suggesting a need for alternative countermeasures.

3.1.2 Antibody therapeutics against infectious pathogens

To reduce the impact and limit influenza virus infections, novel therapeutic approaches are being developed, including new chemical and biological modalities amongst which antibody therapeutics are considered as one of the most promising concepts. Passive immunization unlike conventional vaccines offers advantages of safety in immunosuppressed individuals, does not dependent on maternally derived antibodies (a crucial consideration in poultry) and avoids handling of partially virulent pathogens.

Depending on antibody ability to bind to specific antigens and their epitopes, the stage at which the virus life cycle will be halted and the mechanism of action does vary. For instance, HA-specific antibodies are most likely to interfere during the initial steps of infection, such as binding to host cell receptors or fusion, based on antibody affinity towards HA1 or HA2 domains, respectively, while anti-NA antibodies limit release of new virus particles (Figure 3.1) (166, 310).

However, not all antibodies can induce direct virus neutralization, with some requiring Fc-region-dependent functions leading to cell-mediated immune responses such as ADCC; however, in some instances the presence of an Fc-domain might also induce antibody dependent enhancement (ADE) (149, 150, 153, 409). ADE can potentiate host cell infection and, therefore, more profound pathogenesis due to increased rate of virus entry into host cells following antibody-antigen complex formation (410). Although the concept has been proven, the majority of the evidence for ADE gathered is based on a whole pool of antibodies generated post-vaccination, rather than single antibody isolated and used for therapeutic purposes (411). In addition, ADE is also dependent on Fc-Fc receptor compatibility. Nevertheless, if an Fc-region derived from one species is to be used in another, this can increase therapeutic antibody immunogenicity, or lead to the loss of function if this depends on binding to Fc receptors which might be incompatible (150, 412). To avoid

inaccurate engagement of cellular pathways by Fc domains, various antibody formats retaining only antigen specificity and lacking a constant region have been developed. One of such formats is scFv antibodies offering advantages during production and reduced immunogenicity.

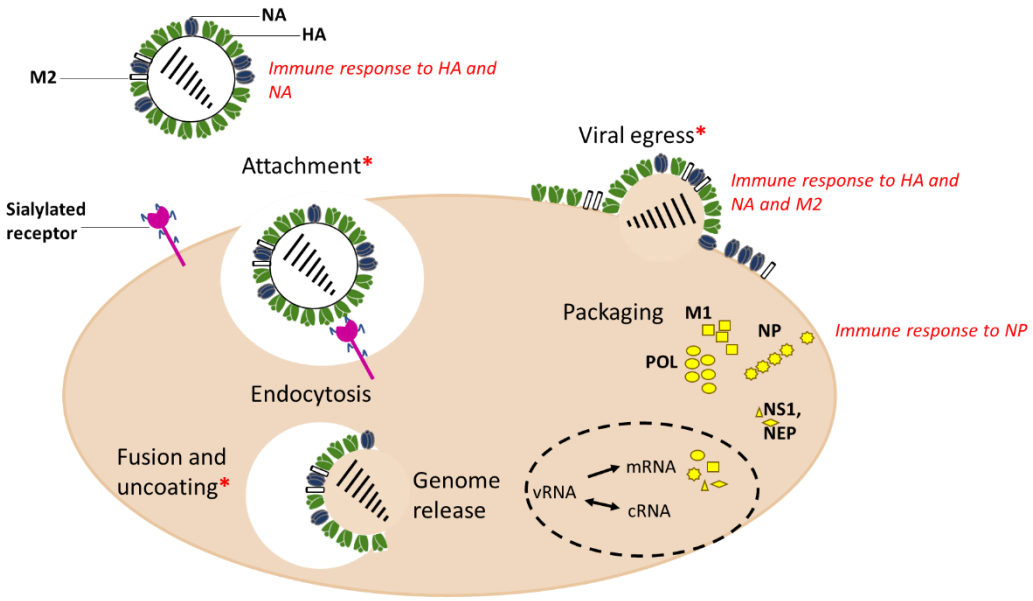

Figure 3.1. Influenza virus life cycle and antibody interference. Upon influenza virus entry into the body, HA initiates attachment to the sialylated host cell receptor. Antibodies targeting the HA head can interfere with this process by binding near the receptor binding site on HA. Endocytosis occurs (if antibody response is not sufficient to inhibit receptor binding) followed by pH mediated fusion of endosomal and viral membranes; this latter step can be inhibited by HA stem-specific antibodies. If fusion is successful, the virus genome is released to enter the nucleus where genome amplification and mRNA production takes place followed by mRNA trafficking to cytoplasm for translation. Some of the newly synthesised virus proteins re-enter the nucleus to support viral RNA synthesis while other components start coming into close proximity with cell surface where immune response might be elicited. Newly formed virions egress by budding from the plasma membrane and are released from the cell by NA-mediated activity. This step can also be prevented if NA-specific antibodies block the enzyme active site. * Indicates stages at which monoclonal antibodies might interfere.

It has been shown that passive immunization with antibodies against the most antigenically relevant virus proteins, delivered pre- or post- exposure to the virus via intravenous injection, intranasal inoculation or via virus vectors or in

a form of purified protein or nucleic acid can prevent disease and abort the virus life cycle in mice, non-human primates and even people (309, 318, 327). Currently, only limited information exists on whether antibody therapeutics would be a feasible approach for AIV control in poultry. Successful proof-of-concept development supporting passive immunization effectiveness and benefits to poultry could provide a basis and direct further research efforts.

3.1.3. Chapter objectives

- To assess if scFv antibodies retain their functionality in vivo when administered intranasally to poultry
- To evaluate if scFv antibodies can reduce infection in directly challenged birds for the proof-of-principle study
- To assess if scFv antibodies can reduce virus shedding into the environment and transmission to contact birds

3.2 Results

3.2.1 Intranasal antibody administration leads to reduced morbidity in birds

In chapter 2 it was observed that three out of six anti-HA antibodies tested retained their functional activity when converted to scFv format. Out of the three useful antibodies, scFv JF7 displayed highest activity in a biologically relevant microneutralization assay. Both CG12 and EC12 antibodies had variable light and heavy chains belonging to the same germlines and maintained similar neutralization profiles when converted to scFvs. When converted to full-length immunoglobulins containing mouse Fc regions, EC12 retained more uniform activity as opposed to CG12 which required much higher concentrations in an IgG2a format for a not well-established reason.

Therefore, for an assessment of scFv effect on disease manifestation, morbidity, and virus transmission *in vivo* scFvs JF7 and EC12 were chosen.

In short, naïve, specified pathogen-free (SPF) chickens were divided into five groups, three of which contained 20 birds each which were further subdivided into subgroups of 10 that received UDL-1/08 virus directly (5×10^5 PFU) or via contact. Chickens in group 1 were non-treated and challenged, in group 2 treated with scFv JF7 (200 µg/dose) and challenged, in group 3 treated with scFv EC12 (300 µg/dose) and challenged. Two additional groups were used for control purposes that were either scFv treated and non-challenged or non-treated and non-challenged, with the overall experiment terminated 14 days post challenge (Figure 3.2). The two different treatment doses were based on slightly different scFv neutralization profiles *in vitro* and were tailored so that the dose would not dramatically exceed 1 mg kg^{-1} delivered during the initial administrations (averaged values for scFv JF7 were 0.666 mg kg^{-1} and for scFv EC12, 1.008 mg kg^{-1}).

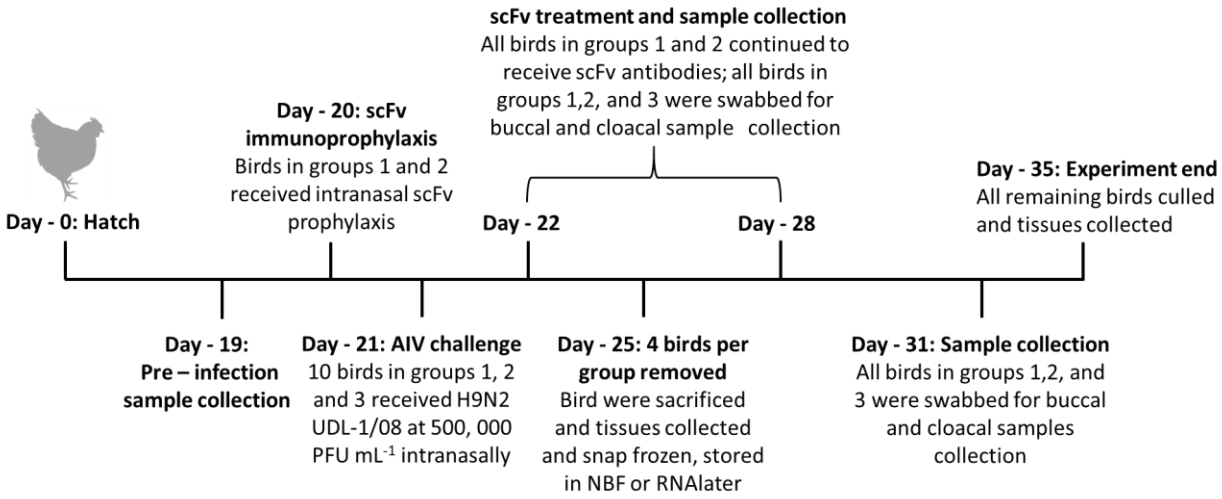

Figure 3.2. Summary of influenza virus infectivity, transmission, and pathogenicity *in vivo* study design. Two-day old (n=76) Rhode Island Red chickens were divided into five groups (n=20/group 1, 2, 3; n=6/group 4; n=10/group 5). All birds were swabbed at 19 days of age and birds from groups 1, 2, and 4 intranasally administered with scFv JF7 (group 1) or scFv EC12 (group 2 and 4) at day 20. Next day 10 birds from groups 1, 2 and 3 were intranasally challenged with 500, 000 PFU mL-1 of UDL-1/08. scFv treatment was continued for 7 days post-challenge in groups 1, 2, and 4. At day 4 post challenge 4 birds from groups 1, 2, 3 and 5 were removed for tissue harvesting. The experiment was terminated at day 35.

Virus infected birds did not demonstrate observable clinical signs (pale comb/wattles, nasal discharge, reddened eyes, snicking, ruffled feathers) in any of the groups throughout the length of study. However, differences in weight gain patterns on days 3 and 4 post challenge (coinciding with the peak of infection as defined by virus shedding), were observable. Amongst directly infected and non-treated birds 70% (7/10) and 30% (3/10) of directly infected and treated with scFv EC12 lost or did not gain weight on day 3 post-challenge (Figure 3.3a). On the other hand, all the birds treated with scFv JF7 were continuing to gain weight at day 3 post infection as were non-infected controls. This led to statistically significant differences between non-infected and infected, non-treated birds or infected, treated with scFv EC12 birds (Figure 3.3b). In addition, non-treated birds lost weight at a significantly higher rate than the scFv JF7 treated group. Nonetheless, two chickens from the latter

group lost 7 g and 17 g of weight next day (day 4 post-infection) leading to an average of ~2.6% and ~5.2% body mass loss with none of the other directly challenged birds continuing to lose weight at this time point (Figure 3.3c).

All birds serving as contacts that received either scFv JF7 or scFv EC12 were continuing to gain weight as opposed to non-treated challenged birds from which 30% (3/10) and 10% (1/10) lost or did not gain weight on days 3 and 4 post-challenge, respectively (Figure 3.3d). In addition, on day 3 post challenge non-treated birds infected by contact have also shown body mass loss as opposed to non-infected birds or chickens that received scFv EC12 prior and during infection (Figure 3.3e). Similarly with directly infected birds, chickens infected by contact and treated with scFv JF7 were showing a lag period in recovering body weight (Figure 3.3f).

Overall, weight changes indicated cease in weight gain of non-treated chickens infected either directly or by contact at day 3 post-challenge; however, all non-treated birds were starting to recover on day 4 post virus inoculation. In contrast, scFv JF7 or scFv EC12 treated birds infected directly or by sharing the same space, food and staying in proximity did not suffer from such a halt in weight gain when percentile average group weight was compared. To sum up, scFv prophylaxis and treatment against influenza virus ensured overall body mass increase at a steady rate in chickens.

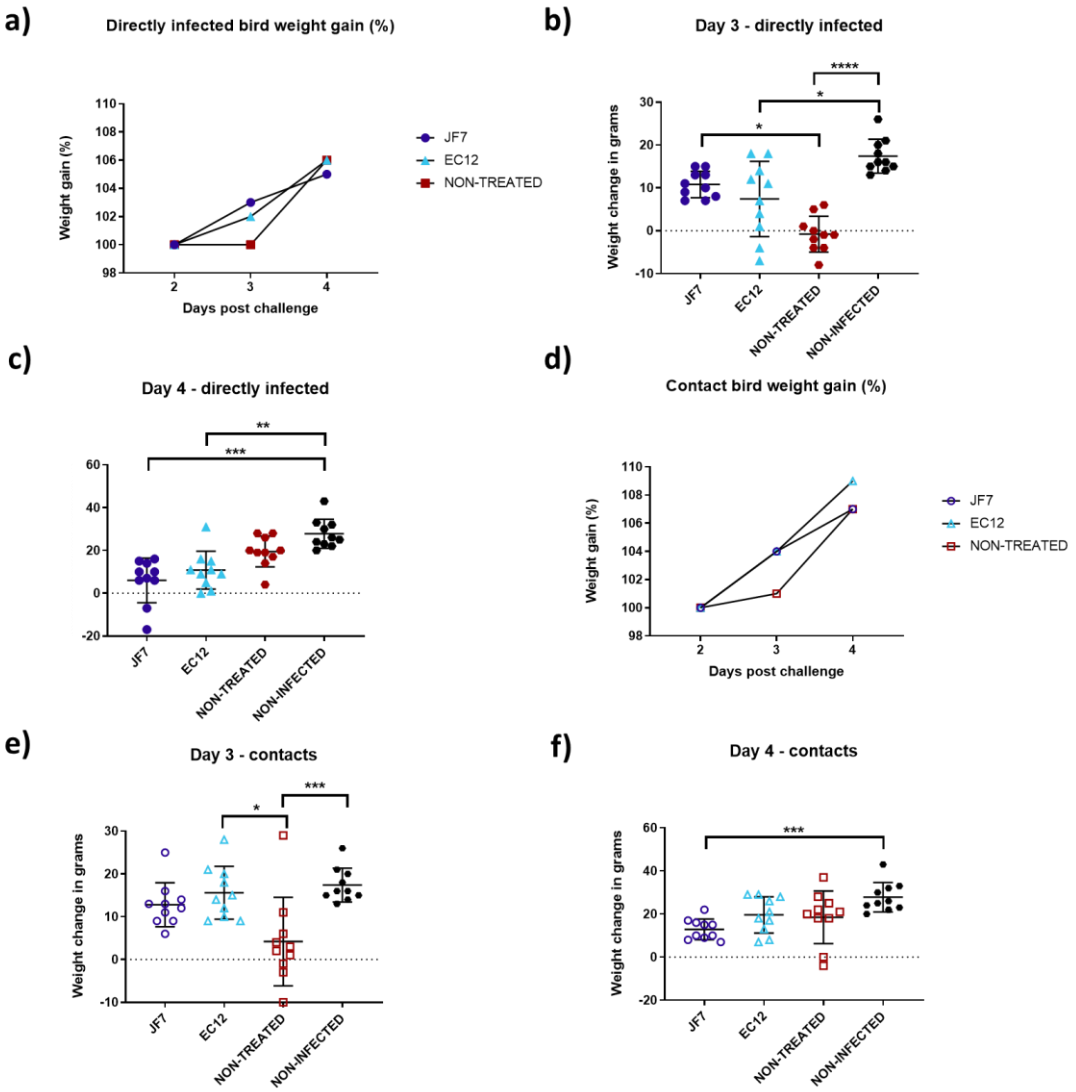

Figure 3.3. Weight changes in birds after H92 UDL-01/08 challenge and scFv treatment. Birds received scFv JF7 (200 µg/dose) or scFv EC12 (300 µg/dose) by intranasal route 24 hours before challenge with 5×10^5 PFU of UDL-1/08 followed by daily treatment till day 7 post virus inoculation. Body weight changes were recorded in grams with an average change recorded in **a)** directly infected and **d)** contact birds and more emphasis provided on days 3 **b, e)** and 4 **c, f)** post virus inoculation in **b, c)** directly infected and **e, f)** contact birds; non-infected and non-treated birds were used as a control with each dot representing an individual bird. Levels of significance were based on p-values from Kruskal–Wallis test (*p*-values of $P \leq 0.05$ were considered significant (Nonsignificant (Ns) = $p > 0.05$; * = $p \leq 0.05$; ** = $p \leq 0.01$; *** = $p \leq 0.001$; **** = $p \leq 0.0001$). Mean for each group ± SD indicated where applicable.

3.2.2 Intranasal scFv JF7 antibody therapy decreases infectious particle virus peak shedding

Having observed weight differences in chickens receiving antibody therapeutics and, the next aim of this study was to test the effect of intranasal scFv administration on virus shedding levels. For this purpose, buccal and cloacal swabs were collected daily from challenged birds and used in plaque assays to determine live virus titers as well as RT- qPCR to identify presence of the virus genome.

Virus recovery from buccal swabs of scFv JF7 treated birds indicated relatively similar virus titers for the first four days post-challenge (4600 - 19000 PFU mL^{-1}) followed by a sharp decline on day 5 post virus inoculation in the directly infected group (Figure 3.4a). On the other hand, non-treated birds had a more defined peak with higher virus titers on day 3 post-infection (~67500 ± 152101 PFU mL^{-1}), resulting in significant differences between the two groups (Figure 3.4e). Virus titers in non-treated infected birds declined more gradually than in scFv JF7 treated birds with no more virus observed by day 5 post-challenge. Shedding from the cloacal cavity was found to be more sporadic and resulting in much lower titers, with virus found in scFv JF7 treated directly infected birds starting at day 2 post-infection (~350 ± 1166 PFU mL^{-1}), peaking on day 3 (~650 ± 1821 PFU mL^{-1}) and gradually decreasing on day 4 (~11 ± 12 PFU mL^{-1}) with no more virus found from day 5 post-challenge (Figure 3.4b). Non-treated birds retained similar virus titers on days 3 (~335 ± 991 PFU mL^{-1}) and 4 (~23 ± 65 PFU mL^{-1}) post-challenge with the only difference on day 2 when none of the swab samples yielded live virus.

With regards to the contact birds, buccal swabs from those that received scFv JF7 indicated a reduced period of virus shedding, as all the birds in the group were able to clear virus by day 5 post-infection with the highest shedding recorded on days 2 (~9025 ± 10567 PFU mL^{-1}) and 3 (~9100 ± 9328 PFU mL^{-1}) (Figure 3.4.c). The non- treated counterparts once again had more defined shedding peak at day 3 post-challenge (~116000 ± 201695 PFU mL^{-1})

resulting in significant differences (Figure 3.4.e). Although virus titers were starting to decrease on day 4 in non-treated chickens swabs, birds were continuing to shed virus on day 5 post-challenge (~1125 ± 2208 PFU mL^{-1}) from buccal cavities leading to statistically relevant differences at this (Figure 3.4.f). As with directly infected birds, contacts were also shedding virus sporadically from cloacal cavities with virus detected in the non-treated group only on day 4 (~20 ± 66 PFU mL^{-1}) but in scFv JF7 treated birds on days 3 (~50 ± 112 PFU mL^{-1}) and 4 (~25 ± 66 PFU mL^{-1}) post-challenge. Overall, these data suggest that intranasal delivery of scFv JF7 can partially limit virus replication and shorten the infectious virus shedding period in both directly infected and contact birds.

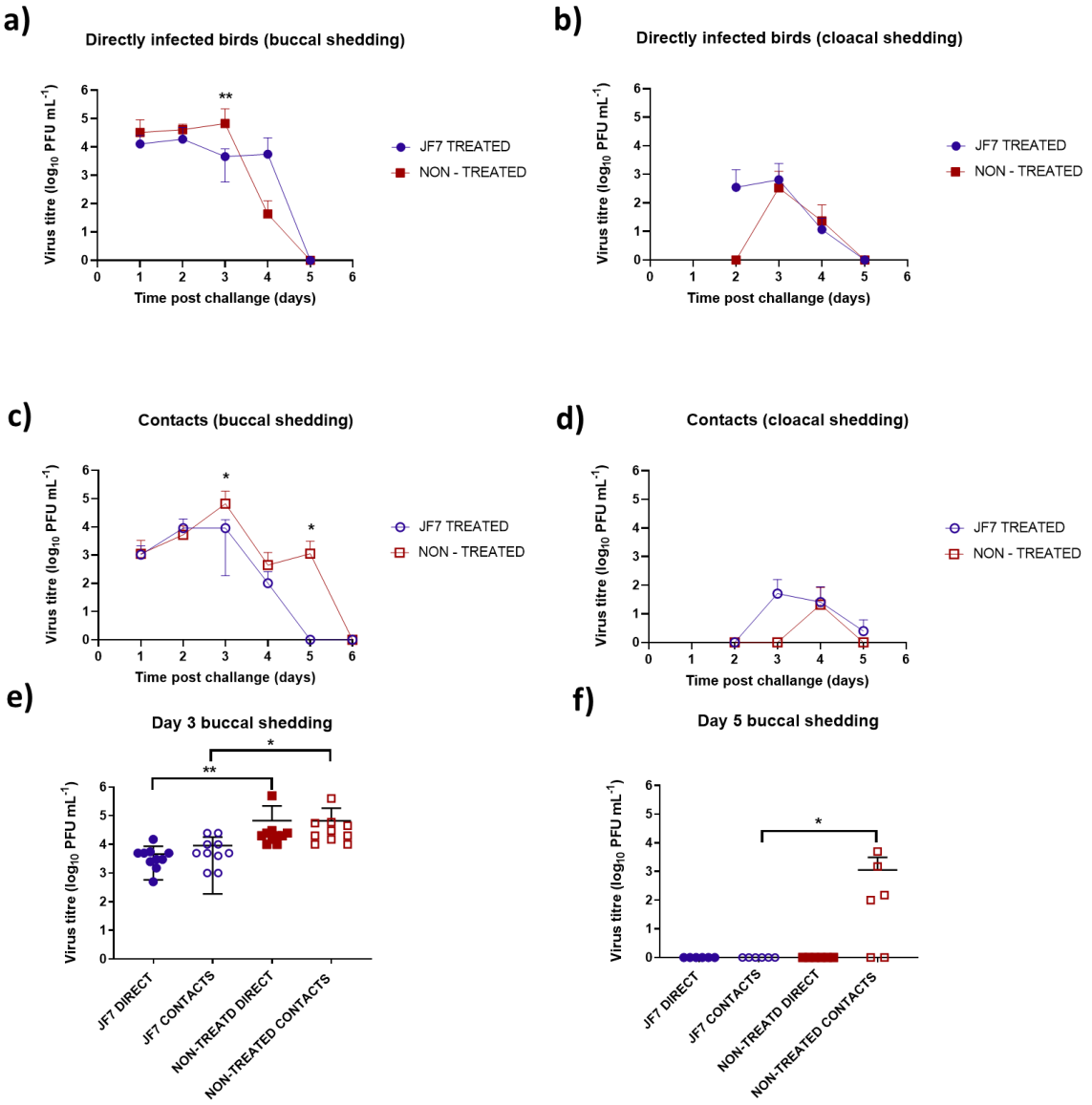

Figure 3.4. Virus shedding from buccal and cloacal cavity in scFv JF7 treated and non-treated birds. Chickens were infected with 5 × 10^5 PFU of UDL-1/08 and daily administered with 200 µg/dose of scFv JF7 by intranasal route starting at day -1 and continued until day 7 post-challenge. Viral titers were determined by plaque forming assay. Mean infectious virus titers from **a)** buccal and **b)** cloacal cavities of directly infected birds; **c)** Mean infectious virus titers from buccal and **d)** cloacal cavities of contact birds; **e)** buccal shedding titers from directly infected and contact birds at day 3 and **f)** day 5 post-challenge with each dot representing individual bird. Levels of significance were based on p-values from Kruskal–Wallis test (Nonsignificant (Ns) = $p > 0.05$; * = $p \leq 0.05$; ** = $p \leq 0.01$; *** = $p \leq 0.001$; **** = $p \leq 0.0001$). Mean for each group ± SD indicated where applicable.

3.2.3 Intranasal scFv EC12 antibody therapy decreases peak virus shedding but prolongs its duration

To evaluate the therapeutic efficacy of scFv EC12, a similar experiment was performed. As indicated in section 3.2.2, live virus recovery from buccal swabs of non-treated directly infected birds reached peak titers at day 3 post-challenge, followed by a sharp decline and complete virus clearance by day 5 post-infection (Figure 3.5.a). EC12 treated birds were found to contain marginally lower titers of infectious virus particles throughout the infection except from day 3 post-challenge (~5250 ± 4421 PFU mL^{-1}) when differences between treated and non-treated directly infected birds differed by at least 10-fold and were found to be significant. All virus in the scFv EC12 receiving group was cleared by day 5 (Figure 3.5.a). Next, virus titers were measured in cloacal swabs, indicating minimal shedding on day 3 and 4 post-infection in both groups with higher titers found on day 3 post virus inoculation, but with only marginal differences between two groups (Figure 3.5.b).

In scFv EC12 treated birds infected by contact, virus titers remained lower than in non-treated birds until day 4 post-challenge, with significantly lower titers found only on day 3 post-infection (~2525 ± 6233 PFU mL^{-1}) (Figure 3.5.c). Interestingly, some of the treated birds were found to have more persistent virus replication as indicated by continuous shedding till day 6 post-challenge (~120 ± 216 PFU mL^{-1}). A similar virus shedding profile was also found after assessment of cloacal swabs, with birds that received scFv EC12 continuing to shed virus on days 4 (~700 ± 2213 PFU mL^{-1}) and 5 (~2 ± 4 PFU mL^{-1}) post-challenge as opposed to non-treated birds which were only positive for live virus on day 4 (Figure 3.5.d). However, cloacal sampling was only sporadic with only 1 out of 10 and 1 out of 6 birds being positive in the treated group on respective days. In general, scFv EC12 was found to supress virus shedding during the peak of infection in both directly infected

and contact groups, but it potentially also contributed to more persistent infection in a fraction of the contact birds.

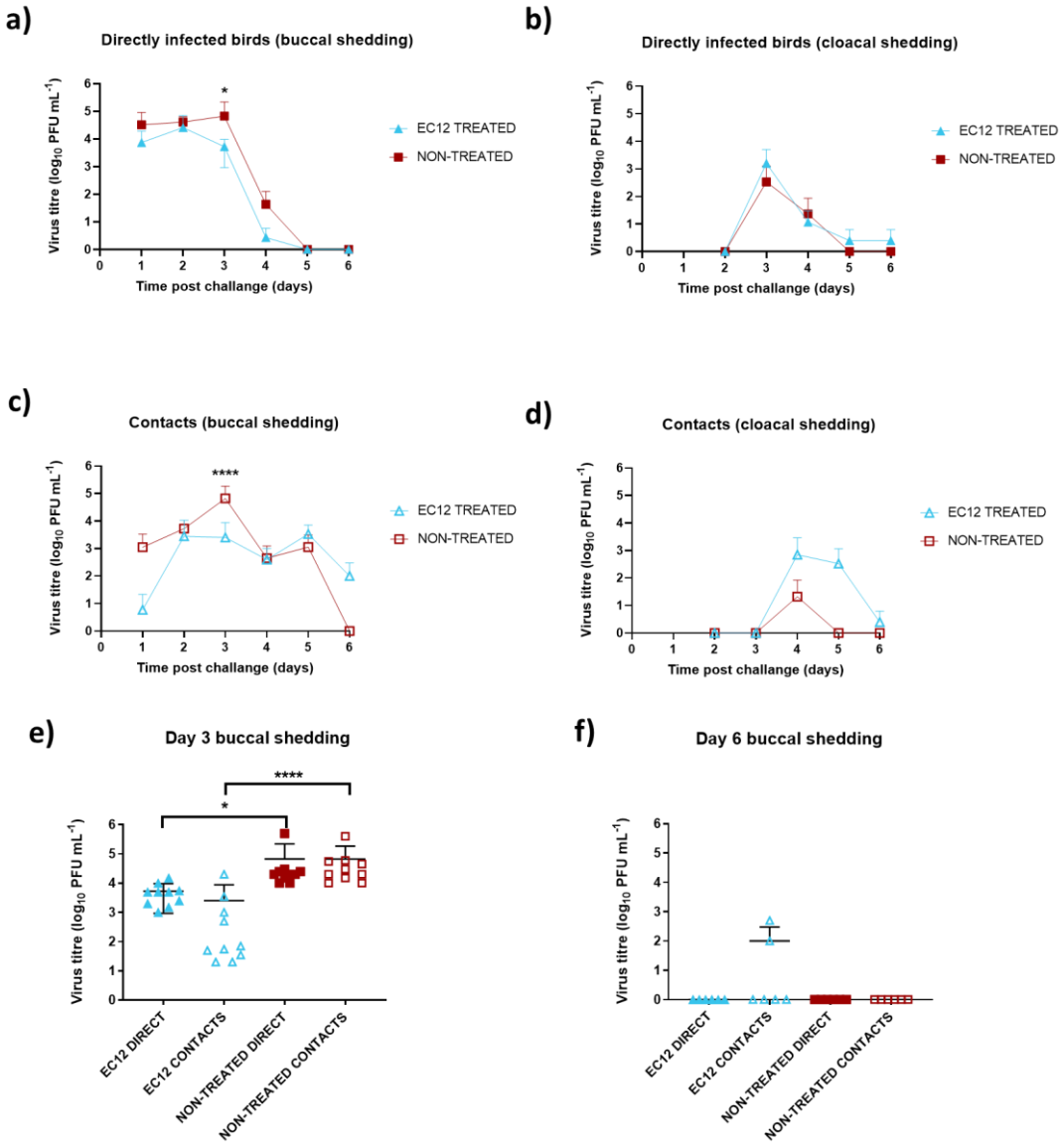

Figure 3.5. Virus shedding from buccal and cloacal cavity in scFv EC12 treated and non-treated birds. Chickens were infected with 5 × 10^5 PFU of UDL-1/08 and daily administered with 300 µg/dose of scFv EC12 by intranasal route staring at day -1 and continued until day 7 post-challenge. Viral titers were determined by plaque forming assay. Mean infectious virus titers from **a)** buccal and **b)** cloacal cavities of directly infected birds; **c)** Mean infectious virus titers from buccal and **d)** cloacal cavities of contact birds; **e)** buccal shedding titers from directly infected and contact birds at day 3 post-challenge and **f)** day 6 post-challenge with each dot representing individual bird. Levels of significance were based on p-values from Kruskal–Wallis test (Nonsignificant (Ns) = $p > 0.05$; * = $p \leq 0.05$; ** = $p \leq 0.01$; *** = $p \leq 0.001$; **** = $p \leq 0.0001$). Mean for each group ± SD indicated where applicable.

3.2.4 Differences in virus titers in buccal swab samples can be seen by ELISA

To further confirm differences seen by plaque assay, day 3 post-challenge swab samples were subjected to ELISA for viral antigen. Briefly, an assay was developed using swab samples for ELISA plate coating in duplicates and probing by anti-NP antibody for virus. OD 450/630 nm values were read and used for further analysis. The results, indeed, indicated statistically significant differences between scFv JF7 or EC12 treated and non-treated birds infected directly or by contact, and scFv EC12 treated and non-treated birds infected by contact (Figure 3.6.a, b). Nevertheless, this statistically significant difference was found to disappear between contact infected scFv JF7 treated and non-treated birds, reflecting the poor significance value (p=0.0222) observed previously by plaque forming assay (Figure 3.4.c).

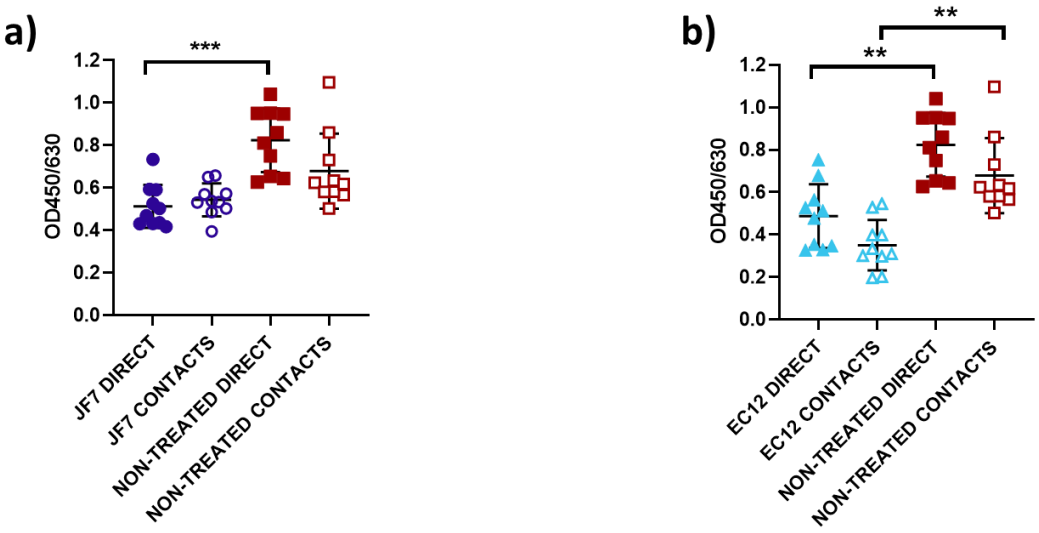

Figure 3.6. Virus antigen levels in buccal swab samples measured by ELISA. Viral titers were determined by measuring levels of NP protein by an anti-NP specific monoclonal antibody. OD450/630 values comparing **a)** scFv JF7 treated vs non-treated birds infected directly or by contact and **b)** scFv EC12 treated vs non-treated birds infected directly or by contact were assessed. Levels of significance were based on p-values from Kruskal–Wallis test (Nonsignificant (Ns) = $p > 0.05$; * = $p \leq 0.05$; ** = $p \leq 0.01$; *** = $p \leq 0.001$; **** = $p \leq 0.0001$). Mean for each group ± SD indicated where applicable.

Overall, this indicates that the NP ELISA could be used to measure virus levels for an initial analysis, providing a good indication for results, but another method of confirmation might be needed to check for assay-to-assay variability.

3.2.5 Intranasal scFv administration does not affect the ability of virus to reach and replicate in internal organs

The known tropism of avian inflIuenza virus towards the respiratory tract and digestive system of poultry led us to investigate if scFvs could limit virus dissemination *in vivo*. For this purpose, some of the most susceptible tissues including nasal turbinates, trachea, lung, spleen and cecal tonsils were harvested at day 4 post-challenge and snap frozen prior to subsequent homogenisation and live virus titration by plaque assay. No infectious virus particles were found in lung, spleen or cecal tonsils (data not shown), however, low levels were recovered from nasal turbinates and trachea (Figure 3.7). With regards to nasal turbinates, virus was found in 1 out of 4 birds treated with scFv JF7 infected directly or by contact as opposed to 2 out of 4 and 3 out of 4 birds that were non-treated and infected directly or by contact, respectively (Figure 3.7.a). On the other hand, none of the scFv EC12 treated birds that received virus inoculum were positive for infectious influenza particles in nasal turbinates whereas 3 out of 4 contacts had virus to an average level of ~112 ± 159 PFU mL^{-1}. Virus recovery from tracheas replicated the same situation of nasal turbinates within scFv JF7 treated groups and the non-treated directly infected group, while only 1 out of 4 birds from non-treated contacts was found to have virus in the trachea (Figure 3.7.b). As seen previously, none of the directly infected birds treated with scFv EC12 had virus in trachea and only 1 out of 4 was positive in contacts group. To sum up, it appeared that virus dissemination was more profound in superficial tissues and primary sites of infection such as nasal turbinates rather than internal organs with fewer birds

testing positive if they were treated with scFv JF7 or scFv EC12 and infected directly. This effect was not large enough to conclude that scFv treatment had any major effect on virus dissemination *in vivo* however.

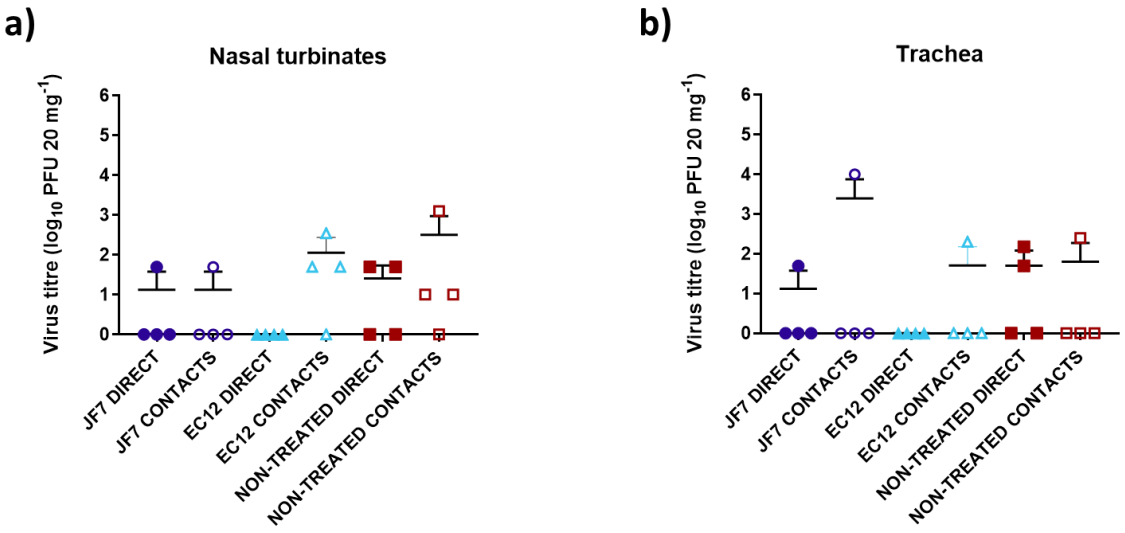

Figure 3.7. Virus detection in tissues from scFv JF7, scFv EC12 treated and non-treated birds. Chickens were infected with 5×10^5 PFU of UDL-1/08 and daily administered with 200 µg/dose of scFv JF7 by intranasal route starting at day -1 and continued until day 7 post-challenge. Viral titers were determined by plaque forming assay in **a)** nasal turbinates and **b)** trachea collected at day 4 post challenge. Levels of significance were based on p-values from Kruskal–Wallis test with *p*-values of $P \leq 0.05$ were considered significant (Nonsignificant (Ns) = $p > 0.05$; * = $p \leq 0.05$; ** = $p \leq 0.01$; *** = $p \leq 0.001$; **** = $p \leq 0.0001$). Mean for each group ± SD indicated where applicable.

3.2.6 Virus genome measurement confirms differences in virus levels during the peak infection, and prolonged shedding in scFv EC12 treated birds infected by contact

To further investigate if the differences in virus replication between treated and non-treated birds could be seen, RT-qPCR to measure M gene transcripts was performed on RNA extracted from buccal swab samples and compared to a segment standard curve to calculate genome copy numbers. M gene transcript

levels were found to remain similar throughout days 1 to 6 post challenge in scFv JF7 treated birds infected directly or by contact, while non-treated birds were found to have higher genome levels on day 1 post challenge that started to decrease from day 2 onwards (Figure 3.8 a, b). Importantly, agreeing with what was seen by plaque assays, statistically significant differences between challenged scFv JF7 treated and non-treated birds were found on day 3 post-infection regardless of the route of infection. In addition, a significant difference was found on day 1 post-challenge in the directly infected group, with more M gene transcripts observed within non-treated birds. Conversely, the difference seen on day 5 post virus inoculation in the contact group was found to be insignificant by genome copy number assessment. Similarly, statistically significant differences on day 1 post-infection were found between non-treated and scFv EC12 treated birds infected directly or by contacts, which was not observed by live virus titration (Figure 3.8 c, d). On the other hand, differences on day 3 post-challenge between scFv EC12 treated and non-treated birds retained statistical significance in directly infected or contact birds. In addition, an increase of M gene transcripts in scFv EC12 treated birds was noted on day 5 post-infection. Overall, this indicates that both live virus and M gene transcripts levels were impacted by scFv treatment during the peak of infection.

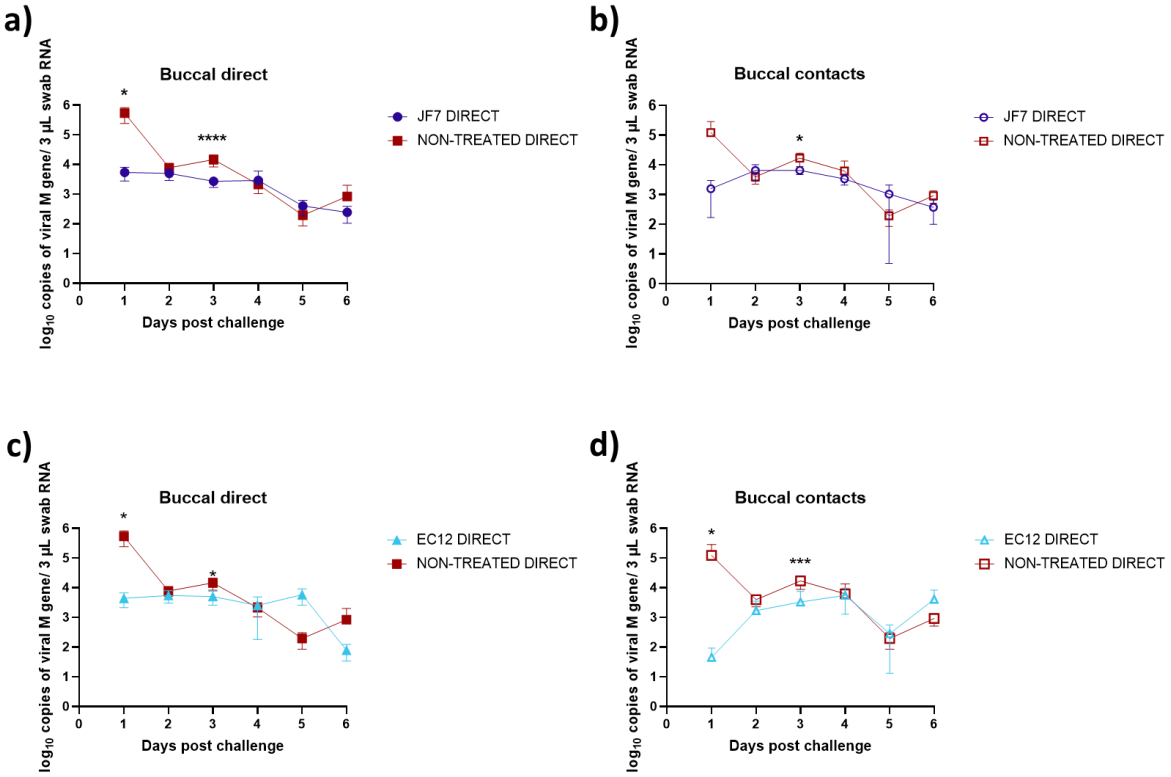

Figure 3.8. Virus M gene transcript levels in buccal swab samples. RNA was extracted from buccal swab samples and RT-qPCR performed to measure M gene transcripts in **a)** scFv JF7 treated vs non treated birds infected directly; **b)** scFv JF7 treated vs non treated birds infected by contact; **c)** scFv EC12 treated vs non treated birds infected directly; **d)** scFv EC12 treated vs non treated birds infected by contact. Kruskal–Wallis test with *p*-values of $P \leq 0.05$ were considered significant (Nonsignificant (Ns) = $p > 0.05$; * = $p \leq 0.05$; ** = $p \leq 0.01$; *** = $p \leq 0.001$; **** = $p \leq 0.0001$). ± SD indicated where applicable.

3.2.7 All birds become seroconverted after virus challenge regardless of scFv therapy

Next, this study aimed to see if antibody therapeutics would not impede immune response generation in challenged birds, as the protective scFv efficacy was not sufficient to completely halt virus replication. Hemagglutinin inhibition (HAI) assays were performed using homologous UDL-1/08 virus with

pre-infection serum and serum collected on days 4 and 14 post-challenge. As expected, none of the birds before infection had antibodies able to bind to HA and, therefore, inhibit subsequent red blood cell agglutination (Figure 3.9.a). An immune response could be detected on day 4 post-infection, with relatively higher titers in directly infected groups than in contact birds regardless of whether scFv treatment was administered or not (Figure 3.9.b). Interestingly, higher HAI titers at day 4 post-infection (indicating earlier seroconversion) were found in chickens that had lower virus levels (as suggested from swab samples and tissues), such as scFv JF7 contact birds than scFv EC12 treated or non-treated birds that were previously found to contain higher infectious virus levels. Nevertheless, all birds had seroconverted (using a cut-off for seroconversion defined as HI > $Log_2$4) by day 14 post-challenge, with HAI titers ranging between 256 and 4096 with no differences found between groups (Figure 3.9.c). These data suggest that scFv prophylaxis and therapy does not delay or interfere with immune response generation if therapy is not 100% efficient.

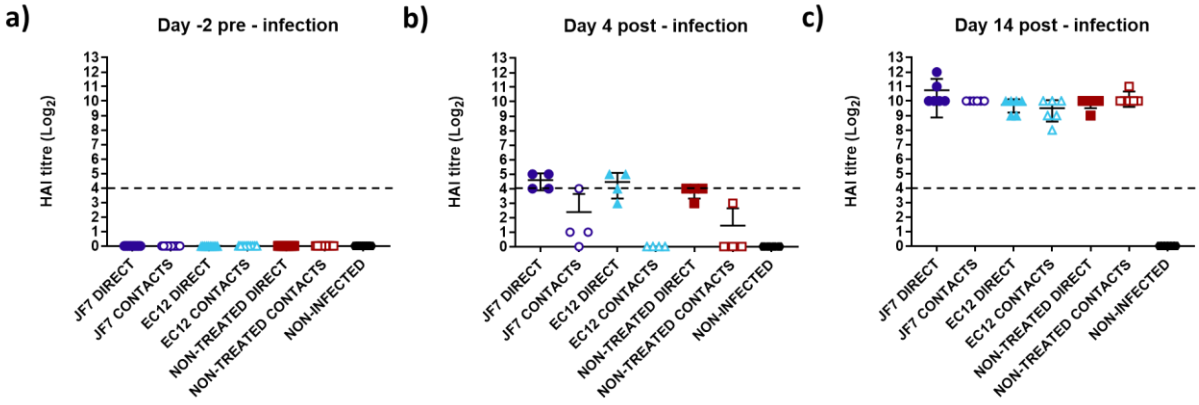

Figure 3.9. HI titers of (non)challenged and scFv treated or non-treated birds. HI titers were measured to assess pre-infection levels and post-infection seroconversion at various time points including **a)** two days before challenge, **b)** 4 days post-challenge and **c)** 14 days post-challenge. HI > $Log_2$4 was considered positive indicated by dotted line. Mean for each group ± SD indicated where applicable.

3.2.8 Higher inflammatory responses were formed within non-treated bird group

The effect of scFv administration on cytokine induction during the virus infection was tested next. Levels of proinflammatory gene transcripts encoding IL-4, IL-6 and IFNγ were measured by RT-qPCR using RNA derived from tissue samples representing the main sites of infection or immune response, including nasal turbinates, trachea, lung, spleen and cecal tonsils harvested at day 4 post-challenge. 28S ribosomal RNA was used as a reference host transcript for data normalisation. No amplification was detected for IL-4 gene transcripts in any of the tissues; in addition, no amplification was found for IL-6 cytokine transcripts in nasal turbinates (data not shown). Although, IFNγ gene transcripts were amplified successfully no differences were found in IFNγ response in any of the tissues for any of the birds over the background of controls as indicated in Figure 3.10. Comparison of 40 - ΔCT values in IL-6 responses, correlating to T-cell differentiation and B-cell maturation, revealed no changes in respiratory tract organs (trachea and lung) over the background levels of non-infected birds (Figure 3.11 a, d). The same outcome was found when IL-6 transcripts were measured within cecal tonsils; however, patterns of IL-6 induction were significantly different within spleen tissue (Figure 3.11 b, c), which is considered to be a peripheral lymphoid organ in chickens (413). Differences in IL-6 responses were found between non-infected and non-treated birds infected directly or by contact, as well as between non-treated and treated with scFv JF7 antibody groups infected either after direct virus inoculation or by space sharing and proximity (Figure 3.11 c). On the other hand, there were no significant differences between non-treated and scFv EC12 treated birds suggesting IL-6 induction in the latter group regardless of the route of infection (Figure 3.11 c). In conclusion, IL-6 transcript levels in spleen correlated with lower virus replication seen in swab samples and

suggests a more widespread inflammatory state in non-treated UDL-1/08 virus challenged birds.

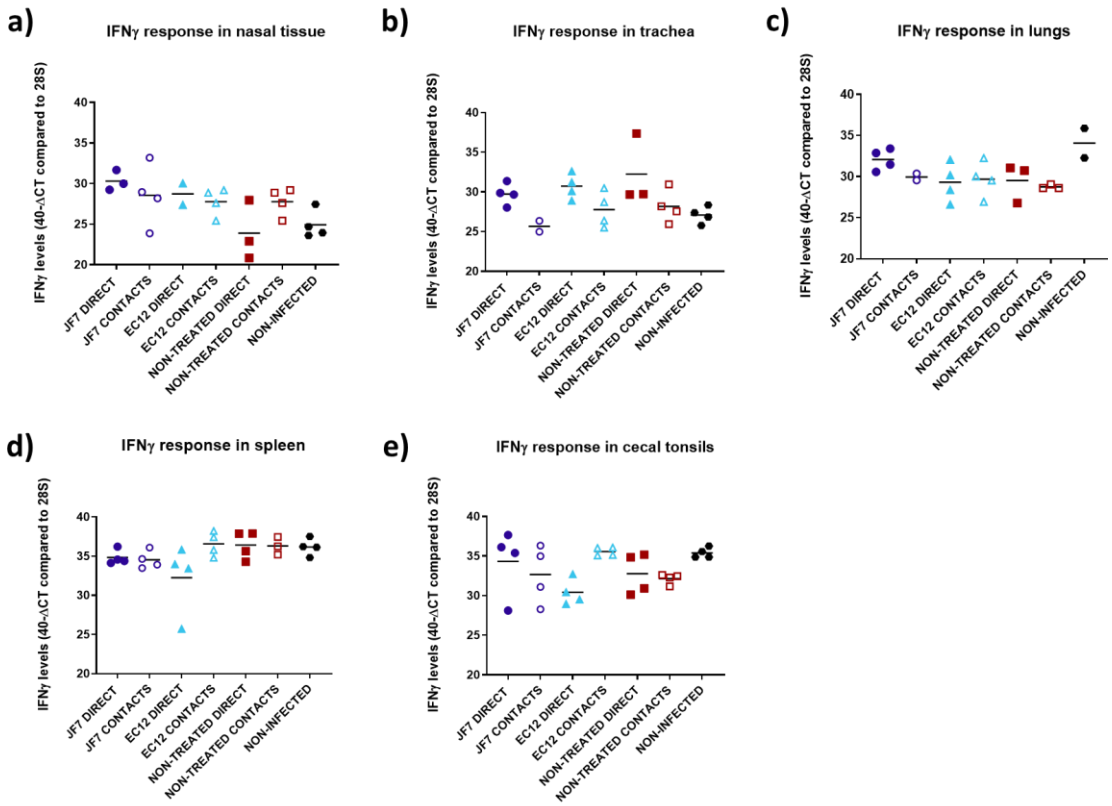

Figure 3.10. IFNγ mRNA expression in tissues of (non)challenged and scFv treated or non-treated birds. RNA was extracted from bird tissues **a)** spleen; **b)** cecal tonsils; **c)** lungs; **d)** trachea; **e)** nasal tissue and RT-qPCR performed for the IFNγ transcripts as well as 28S rRNA as a reference RNA. Values are represented as 40-ΔCT values after normalization to 28S rRNA with means for each group indicated. A one-way ordinary ANOVA test was run for statistical analysis. *p*-values of $P \leq 0.05$ were considered significant (Nonsignificant (Ns) = $p > 0.05$; * = $p \leq 0.05$; ** = $p \leq 0.01$; *** = $p \leq 0.001$; **** = $p \leq 0.0001$).

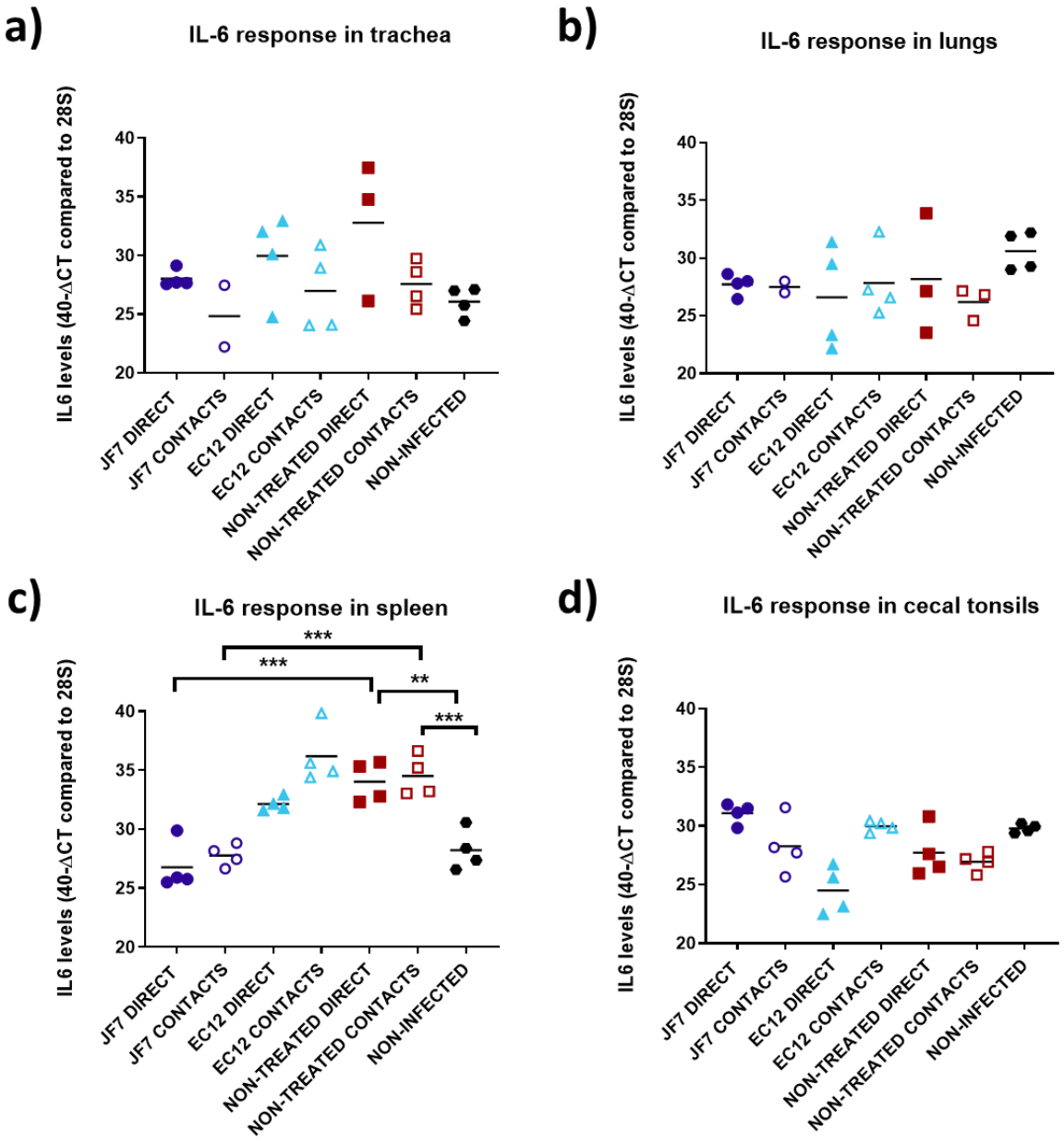

Figure 3.11. IL-6 mRNA expression in tissues of (non)challenged and scFv treated or non-treated birds. RNA was extracted from bird tissues **a)** spleen; **b)** cecal tonsils; **c)** lungs; **d)** trachea and RT-qPCR performed for the IL-6 transcripts as well as 28S rRNA as a reference RNA. Values are represented as 40-ΔCT values after normalization to 28S rRNA with means for each group indicated. A one-way ordinary ANOVA test was run for statistical analysis. *p*-values of $P < 0.05$ were considered significant (Nonsignificant (Ns) = $p > 0.05$; * = $p \leq 0.05$; ** = $p \leq 0.01$; *** = $p \leq 0.001$; **** = $p \leq 0.0001$).

3.2.9 scFv therapeutics induce virus escape mutant formation

The previously seen trend of prolonged infection in scFv EC12 treated chickens infected by contact led to the hypothesis that viral escape mutants might be formed after the challenge, following treatment of antibodies binding next to the HA RBS. This was tested by HA1 gene sequencing using nucleic acid recovered from day 4 post-infection swab samples from the birds confirmed to carry the highest virus loads from each group. This included 5 samples (2 direct and 3 contacts) from the group treated with scFv JF7, 6 samples (2 direct and 4 contacts) from scFv EC12-treated group and 4 (2 direct and 2 contacts) from the non-treated control group. The virus inoculum used to challenge birds served as a further control. All sequences were aligned with the UDL-1/08 HA gene sequence deposited in the NCBI database (accession number CY038466). No changes from the publicly available sequence were found in the virus that was used for inoculation or in the swab samples from non-treated birds, whether infected directly or by contact. Contrarily, some virus samples from birds that received scFv JF7 or EC12 treatment were found to carry three simultaneously occurring non-synonymous single point mutations causing the following amino acid changes: K147N, L212P, I217T (H9 numbering used throughout) (Figure 3.12 b, c, d). Mutations were found in 1 out of 5 samples from the scFv JF7 treated group in the swab belonging to a directly infected bird and in 2 out of 6 samples (1 directly infected and 1 contact) from scFv EC12 treated birds. Importantly, mutations at positions 212 and 217 are located near the HA RBS (Figure 3.12. a) and have been previously implicated in immune escape variant formation (together with other amino acid changes at positions 145, 183, 234) when UDL-1/08 was cultured in the presence of hybridoma derived antibodies in vitro (330). Position 147 is located outside of RBS. Overall, data – the data support the hypothesis that escape mutants were generated by the scFv treatment.

To analyse if the mutations found here were relevant only to this study or are present in already circulating H9 subtypes, HA gene sequences deposited to publicly available Influenza Research database were analysed to compare amino acid variation at residues 147, 212 and 217. Alignment of 6500 H9 HA sequences available and extracted from Influenza Research Database (no filter for date range or geographical restrictions for sequences was applied) showed the consensus amino acid at position 147 being Lys, followed by a small fraction of viruses containing Glu, Asn, Arg, Gln and Thr (Table 3.1). On the other hand, position 212 was dominated by Leu with the next most common residues being Ile, Arg, His, Pro and Phe, while Met was the most common amino acid at position 217 but with a high incidence of Gln, Ile and Thr. Thus all mutations that occurred in this study are substitutions to residues that are present in viruses naturally circulating in poultry.

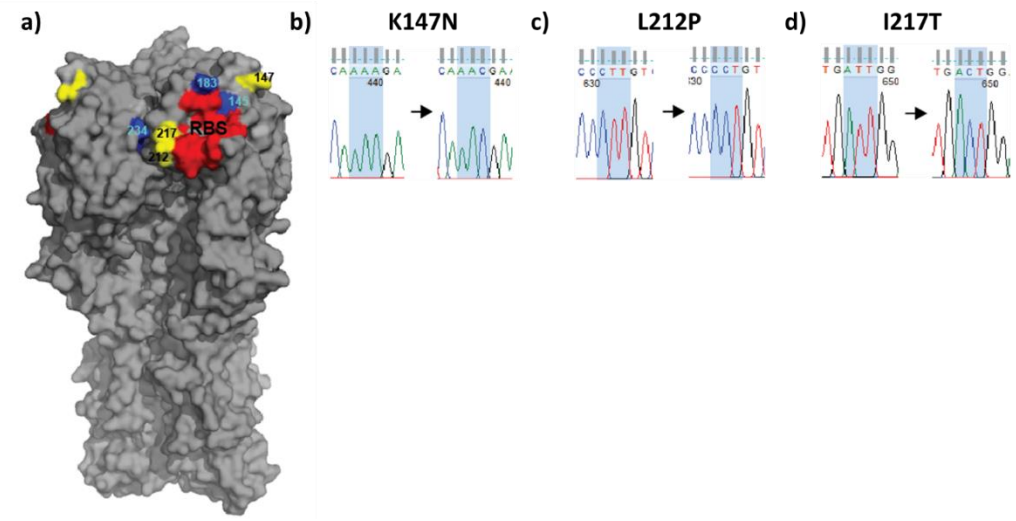

Figure 3.12. Locations of mutant residues and sequencing traces. a) HA head is in grey, receptor binding site (RBS) in red with highlighted residues P92, G128, T129, S130, S131, A132, W143, N173, V180, L184, Y185, N214, G215, L216, G218 and R219. Mutations recorded in this study are in yellow at positions 147, 212 and 217. Mutations found previously with monoclonal antibodies derived from hybridoma clones F965-ID2, F965-JF7 and F965-EC12 are in blue. Numbering and figure is based on mature H9 protein (PDB ID 1JSD), and figure generated using PyMOL software. **b)** K147N resulting from one nucleotide substitution; **c)** L212P resulting from one nucleotide substitution; **d)** I217T resulting from one nucleotide substitution

Table 3.1. Analysis of single nucleotide polymorphisms within the H9 HA gene. 6500 H9 HA sequences were downloaded from the Influenza Research Database and the incidence of each amino acid at positions 147, 212 and 217 assessed.

POSITION	CONSENSUS	ALA	ARG	ASN	ASP	CYS	GLN	GLU	GLY	HIS	ILE	LEU	LYS	MET	PHE	PRO	SER	THR	TRP	TYR	VAL
147	LYS		4	5	1		4	6			1	1	6468			1		2			
212	LEU		19							12	58	6368			10	11	1	4			6
217	MET	2	2	1			1398			4	654	4		4383	2			41			1

In general, even though scFv can limit virus replication to some extent, identification of virus mutants formed following scFv treatment suggests single antibody administration is likely to induce faster antigenic drift due to pressure

generated only towards a single antigenic epitope. This indicates a need for careful selection of therapeutic antibodies.

3.3 Discussion

The assessment of the therapeutic potency *in vivo* of two HA1 targeting antibodies performed herein is a follow up from Chapter 2, where monoclonal antibodies and their scFvs were generated recombinantly using hybridoma derived immunoglobulin variable domain sequences and characterised for specificity against an array of H9N2 viruses (330). On the basis that passive immunization would be aimed at poultry, chickens, being economically and epidemiologically important hosts of AIV (406, 414, 415), were selected as an animal model for this study. In short, after assessment of live virus titers measured by plaque assays and M gene transcript levels measured by RT-qPCR, it was found that scFv prophylaxis and treatment led to lower virus titers in buccal swabs during the critical stages of infection (more specifically day 3 post-challenge) when compared to non-treated controls. In addition, scFv JF7 treated birds infected by contact had a reduced virus shedding period while scFv EC12 treated, directly infected birds had a slightly earlier infection peak. This also affected weight gain patterns, indicating a lower disease burden in birds that received passive immunization. This could be an important factor considering the impact and value of each gram lost per bird and the total amount it would contribute to if the whole poultry chain was affected.

Interestingly, estimation of M gene transcript levels showed higher amounts of virus genome in non-treated birds at day 1 post-infection that was not observable by plaque assay, suggesting either a higher level of non-infectious particles containing genome generated during this initial stage post-challenge in non-treated birds, or perhaps the result of non-standardised RNA concentrations used for RT-qPCR. In addition, it was noted that scFv administration did not impact natural immune response formation after

intranasal challenge as assessed by seroconversion levels, also agreeing with previous reports that indicate day 4 post-infection as a starting point for positive HI titers in chickens (416). As all birds became seroconverted after the challenge it would be interesting to investigate if scFv treatment and induction of virus escape mutants has led to generation of potentially more cross-reactive serum with heterologous HA antigens. In this instance, this was outside the scope of the project.

Several similar studies investigating monoclonal antibody efficacy against HA of influenza virus have been performed in other species including but not limited to mice, ferrets, non-human primates, swine and even humans, demonstrating the potential for this approach (150, 155, 327, 417). Although a few studies tried to assess the effect of antibodies targeting other virus antigens such as NA, NP or M, with some demonstrated success, the major focus remains on HA due to high antigen exposure and easy access for monoclonal antibodies that can support a robust inhibitory effect (417-419). However, the limitation of anti-HA antibodies often comes at a cost of antigenic flexibility allowing virus escape mutant formation (327, 420), as also likely seen in this study. To avoid this, HA2 subunit specific antibodies are preferred over HA1 targeting immunoglobulins for two major reasons: i) higher HA2 conservation amongst heterologous viruses increases antibody breadth; ii) higher conservation comes at greater fitness costs for the virus to form immune escape mutants (143, 332, 334). Such broadly neutralizing antibodies can be exemplified by MEDI8852, CR6261 or F16 that are more likely to interfere with virion and endosomal membrane fusion rather than initial attachment to the host receptor(153, 332, 334). Nevertheless, in several instances the activity of broadly neutralizing antibodies has been demonstrated to depend on Fc-region function, restricting the species in which a particular immunoglobulin would remain functional (149, 150, 229). In addition, although HA is the major antigenic determinant of influenza virus, epitopes located within the HA stem

are often of limited accessibility, partially compromising usage of such antibodies and potentially necessitating increase in dosages for administration and thus associated costs for antibody production. It is expected that antibodies in this study were inhibitory during initial virus attachment rather than later stages.

scFv antibody format was chosen for passive immunization purposes after it was shown to be as effective at neutralising virus as full-length monoclonal antibody *in vitro* in Chapter 2, with the anticipation that the scFv functional profile would remain similar *in vivo*. Obtaining proof-of-principle that scFv antibodies can retain functionality *in vivo* was aimed to establish a future premise to generate a 'polyclonal' antibody format containing several scFvs targeting different virus epitopes and, therefore, increasing the breadth and versatility of antibody therapeutics. Such multivalent molecule generation would aid not only in targeting multiple epitopes but would also contribute to higher stability and pharmokinetical profile due to an increased molecule size. Similar concepts have been looked at with single domain antibodies, as illustrated by the generation of multivalent MD3606 antibody and its subsequent linkage to a human IgG1 Fc-region, or by generation of FLU BiTE by fusing two different specificity antibodies (421, 422). The short *in vivo* half-life of scFvs is one of the main reasons this antibody format is rarely chosen for therapeutic purposes (423). This study did not investigate the half-life of scFvs in chickens after intranasal delivery, although it could be a rate limiting step that decreases treatment efficacy.

Intranasal antibody administration was chosen as it has previously been demonstrated to be superior to systemic delivery in mice models, providing complete protection against lethal challenge (166, 424, 425). Such high potency with intranasal delivery can be explained by interference with the virus-cycle at the primary site of infection. In this study, 200 µg/dose and 300

µg/dose of scFv JF7 and EC12 were chosen, respectively, so as not to exceed 1 mg kg^{-1} dosage at any time point during infection. Alternative delivery measures to be considered should be aerosols, that would significantly reduce labour costs, and which might ensure better distribution into the target organs such as lungs (328, 426). Mass vaccination of chickens using aerosols is an approved method in large poultry flocks. Alternatively, antibody incorporation into the food pellets could be considered, as LPAI H9N2 infection has a tropism for the gastrointestinal tract (GI) in poultry as has been demonstrated by several studies (427, 428) and suggested by the cloacal virus shedding seen in this study. Although a similar approach has been developed and shown to be effective using genetically transgenic pea shred expressing antibody against *Eimeria* (171), the feasibility of such approach for treatment of AIV remains to be investigated. Specifically, the questions of antibody levels generated and subsequent stability during food processing and storage need to be addressed, in addition to antibody stability in the low pH of the GI. However, while both approaches benefit mass vaccination, they have the major drawback of uncontrollable dosage, which might be crucial for antibody therapeutics to avoid virus mutant formation. This study has shown that intranasal antibody delivery to birds led to altered virus shedding kinetics possibly due to antibody starting to act in nasal passages where the virus naturally replicates, but it remains to be analysed which administration route would be the most advantageous for passive immunization in farmed animals. In addition, having observed virus mutant formation in the first four days of infection and virus clearance within five to six days, for the future it might be beneficial to use the highest antibody concentration possible for the shortest amount of time (preferably only first two to three days post challenge) - such precise timing, however, might become challenging in natural ‘field’ conditions. Nevertheless, antibody therapeutics can be delivered not only in a purified protein format, but also as a nucleic acid with multiple studies reporting efficient protection and high levels of long-term antibody secretion systemically using

this approach (175, 429, 430). In addition, this can significantly reduce production costs. Viral vectored immunoprophylaxis using viral vectors that are already administered to poultry at early age, such as herpesvirus of turkeys or Newcastle disease virus encoding an antibody gene that gets expressed *in vivo* could be yet another approach which would provide extra layer of protection from an early age, when maternal antibodies are present at low levels but the bird's immunity is not fully formed (177, 431). Success with a persistently expressed scFv antibody carrying hydrolytic activity towards RNA and DNA viruses has been demonstrated by generating a transgenic chicken line (114).

To investigate if scFv administration would interfere with cellular immune response formation and to assess any underlaying signs of infection, pro-inflammatory cytokine transcripts levels were assessed by RT-qPCR. Results indicated IL-6 upregulation in challenged, non-treated or infected, scFv EC12 treated birds' spleens, indicating more widespread inflammation status in those animals. Elevated IL-6 levels in internal organs including the spleen in H9N2 infected birds or serum samples of influenza virus infected primates has been observed previously (327, 432). No changes in IFNγ response over the background of non-infected animal samples was observed here. Similar outcomes measuring IFNγ transcript upregulation in peripheral blood lymphocytes were reported previously, with cytotoxicity-associated gene induction after 7 days post-infection (433). In addition, when day 4 post-challenge samples were assessed for IL4, another pro-inflammatory cytokine IL-4 corresponding to T helper 2 response induction, levels were undetectable, agreeing with what has been demonstrated previously from primate serum samples (327). Furthermore, no changes in IL-4 expression in chickens following H9N2 infection has also been described elsewhere (433).

Analysing virus shedding results, it was observed that scFv EC12 treated chickens had a prolonged shedding profile which was hypothesised to be caused by virus escape mutant formation. This was supported by Sanger sequencing of the HA1 domain from these virus samples. Interestingly, three mutations identified (K147N, L212P, I217T) were found in both scFv EC12 and scFv JF7 treated birds, suggesting similar binding epitopes by both antibodies. Escape mutant formation at day 5 post influenza virus infection in monoclonal antibody treated animals has been demonstrated by Itoh et al (327). From the samples analysed here, all mutations were found to occur simultaneously, indicating that potentially some of the sites, in particular 147 might represent a compensatory mutation rather than being induced due to direct interaction with antibody. Any effect of the mutations' impact on virus fitness remains to be addressed (as well as a direct test that they affect scFv-binding); however, it would not be expected to result in higher pathogenicity as all scFv JF7 and scFv EC12 treated birds cleared virus infection successfully. From the data gathered, it appears that the mutations arose soon after infection, as both directly infected and contact birds were found to harbour virus with the substitutions within HA1. It is not expected that the escape mutations increased virus transmission, as treated contact birds had virus titers similar and to some extent lower than non-treated chickens. To address whether the mutations introduced would significantly affect virus replication, it would be beneficial to rescue the presumed virus escape mutants and characterise them in cell culture. In addition, NGS sequencing could be performed to detect if any further minor virus populations were present. It is possible to predict and reduce the likelihood of such phenomenon by standard *in vitro* techniques allowing selection of the antibody combination least likely to generate escape mutants. Indeed, analogous mutations at positions 212 and 217 have been reported to occur *in vitro* using full length monoclonal antibodies; however, those mutations coincided with changes in other positions such as 145, 183 or 234, which were not found to *change in vivo* after the first round of infection

(330). In addition, position 147 was found only to change *in vivo* here, but not *in vitro* in the published study (330).

Having analysed single nucleotide polymorphisms of H9N2 viruses detected in nature it was found that all three mutations can occur naturally, and this study did not generate mutations that have not been previously circulating in poultry, based on 6500 H9 HA sequences submitted to the Influenza Research Database. Noteworthy, positions 217 was much more permissive to variation than positions 147 and 212, indicating a higher likelihood of this position to be involved in natural virus antigenic repertoire formation. In addition, previous work has demonstrated that all three mutations are involved in antigenic residue formation which when occurring separately, were proven to not induce significant changes in HAI assays with UDL-1/08 antisera (330, 434, 435). A literature analysis of mutated residue contribution to HA function revealed position 217 as being involved in receptor binding and mammalian adaptation in multiple subtypes, suggesting a change from Met to Thr might have led to differences in preference for sialylated receptors, although the exact role of Met at this position remains to be determined (436, 437). Less evidence exists on how the amino acid side chains at positions 147 and 212 contribution to virus antigenicity, virulence, or immunogenicity.

To sum up, as a proof-of-concept, this chapter has shown that antibody therapeutics against HA could be used to tackle avian influenza virus, suggesting similar strategy could also be applicable for other virus pathogens affecting poultry. Although, HA head targeting antibodies might induce virus evolution, it is anticipated that the combination of several such antibodies would reduce level of antigenic changes or would result in fitness impairment of progeny virus.

Chapter 4 WOULD HERPESVIRUS OF TURKEYS ACT AS AN EFFICIENT VIRAL VECTOR FOR THERAPEUTIC ANTIBODY EXPRESSION *IN VITRO* AND *IN VIVO*?

Current control measures for avian influenza virus in poultry include vaccination with the antigen of choice. Previously, this study has shown that passive immunization with scFv antibodies targeting HA head can limit virus replication in birds but induce virus escape mutant generation. Herein, herpesvirus of turkeys (HVT) was investigated as a potential vector for delivery of encoded protective antibodies in poultry. For this purpose, an alpaca derived VHH antibody known to bind to HA stem and to cross neutralize multiple virus subtypes was chosen and converted to bivalent format. Antibody was produced in S2 cell culture and assessed for functional activity prior to targeted, CRISPR-Cas9 based, insertion into the HVT vector. Virus was rescued in CEF cells and passaged for 20 times to assess insert stability and recombinant virus growth kinetics. Antibody expression levels remained sufficient after multiple passages, but virus growth kinetics were altered. Nevertheless, rHVT was used to observe if virus could replicate *in ovo* and *in vivo* and express sufficient antibody titers in birds. A tolerability study performed in hatched birds revealed antibody not being secreted to detectable levels at a time points when samples were obtained but an anti-antibody response was found to be mounted. These data indicate that HVT virus can be used for antibody production purposes *in vitro* but it cannot act as sufficient means of antibody gene delivery to birds to the best of this work knowledge.

4.1 Introduction

4.1.1 Vectored antibody gene transfer

One of the solutions for high production cost and a need of repeated administrations for recombinant therapeutic antibodies is viral mediated antibody gene transfer also referred as vectored immunoprophylaxis (VIP). This approach can ensure continuous release of desired antibodies into target tissues or systemically. Nevertheless, pre-existing immunity towards the virus vector and its possible immunogenicity are amongst possible issues (438). Currently adeno-associated virus (AAV) is preferred means for the development of gene therapy strategies against multiple chronic illnesses and some acute infectious diseases affecting humans (439-441). Numerous studies in mice and non-human primates have shown recombinant AAV (rAAV) vectors providing long term, high level expression of transgenes *in vivo* (175, 442, 443). In addition, with regards to rAAV use for VIP purposes challenge models have been established and shown that therapeutic antibodies against viral pathogens such as HIV or influenza viruses, can protect animals against disease development and limit its further spread (173, 175, 185, 442). Despite these findings, the veterinary field prefers and has approved the use for distinct viral vectors.

4.1.2 Avian viral vectors

Poxvirus vectors represented by fowlpox, herpesvirus vectors including avian infectious laryngotracheitis virus, herpesvirus of turkeys and duck enteritis virus, paramyxovirus and adenovirus vector families exemplified by Newcastle disease virus and avian adenovirus respectively, - have all been used as viral vectors against heterologous avian pathogens (177, 178, 444-446). Amongst

all herpesvirus of turkeys (HVT) also known as maleagrid herpesvirus 1 has shown an exceptional potential in development of viral vectored poultry vaccines as illustrated by licensing and commercialisation of Vaxxitex HVT + IBD, Poulvac Procerta HVT ND and Vectormune® AI (447-449). Being genetically and antigenically related to Marek's disease virus (MDV) that causes persistent, apathogenic infections in chickens HVT provides protection against MD (450). HVT, similarly to other herpesviruses, contains double stranded DNA genome that is divided into unique short (US) and unique long (UL) regions encoding nearly 100 proteins (450). Some of the sites within HVT genome are classified as 'non – essential' (i.e., US1, US2, US10, UL3/4, UL45/46, and thymidine kinase (TK) loci) which, therefore, can sustain insertion of foreign genes and facilitate production of viral vectored vaccines offering synergistic effect and simultaneous protection against MD and antigen of choice (431, 451).

4.1.3 Approaches for viral vector generation

Strategies for recombinant HVT generation employed in the past include homologous recombination, bacterial artificial chromosome (BAC) or fosmid vectors (452, 453). However, development of clustered regularly interspaced short polindromic repeat (CRISPR) – CRISPR associated protein 9 (Cas9) technology allows to achieve more precise genome editing in a time and labour efficient manner (454). It is based on *Streptococcus pyogenes* immune system mechanism wherein all foreign sequences are memorized by CRISPR DNA family which later facilitates exogenous DNA recognition by guide RNA (gRNA) and its cleavage by DNA endonuclease enzyme – Cas9 (455-457). Design of gRNA complimentary to the sequence of interest and its insertion into an expression plasmid carrying Cas9 enzyme ensures targeted introduction of double stranded DNA breaks in transfected cells. Deletions or insertions can

be generated within the target genome mediated via non-homologous end joining (NHEJ) or homology directed repair (HDR) (458). NHEJ is an error prone mechanism of direct broken ends ligation leading to high rates of unspecific changes (insertions or deletions) which often have detrimental effects (459). On the other hand, HDR-dependent CRIPR/Cas9 requires homology arms which facilitate accurate repair allowing more specific genome modifications (460).

4.1.4 Chapter objectives

- Production of broadly neutralising antibody and its characterization *in vitro.*
- Generation of recombinant HVT viral vector carrying broadly neutralising antibody using a CRISPR/Cas9 approach.
- Characterisation of a recombinant HVT virus ability to express the transgene *in vitro* and investigate how this affects viral replication.
- Evaluation of recombinant HVT as viral vector for vectored immunoprophylaxis purposes *in ovo* and *in vivo*.

4.2 Results

4.2.1 R1aB6 bivalent antibody generation as purified protein

Having observed HA head binding scFvs promoting virus escape mutant generation it was sought to replace antibody fragments derived from hybridomas with HA stem region (HA2) binding VHH antibodies carrying higher cross-reactivity with diverse AI viruses and potentially having reduced impact on virus escape mutant formation due to interaction with more conserved

epitopes. For this purpose, bivalent R1aB6 antibody was chosen which was previously described as potent broad cross-subtype neutralizing antibody recovered from 2009 A(H1N1) HA immunized alpacas and which sequence was kindly obtained from Simon E. Hufton, NIBSC (461). As described in section 2.1.2 bivalent R1aB6 antibody was produced in S2 cell culture supernatant and its purity was assessed by SDS-PAGE. A single band observed at ~30 kDa indicated no contaminants present in eluted and dialysed protein (Figure 2.1).

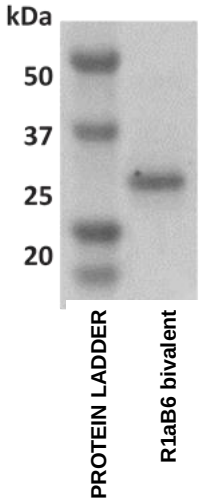

Figure 4.1. SDS-PAGE of R1aB6 bivalent VHH antibody. Antibody was purified from S2 cell culture supernatant and dialysed into PBS pH 7.4 after purification. 5 µg of purified protein was mixed with protein loading buffer, and denatured. Purified nanobody was run on 12% Bis – Tris polyacrylamide resolving gel and visualised by Coomassie blue staining

4.2.2 R1aB6 bivalent antibody shows binding to H9N2 and cross-reactive neutralization profile

Following the overall focus of the study in generation of therapeutic approaches for AIV purified bivalent R1aB6 antibody affinity towards the panel of H9N2 and H5N1 viruses was assessed. Six H5N1 viruses chosen were representatives of major H5 HA clades while H9N2 viruses remained same as

in Chapter 2. ELISAs were performed as described previously (section 2.1.2.2.). Results indicated the antibody's ability to cross-react with a range of H9N2 viruses (Figure 4.2.a). The highest binding profile was determined to be towards Egy/D7100 and Env/BD, an intermediate binding profile towards UDL-1/08, UDL-2/08, India/WB, UAE/D1556 and VN/38 and limited binding towards WZ/606 (Figure 4.2.a). On the other hand, none of the H5N1 viruses tested were able to bind to bivalent R1aB6 antibody efficiently during this study with only Egy/137 found to yield signal slightly over the background levels (Figure 4.2.b). Assessment of the purified bivalent R1aB6 function in MNT assay and a panel of H9N2 viruses tested indicated only India/WB maintaining functional activity and ability to inhibit virus growth with the concentration as high as 25 µg mL $^{-1}$ required (Table 4.1). Although, no binding to H5N1 was observed by ELISA R1aB6 was able to neutralize VN/OIE/6022 showing broad neutralizing activity. Positive control of heat-inactivated serum raised against UDL-1/08 or VN/OIE/6022 for H9N2 and H5N1 viruses were used, respectively. Negative control of wR1a-28 VHH antibody (gifted from Dr Simon E. Hufton, NIBSC) specific to H7 HA was used to examine and confirm the assay's reliability.

Overall, these results indicate that bivalent R1aB6 antibody has strong affinity towards multiple H9N2 viruses and very limited to H5N1 but it can efficiently neutralize India/WB and VN/OIE/6022 viruses representing this antibody's potential against multiple AIVs.

Chapter 4 WOULD HERPESVIRUS OF TURKEYS ACT AS AN EFFICIENT VIRAL VECTOR FOR THERAPEUTIC ANTIBODY EXPRESSION *IN VITRO* AND *IN VIVO*?

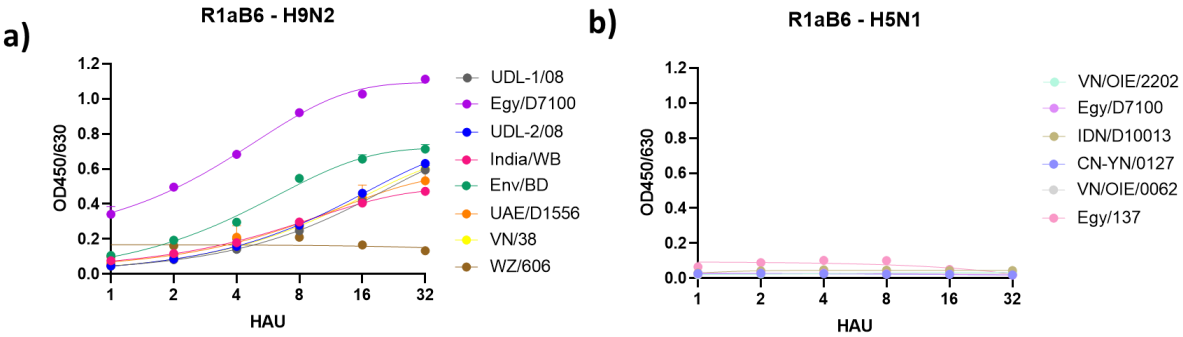

Figure 4.2. ELISA assessing R1aB6 bivalent VHH antibody binding to a) H9N2 viruses**; b)** H5N1 viruses. 32 HAU units of each virus was used for coating and 2-fold dilutions. Purified antibodies were used at 1 µg mL^{-1} and probed by an anti C-tag antibody conjugated to biotin which was detected using HRP-conjugated streptavidin. The variable heavy chain of the heavy chain only antibody wR1a-28 specific to H7 HA non-binding UDL-1/08 was used as a negative control. Binding was measured in technical duplicate and the average OD 450/630 nM was plotted with error bar representing ±SD, curve fitting was performed following a nonlinear regression model.

Chapter 4 WOULD HERPESVIRUS OF TURKEYS ACT AS AN EFFICIENT VIRAL VECTOR FOR THERAPEUTIC ANTIBODY EXPRESSION *IN VITRO* AND *IN VIVO*?

Table 4.1. R1aB6 bivalent VHH antibody activity in virus microneutralization assay. To assess antibody functional activity assay was performed in technical and biological triplicates. Values represented show antibody concentration required for complete virus neutralization. Serum samples raised against UDL-1/08 or VN/OIE/6022 were used as a positive control. Average data is shown with ± SD where applicable. - indicates no activity found with detection limit 100 µg mL^{-1}.

Virus / Antibody	R1aB6 µg mL^{-1}
A/chicken/Pakistan/UDL-01/2008	-
A/chicken/Egypt/D7100/2013	-
A/chicken/Pakistan/UDL-02/2008	-
A/chicken/India/WB-NIV1057169/2010	25
A/environment/Bangladesh/10360/2011	-
A/quail/UAE/D1556/2011	-
A/Chinese hwamei/Vietnam/38/2006	-
A/chicken/Wenzhou/606/2013	-
A/chicken/Nepal/T-359/2014	-
A/duck/Vietnam/OIE-0062/2012	-
A/duck/Vietnam/OIE-2202/2012	50
A/tree sparrow/Indonesia/D10013/2010	-
A/turkey/Egypt/137/2013	-
A/Yunnan/0127/2015	-

4.2.3 Bivalent R1aB6 can be used to generate rHVT using CRISPR-Cas9 knock-in approach

In Chapter 3, it was demonstrated that intranasal delivery of purified scFv antibodies binding to hemagglutinin head region (HA1) can reduce virus peak shedding *in vivo*. However, costs of antibody purification and a need of repeated administrations makes such strategy unattainable for use in poultry.

To assess further means of therapeutic antibody delivery recombinant HVT virus carrying therapeutic antibody was generated and tested *in vitro, in ovo* and *in vivo*.

To generate recombinant HVT virus expressing therapeutic antibody, plasmid otherwise identical to pUC18 backbone, was modified to allow introduction of expression cassette containing i) murine cytomegalovirus immediate-early promoter adjacent to synthetically generated ii) SV40 poly(A) polyadenylation site located between partial (HVT087) SORF3 and partial (HVT088) US2 sequences homologous to HVT genome. Resulting plasmid was used for ORF encoding CD33 secretion signal, bivalent VHH antibody and V5/C-tag sequence insertion via restriction enzyme dependent cloning. To engineer bivalent nanobody format, VHH sequence specific for R1aB6 was repeated twice and linked by $(Gly_4Ser)_6$ linker as described previously.

DNA of resultant plasmid was co-transfected with pSpCas9(BB)-2A-Puro (PX459) V2.0 (Addgene plasmid #62988) carrying green fluorescent protein (GFP) specific sgRNA and expressing *S.pyogenes* Cas9 protein into chicken embryo fibroblast (CEF) cells. Subsequently, cells were infected with HVT_GFP virus, derived from the FC-126 strain, to facilitate targeted cleavage and HDR repair of viral genome (Figure 4. 3.).

Chapter 4 WOULD HERPESVIRUS OF TURKEYS ACT AS AN EFFICIENT VIRAL VECTOR FOR THERAPEUTIC ANTIBODY EXPRESSION *IN VITRO* AND *IN VIVO*?

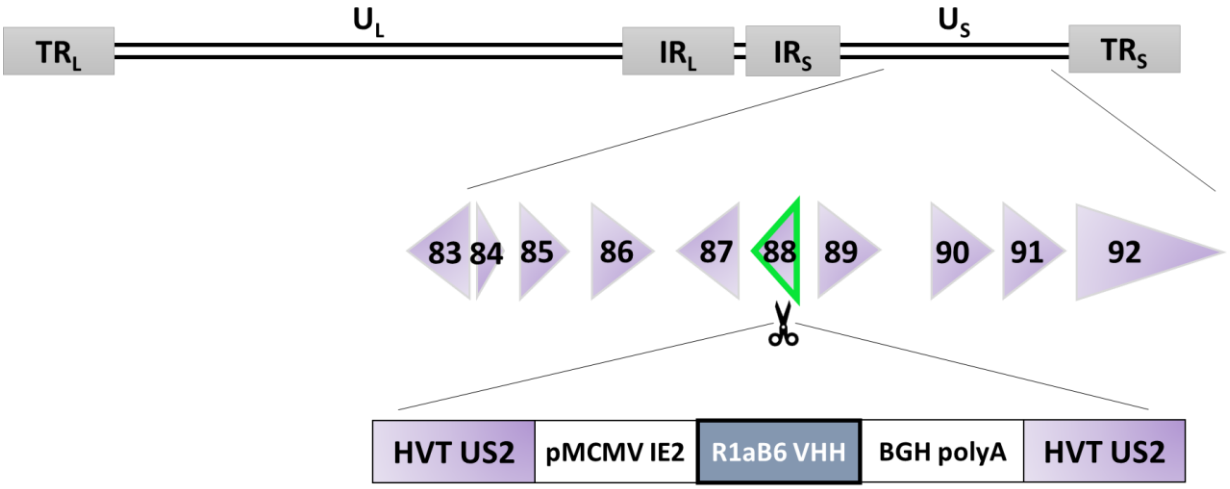

Figure 4.3. Homology dependent repair mediated knock-in of R1Ab6 VHH antibody expression cassette into Herpesvirus of turkeys (HVT) genome. Unique short locus of HVT genome encoding 10 genes (numbered 83 – 92) was used for foreign gene insertion. Specifically, gene 88, also known as the US2 gene site, already carrying GFP expression cassette was targeted by gRNA as indicated by a scissor icon. gRNA induced double stranded break was repaired in the presence of donor plasmid carrying homology arms for US2 site and a transgene cassette containing mCMV IE2 promoter, transgene R1aB6 and BGH polyadenylation signal.

Transfected/infected cells were passed 3 days post infection and left in the cell culture until visible plaques were noted to form. Recombinant virus plaques without GFP signal had comparable size and morphology with HVT - GFP virus and were isolated for DNA extraction (Figure 4.4.).

Chapter 4 WOULD HERPESVIRUS OF TURKEYS ACT AS AN EFFICIENT VIRAL VECTOR FOR THERAPEUTIC ANTIBODY EXPRESSION *IN VITRO* AND *IN VIVO*?

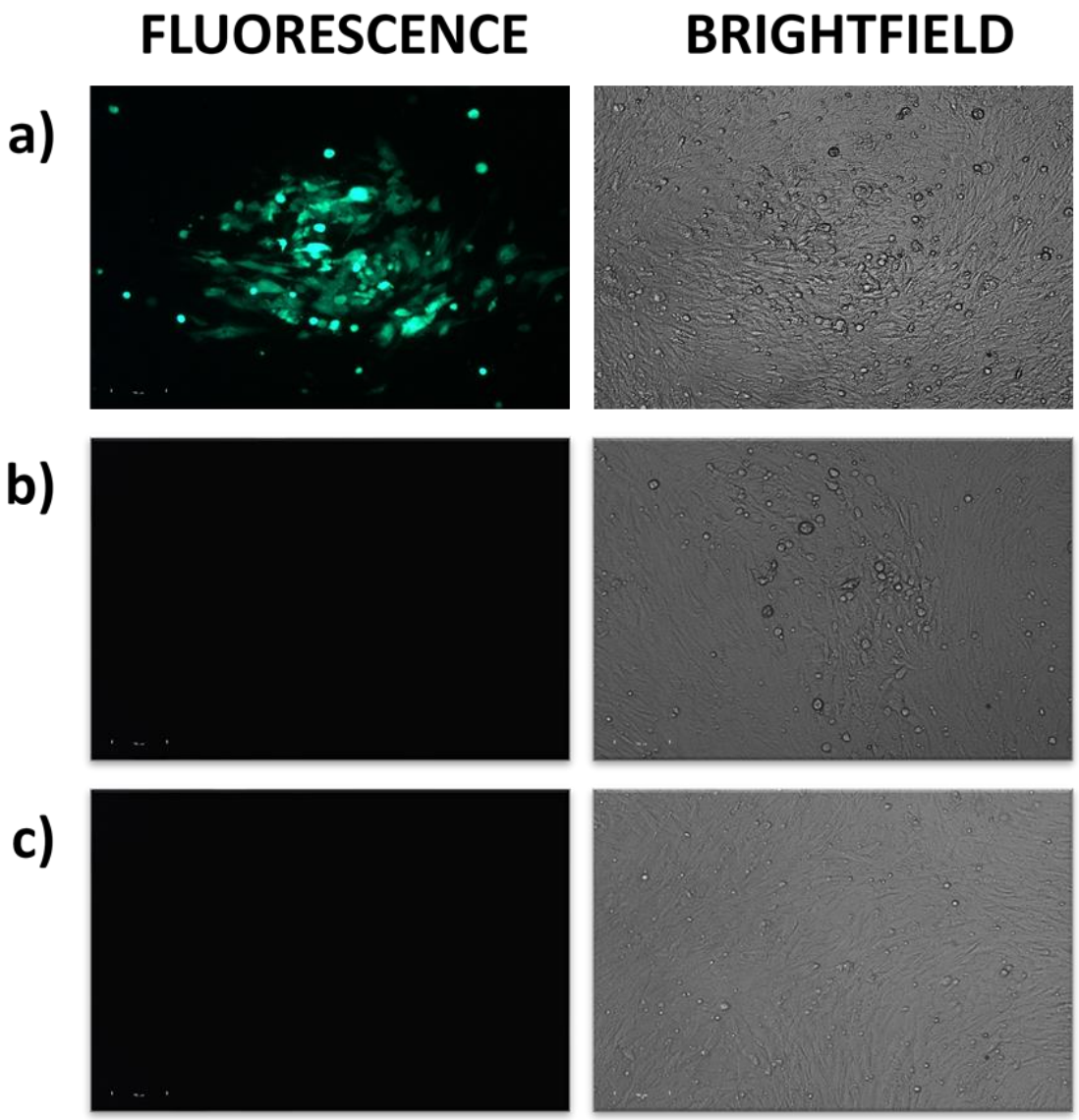

Figure 4.4. Cytopathic effect and plaque formation in CEF cells. a) Cells transfected and infected with HVT – GFP virus displaying GFP signal indicating no genome editing events. Plaque (left panel) morphology observed under UV excitation and in phase contrast (right panel). **b)** Cells transfected and infected with HVT – GFP virus which has undergone genome editing. Plaque (left panel) morphology observed under UV excitation and in phase contrast (right panel). **c)** Transfected, non-infected cells displaying no fluorescence signal (plaques) under UV excitation (left panel) and no CPE under brightfield microscopy (right panel). Scale bar at the left corner of each panel is representative for 100 μm.

Chapter 4 WOULD HERPESVIRUS OF TURKEYS ACT AS AN EFFICIENT VIRAL VECTOR FOR THERAPEUTIC ANTIBODY EXPRESSION *IN VITRO* AND *IN VIVO*?

The presence of nanobody expression cassette at US2 locus was confirmed by PCR analysis using site - and gene - specific primers (Figure 4.5.). WT HVT (Fc-126) was used as negative control for site - and gene - specific PCRs with no product obtained in either of the reactions, HVT-GFP and plasmid used for transfection served as positive controls with bands seen at the expected sizes of ~1500 bp and ~600 bp for site - and gene - specific PCRs, respectively (Figure 4.5.). From a panel of 24 plaques picked and tested ~54% (13/24) were found to have amplicon within US2 site while ~33% (8/24) had amplicon corresponding to the size of gene specific product. Only ~16% efficiency rate (4/24) was determined for successful knock-in events that were double positive using site - and gene - specific primers. These were then subjected to another two rounds of purification and PCR confirmation to obtain pure recombinant virus (Figure 4.5.).

Chapter 4 WOULD HERPESVIRUS OF TURKEYS ACT AS AN EFFICIENT VIRAL VECTOR FOR THERAPEUTIC ANTIBODY EXPRESSION *IN VITRO* AND *IN VIVO*?

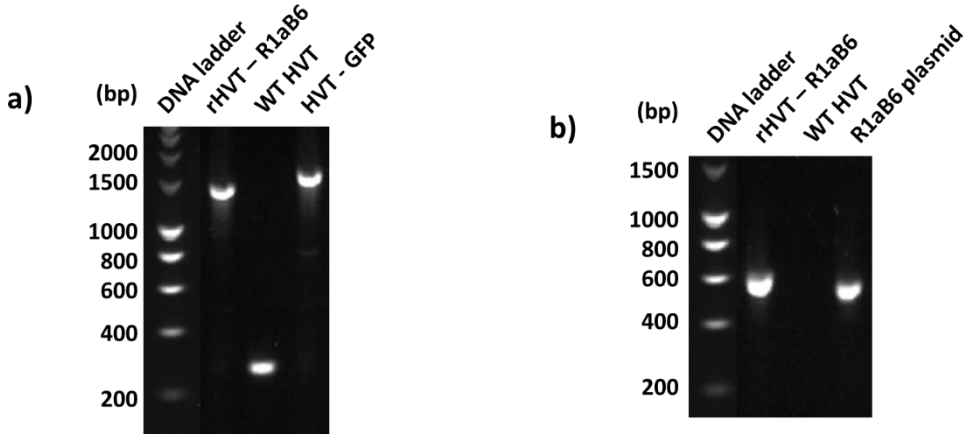

Figure 4.5. PCR analysis of DNA from HVT virus infected CEF cells. a) DNA from CEF cells infected with HVT virus was amplified using primers flanking insertion sites. Upper bands ~1500 bp (for rHVT – R1aB6 and HVT - GFP) show the presence of foreign gene cassettes, lower band for WT HVT (~260 bp) indicates absence of a transgene at the US2 site. **b)** DNA from CEF cells infected with HVT virus or the plasmid used for CEF transfection was amplified using gene specific primers. Amplification was confirmed in positive control sample and rHVT (~600 bp) but not WT HVT infected CEF cells. PCR products were run on 1% agarose gels at 50V for 2 hours.

Overall, this indicates that, antibody gene can be integrated into HVT genome via CRISPR-Cas9 HDR mechanism but multiple plaques corresponding to different clones must be picked and carried out for at least few rounds of purification to obtain pure recombinant virus stocks.

4.2.3.1 rHVT – mediated expression of HA targeting antibodies in cell culture

Having confirmed antibody gene integration into HVT genome the expression of the transgene was investigated. CEF cells were used for virus growth and the secretion of R1aB6 nanobody was assessed by western blot and ELISA using the supernatant of cells infected with WT HVT or rHVT – R1aB6 virus. A Following protein transfer onto a nitrocellulose membrane nanobody was

probed by CaptureSelect™ Biotin Anti-C-tag Conjugate and virus detected by an HVT-vNr-13-specific monoclonal antibody. Distinct bands at expected sizes (~33 kDa) for rHVT-R1aB6 and a purified protein used as a positive control were observed corresponding to the bivalent VHH antibody. This was absent in sample containing the supernatant of WT HVT infected CEF cells and the non – infected control (Figure 4.6.). Both, rHVT-R1aB6 and WT HVT samples were positive for HVT-vNr-13 (~15 kDa) which was absent in mock infected and purified protein samples, serving as the control of infection.

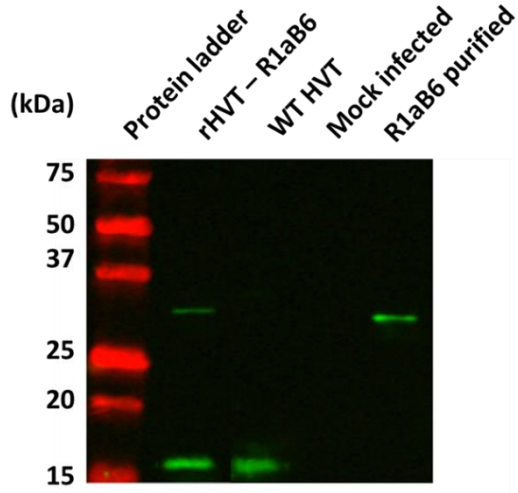

Figure 4.6. WB analysis of R1aB6 expression by rHVT infected CEF cells. Supernatant of infected cells were harvested and mixed with protein loading buffer and denatured prior to loading onto 12% Bis – Tris polyacrylamide resolving gel. After the run proteins were transferred onto nitrocellulose membrane for Western blotting with anti-C-tag specific antibody to detect recombinant R1aB6 production (~33kDa) whilst HVT-encoded Bcl-2 homolog vNr-13 (~18 kDa) serving as the control of infection.

Similarly, CaptureSelect™ Biotin Anti-C-tag Conjugate was used to probe the supernatants from CEF cells infected with rHVT-R1aB6 and WT HVT and used for ELISA plate coating. Nine clones were tested for their ability to secrete R1aB6 nanobody that represented two main clone families (2 and 11) obtained

during first selection step. However, at this stage the virus used to infect CEF cells was not titrated (data is from P2 virus after the rescue), therefore, differences in transgene secretion levels might also account for differences in virus growth kinetics. In general, levels of nanobody secreted were similar between different clones, however, significantly lower expression was noted for clones 11.1.3, 11.1.6 and 11.1.10 (Figure 4.7.). Two of the highest expressing clones, from different clone families, 11.1.2 and 2.2.4 as determined by ELISA (OD450/630 = 1.4 ± 0.02 and OD450/630 = 1.4 ± 0.18, respectively) were chosen for further virus characterisation and virus stability assessment *in vitro*.

These results indicate that antibodies can be expressed by rHVT growing in infected primary cells, but transgene expression levels might vary between different clones.

Chapter 4 WOULD HERPESVIRUS OF TURKEYS ACT AS AN EFFICIENT VIRAL VECTOR FOR THERAPEUTIC ANTIBODY EXPRESSION *IN VITRO* AND *IN VIVO*?

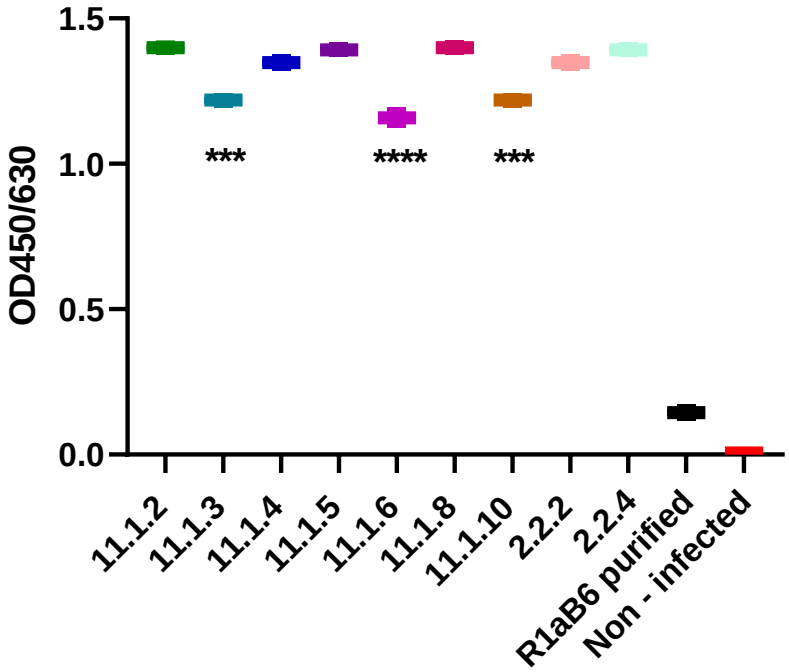

Figure 4.7. R1aB6 expression levels from different HVT clones. ELISA was performed on CEF cells culture supernatants infected with nine different clones of rHVT virus at passage 2. Transgene secretion levels were assessed by probing C-tag presence via anti C-tag antibody. Purified R1aB6 antibody was used as a positive control at 1 µg/well. Non - infected cell supernatant was used as a negative control. Binding was measured in technical duplicate and the average OD450/630 nM was plotted with error bar representing +/-SD. Levels of significance were based on P – values from ordinary one - way ANOVA with multiple comparisons test (Nonsignificant (Ns) = $p > 0.05$; * = $p \leq 0.05$; ** = $p \leq 0.01$; *** = $p \leq 0.001$; **** = $p \leq 0.0001$).

4.2.3.2 rHVT carrying antibody expression cassette stability in vitro

Next, the genetic stability of both rHVT – R1aB6 clones was assessed. For this purpose, rHVT alongside WT HVT was sequentially passaged for 20 times in primary CEF cells. Viral DNA was extracted after every 5 passages and analysed using R1aB6 gene - and US2 site - specific PCRs. No changes were

observed in the size and amount of R1aB6 gene product indicating stable transgene insertion into the HVT genome, WT HVT DNA was used as a negative control with no amplification observed in the reaction while plasmid used for initial transfection served as a positive control indicating size of expected band from rHVT DNA (Figure 4.8.a). As expected, the same results of no knock-out events were confirmed by site- specific PCRs where controls of WT HVT and HVT-GFP were used (Figure 4.8.b).

Chapter 4 WOULD HERPESVIRUS OF TURKEYS ACT AS AN EFFICIENT VIRAL VECTOR FOR THERAPEUTIC ANTIBODY EXPRESSION *IN VITRO* AND *IN VIVO*?

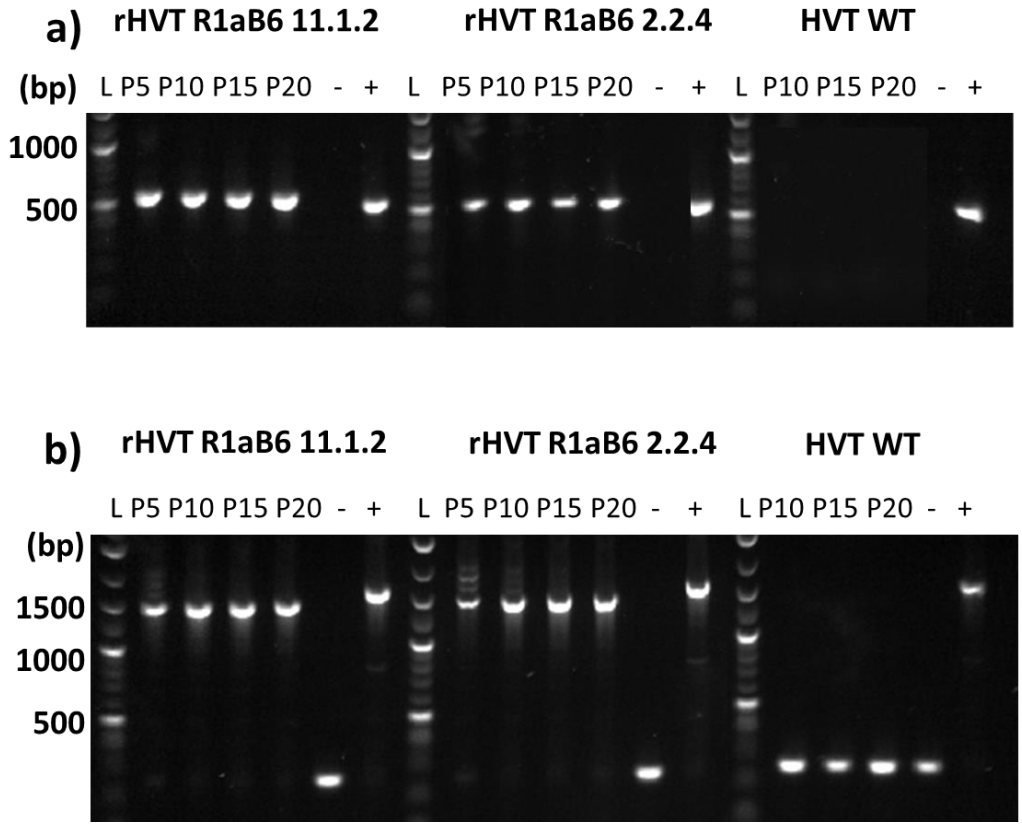

Figure 4.8. Analysis of rHVT - R1aB6 stability by PCR. a) DNA from CEF cells infected with rHVT or WT HVT virus was harvested every 5 passages and amplified using gene specific primers. The plasmid used for CEF transfection served as a positive control. Amplification was confirmed in positive control sample and rHVT (~600 bp) but not WT HVT infected CEF cells; **b)** DNA from CEF cells infected with HVT virus was harvested every 5 passages and amplified using primers flanking insertion sites. Upper bands ~1500 bp for rHVT – R1aA5 show the presence of foreign gene cassettes, lower bands for WT HVT (~260 bp) indicates absence of the transgene at the US2 site. HVT – GFP DNA served as a positive control. PCR products were run on 1% agarose gels at 50V for 2 hours.

To further confirm rHVT stability and nanobody expression plaque immunostaining was performed (Figure 4.9.). Briefly, cells were infected with P20 rHVT - R1aB6, P20 WT HVT or mock infected and left for 72h to allow

plaque formation before fixation with methanol: acetone and immunostaining with Odyssey compatible antibodies. HVT specific chicken serum was used to detect virus specific plaques under the red channel and anti – C – tag antibody was used to probe plaques expressing recombinant nanobody under the green channel. WT HVT served as a control and was positive when probed with chicken antisera but not anti – C – tag antibody, mock infected cells showed no staining with either of the antibodies. Most of rHVT plaques double stained for both virus and insert specific antibodies, however, a proportion of plaques was found to have the phenotype of WT HVT virus. Clone 11.1.2 had slightly higher recombinant and wildtype HVT ratio with 34 out of 250 plaques probed by antiserum but not C-tag antibody. Clone 2.2.4 had 29 out of 250 plaques which were lacking transgene expression. There were no observable differences in plaque morphology between wildtype and recombinant HVT viruses.

These results suggested that stability of antibody expression cassette was affected by recombinant virus passaging in primary CEF cells after 20 passages with up to 15 % of plaques (~14 % for clone 11.1.2 and ~11 % for clone 2.2.4) reverting to wildtype. In addition, the immunostaining experiment appeared to be more sensitive method for the assessment of rHVT stability *in vitro* than conventional PCR.

Chapter 4 WOULD HERPESVIRUS OF TURKEYS ACT AS AN EFFICIENT VIRAL VECTOR FOR THERAPEUTIC ANTIBODY EXPRESSION *IN VITRO* AND *IN VIVO*?

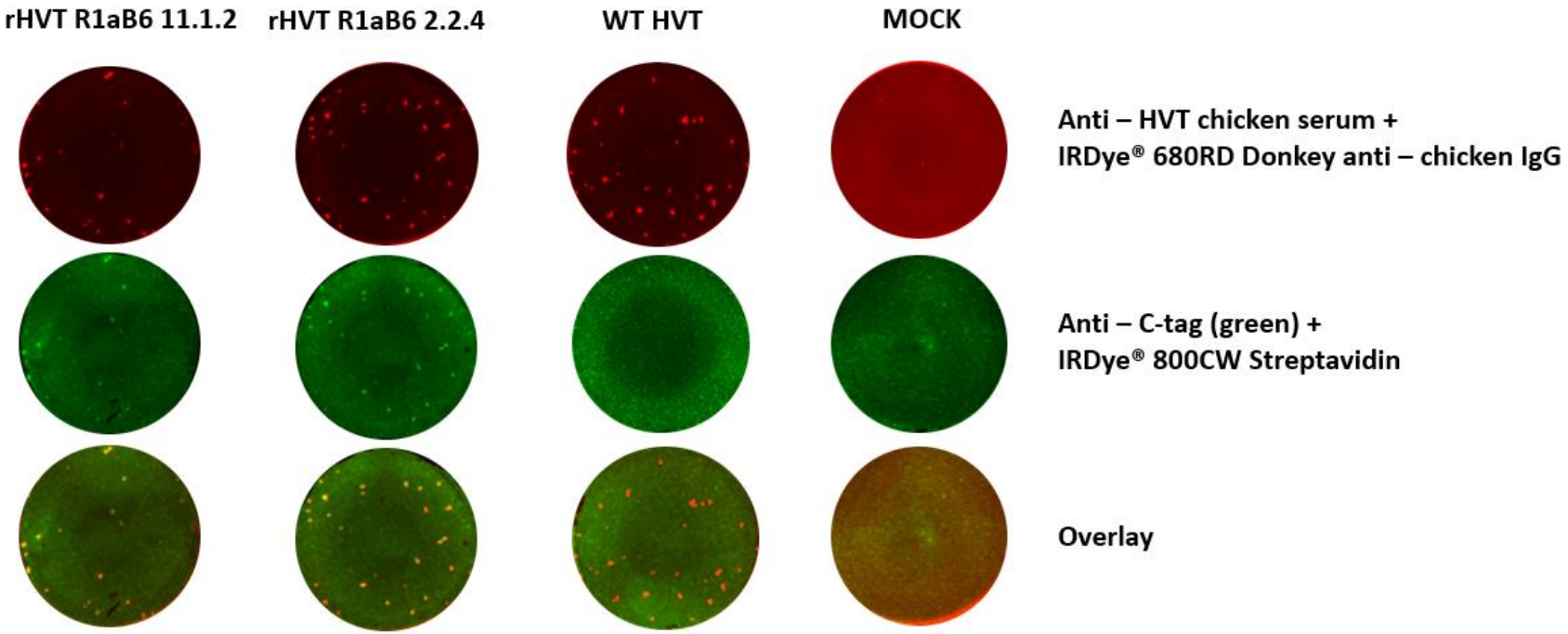

Figure 4.9. Analysis of passage 20 rHVT - R1aB6 stability by immunofluorescence staining. CEF cells were infected with P20 virus for 72h and fixed with methanol: acetone prior to staining with anti – HVT chicken serum (red) and anti C-tag antibody (green). Merged images of double stained cells were obtained by scanning 6 – well plates using Odyssey CLx. **a)** rHVT – R1aB6 clone 11.1.2; **b)** rHVT – R1aB6 clone 2.2.4; **c)** WT HVT; **d)** MOCK – infected cells.

Chapter 4 WOULD HERPESVIRUS OF TURKEYS ACT AS AN EFFICIENT VIRAL VECTOR FOR THERAPEUTIC ANTIBODY EXPRESSION *IN VITRO* AND *IN VIVO*?

4.2.3.3 Insertion of therapeutic antibody expression cassette does alter HVT growth kinetics

To assess whether recombinant viruses were attenuated or had identical replication with wildtype HVT low multiplicity of infection (MOI) growth curves in CEF cells were performed with 20 times passaged viruses which were previously confirmed to contain antibody transgene. DNA was extracted at 6 h, 12 h and then every 24 h post infection until 144 h time point was reached. The viral genome copy numbers per 10 000 cells were used for qPCR to determine virus replication rates. An ovotransferin gene transcript amplification was used as an internal control and for the purposes of DNA quality assessment. Differences between wildtype and recombinant HVT as well as between two clones expressing same nanobody were observed (Figure 4.10.a).

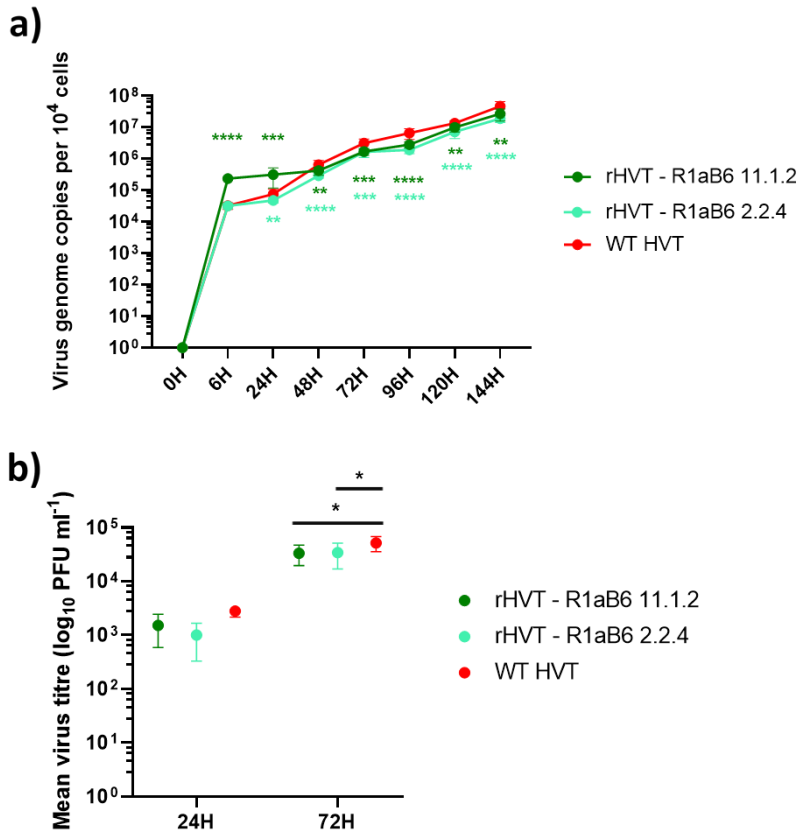

Figure 4.10. Replication kinetics of rHVT – R1aB6 viruses in CEF cells. a) In vitro growth rates of passage 20 rHVT viruses were measured by TaqMan qPCR. DNA samples were extracted from infected CEF cells harvested at various time points over a 144h period (shown on the x axis) to and the viral genome copy numbers per 10 000 cells (shown on the y axis) were assessed. The growth curve experiment was run in technical triplicates and biological duplicates, the qPCR was run in technical triplicates. Levels of significance were based on P – values from two - way ANOVA with multiple comparisons test (Nonsignificant (Ns) = p > 0.05; * = p ≤ 0.05; ** = p ≤ 0.01; *** = p ≤ 0.001; **** = p ≤ 0.0001); **b)** In vitro growth rates of passage 20 rHVT viruses as measured by plaque assay. CEF cells were infected with P20 rHVT or WT HVT (MOI of 0.0001) and left for 24h or 72h before harvesting. Harvested viruses were titrated on fresh CEF cells that were fixed and stained probing virus by an HVT specific chicken serum. The growth curve experiment was run in technical triplicates and biological duplicates, plaque assay was run in a single replicate. Levels of significance were based on P – values from two - way ANOVA with multiple comparisons test (Nonsignificant (Ns) = p > 0.05; * = p ≤ 0.05; ** = p ≤ 0.01; *** = p ≤ 0.001; **** = p ≤ 0.0001).

Chapter 4 WOULD HERPESVIRUS OF TURKEYS ACT AS AN EFFICIENT VIRAL VECTOR FOR THERAPEUTIC ANTIBODY EXPRESSION *IN VITRO* AND *IN VIVO*?

The early time point of infection (6 h post infection) indicated no statistically significant difference between clone 2.2.4 and WT HVT virus genome copy number. At the same time point clone 11.1.2 appeared to produce much higher genome copy titers ($p < 0.0001$) indicating higher replication potential lasting until 48 h post infection. Starting at 24 h post infection clone 2.2.4 was indicated to have reduced replication potential when compared to WT HVT. This was maintained till the end of experiment (144 h post infection) with varying degrees of significance ($p = 0.0068$ at 24 h; $p \leq 0.0001$ at remaining time points). On the other hand, clone 11.1.2 was also noted to produce lower amount of genome copies, starting at 48 h post infection with differences ranging between ~20 000 and ~ 200 000 00 virus genome copies per 10 000 cells at 48 h and 144 h time points, respectively (variation of $p \leq 0.0011$ - 0.0001). There were also statistically significant differences between clones 2.2.4 and 11.1.2 at most of the time points with clone 11.1.2 having slight fitness advantage as determined by higher virus genome copy numbers.

The qPCR results were further confirmed by plaque assays with 24 h and 72 h post infection time points chosen for live virus quantification. Briefly, pre-seeded CEF cells were infected with cell - associated an HVT samples harvested during the growth curves and left for 72 h for plaques to develop. These were fixed and probed by HVT specific chicken serum and secondary anti-chicken HRP antibody visualised by DAB + Substrate Chromogen System (Figure 4.10.b). Although observed plaques numbers at 24 h post infection showed non-significant differences for both clone 2.2.4 (1000 ± 670 PFU mL^{-1}) and clone 11.1.2 (1667 ± 701 PFU mL^{-1}) compared to the wildtype HVT (2792 ± 620 PFU mL^{-1}). However, the 72 h time point reflected qPCR data with a statistically higher replication rate of wildtype virus (51667 ± 16020 PFU mL^{-1}) versus two recombinant HVT clones (33333 ± 13662 PFU mL^{-1} for clone 2.2.4 and 34167 ± 17151 PFU mL^{-1} for clone 11.1.2) (Figure 4.10.b). Overall,

this indicates that nanobody insertion at US2 site does affect virus growth kinetics with wildtype virus displaying higher genome copy numbers and higher rates of live virus replication. Differences seen were also noticed to depend on clone-to-clone variability with higher replication rates observed in a less stable clone 11.1.2 carrying higher wildtype to recombinant virus ratio as previously examined by immunostaining.

4.2.3.4 Therapeutic antibody secretion into the cell culture supernatant coincides with viral replication but changes with virus passages

Having observed differences in growth kinetics between two rHVT clones tested, the supernatant of infected CEF cells was harvested and used for ELISA to determine nanobody release throughout the infection. The same time points were used, as per growth curves described previously, with P20 viruses. Regardless of a slightly lower replication potential clone 2.2.4 was able to produce almost twice as much protein as clone 11.1.2 with differences starting to appear 72 h post infection (Figure 4.11.a). The peak protein expression for both clones was reached at 120 h post infection with levels plateauing or even slightly decreasing afterwards.

Chapter 4 WOULD HERPESVIRUS OF TURKEYS ACT AS AN EFFICIENT VIRAL VECTOR FOR THERAPEUTIC ANTIBODY EXPRESSION *IN VITRO* AND *IN VIVO*?

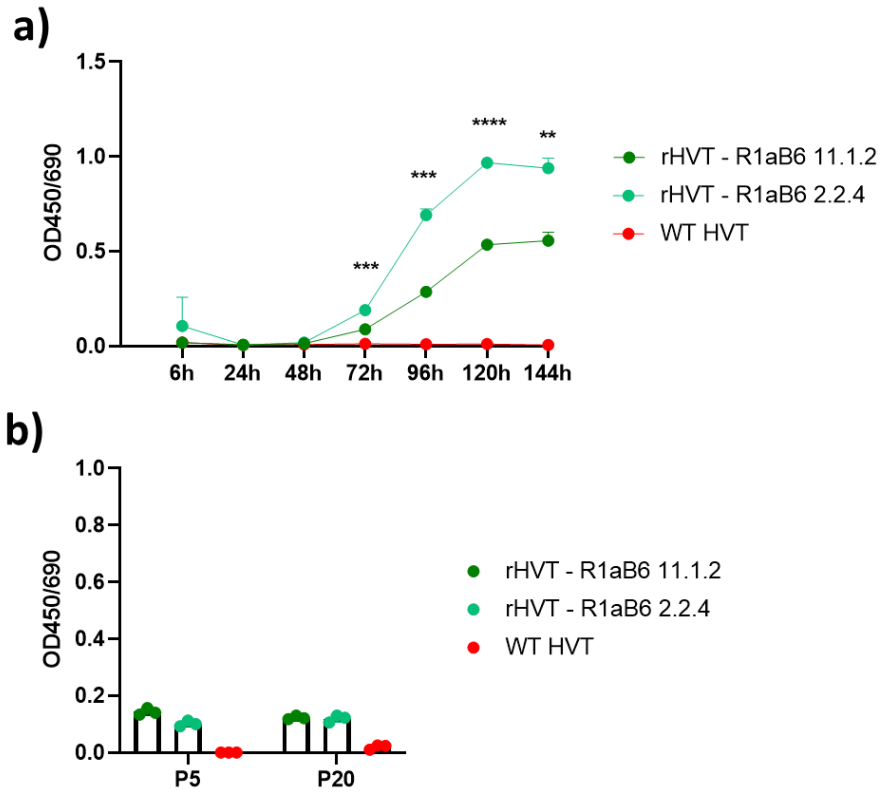

Figure 4.11. R1aB6 secretion to cell culture supernatant. a) R1aB6 levels were measured at a 24 h intervals throughout 144 h period post CEF infection. Infection experiments were performed in triplicates and ELISAs were based on R1aB6 detection via C-tag. Levels of significance were based on P – values from two - way ANOVA with multiple comparisons test (Nonsignificant (Ns) = $p > 0.05$; * = $p \leq 0.05$; ** = $p \leq 0.01$; *** = $p \leq 0.001$; **** = $p \leq 0.0001$); **b)** R1aB6 levels were compared in supernatant samples of CEF cells infected with P5 and P20 rHVT – R1aB6 or WT HVT viruses as described previously.

Next, to investigate whether different passages have an impact on nanobody release, CEF cells were infected with recombinant or wildtype virus and supernatant was harvested after 48 h for analysis (Figure 4.11b). Nanobody levels for both clones remained similar at both P5 and P20 viruses infected cells revealing transgene expression remaining stable

All in all, this and previous data suggest that recombinant HVT virus retains its ability to produce protein throughout passaging in cell culture. As expected, higher levels of transgene were found in a relatively more stable clone. In addition, variation in protein production by different passage viruses should be taken into consideration if recombinant virus is to be used for further evaluation *in vivo*.

4.2.4 Characterisation of rHVT expressing therapeutic antibody *in ovo*

To determine whether HVT virus can replicate and express transgene not only in cell culture but also *in ovo* short study in eggs was performed. For this purpose, embryonation day 10 eggs were divided into three groups receiving either rHVT – R1aB6 clone 2.2.4, clone 11.1.2 or WT HVT at 20, 000 PFU into the allantoic cavity. Eggs were chilled at 24h or 72h post infection (five mock infected eggs were also included at the later time point). Embryo's limbs were used for DNA extraction and subsequent qPCR to evaluate HVT potential to reach and replicate in the chicks' embryos body. None of the main organs (spleen, lungs, bursa) were developed enough for differentiation at these time points. 24h post infection HVT genome was detected in one out of five embryos infected with clone 2.2.4 or clone 11.1.2 and three out of five embryos infected with WT HVT (Figure 4.12a).

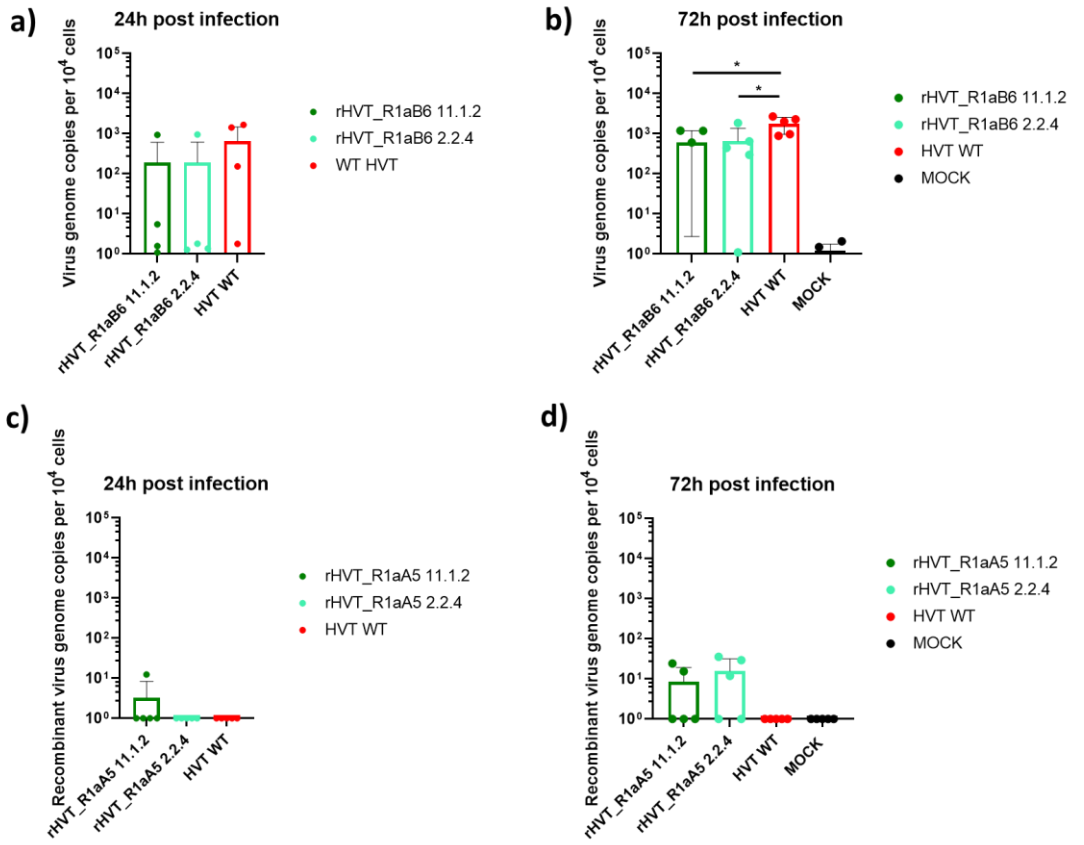

Figure 4.12. HVT replication *in ovo*. *In ovo* growth rates of passage 5 rHVT or WT viruses were measured by TaqMan qPCR with primers specific to virus at **a)** 24h and **b)** 72h time points post infection. Alternatively, TaqMan qPCR was performed with primers specific to insert at **c)** 24h and d**)** 72h time points post infection DNA samples were extracted from leg muscle tissue and the viral genome copy numbers per 10 000 cells (shown on the y axis) were assessed. qPCR was run in technical triplicates.

All embryos were positive for amplification of ovotransferin gene indicating satisfactory DNA quality. At 24 post-infection HVT mean titers in positive samples varied between ~136±346 to ~191±396 viral genome copy numbers per 10 000 cells for clones 2.2.4 and 11.1.2, respectively. On the other hand, ~699±789 viral genome copy numbers per 10 000 cells was detected for WT HVT in positive samples resulting in no statistically significant differences

between three viruses as assessed by one – way ANOVA. Although, levels of genome copy numbers were similar between recombinant and wildtype viruses at 24h post-infection significant differences in replication were observed at later time point (72h post - infection) (Figure 4.12b). Data analysis revealed four out of five (rHVT – R1aB6 clone 2.2.4), three out of five (rHVT – R1aB6 clone 11.1.2) and five out of five (WT HVT) embryos positive for HVT genome at 72h post – infection. Importantly, mean genome copy number titers varied between ~597±577, 650±683 and ~1775±814 per 10 000 cells suggesting a higher replication potential of WT HVT virus. Mock-infected eggs contained no detectable virus.

Moreover, alternative primers specific for nanobody DNA were designed to test recombinant virus levels. No amplification was found for wildtype or mock infected eggs at 24h and 72h post-infection time point (Figure 4.12.c, d). Recombinant virus titers detected were lower than those found using gene specific primers averaging to ~4±3 for clone 11.1.2 at 24h post-infection and a further increase to ~53±75 or ~112±127 per 10 000 cells at 72h time-point for clones 11.1.2 and 2.2.4, respectively.

Overall, qPCR data obtained suggests that both rHVT and WT HVT were able to infect and replicate in embryos but rHVT showed attenuated profiles as previously observed in growth kinetics profile assessed in primary cell tissue culture.

4.2.5 Characterisation of rHVT expressing therapeutic antibody in vivo

Following rHVT ability to replicate *in vitro* and *in ovo* enabling nanobody release into cell culture supernatant it was aimed to assess if this could be an efficient strategy of therapeutic antibody delivery to hatched chickens. rHVT –

R1aB6 clone 2.2.4 with higher antibody production titers was selected to determine its infectivity, ability to generate recombinant antibody and tolerability in birds. Briefly, two groups of nine naïve, specific – pathogen free (spf) chickens were administered with maximum virus titers attained after stock propagation resulting in either 37600 PFU/dose of rHVT at P5 or 27200 PFU/dose of WT HVT at P5 (Figure 4.13).

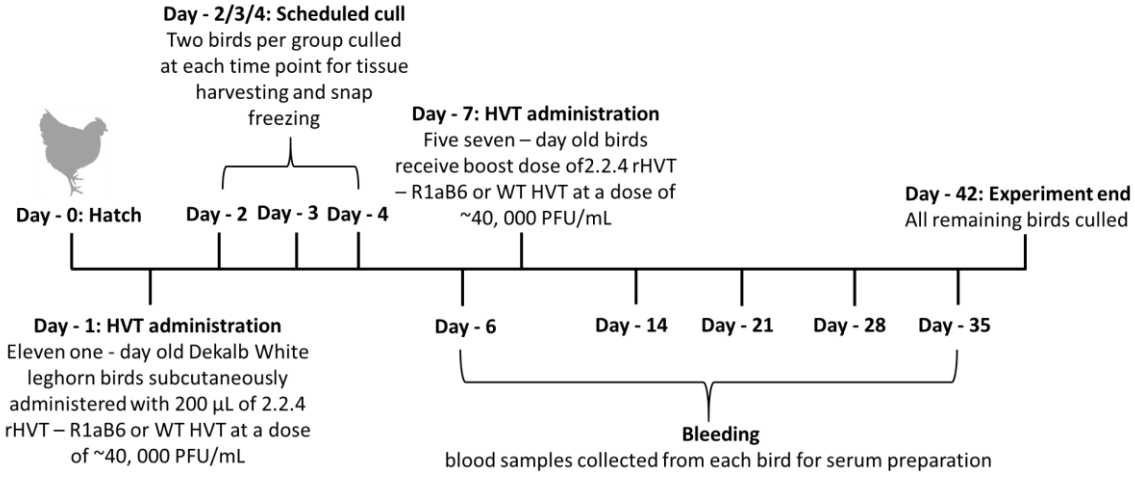

Figure 4.13. Summary of HVT tolerability study design in vivo. One day old (n=22) Dekalb White leghorn chickens were divided into two groups (n=11/group) and subcutaneously administered with 2.2.4 rHVT – R1aB6 or WT HVT at a dose of ~40, 000 PFU mL^{-1}. Two birds per group were sacrificed at day 1, 2 and 3 post vaccination for tissue harvesting. A booster dose of ~40, 000 PFU mL^{-1} of 2.2.4 rHVT – R1aB6 or WT HVT for remaining five birds per group was administered at day 7 post first vaccination. Blood samples were collected prior to booster vaccination and then weekly starting at day 14 with the experiment terminated at day 42.

The viral vector was delivered via subcutaneous inoculation at day 1 post hatch with repeated administration given at day 7 post hatch. Birds from each group were humanely culled at 24 h, 48 h and 72 h post primary vaccination and tissues were analysed for live virus quantification. PBMCs were extracted from

whole spleen samples and co-cultured with pre-seeded primary CEF cells for seven days with no virus detected by microscopical evaluation and lack of visible cytopathic effect which was further confirmed after immunostaining of cells. The remaining birds were bled at weekly intervals with the experiment terminated at day 42 post primary vaccination when tissue samples were harvested for further analysis. As previously, no live virus could be detected under co-culture conditions from day 42 samples by immunostaining.

To assess if genome of HVT virus can be found in vaccinated birds, tissue samples collected were subjected to DNA extraction and qPCR analysis. Due to HVT tropism towards PBMCs, feather and skin tissues, these in addition to lung samples were tested from day 42 post vaccination. There was no virus genome detected in lung or PBMCs (Ct ≥30). Three out of five birds vaccinated with rHVT -R1aB6 displayed a positive signal in feather samples and all birds from both groups, administered with rHVT -R1B6 or WT HVT, were positive when skin was subjected for HVT genome quantification (Figure 4.14). In this instance DNA amount was not sufficient to repeat the same experiment using gene specific primers.

An internal control of ovotransferrin and successful amplification of this gene in all the tissues for all the birds suggested satisfactory DNA quality. An additional negative and positive control of primary CEF cells uninfected or infected with WT HVT, respectively, were run alongside with amplification seen as expected.

Chapter 4 WOULD HERPESVIRUS OF TURKEYS ACT AS AN EFFICIENT VIRAL VECTOR FOR THERAPEUTIC ANTIBODY EXPRESSION *IN VITRO* AND *IN VIVO*?

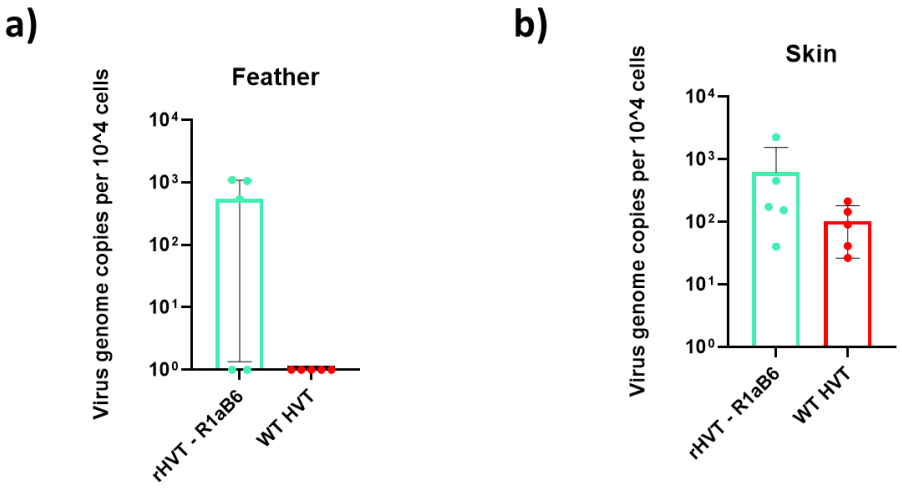

Figure 4.14. HVT genome detection in vivo. Tissues samples **a)** feather and **b)** skin were harvested and snap frozen at the end of experiment. 20mg of each tissue from individual birds was used for DNA extraction and qPCR analysis to measure HVT virus genome copy numbers normalised to 10, 000 cells (shown on the y axis). The experiment was run in triplicates.

4.2.5.1 rHVT viral vector does not express detectable protein levels systemically

Next, recombinant HVT virus ability to express detectable levels of antibodies systemically was assessed. Blood samples collected at weekly intervals were subjected for serum preparation which then was used for previously described ELISA protocol allowing transgene detection. In this instance, no signal above the background controls of WT HVT inoculated birds was found for any of samples derived from birds (Figure 4.15.). A positive control of recombinantly expressed and purified protein indicated assay working with the detection limit of ~7.66 ng mL^{-1}. No further antibody detection in any other tissues was performed based on the lack of data obtained by qPCR supporting virus presence there.

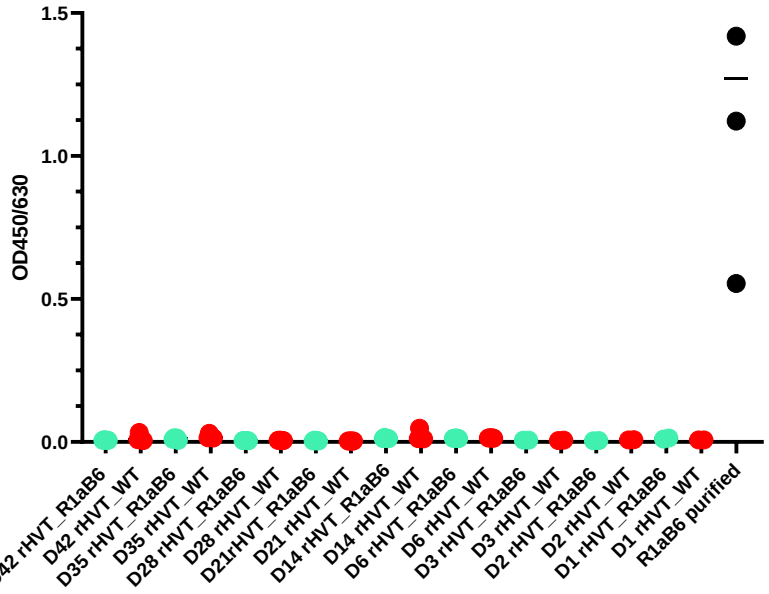

Figure 4.15. R1aB6 antibody detection in serum samples. R1aB6 antibody levels were assessed by ELISA. The plate was coated with serum samples from individual birds and probed by anti-C-tag conjugated antibody and streptavidin conjugated HRP. Antibody levels were assessed daily for the first three days after HVT administration and on day 6 post hatch, antibody levels were measured at weekly intervals after the booster dose. Responses in individual birds were measured in duplicates and are shown as OD450/630 nM, purified R1aB6 was used as positive control.

4.2.5.2 rHVT vectored antibody induces anti – antibody response in vivo

Finally, serum samples were subjected to test if anti-idiotypic antibodies have been generated. To detect chicken antibodies against camelid derived R1aB6 encoded and delivered by rHVT virus vector serum samples were diluted 1 in 1000 and used for probing of ELISA plates coated with a bivalent form of purified R1aB6. Chicken anti – antibodies were detected in rHVT vaccinated birds starting at day 21 post vaccination with levels slightly decreasing at days 35 and 42 post vaccination (Figure 4.16). Anti – idiotypic antibodies were

recorded in three out of five birds, two of which were also positive for rHVT genome in feather samples by qPCR.

These data suggest rHVT ability to deliver transgene *in vivo* and mediate its expression to the levels that can induce an immune response. However, such induction of a humoral immune response and idiotypic antibodies shows a limitation in HVT use for therapeutic antibody gene transfer. Further analysis will be needed in future to better understand if this vector can serve for vectored immunoprophylaxis purposes.

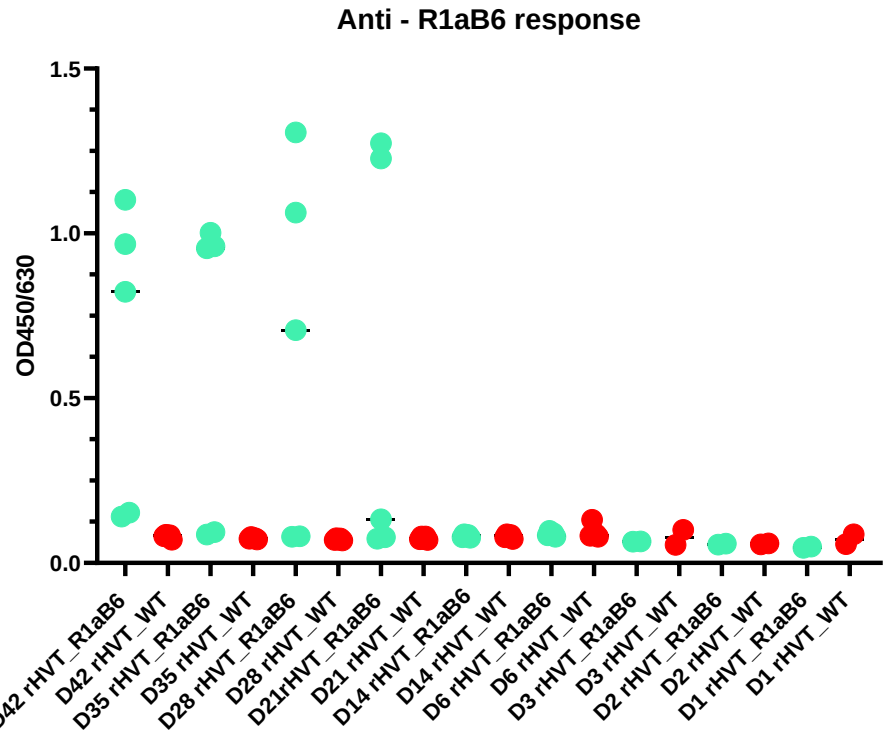

Figure 4.16. Anti – antibody response *in vivo*. Anti – R1aB6 antibodies were assessed by ELISA. The plate was coated with purified R1aB6 and serum samples from individual birds were probed by HRP conjugated anti – chicken IgY. Immune response was assessed daily for the first three days after HVT administration and on day 6 post hatch, antibody levels were measured at weekly intervals after booster dose. Responses in individual birds were measured in triplicates and are shown as OD450/630 nM.

Chapter 4 WOULD HERPESVIRUS OF TURKEYS ACT AS AN EFFICIENT VIRAL VECTOR FOR THERAPEUTIC ANTIBODY EXPRESSION *IN VITRO* AND *IN VIVO*?

4.3 Discussion

In this chapter the bivalent R1aB6 antibody was produced and characterized *in vitro* followed by generation of recombinant herpesvirus of turkeys expressing this antibody. The sequence used for bivalent antibody generation was kindly shared by Simon E.Hufton (NIBSC) who has previously indicated bivalent format being more cross-reactive with more diverse antigens (461). Antibody was purified from S2 cell culture supernatant resulting in elution of ~30 kDa protein corresponding to the size of the bivalent antibody. When assessed for affinity towards H9N2 and H5N1 viruses R1aB6 remained more cross-reactive with H9N2 viruses but not H5N1 viruses tested. This was somewhat unexpected as previous data suggest antibody to have cross reactivity with H5N1 in particular clades 1 and 2.1.3.2 (461). Several explanations for differences observed include i) monovalent vs bivalent antibody being characterised in Hufton *et al* publication and this study; ii) inconsistent antigen concentrations used for coating; iii) insufficient concentrations of R1aB6 used in this study; iv) H5N1 antigens chosen had distinct epitopes resulting in a loss of antibody binding. Although, out of eight H9N2 viruses tested all except WZ/606 were able to bind bivalent R1aB6 in ELISA only one was neutralized in the presence of R1aB6 at a concentration of 25 µg mL^{-1}. The concentration required for functional activity in this study was much higher than published data indicating H9N2 neutralization in the presence of ~0.6 ng mL^{-1} of R1aB6 (461). Differences in viruses used is the most reasonable explanation for this. Interestingly, neutralizing activity against VN/OIE/2202 belonging to clade 2.3.2.1c was observed at this study with higher concentration of antibody required again. To confirm this ELISAs should be repeated using 30 µg of purified antibody instead of 1 µg used. Overall, this study was able to identify two new antigens which were not previously

identified, combining this and published data R1aB6 becomes a promising model for antibody therapeutics against AIVs.

Generation of recombinant virus vector was based on an established CRISPR/Cas9 approach frequently used for the development of HVT vectored poultry vaccines (454). A multitude of studies has investigated HVT potential to carry foreign heterologous antigens and induce protective antibody levels against transgene with the vector being licensed for veterinary use in multiple countries (178, 408, 462). This work is the first to incorporate therapeutic antibody gene into the virus genome and assess HVT as vector for immunoprophylactic purposes.

Advantages of HVT for the use as viral vector include lack of maternally derived antibodies in chickens providing early - life vaccination ability, persistence of virus in birds and ability to accommodate multiple inserts due to large genome size (408, 463). Another important HVT feature is ability to produce cell - associated or cell - free form of viral vector (65). In this study cell-associated virus was used. Some studies imply on viral vector form ability to impact on vaccine efficacy and immunogenicity whilst others demonstrated no effect on transgene expression and levels of protection when two different forms of HVT has been administered to birds (462, 464). Generally, cell – associated form is easier to prepare and handle whilst cell- free form provides additional benefits during storage and transportation (462).

Herein, it was found that a nanobody gene cassette can be inserted into US2 site of HVT genome with around one in ten plaques displaying phenotypic changes (loss of GFP signal) from which ~16% of the plaques were confirmed to be positive for gene - and site - specific insertion as assessed by PCR. The percentage of HDR efficiency for targeted knock-in into US2 site of HVT genome has not been previously characterised. However, some evidence suggests that the same strategy can result in ~6% insertion efficiency when

the intergenic region located between UL45 and UL46 loci is targeted (465). Different insertion success rates are likely to be mediated by a variety of factors including but not limited to site of expression cassette integration (US2 vs UL45/46), size of cassette to be inserted, gRNA and protocol variations such as dose and timing of cell transfection and infection. Relatively low efficiency of HDR mediated insertion results from this pathway being engaged only in synthesis (S) and growth 2 (G2) phases of cell cycle as opposed to NHEJ which can take place throughout the cell division (460). Although no side-by-side comparison of two repair mechanisms being employed for recombinant HVT generation has been performed to the best of this study knowledge; NHEJ is still considered as a more efficient genome editing mechanism. Nevertheless, lack of homologous arms representing a higher risk of unintended indel mutations or bi-directional transgene cassette insertion has led to HDR approach being adopted herein (459). In this study, for the comparative purposes two clones (clone 2.2.4 and 11.1.2) of rHVT – R1aB6 were selected and their ability to produce recombinant antibody, to remain stable under continuous viral passages and to replicate *in vitro* were assessed. In general, both clones were able to produce recombinant antibody as seen by ELISA. Multiple factors are contributing to transgene expression efficiency from rHVT virus vector. For example, US2 site has been previously shown to potentially mediate higher transgene expression than that of US10 (431). In addition, a crucial role is played by promoter used for transcription initiation with CMV/β-actin chimera promoter (Pec) promoter demonstrated to be higher inducer than CMV (466). In this study mCMV ie2 promoter was used which is known to drive high level protein expression across multiple cell subtypes and species. Interestingly, herein variation in transgene production levels was seen during the initial screening which remained prominent in subsequent analysis at later virus passages. Such differences at early time points could be

explained by differences in virus growth kinetics as titre at that stage for the recombinant virus was not possible to determine due to virus just being rescued and not expanded enough. For the proof-of-concept study there was also limited capacity of resources to carry multiple clones into the next stage, therefore, a high likelihood that the best producer was also the best replicating virus remains. Variation in transgene levels produced at the later passages could be a true reflection of clonal differences in combination to stability and reversion to wildtype phenotype which was more prominent with 11.1.2 also coinciding with lower antibody expression. This is the first report investigating recombinant HVT virus clonal differences. On the other hand, it must be noted that traditional incorporation of antigens serving an immunogen role has in essence a completely different purpose of immune response induction where levels of transgene produced might be lower to those expected to be found when transgene is used for immunoprophylactic purposes.

In addition to inter-clonal differences, herein, significant variation in recombinant and wildtype virus growth kinetics were found. Such differences were likely to account on transgene interference with virus life cycle. Such hypothesis can be further strengthened by higher replication observed by clone 11.1.2 which was shown to have higher wildtype: recombinant virus ratio at P20 and induced lower levels of protein production. Nevertheless, multiple genomic loci have been deemed to be able to facilitate transgene insertion with no effect on virus replication including US2 site (451, 466). Moreover, other studies have shown that rHVT carrying up to three distinct expression cassettes integrated in multiple positions within the virus genome retain growth kinetics identical to wildtype HVT (408). The hypothesis of R1aB6 toxicity and interference with virus replication can also explain emergence of a small population of WT HVT after serial passages which could only be picked up by immunostaining allowing to track each plaque separately. It is not expected

that a sub-population of wildtype virus was present since the initial virus rescue as multiple rounds of selection in a 96 - well plate containing single plaques was performed. In addition, although there is not much evidence in literature personal communication has suggested knock-out events occurring regularly independently from the insert. Reversion to the wildtype is one of the main limitations if recombinant virus is to be used *in ovo* and *in vivo* and is one of the reasons why the earliest passages possible were used for further experiments.

Overall, based on *in vitro* work it was concluded that different clones should be evaluated against a wide range of factors to allow selection of the most stable clone, secreting highest levels of protein of interest. Although such analysis is likely to be performed by industry prior to vaccine approval, clone screening for the proof-of-principle studies is rare.

To further investigate if rHVT can replicate not only *in vitro* but also in eggs a short study was performed. HVT vaccines are typically suitable for *in ovo* inoculation at ED18 that does result in immune response generation at an early life of vaccinated birds (467-469). Egg susceptibility to HVT at an earlier embryonic development has been demonstrated by several studies. Interestingly, HVT has been noted to be pathogenic causing lesion formation if delivered to ED10-12 eggs with this effect disappearing from ED16 onwards (470, 471). Adherent lung cells are known to be the primary cell population infected in developing embryos with virus starting to replicate at day 1 post inoculation and its titers peaking at day 3 (472). Following *in ovo* virus replication it was decided to assess if rHVT – R1aB6 can sustain antibody production in birds. It is established that primary infection sites for MDV and vaccine strains (CVI988; HVT) against MD are lymphoid organs such as a bursa of Fabricius, thymus and spleen where it can also persist for several

weeks. Although it is known that HVT levels peak 2-3 weeks after inoculation it is not clear when virus starts replicating and spreads to different tissues which is crucial for passive immunization purposes (178). For this reason, splenocytes of vaccinated birds have been extracted 24 h, 48 h and 72 h post – inoculation and co-cultured with CEF cells. No virus was recovered in this instance indicating suboptimal sampling timing and suggesting limited recombinant virus replication and spread for at least first three days post vaccination.

Next, virus levels were assessed at the end of experiment at day 42 post vaccination. Feather samples were chosen as one of the tissues to analyse as epithelium of feather follicles is known to sustain persistent HVT infection. Three out of five birds vaccinated with recombinant HVT form were positive for virus genome by qPCR and had a median of viral load equivalent to 10^5 genome copies per million cells. This finding is somewhat different to what has been previously reported suggesting lower virus titers reaching only up to 10^4 genome copy numbers in a million cells in several chicken lines including those carrying maternally derived antibodies (473). Such differences are likely to depend on the rHVT dose delivered upon vaccine inoculation with standard practises indicating ~10-fold lower virus titers being used only at day 1 post hatch whilst here higher dose was given twice to make sure vaccination has been successful. A lack of amplification of HVT genome from some of the bird feather follicle samples could be an indication of either truly negative samples due to cleared HVT infection or limitations in sampling procedures when only several feathers are representing totality of thousands of feathers covering bird. A trend of irregularity for genome amplification from feathers taken from the same bird throughout animal experiment has been observed previously which could also be explained by infection being cleared up in some feathers but continuing to persist or re-infect others. No amplification of HVT genome

in other tissue samples tested (lung, PBMCs) most likely indicated lack of virus in those organs, however, a presence of HVT below the threshold of qPCR sensitivity must be taken into consideration. Overall, timings of tissue harvesting chosen in this experiment might be outside the optimal HVT replication period and further experiments with larger number of birds should be performed.

This study was not able to provide evidence that rHVT encoded antibody is produced systemically at the detectable levels. Whether this was due to the low protein expression by virus itself or was a result of rapid clearance due to the low molecular weight (~30 kDa) of the molecule needs to be yet established. However, no evidence supporting systemic transgene expression from rHVT virus has been found in literature suggesting its limitations to enter circulation in the first place. On the other hand, limited stability of low molecular weight molecules *in vivo* is undeniable (442, 474). This has been illustrated by monovalent nanobody incorporation into AAV vector which when administered to mice did result in serum concentrations of 0.36 µg mL^{-1} as opposed to 560 µg mL^{-1} - 1100 µg mL^{-1} when antibody was formatted into mouse IgG1 or IgG2a isotypes (442). Interestingly, even the lowest concentration could delay infection in challenged animals suggesting challenge model might be crucial for further studies (442). Even though several reports have indicated Fc addition interfering with tissue penetration and reduced pharmacokinetics, Fc-domain incorporation should be considered before the next step as it could not only benefit in half-life extension but can also potentially enhance antibody function by mediating ADCC, ADCP, or CDC response as reported by others (475-479). In this study, high anti-antibody response was observed starting at day 21 post virus inoculation. This coincides with typical immune response generation to the antigen delivered by rHVT vector (178). These data suggest antibody acting a role of antigen when delivered by HVT with further analysis

required to evaluate limit to which humoral response against transgene can contribute to its expression. Interestingly, anti-antibody response generation during VIP is often associated with low levels of transgene generated by viral vector (480). This can rely on both B and T - cell specific immunity against foreign proteins. Strategies to reduce anti-idiotypic antibody generation include codon optimisation or other approaches aiming to diminish immune response against vector itself rely on vector genome modifications such as CpG dinucleotide depletion, addition of Toll-like receptor inhibitory sequences or immunosuppressive therapy course following VIP administration (481-484). However, this would not be plausible with HVT which purpose is to act as immunogen and to provide protection against MDV.

Based on the results generated in this chapter for future work alternative virus vectors should be considered. As it was mentioned previously, up to date most promising viral vector for VIP is AAV which can successfully express therapeutic antibodies in mice and non-human primates for up to 11 months or longer (175, 485). AAV tropism towards multiple muscle types is thought to contribute to extended transgene expression due to limited cell renewal and division. In addition, AAV can also be delivered intranasally which is especially relevant for respiratory tract infections (486). However, inter-species variation towards AAV susceptibility exists with a limited understanding of poultry permissiveness to AAV. Nevertheless, some evidence exists supporting poultry specific avian adeno associated virus as viral vector for transgene expression in chick embryos (487). Other viral vectors that could be considered for passive immunization purposes in poultry include NDV, FPV or fowl adenovirus vector (FAdV). In particular, FAdV has been shown to be a potent vector for delivery of heterologous antigens as well as for VIP purposes delivering antibody fragments that were reaching protective levels against IBDV *in ovo* (430). In addition, adenovirus serotype 5 has been used in

chickens and shown to induce protective response against the target antigen (488). However, some of these vectors are susceptible to maternally derived antibodies which might become rate limiting if vaccination must be done *in ovo* or at early age. Therefore, a range of alternative viral vectors for immunoprophylactic purposes in birds should be tested.

Chapter 4 WOULD HERPESVIRUS OF TURKEYS ACT AS AN EFFICIENT VIRAL VECTOR FOR THERAPEUTIC ANTIBODY EXPRESSION *IN VITRO* AND *IN VIVO*?

Chapter 5 FINAL CONCLUSIONS AND DISCUSSION

5.1 Conclusions

The objective of this study was to develop and evaluate feasibility of passive immunization, using recombinantly produced neutralizing antibody fragments, in poultry based on avian influenza virus H9N2 subtype (A/chicken/Pakistan/UDL-01/2008) as a disease model. As a proof-of-principle this work set the basis and directions for future work focusing on the antibody choice, production systems, routes, and dosages of therapeutic antibody delivery to poultry in a form of recombinant protein or nucleic acid whilst utilizing recombinant viral vectors.

The primary focus of Chapter 2 was sequence analysis of a panel of six antibodies produced from mouse hybridomas specific to AIV H9 HA protein (330). CDR comparison with well described, publicly deposited allelic germline sequences revealed diversity in the antibody repertoire for both variable heavy and light chains. Furthermore, assessment of antibody sequence diversification from assigned germline sequences indicated most of the mutations were harboured within framework rather than complementarity determining regions suggesting an effect on overall antibody structure and confirmation. Interestingly, one of the antibodies (HA9) was found to have a completely abrogated FR1 region resulting in insufficient data for variable domain model prediction. On the other hand, remaining antibodies retained structural similarity with only two antibodies JF7 and JF8 having observably more defined, longer CDRH3 loops reflecting on longer sequences. To follow on, all six antibodies were recombinantly produced in mouse IgG1, IgG2a and scFv format and purified from cultured cell supernatants for affinity and activity comparison using ELISAs and functionally relevant virus microneutralization assays with homologous and heterologous H9N2 viruses. Briefly, antibodies

retained binding and neutralizing profile with least diverged antigens such as Egy/D7100 or UDL-02/08 which was gradually lost upon testing with antigenically distinct viruses including VN/38 or WZ/606. In general, binding to antigens was slightly lower by antibodies in an scFv format (as demonstrated by OD450/630 results) than full length mouse IgG1 or IgG2a subclasses potentially due to structural changes likewise lost bivalency. Similar results were also found in MNT assay with slightly higher concentrations of scFvs required for virus neutralization, however, the increase in concentration for three antibodies was not statistically significant. In addition, HA9 which was previously shown to lack one of the framework regions was able to efficiently neutralize an array of viruses in all formats while some antibodies (i.e., JF8) lost functional relevance after format change. Overall, this work has shown that engineered antibody fragments can maintain functional activity comparable with full-length monoclonal immunoglobulin molecules *in vitro*.

Next, in chapter 3 it was explored if scFvs which were found to have superior neutralizing profiles *in vitro* could serve for therapeutic purposes to homologous virus challenged birds when delivered intranasally *in vivo*. Data obtained indicated that scFv delivery as a prophylaxis before challenge and as a treatment after infection can partially reduce morbidity levels and virus peak infection titers. This was further confirmed after cytokine, specifically IL-6, transcript level analysis in spleen tissues, indicating more widespread inflammation in non-treated birds. However, immune pressure applied to a highly variably HA head has led to virus escape mutant generation. In this instance, three mutations were found to occur near HA receptor binding site with all three changes identified as naturally occurring in other virus strains after publicly deposited sequence analysis. In general, this work has served as a proof-of-concept that intranasal neutralizing antibody delivery to chickens can limit virus infection to a certain extent, but several limiting factors such as antibody propensity to provoke virus evolution, presumably short life of scFvs,

requirement of each bird handling for antibody administration daily in addition to several other factors must be overcome to progress this work further.

For this reason, it was hypothesised that a previously described alpaca derived broadly neutralizing R1aB6 antibody targeting HA stem would be the best choice for next part of work described in chapter 4 (461). In this chapter it was asked if a vaccine vector – herpesvirus of turkeys could act as an efficient viral vector for therapeutic antibody gene transfer and continuous high-level antibody expression *in vivo* as has been widely demonstrated with adeno associated virus in other species (175, 439, 440). To answer this question recombinant virus vectors carrying bivalent R1aB6 antibody gene was generated based on the CRISPR/Cas9 approach. Characterization of two separate recombinant HVT clones has shown that presence of antibody expression cassette interfered and led to reduced virus growth kinetics as opposed to wildtype control, however, antibody expression and secretion into the supernatant remained sufficient. In addition, it was found that after multiple passages a tendency for reversion into the wildtype was established. A similar profile was also seen after recombinant virus delivery into 10-day old embryos via the allantoic cavity. To further investigate if HVT could serve as a viral vector for therapeutic antibody delivery *in vivo* small tolerability study was performed where 1-day old chickens were administered with either recombinant or wildtype virus. Bivalent R1aB6 antibody production levels were undetectable systemically, however, anti-antibody response was found to form in birds that have received recombinant HVT indicating virus was successfully delivered and some antibody expression was occurring. The data obtained in this chapter implies that alternative virus vectors should be explored for use in poultry in combination with alternative antibody formats.

5.2 Limitations and future work directions

Several of the key areas remain in each chapter that were not addressed in this study due to the time constrains but would contribute to fundamental

knowledge if investigated further. In general the work described and data generated herein should be considered as a proof-of-concept contributing to a general understanding and providing a basis for certain hypotheses and conclusions to be drawn about antibody therapeutics feasibility in poultry. Follow-up work would be required to gain more in-depth knowledge and to further optimise each of the aspects analysed here.

To begin with, herein, functional antibody characterisation *in vitro* was mainly based on two assays ELISA and MNT. Although, virus neutralization assay is the most reliable assay that could be performed to evaluate if influenza virus life cycle can be halted in the presence of antibodies alternatively plaque reduction neutralization test (PRNT) could be incorporated. PRNT unlike MNT can provide further information beyond antibody neutralizing titre informing if antibody presence at sub-neutralizing levels would lead to changes in plaque sizes. Previously it has been shown that whole serum as well as individual monoclonal antibodies can lead to decrease in both plaque numbers and size. However, such a phenomenon is more often associated with NA, M2e targeting antibodies or HA specific immunoglobulins that do not contain neutralization activity and are involved in interfering with new virus particle release (489-492). In addition, it has been shown that presence of antibodies can also impact newly generated virion morphology decreasing the likelihood of filamentous particle formation *in vitro* (315). Another aspect that could be improved in chapter 2 was characterisation of antibody affinity towards various antigens. In multiple recent studies the ELISA assay is being replaced by bio-layer interferometry or surface plasmon resonance spectroscopy technologies allowing more precise measurement of antigen-antibody binding kinetics which was not used in this instance but would be beneficial addition in future studies (461, 493). In addition, the combination of any two antibodies was not fully tested using the whole panel of six antibodies based on some preliminary data form previous work and results prepared for publication suggesting that antibody activity for some of the antibody pairs when combined resulted in

either no changes observed or led to decrease of activity possibly due to binding to nearby epitopes and competing profiles (330, 381). However, lack of these data restrict generation of more definite conclusions.

Nevertheless, the most crucial factor playing key role in successful regime of passive immunization is choice of monoclonal antibodies. In this study H9 HA head targeting antibodies derived from mice hybridomas were used that inevitably resulted in virus escape mutant generation *in vivo*, described in chapter 3. Such a phenomenon has been observed before and, therefore, efforts are put towards antibody recovery that would be targeting more conserved epitopes providing additional hurdles for virus escape formation and increasing breadth of antibodies enabling recognition of more diverse viral antigens. Nonetheless, continuous arms race with virus has revealed its ability to overcome and create resistance even in the presence of broadly cross-neutralizing HA stalk-binding antibodies (494). Further investigations indicated higher predisposition for such mutation acquisition by certain influenza subtypes (495). Taken together, in the eyes of this thesis, such evidence suggests discovery of new epitopes should be continued and if taken forwards it is likely to become a process similar to yearly vaccine candidate matching. Therefore, to increase antibody therapeutics success rates combination of several immunoglobulins targeting multiple virus antigens (ie. HA, NA, M2e, NP) delivered as an antibody 'cocktail' or formatted into a multispecific format is likely to be necessary to minimise or ideally completely prevent virus changes. In addition, antibody effector function and a general antibody format improvement allowing optimisation of FcγR mediated functions, complement mediated function, pharmacokinetic profile and antigen binding might be necessary for optimal results.

This potentially implicates another limitation of this study where mouse derived antibodies were used in poultry. To overcome Fc-domain and receptor incompatibility and possible immunogenicity the Fc-region was removed

altogether generating scFv antibodies which were shown to have noticeable but not statistically significant changes in activity when compared to antibodies containing mouse IgG1 or IgG2a Fc-domains *in vitro*. For future studies it would be worth checking if chicken derived Fc-domain incorporation instead of mouse constant regions would result in completely restored and identical functional activity observed with full mouse hybridoma-like antibodies. Some preliminary work has been carried out in the timeframe of this study, however, data generated was inconclusive indicating further characterisation and generation of larger antibody amounts is required. Although due to the small size scFvs would potentially be beneficial in multispecific format generation in this study single monomeric scFvs were expected to have further limitation of reduced half-life *in vivo.*

Although, multiple reports have shown successful antibody recovery from human donors this area in poultry is lagging due to multiple constrains including a lack of well-defined reagents such as antibodies required for cell sorting in livestock species. To the best of this works' knowledge only a single study has shown successful antibody recovery from chickens and other host species (77). To overcome this problem protocols in the avian influenza group at the Pirbright Institute are being established allowing antibody recovery from challenged or vaccinated bird splenocytes suggesting the work that has been started herein will be continued focusing on the improvement on these key areas.

Intranasal antibody delivery has been chosen in this study. Such an approach works well in the experimental conditions and importantly it ensures accurate control of antibody dose reaching each bird. However, considering the magnitude of poultry flocks and requirement of each bird handling intranasal antibody delivery would not be efficient logistically. As discussed in chapter 3 spray immunization already in use for massive vaccination is one of the best alternative variants. This could be further improved by introducing antibody

formulation into nanoparticles. For instance, some of the potential platforms that have not been discussed previously include SpyTag/SpyCatcher protein ligase concept allowing self-assembling nanoparticle generation or induction of spontaneously forming multispecific antibody formats (496-499).

The animal experiment study testing scFv efficacy against H9N2 virus has addressed main questions evaluating morbidity levels and changes in virus titers in scFv treated vs non-treated birds. Several areas that were not addressed but would be beneficial to look at include investigation if therapeutic antibodies play immunomodulatory role and whether passive immunization leads to any differences in immune response generation in birds. Although, the HI assay performed in this study did not show any differences in serum ability to prevent red blood cell agglutination by UDL-01/08 virus, as this method can only assess levels of virus HA antigen head specific antibodies. Further assays examining the proportions of each antibody subclass generated could be performed in addition to a comparison of serum ability to neutralize homologous and heterologous antigens assessed by the MNT test. Although, in this instance the Fc-region in scFv antibodies was absent other studies demonstrated that immune complex formation between antigen and full-size antibody can lead to enhanced antigen uptake and presentation, therefore, leading to stronger and broader immune response that might also be possibly formed while therapeutic antibodies containing Fc-domain are administered (156). Moreover, only three cytokines (IL-6, IL-4 and IFNγ) were tested in the study corresponding to the acute phase response, Th2 stimulation and macrophage activation in poultry. Recent work also suggests high involvement of poly (ADP-ribose) polymerase (PARP), 2'-5'-oligoadenylate synthetase-like (OASL), myxovirus resistance 1 (MX1) and C-X-C Motif Chemokine Ligand 1 (CXCLi1) amongst other immune-related gene expression following H9N2 infection, assessment of which could have provided further insights into levels of protection development during subsequent exposures (433). Having seen rapid virus clearance it is envisaged that a shorter therapeutic administration

window would be sufficient and the use of maximal dosages rather than prolonged periods at smaller doses would be advisable for future studies. A further point can be raised addressing virus dose used for bird challenge with some school of thought supporting virus titration by 50% egg infectious dose (EID50) rather than plaque assays due to the relevance in poultry infection (433, 500, 501). However, the later method chosen herein was well-established and proven to work in multiple studies suggesting if the infectious virus dose is adjusted the method used for virus titration should not have significant effect on study outcome (502, 503). Another potential shortcoming in this work was use of challenged, non-treated birds as a negative control instead of administering different specificity or 'scrambled sequence' antibody which would be beneficial to include in any other future studies. In addition, environmental sample analysis (such as water and food) could contribute to better understanding of therapeutic antibody effect on virus circulation in the environment.

Nevertheless, conventionally purified antibodies are expensive to produce revealing another challenge with the costs of therapeutic antibodies likely exceeding the costs of pre-emptive stamping out of poultry if the outbreak occurs. Therefore, the next part of work focused on viral vectored immunoprophylaxis generation and this approach feasibility evaluation in poultry. One of the main advantages of antibody gene delivery by viral vector is once a lifetime administration ensuring antibody secretion at sufficient levels for prolonged periods of time. For this reason, careful selection of viral vector with tropism only to target tissues, likewise, respiratory tract for the delivery of influenza virus specific antibodies would be beneficial. In addition, controlled transgene expression *in vivo* can be achieved in several ways with some success demonstrated with inducible promoters incorporating tetracycline-responsive transcriptional elements, micro RNAs or steroid dependant switches (504-506). The rationale of this study to use HVT virus as viral vector was based on licensed approval of this vector for various antigen delivery in

poultry and reagent availability. One factor within *in ovo* studies that would have been interesting to investigate was recombinant virus administration to older embryos (day 16-17) that would have specific tissues developed to allow tissue differentiation for susceptibility towards HVT and permissibility for therapeutic antibody expression. In addition, *in ovo* vaccinations with HVT are typically administered to amniotic rather than allantoic cavity; the impact of route of delivery should be assessed to understand how it can impact virus replication and distribution. Another important question that was not addressed in this study but would need further investigation is on the role of anti-antibody response and whether it would interfere with VHH binding to the antigen or its functional activity.

Alternative approaches to viral vectored immunoprophylaxis that could sustain therapeutic antibody expression *in vivo* could be via delivery of DNA plasmid encoded antibodies into the muscle tissues or local mRNA formulated in a liposomal formulation administration (429, 507). In addition, even more complex approaches such as of engineering of target species and development of transgenic animals incorporating antibody genes into the host genome have been demonstrated as an efficient mechanism. This has been proven with generation of *Aedes Aegypti* mosquitoes carrying scFv antibody neutralizing multiple dengue virus subtypes or transgenic chickens carrying 3D8 scFv with hydrolysing ability specific to nucleic acid (115, 508).

Finally, as of current knowledge and understanding two major hurdles for passive immunization in poultry exist including therapeutic antibody production costs and with regards to avian influenza virus high virus ability to adapt and overcome selective pressure of immunoglobulin molecules. Although production costs can be greatly reduced by delivery of nucleic acid encoding desired antibody compatibility with massive immunization advantages would be extremely beneficial if poultry and other livestock becomes one of the target hosts. Regarding choice of antibodies, it appears that combination of several

immunoglobulins targeting diverse, yet well conserved epitopes might be required. Alternatively, to further enhance passive immunization effects combined therapies with antivirals might be necessary. However, current rules do not allow antiviral usage in poultry to prevent virus evolution; whether the same will not happen with therapeutic antibodies remains uncertain. Nevertheless, it is expected that for some antigens the choice of antibodies might be much easier and passive immunization approach more applicable as illustrated with well-established RSV example in humans. Plausibly if therapeutic antibodies are established in case of the emergence of the outbreak to achieve the best results a combination of nucleic acid encoding therapeutic antibodies and purified protein delivery should be considered that will act as additional control measures alongside vaccination.

Chapter 6 MATERIALS AND METHODS

6.1 Materials

6.1.1 General reagents

2- Mercaptoethanol	Sigma Aldrich (M6250-10ML)
3,3′,5,5′-tetramethylbenzidine (TMB) substrate	BD Biosciences (555124)
30% Acrylamide/Bis solution 37.5:1	Bio-Rad (1610158)
Acetone analar	Sigma Aldrich (32201-2.5L)
Amersham™ Protran® Western blotting membranes, nitrocellulose	Sigma Aldrich (GE10600002)
Ammonium persulphate (APS)	Sigma Aldrich (A3678-25G)
Ampicillin ready-made solution	Sigma Aldrich (A5354-10ML)
Bovine Serum Albumin (BSA)	Sigma Aldrich (A7906-100G)
Bromophenol blue	Sigma Aldrich (B0126-25G)
CaptureSelect™ C-tag Affinity Matrix	Thermo Fisher Scientific (191307005)
Crystal violet solution	Sigma Aldrich (V5265-500ML)
DAB Chromogen and Substrate Buffer	Agilent (K3468)
dNTP set	Thermo Fisher Scientific (10297018)
DTT	Sigma Aldrich (10197777001)
ELISA coating buffer	The Pirbright Institute, cell culture services
Ethanol absolute ≥99.8%	VWR International (20821.321)

GelRed Nucleic Acid Gel Stain 10,000X in water	Biotium (BT41003-5)
Glycine	Sigma Aldrich (G8898)
HistoPaque 1083	Sigma Aldrich (10831-100ML)
Hyperladder™ 1 kb Bioline	Bioline (BIO-33026)
Protein G IgG Binding Buffer	Thermo Fisher Scientific (21011)
IgG Elution Buffer	Thermo Fisher Scientific (21004)
Kanamycin solution from Streptomyces	Sigma Aldrich (K0254-20ML)
LB Broth (Miller)	Sigma Aldrich (L3522-1KG)
Methanol analar	Sigma Aldrich (32213-2.5L)
$MgCl_2$	Sigma Aldrich (M8266-1KG)
Molecular Biology Grade Agarose for gel electrophoresis	EUROGENTEC (18037G)
PageBlue™ Protein staining solution	Thermo Fisher Scientific (24620)
Phosphate buffered saline (PBS)	The Pirbright Institute, cell culture services
PBS'a' (PBS without calcium, magnesium)	The Pirbright Institute, cell culture services
Pierce™ BCA protein assay	Thermo Fisher Scientific (23225)
Pierce protein G agarose	Thermo Fisher Scientific (20397
Precision Plus Protein™ All Blue Prestained Protein Standards	Bio-Rad (1610373)
Purified agar for plaque assay	Oxoid (LP0028)
QIAamp® One-For-All Nucleic Acid kit	Qiagen (965672)
Qiagen DNA blood and tissue kit	Qiagen (69504)
Qiagen Proteinase K	Qiagen (19131)

Qiagen Qiafilter plasmid filter maxi kit	Qiagen (12162)
Qiagen Qiaprep miniprep kit	Qiagen (27106)
Qiagen Qiaquick gel extraction kit	Qiagen (28704)
Qiagen RNeasy mini kit	Qiagen (74104)
Skimmed milk powder	Marvel
Super Optimal broth with Catabolite repression (SOC) medium	Thermo Fisher Scientific (15544034)
Tetramethylethylenediamine (TEMED)	Bio-Rad (161-0800)
Tris	Sigma Aldrich (T1503-25G)
Tris Glycine SDS PAGE Buffer (10X)	National diagnostics (EC-8700)
Tween 20	Sigma (P1379-1L)
Ultra-pure Tris/borate/EDTA (TBE) buffer	Thermo Fisher Scientific (15581044)
UltraPure™ DNase/RNase-Free Distilled Water	Thermo Fisher Scientific (10977049)

6.1.2 Enzymes and master mixes

ABsolute Blue qPCR Low ROX mix	Thermo Fisher Scientific (AB4318B)
GoTaq® Green Master Mix	Promega (M7123)
PfuUltra II Hotstart 2x Master mix	Agilent (600852)
Restriction enzymes	New England Biolabs
Superscript III one-step RT-PCR with PlatinumTM Taq DNA polymerase	Thermo Fisher Scientific (1257435)

T4 DNA ligase	New England Biolabs (M0202)
T4 DNA polymerase	New England Biolabs (M0203S)

6.1.3 Antibodies

Table 6.1. Antibodies used in this study

Antibody	Type	Source	Notes
ID2	IgG1 mouse monoclonal	This study	Raised against UDL-1/08 H9HA
JF7	IgG1 mouse monoclonal	This study	Raised against UDL-1/08 H9HA
EC12	IgG1 mouse monoclonal	This study	Raised against UDL-1/08 H9HA
HA9	IgG1 mouse monoclonal	This study	Raised against UDL-1/08 H9HA
CGA12	IgG1 mouse monoclonal	This study	Raised against UDL-1/08 H9HA
JF8	IgG1 mouse monoclonal	This study	Raised against UDL-1/08 H9HA
ID2	IgG2a mouse monoclonal	This study	Raised against UDL-1/08 H9HA
JF7	IgG2a mouse monoclonal	This study	Raised against UDL-1/08 H9HA
EC12	IgG2a mouse monoclonal	This study	Raised against UDL-1/08 H9HA
HA9	IgG2a mouse monoclonal	This study	Raised against UDL-1/08 H9HA
CGA12	IgG2a mouse monoclonal	This study	Raised against UDL-1/08 H9HA

JF8	IgG2a mouse monoclonal	This study	Raised against UDL-1/08 H9HA
ID2	scFv fragment	This study	Raised against UDL-1/08 H9HA
JF7	scFv fragment	This study	Raised against UDL-1/08 H9HA
EC12	scFv fragment	This study	Raised against UDL-1/08 H9HA
HA9	scFv fragment	This study	Raised against UDL-1/08 H9HA
CG12	scFv fragment	This study	Raised against UDL-1/08 H9HA
JF8	scFv fragment	This study	Raised against UDL-1/08 H9HA
R1aB6	Bivalent VHH fragment	This study	Raised against pdm/09

Table 6.2 Primary antibodies used in this study

Antibody	**Application (dilution)**	**Source**
CaptureSelect™ Biotin Anti-C-tag Conjugate	WB, ELISA, immunostaining (1:500 – 1:5000)	Thermo Fisher Scientific
Polyclonal chicken anti-HVT serum	Immunostaining (1:500)	In house raised by Iqbal group
vNr-13 anti HVT-encoded Bcl-2 homologue clone EG2	WB (1:20)	Avian Oncogenic Viruses group, The Pirbright Institute

Table 6.3. Secondary antibodies used in this study

Antibody	Application	Source
Streptavidin – HRP conjugate	ELISA (1:500)	Thermo Fisher Scientific
Polyclonal rabbit anti-mouse immunoglobulins HRP	ELISA (1:2000)	Agilent
Anti-chicken IgY (IgG) (whole molecule) − peroxidase antibody	ELISA (1:10, 000)	Sigma Aldrich
IRDye® 680RD Donkey anti-Chicken IgG (H + L)	WB (1:10, 000)	LI-COR Biosciences
IRDye® 680RD Donkey Anti-Chicken Secondary Antibody	WB (1:10, 000)	LI-COR Biosciences
IRDye® 800CW Streptavidin	WB (1:2000)	LI-COR Biosciences

6.1.4 Plasmids

Table 6.4. Plasmids used in this study

Name	Description	Source
pExpres2.1	Expression plasmid for S2 cells	ExpreS2ion Biotechnologies
pNeoSec	Expression plasmid for ExpiCHO cells	The UK Immunological Toolbox
pUC18	Donor plasmid carrying homology arms for recombinant HVT virus rescue	Addgene (Cat no. #50004)
pSpCas9(BB)-2A-Puro (PX459) V2.0	Plasmid for guide RNA insertion and	Addgene (Cat no. #62988)

	recombinant HVT virus rescue	
pHVT-BAC3	Plasmid for HVT qPCR standards	Avian Oncogenic Viruses group, The Pirbright Institute
pGEMT-Ovo	Plasmid for ovotransferrin qPCR standards	Avian Oncogenic Viruses group, The Pirbright Institute

6.1.5 Eukaryotic cell culture

Table 6.5. Cell lines used in this study

Cell line	**Notes**	**Source**
S2	Drosophila Schneider 2 cells	ExpreS2ion Biotechnologies
ExpiCHO	Chinese Hamster Ovary cells	Thermo Fisher Scientific
MDCK	Madin darby canine kidney cells	ATCC
CEF	Chicken embryo fibroblast	The Pirbright Institute

6.1.5.1 *Cell culture reagents*

Calcium Phosphate transfection kit	Thermo Fisher Scientific (K278001)
Dextran hydrochloride	Sigma Aldrich (D-9885-50G)
Dulbecco's modified Eagle's medium	Sigma Aldrich (D6429-6X500ML)
EX-CELL® 420 Serum-Free Medium for Insect Cells	Sigma Aldrich (14420C-1000ML)
ExpiCHO™ Expression Medium	Thermo Fisher Scientific (A2910001)

ExpiCHO™ expression system kit	Thermo Fisher Scientific (A29133)
Foetal bovine serum (FBS) sterile filtered - Brazil	Life Science Production (S-001A-BR)
Gentamicin sulphate salt bioreagent	Sigma Aldrich (G1264-1G)
Hepes solution	Sigma Aldrich (H0887-100ML)
L-glutamine	Thermo Fisher Scientific (25030024)
Medium 199	Sigma Aldrich (M4530-6X500ML)
Minimum Essential Medium	Sigma Aldrich (M027-100ML)
Nystatin bioreagent	Sigma Aldrich (N6261-500KU)
Ofloxacin HCl	Sigma Aldrich (O8757)
OptiMEM, reduced serum medium, no phenol red	Thermo Fisher Scientific (11058021)
Penicillin G potassium salt bioreagent	Sigma Aldrich (P7794-1MU)
Penicillin-Streptomycin (10,000U/ML)	Thermo Fisher Scientific (15140122)
Polymyxin B sulphate salt bioreagent	Sigma Aldrich (P4932-5MU)
Roswell Park Memorial Institute (RPMI) medium	Sigma Aldrich (R8758-6X500ML)
Schneider’s insect medium	Sigma Aldrich (S0146-6X500ML)
Sodium bicarbonate solution	Sigma Aldrich (S8761-100ML)
(SDS)	Sigma Aldrich (L3771)
Streptomycin sulphate salt bioreagent	Sigma Aldrich (S9137-25G)
Sulfamethoxazol vetranal	Sigma Aldrich (31737-250MG)
TPCK trypsin	Sigma Aldrich (T8802-100MG)

*Trans*IT-X2® Dynamic Delivery System	MirusBio (MIR 6003)
Trypsin (2.5%), no phenol red	Thermo Fisher Scientific (15090046)
Tryptose phosphate broth (TPB)	Sigma Aldrich (T8159-100ML)
Versene	Thermo Fisher Scientific (15040033)
Zeocin	Invivogen (ant-zn-5p)

Table 6.6 Cell culture media composition used in this study

CEF growth media	5% v/v FCS
	10% v/v TPB
	Medium 199
MDCK growth media	10% v/v FCS
	DMEM
S2 growth media	10% v/v FCS
	Schneider's insect medium
Influenza virus plaque assay overlay media composition	0.0005% dextran hydrochloride
	0.15% w/v sodium hydrocarbonate
	0.2% w/v BSA
	100 U mL^{-1} Pen/Strep
	10 mM Hepes
	10x Minimum Essential Medium

	2 mM L-glutamine
	2µg mL^{-1} TPCK trypsin
Virus transport media (adjusted to Ph 7.4)	0.5% v/v BSA,
	Gentamicin 250 mg L^{-1}
	Medium 199,
	Nystatin 5x 105 U L^{-1}
	Ofloxacin HCl 60 mg L^{-1}
	Penicillin G 2 x 10^6U L^{-1}
	Polymyxin B 2 x 10^6 UL $^{-1}$
	Streptomycin 200 mg L^{-1}
	Sulfamethoxazol 0.2 g L^{-1}

Table 6.7. Bacteria culture media composition used in this study

Luria Broth (LB) medium	LB Broth (Miller)
	100 µg mL^{-1} ampicillin or 50 µg mL^{-1} kanamycin or 25 µg mL^{-1} zeocin
LB agar plates	Pre-made LB medium
	1.5% w/v agar
	100 µg mL^{-1} ampicillin or 50 µg mL^{-1} kanamycin or

	25 µg mL^{-1} zeocin

6.1.6 SDS PAGE gels composition

Stacking gel – always cast at 4%

MQ Water	2.1 mL
30% Acrylamide/Bis solution 37.5:1	0.5 mL
1.0 M Tris-HCL (pH 6.8)	0.38 mL
10% SDS	0.03 mL
10% APS	0.03 mL
TEMED	0.003 mL

Resolving gel - 8%

MQ Water	2.3 mL
30% Acrylamide/Bis solution 37.5:1	1.3 mL
1.0 M Tris-HCL (pH 8.8)	1.3 mL
10% SDS	0.05 mL
10% APS	0.05 mL
TEMED	0.005 mL

Resolving gel - 10%

MQ Water	1.9 mL

30% Acrylamide/Bis solution 37.5:1	1.7 mL
1.0 M Tris-HCL (pH 8.8)	1.3 mL
10% SDS	0.05 mL
10% APS	0.05 mL
TEMED	0.005 mL

Resolving gel - 12%

MQ Water	1.6 mL
30% Acrylamide/Bis solution 37.5:1	2.0 mL
1.0 M Tris-HCL (pH 8.8)	1.3 mL
10% SDS	0.05 mL
10% APS	0.05 mL
TEMED	0.005 mL

6.1.7 Buffers/solutions

*All buffers/solutions prepared in distilled water unless otherwise stated.

Table 6.8. Buffers and solutions used in this study

Crystal violet solution	0.1% v/v crystal violet
	20% Methanol
ELISA blocking buffer/antibody dilution	PBS 5% w/v BSA
ELISA stop solution	2 M H2SO4

Immunostaining blocking buffer	PBS 5% v/v FCS
Methanol:acetone 1:1	50% methanol
	50% acetone
SDS loading dye	8 M urea
	2% w/v SDS
	10 mM Tris HCl pH 6.8
	0.01% v/v Bromophenol blue
Wash buffer (WB/ ELISA/ immunostaining)	PBS/0.1% v/v Tween20
Western blot antibody dilution	PBS/0.1% v/v Tween20
	1% w/v skimmed milk
Western blot blocking buffer	PBS/0.1% v/v Tween20
Western blot transfer buffer	25 mM Tris,
	192 mM glycine
	20% v/v methanol

6.1.8 Viruses

Table 6.9. Viruses used in this study

Strain	**Alias**	**Notes**
A/Chicken/Egypt/D7100/2013 (H9N2)	Egy/D7100	1:1:6 recombinant with Egy/D7100 HA, UDL-1/08 NA and PR8 internals
A/Chicken/India/WB-NIV1057169/2010 (H9N2)	India/WB	1:1:6 recombinant with India/WB HA, UDL-1/08 NA and PR8 internals

A/Chicken/Pakistan/UDL-01/08 (H9N2)	UDL-1/08	2:6 recombinant
A/Chicken/Pakistan/UDL-02/08 (H9N2)	UDL-2/08	1:1:6 recombinant with UDL2/08 HA, UDL-1/08 NA and PR8 internals
A/Chicken/Wenzhou/606/2013 (H9N2)	WZ/606	1:1:6 recombinant with WZ/606 HA, UDL-1/08 NA and PR8 internals
A/Chinese Hwamei/Vietnam/38/2006 (H9N2)	VN/38	1:1:6 recombinant with VN/38 HA, UDL-1/08 NA and PR8 internals
A/environment/Bangladesh/10306/2011 (H9N2)	Env/BD	1:1:6 recombinant with env/BD HA, UDL-1/08 NA and PR8 internals
A/Quail/United Arab Emirates/D1556/2014 (H9N2)	UAE/D1556	1:1:6 recombinant with UAE/D1556 HA, UDL-1/08 NA and PR8 internals
A/Chicken/Nepal/T-359/2014 (H5N1)	Npl/T-359	1:6 recombinant with Npl/T-359 HA, PR8 NA and internals
A/Duck/Vietnam/OIE-0062/2012 (H5N1)	VN/OIE/0062	1:6 recombinant with VN/OIE/0062 HA, PR8 NA and internals
A/Duck/Vietnam/OIE-2202/2012 (H5N1)	VN/OIE/2202	1:6 recombinant with VN/OIE/2202HA, PR8 NA and internals
A/Tree Sparrow/Indonesia/D10013/2010 (H5N1)	IDN/D10013	1:6 recombinant with IDN/D10013 HA, PR8 NA and internals

A/Turkey/Egypt/137/2013 (H5N1)	Egy/137	1:6 recombinant with Egy/137 HA, PR8 NA and internals
A/Yunnan/0127/2015 (H5N1)	CN-YN/0127	1:6 recombinant with CN-YN/0127 HA, PR8 NA and internals
A/California/7/2009 (H1N1)	09/pdm	Full virus
Fc126 HVT	WT HVT	Full virus
Fc126 HVT - GFP	GFP HVT	Recombinant virus with GFP at US2 site
Fc126 HVT – R1aB6 2.2.4	2.2.4 rHVT R1aB6	Recombinant virus with GFP at US2 site clone 2.2.4
Fc126 HVT – R1aB6 11.1.2	11.1.2 rHVT R1aB6	Recombinant virus with GFP at US2 site clone 11.1.2

6.1.9 Eggs

Table 6.10. Eggs used in this study

Species	**Supplier**	**Age (from – to)**	**Use**
VALO Biomedia clean eggs	VALO Biomedia	Embryonic day 10 - Embryonic day 12	Influenza virus stocks growth
		Embryonic day 12	Production of CEF cells
		Embryonic day 16 - Embryonic day 19	Assessment of HVT virus replication in eggs
Dekalb White leghorn	VALO Biomedia	Day 1 post hatch - 42 days old	Assessment of HVT virus tolerability in adult birds

Rhode Island Red	National Avian Research Facility	20 days old - 42 days old	Influenza virus challenge study

6.1.10 Primers

Table 6.11. cDNA primers used in this study

Name	Sequence	Description
UniHA FW	AGCAAAAGCAGGGG	Complementary to the 5' end of vRNA of IAV HA segment
UniHA RV	AGTAGAAACAAGGGTGTTTT	Complementary to the 3' end of vRNA of IAV HA segment

Table 6.12. qPCR primers and probes used in this study

Name	Sequence	Description
Influenza M FW	AGATGAGTCTTCTAACCGAGGTCG	Designed to amplify influenza M segment
Influenza M RV	TGCAAAAACATCTTCAAGTCTCTG	
Influenza M probe	AM-TCAGGCCCCCTCAAAGCCGA-TAMRA	
IL-4 FW	AACATGCGTCAGCTCCTGAAT	
IL-4 RV	TCTGCTAGGAACTTCTCCATTGAA	

IL-4 probe	FAM-AGCAGCACCTCCCTCAAGGCACC-TAMRA	Designed to amplify chicken IL-4
IL-6 FW	GCTCGCCGGCTTCGA	Designed to amplify chicken IL6
IL-6 RV	GGTAGGTCTGAAAGGCGAACAG	
IL-6 probe	FAM-AGGAGAAATGCCTGACGAAGCTCTCCA-TAMRA	
IFNγ FW	GTGAAGAAGGTGAAAGATATCATGGA	Designed to amplify chicken IFNγ
IFNγ RV	GCTTTGCGCTGGATTCTCA	
IFNγ probe	FAM-TGGCCAAGCTCCCGATGAACGA-TAMRA	
28S FW	GGCGAAGCCAGAGGAAACT	Designed to amplify chicken ribosomal protein 28S
28S RV	GACGACCGATTTGCACGTC	
28S probe	FAM-AGGACCGCTACGGACCTCCACCATAMRA	
HVT FW	GGCAGACACCGCGTTGTAT	Designed to amplify HVT virus ORF1
HVT RV	TGTCCACGCTCGAGACTATCC	
HVT probe	FAM-AACCCGGGCTTGTGGACGTCTCC-BHQ1	
Ovo FW	CACTGCCACTGGGCTCTGT	Designed to amplify Chicken ovotransferrin
Ovo RV	GCAATGGCAATAAACCTCCAA	
Ovo probe	YAKIMA YELLOW-AGTCTGGAGAAGTCTGTGCAGCCTCCA-TAMRA	
R1aB6 FW	CGCTGCCGGTAAGCCTAT	Designed to amplify R1aB6 transgene
R1aB6 RV	TGGGCCTCGAAGATGTCGTT	

R1aB6 probe	FAM-TAACCCTCTCCTCGGTCTCGATT-BHQ1	

Table 6.13. Sequencing primers used in this study

Name	Sequence	Description
pExpres2.1 sequencing FW	GACTCTTGCGTTTCTGATAGG	Sequencing of 5' end of insert in pExpres2.1
pExpres2.1 sequencing RV	GGAGTGTGTAAATGGACAA	Sequencing of 3' end of insert in pExpres2.1
pNeoSac Mm IgG1	TAGTTTGGGCAGCAGATCCA	Sequencing of 3' end of insert in pNeoSac Mm IgG1
pNeoSac Mm IgG2a	CACCGAGGAGCCAGTTGTAT	Sequencing of 3' end of insert in pNeoSac Mm IgG2a
pNeoSac Mm kappa	CACCTCCAGATGTTAACTG	Sequencing of 3' end of insert in pNeoSac Mm kappa
pUC18 FW	CACACGTCAGCTCATCGGTTAGC	Sequencing of 5' end of insert in pUC18
pUC18 RV	GTACCGTCGCAGTCTTCGGTCT	Sequencing of 3' end of insert in pUC18
M13 FW	TGTAAAACGACGGCCAG	Sequencing of PCR products containing M13 extension

Table 6.14. Cloning primers used in this study

Name	Sequence	Description
CD33 FW	ATGCCGCTGCTGCTACTGCTGCCC	scFv ID2, scFv JF7, scFv EC12, R1Ab6 subloning into pExpres2.1 from GeneArt gene synthesis product
C-tag RV	TTAAGCCTCTGGCTCCTCGTGCCA	
CG12/HA9/JF8 VL FW	ATAGAATTCATGGGGATCCTTCCCAGCCCTGGGATGCCTGCGCTGCTCTCCC	CG12 subcloning from IgG2a into scFv format
CG12 VL linker RV	TCCGCTTCCTCCGCCGCCACTTCCGCCTCCGCCATCAGCCCGTTTGA	
CG12 VH linker FW	GGCGGCGGAGGAAGCGGAGGCGGAGGATCCGAGGTGCAGCTGGAGCAGTCA	
CG12 VH RV	ATAAGGCCTGGCTGTTGTTTTGGCTGAGGAGACTGTGAGAGTGGAGCCTTGGCCCCAGTAGTCAAAACCCCAGTGAT	
HA9 VL linker RV	TCCGCTTCCTCCGCCGCCACTTCCGCCTCCGCCTGGTGCAGCATCAGCCC	HA9 subcloning from IgG2a into scFv format
HA9 VH linker FW	GGCGGCGGAGGAAGCGGAGGCGGAGGATCCGGAGGCTTAGTGCAGCCT	
HA9 VH RV	GTTCAGGCCTTTTGGGGCTGTTGTTTTGGCTGAGGAGACTGTGAGAGTGGTGCCTTGGCCCCA	
JF8 VL linker RV	TCCGCTTCCTCCGCCGCCACTTCCGCCTCCGCCATCAGCCCGTTTTATTTCCA	JF8 subcloning from IgG2a into scFv format
JF8 VH linker FW	GGCGGCGGAGGAAGCGGAGGCGGAGGATCCGAGGTGCAGCTGCAGGAGTCT	

JF8 VH RV	ATAAGGCCTGGCTGTTGTTTTGGC TGAGGAGACTGTGAGAGTGGTGC CTTGGCCCC	
ID2 pNeoSec MmFc IgG1 FW	TGGGTTGCGTAGCTGAGTTCCAC CTGCAGCAG	VH chain of ID2 subcloning into pNeoSec MmFc IgG1 from scFv format
ID2 pNeoSec MmFc IgG1 RV	GGGTGTCGTTTTGGCTGAGGAGA CGGTGAC	
ID2 pNeoSec MmFc IgG2a FW	TGGGTTGCGTAGCTTCTGAGTTCC ACCTGCAGCAGTC	VH chain of ID2 subcloning into pNeoSec MmFc IgG2a from scFv format
ID2 pNeoSec MmFc IgG2a RV	GGCTGTTGTTTTGGCTGAGGAGA CGGTGACTGAGGTTCC	
ID2 pNeoSec MmFc kappa FW	TGGGTTGCGTAGCTGACATCCAG ATGACTC	VL chain of ID2 subcloning into pNeoSec MmFc kappa from scFv format
ID2 pNeoSec MmFc kappa RV	TGCAGCATCAGCCCGTTTGATTTC CAGCTT	
JF7 pNeoSec MmFc IgG1 FW	TGGGTTGCGTAGCTCAGGTCCAA CTGCAGCAGCCT	VH chain of JF7 subcloning into pNeoSec MmFc IgG1 from scFv format
JF7 pNeoSec MmFc IgG1 RV	GGGTGTCGTTTTGGCTGAGGAGA CGGTGACTGAGGTT	
JF7 pNeoSec MmFc IgG2a FW	TGGGTTGCGTAGCTCAGGTCCAA CTGCAGCAGCCT	VH chain of JF7 subcloning into pNeoSec MmFc IgG2a from scFv format
JF7 pNeoSec MmFc IgG2a RV	GGCTGTTGTTTTGGCTGAGGAGA CGGTGACTGAGGTTCC	
JF7 pNeoSec MmFc kappa FW	TGGGTTGCGTAGCTAACATTGTAA TGACC	VL chain of JF7 subcloning into

JF7 pNeoSec MmFc kappa RV	GGTCATTACAATGTTAGCTACGCA ACCCAT	pNeoSec MmFc kappa from scFv format
EC12 pNeoSec MmFc IgG1 FW	TGGGTTGCGTAGCTGAAGTGAAG CTGGTGGAGTCTGA	VH chain of EC12 subcloning into pNeoSec MmFc IgG1 from scFv format
EC12 pNeoSec MmFc IgG1 RV	GGGTGTCGTTTTGGCTGAGGAGA CTGTGAGAGTGGT	
EC12 pNeoSec MmFc IgG2a FW	TGGGTTGCGTAGCTGAAGTGAAG CTGGTGGAGTCTGA	VH chain of EC12 subcloning into pNeoSec MmFc IgG2a from scFv format
EC12 pNeoSec MmFc IgG2a RV	GGCTGTTGTTTTGGCTGAGGAGA CTGTGAGAGTGGTGCC	
EC12 pNeoSec MmFc kappa FW	TGGGTTGCGTAGCTGAAATCCAGA TGACA	VL chain of EC12 subcloning into pNeoSec MmFc kappa from scFv format
EC12 pNeoSec MmFc kappa RV	TGCAGCATCAGCCCCTTTGATTTC CAGCTT	
CG12 pNeoSec MmFc IgG1 FW	TGGGTTGCGTAGCTGAGGTGCAG CTGGAGCA	VH chain of CG12 subcloning into pNeoSec MmFc IgG1 from scFv format
CG12 pNeoSec MmFc IgG1 RV	GGGTGTCGTTTTGGCGGCTGTTG TTTTGGCT	
HA9 pNeoSec MmFc IgG1 FW	TGGGTTGCGTAGCTGGAGGCTTA GTGCAGCC	VH chain of HA9 subcloning into pNeoSec MmFc IgG1 from scFv format
HA9 pNeoSec MmFc IgG1 RV	GGGTGTCGTTTTGGCTGGGGCTG TTGTTTTG	
JF8 pNeoSec MmFc IgG1 FW	TGGGTTGCGTAGCTGAGGTGCAG CTGCAGGA	VH chain of JF8 subcloning into pNeoSec MmFc IgG1 from scFv format
JF8 pNeoSec MmFc IgG1 RV	GGGTGTCGTTTTGGCGGCTGTTG TTTTGGCT	

R1aB6 pUC18 FW	ATTGTCGACGGTACCTTAAGCCTC TGGCTCCTCGTGCCA	R1aB6 subcloning into pUC18 from pExpres2.1
R1aB6 pUC18 RV	TCCACCGGTCGCCACCATGCCGC TGCTGCTACTGCTGC	

6.2 Methods

6.2.1 Molecular cloning techniques

6.2.1.1 Sequencing of monoclonal antibodies variable domains

Variable domain sequences of monoclonal antibodies derived from mice hybridomas F965-ID2, F965-JF7, F965-EC12 were obtained using Absolute Antibody Ltd services. Alternatively, variable domains from F965-HA9, F965-CG12, F965-JF8 were determined using The UK Immunological Toolbox services, managed by The Pirbright Institute. All sequences, regardless of the provider, were obtained using Sanger sequencing of PCR products amplified via rapid amplification of cDNA ends (5′RACE) for variable heavy chains and V-region PCR for variable light chains. Briefly, total mRNA extraction from hybridomas was followed by conversion into cDNA. To facilitate variable heavy chain retrieval a homopolymer tail was added to 3’ of cDNA whilst variable light domains were determined in the presence of primers specific to signal peptide and framework region 1.

6.2.1.2 *In silico* cloning

A) Design of scFv, VHH antibody expression vectors

Variable domain sequences were used for scFv generation *in silico* utilizing SnapGene software. To produce scFv ORF V_L and V_H domains were fused via

a $(Gly_4Ser)_4$ linker, a CD33 secretion signal sequence (*Homo sapiens*; accession number NM_001772.4) was incorporated at the 5'-end of scFv and C-tag sequence (EPEA) was added to the 3'-end. *EcoRI* and *SacII* restriction enzyme sites were added to 5' and 3' ends, respectively. The same strategy was used for bivalent R1aB6 generation by linking two R1aB6 sequences by a $(Gly_4Ser)_4$ linker. R1aB6 amino acid sequence was kindly provided by Simon Hufton (NIBSC). Constructs were inserted into pExpres2.1 vector (ExpreS2ion Biotechnologies) and checked for open reading frame (ORF) retention. The whole constructs for ID2, JF7, EC12 and bivalent VHH R1aB6 were submitted for commercial synthesis (GeneArt). Alternatively, primers were designed, and variable domains amplified from hybridoma clones F965-HA9, F965-CG12, F965-JF8 following scFv generation via overlapping PCR.

B) Design of different mice isotype antibody expression vectors

In silico cloning of variable domains into vectors containing different mouse antibody Fc regions was performed utilizing SnapGene software. Variable domain sequences were used for incorporation into pNeoSec vectors carrying mouse IgG1, IgG2a or kappa constant regions and checked for ORF retention. V_L sequences were inserted into pNeoSec-Mm-Lc-κ plasmid map between *KpnI* and *PstI* restriction enzyme sites while V_H chains were inserted into pNeoSac-MmFc-IgG1 or pNeoSac-MmFc-IgG2a using the same restriction enzyme sites. pNeoSec vectors were obtained from The UK Immunological Toolbox. Overlapping primers matching vector and insert sequence were designed for each of the constructs to facilitate ligation independent cloning.

C) Design of CRISPR-Cas9 donor vectors

For bivalent R1aB6 antibody ORF insertion into the pUC18 backbone (Addgene) carrying i) murine cytomegalovirus immediate-early promoter adjacent to synthetically generated ii) SV40 poly(A) polyadenylation site located between partial (HVT087) SORF3 and partial (HVT088) US2 sequences homologous to HVT genome *AgeI* and *SalI* restriction enzyme sites were used. ORF retention was checked in SnapGene software and primers

designed allowing sub-cloning from pExpres2.1 vector (ExpreS2ion Biotechnologies).

For guide (g) RNA insertion into pSpCas9(BB)-2A-Puro (PX459) V2.0 (Addgene) *BbsI* restriction enzyme site was used. The complete plasmid map and plasmid was kindly shared by Avian Oncogenic viruses group from The Pirbright Institute.

6.2.1.3 PCR amplification

A) PCR amplification of DNA for cloning or sequencing reactions

PCR reactions requiring maximum polymerase precision were performed using PfuUltra II Hotstart 2x Master mix (Agilent) according to the manufacturer's protocol. Briefly, 25 µL reaction contained 1 µL of forward and 1 µL of reverse primers (10 µM each), 1 µL of DNA (10 - 100 ng) and 12.5 µL master mix, the remaining volume was made up with nuclease-free water. Thermocycling conditions were as following i) 2 min denaturation at 95 °C, ii) 20 sec denaturation at 95 °C, iii) 20 sec primer annealing at temperature as determined by Sigma oligonucleotide analysis tool, iv) 15 sec elongation at 72 °C per 1 kb, with steps ii) – iv) performed for 30 cycles, and v) final 3 min elongation step at 72 °C.

B) PCR amplification of DNA to confirm transgene insertion in HVT genome

PCR reactions, to characterize an insert in recombinant HVT virus, were performed using GoTaq® Green Master Mix (Promega). Briefly, 25 µL reaction contained 1 µL of forward and 1 µL of reverse primers (10 µM), 1 µL of DNA template (extracted from infected cells) and 12.5 µL master mix, the remaining volume was made up with nuclease-free water. Thermocycling conditions were as following i) 3 min denaturation at 94 °C, ii) 45 sec denaturation at 94 °C, iii) 30 sec primer annealing at temperature as determined by Sigma oligonucleotide analysis tool, iv) 1 min elongation at 72 °C per 1 kb, with steps ii) – iv) performed for 30 cycles, and v) final 10 min elongation step at 72 °C.

6.2.1.4 Restriction enzyme digestions

Restriction enzyme digestions of vectors and inserts were performed using a single restriction enzyme or a combination of two enzymes per reaction as required. A typical reaction volume of 15 µL consisted of 1 µL (10 – 20 units) of restriction enzyme (New England Biolabs), 1.5 µL of appropriate 10x buffer as suggested by manufacturer, the remaining volume was made up by target DNA (10 – 1000 ng) and nuclease-free water. Digestions were carried out at 37 °C for 6 h.

6.2.1.5 Agarose gel electrophoresis

PCR and restriction digestion products were run on a 1% (w/v) agarose gel. Molecular Biology Grade Agarose (EUROGENTEC) was boiled in 60 mL of 1x Tris/borate/EDTA (TBE) buffer (100 mM Tris, 90 mM boric acid, and 1 mM EDTA, pH 8.3) (Thermo Fisher Scientific). 1 µL of 1x GelRed nucleic acid stain (Biotium) was added to cooled molten agarose and then allowed to set. Each sample was mixed with 1x DNA loading dye (final concentration) prior to loading onto the set gel. Hyperladder™ 1 kb (Bioline) were used as standards for sample DNA size estimation. Gels were run in H1-Set Easigel Fast-Mini Gel Units (CamLab) between 50 - 70V for the required amount of time. DNA was visualised using a Gel Doc™ EZ Imager (BioRad) using the ‘GelRed’ setting.

6.2.1.6 Ligation independent cloning

Ligation independent cloning was performed using T4 polymerase (New England Biolabs). Briefly, vectors were linearized by KpnI and PstI restriction enzymes and treated with 3 units of T4 DNA polymerase in a total volume of 20 µL. The reaction mix contained 50 ng digested vector, 100 mM dTTP, 100 mM DTT, 2 µL 10x BSA, 2 µL of 10x NEB buffer 2 and nuclease-free water. Alternatively, PCRs were performed as described in step 6.2.1.3 on the

amplicon to be inserted with overhang containing primers listed in Table 6.14. The inserts were subjected to T4 DNA polymerase treatment as above with the only difference of 100 mM dTTP substituted by 100 mM dATP. Both vector and insert reaction mixtures were incubated at 22 °C for 30 min followed by 75 °C for 20 min. Annealing reaction was done using 1:3 vector to insert ratio in 15 µL reaction volume with the remaining volume made up by nuclease free water. Reactions were kept at room temperature for 5 min before addition of 1 µL 25 mM EDTA and further 5 min incubation at room temperature followed by immediate bacteria transformation.

6.2.1.7 Ligation

All ligation reactions were performed using 400 units of T4 DNA ligase (New England Biolabs) equivalent to 1 µL and 1.5 µL of 10x buffer provided by manufacturer. Ligations were set using 1:3 molecular ratio of vector to insert in 15 µL reaction volume. Reactions were incubated for 2 h at room temperature.

6.2.1.8 Bacteria transformation

In-house made competent *E.coli* bacteria cells (DH5α, TOP10) were used for transformation with plasmid DNA. Typically, 1-2 µL of ligation reaction or ligation independent cloning product was added to freshly thawed cells and incubated on ice for 30 min. Cells were heat shocked at 42 °C for 45 sec and kept on ice for further 2 min. 250 µL of SOC medium (Thermo Fisher Scientific) was added onto the heat shocked cells and incubated at 37 °C for 1 h while shaking. 100 µL of cells were plated onto appropriate antibiotic LB agar plates and incubated at 37 °C overnight. Single colonies were selected and grown in 10 mL of LB medium supplemented with appropriate antibiotic (37 °C, overnight, shaking).

6.2.1.9 DNA purification from bacteria, gel extraction

DNA purification from bacteria or agarose gel was performed using Qiagen's kits (Qiagen). QIAprep spin miniprep or maxiprep kit was used for DNA extraction from bacterial pallets. Briefly, 10 mL of LB broth with appropriate antibiotic was inoculated for miniprep and 250 mL for maxiprep and grown at 37 °C, overnight while shaking. Bacterial cells were pelleted by centrifugation (1,600x g, 15 min, 4 °C), the supernatant discarded, and cells processed as per manufacturer's instructions. QIAquick gel extraction kit was used for gel extractions as per manufacturer's instructions. DNA was eluted in the nuclease-free water and the nucleic acid concentration and quality was assessed by NanoPhotometer® NP80 (Implen).

6.2.1.10 Plasmid sequencing

Newly prepared DNA plasmids were sent for sequencing to ensure correct modifications. Sanger sequencing was performed by Source Bioscience and the results were analysed using MEGA7 software.

6.2.2 Cell culture and eggs

6.2.2.1 Passaging of continuous cell lines

Drosophila Schneider 2 (S2) cells were obtained from Thermo Fisher Scientific and maintained in Schneider's insect medium (Sigma Aldrich) supplemented with 10% foetal bovine serum (FBS). Media was switched to EX-CELL® 420 Serum-Free Medium for Insect Cells (Sigma Aldrich) after stable cell line establishment. Cells were grown at 25 °C without CO_2 and passaged every 4 - 5 days.

ExpiCHO cells were obtained from Thermo Fisher Scientific, maintained in vented, non-baffled flasks using ExpiCHO™ Expression Medium (Thermo

Fisher Scientific). Cells were grown at 37 °C with 8% CO_2 under continuous shaking and passaged every 3 - 4 days.

MDCK cells were obtained from ATCC, maintained in Dulbecco's modified Eagle's medium (DMEM) (Sigma Aldrich) supplemented with 10% FBS. Cells were grown at 37 °C, 5% CO_2 and passaged every 4 - 5 days.

6.2.2.2 Preparation and maintenance of primary cell lines

Chicken embryo fibroblast (CEF) cells were prepared in-house from embryonic day 10 - 16 eggs. Briefly, chicken embryos were removed from the egg and decapitated. Each embryo was eviscerated, and feet were removed prior to whole body shredding via 10 mL syringe. The mashed embryos were washed in PBS'a' and trypsinized in 20 mL of 0.05% Trypsin/Versene for 2 min under magnetic stirrer agitation. Supernatants were collected and neutralized with FBS, trypsinization process was repeated for 3 times. Isolated cells were centrifuged at 500x g for 5 min. Pelleted cells were resuspended in Medium 199 (Sigma Aldrich) supplemented with 10% tryptose phosphate broth (TPB) (Sigma Aldrich), 5% FCS and 100U/ml Penicillin-Streptomycin and passed through 40 µm nylon cell strainers. The resulting cells were counted and maintained at 37 °C, 5% CO_2.

6.2.2.3 Embryonated chicken eggs

Embryonated eggs were delivered to lab at embryonic day 10-16 and kept at Brinsea Ova-Easy 380 Advance Series II Incubator (Brinsea Incubation Specialists) supporting 37 °C, relative humidity and continuous egg turning.

6.2.3 Antibody production and characterization

6.2.3.1 Antibody expression in mammalian cell culture

Full length antibodies were produced in ExpiCHO cells following supplier's protocol for high titre protein production in a 25 mL cell culture volume. Briefly,

the day before transfection cells were split to have 3 x 10^6 cells mL^{-1} and diluted to 6 x 10^6 cells mL^{-1} with pre-warmed medium on the day of transfection. Total amount of 80 µg plasmid DNA (1:1 ratio for heavy and light chain plasmids) was diluted in 1 mL of cold OptiPRO™ medium. A separate tube with 80 µL of ExpiFectamine™ CHO Reagent diluted with 920 µL OptiPRO™ medium was prepared. Diluted ExpiFectamine™ CHO Reagent was added to diluted DNA and incubated at room temperature for 5 min. Complexed DNA was added onto the cells dropwise and returned into 37 °C, 8% CO_2 incubator supporting continuous flask shaking. 18 h post transfection 150 µL of ExpiFectamine™ CHO Enhancer and 6 mL of ExpiCHO™ Feed was added onto the cells. Cells were returned to 32 °C, 5% CO_2 with continuous shaking. Supernatants were harvested 10 days post transfection by centrifugation at 1,600x g at 4 °C for 30 min.

6.2.3.2 Antibody fragment expression in insect cell culture

Antibody fragments were generated in S2 cells establishing stably expressing cell lines. Briefly, S2 cells were seeded to 1 x 10^6 cells mL^{-1} density on the day prior transfection and transfected using Calcium Phosphate Transfection Kit (Thermo Fisher Scientific). Solution A (total volume of 500 µL) was prepared containing 32 µg plasmid DNA, 60 µL of 2 M $CaCl_2$ with remaining reaction volume made up using nuclease-free water. Solution B consisted of 500 µL 2x HEPES – buffered saline (HBS) (pH 7.05; pH was measured using Mettler Toledo 30130862 SevenCompact™ S210 Basic pH/mV BenchTop Meter). To facilitate calcium phosphate – DNA precipitate formation, solution A was added onto continuously aerated HBS. The reaction was left for 30 min at room temperature prior to addition onto the cells. 24 h post transfection the media were changed, and 72 h post transfection antibiotic selection was started. Antibiotic selection was carried out for a minimum of four weeks using Zeocin (Invivogen) at a concentration of 750 µg ml^{-1} for the first two weeks and 1500

µg ml^{-1} for the next two weeks prior to single cell clone isolation via limiting dilution. Successful single clones were screened by ELISA for protein production and clones showing the highest expression levels expanded and maintained in EX-CELL® 420 Serum-Free Medium for Insect Cells.

6.2.3.3 Antibody purification from cell culture supernatants

A) Antibody purification via protein G

Harvested cell supernatants were passed through a 0.22 µm filter. Full length antibodies were purified via Protein G column (Thermo Fisher Scientific). Briefly, Protein G resin was loaded onto the column, left to set for 1 h and equilibrated with 10 column volumes of Na_3PO_4 with 0.02% (v/v) sodium azide (pH 5) wash buffer. Supernatant samples containing full length antibodies were loaded onto the column and washing step with 10 column volumes of wash buffer was performed to eliminate non-specifically bound proteins. Antibodies were eluted with 0.1 M glycine (pH 3) in 1 mL fractions that were immediately neutralized with 100 µL of 1 M Tris HCl (pH 9). The column was washed with an additional 10 column volumes of 0.1 M glycine (pH 3) and re-equilibrated with wash buffer. The eluted fractions were pooled and dialysed into PBS overnight at 4 °C after which purified protein concentration was assessed.

B) Antibody fragment purification via CaptureSelect™ C-tag affinity matrix

Antibody fragments produced in insect cell culture were purified via a C-tag column. Briefly, as with protein G, supernatants were filtered through 0.22 µm filter and CaptureSelect™ C-tag Affinity Matrix (Thermo Fisher Scientific) was loaded onto the column, left to set for 1 h and equilibrated with 10 column volumes of PBS wash buffer. The filtered supernatant was loaded onto the column followed by washing step with PBS. The bound protein was eluted with 2 M $MgCl_2$ (pH 7.1, pH was measured using Mettler Toledo 30130862 SevenCompact™ S210 Basic pH/mV BenchTop Meter) and dialysed into PBS

overnight at 4 °C after which the purified protein concentration was assessed. The column was washed with 10 column volumes of 0.1 M glycine (pH 3) and re-equilibrated with PBS for long-term storage.

6.2.3.4 BCA assay

To determine the protein concentration Pierce™ BCA protein assay (Thermo Fisher Scientific) was performed as per manufacturer's instructions. Briefly, 25 µL of albumin standards (2000 µg mL^{-1} - 0 µg mL^{-1}) or the protein of interest was added to Nunc™ MicroWell 96-well plates (Thermo Fisher Scientific). 200 µL of bicinchoninic acid working reagent was added on top and the plates were left for 30 min at 37 °C. Reactions were read at 562 nm absorbance using Thermo Scientific™ Multiskan™ GO Microplate Spectrophotometer (Thermo Fisher Scientific). A standard curve was generated from known sample concentrations to allow interpolation of unknown protein concentrations.

6.2.3.5 Protein electrophoresis

Sodium dodecyl sulphate-polyacrylamide gel electrophoresis (SDS-PAGE) was used to separate proteins based on molecular weight differences. SDS gels were prepared in-house using 0.75 mm spacer plates with appropriate short plates and Bio-Rad reagents and buffers according to the manufacturer's instructions. Stacking gels were always cast at 4% while resolving gel percentage was adjusted; depending on the size of the protein, by changing concentration of acrylamide: bisacrylamide (37.5:1) solution (whole recipes can be found in section 6.1.). Each sample was mixed with 1x protein loading buffer (final concentration) and if required 5% of 2 – Mercaptoethanol (final concentration). All samples were boiled for 5 min at 95 °C, briefly spun and loaded onto the gel alongside Precision Plus Protein™ All Blue Prestained Protein Standards (Bio-Rad). Gels were run at 70 V for the required amount of time in a Mini - PROTEAN tetra system (Bio-Rad).

6.2.3.6 *SDS gel staining and Western blotting*

Polyacrylamide gels with separated proteins were used either for Coomassie staining or transferred onto nitrocellulose membrane. Briefly, for whole protein detection gels were washed thrice for 10 min in Milli-Q water and incubated in PageBlue™ Protein staining solution (Thermo Fisher Scientific) for 1 h at room temperature while rocking. Excess of colloidal coomassie G-250 dye was washed overnight in Milli-Q water.

For western blotting gels were briefly washed in Milli-Q water and equilibrated in Western blot transfer buffer together with nitrocellulose membrane and filter papers. To assemble the transfer sandwich 3 filter papers were placed on a positive anode side of Trans-Blot Turbo Transfer System (Bio-Rad) followed by a nitrocellulose membrane, the SDS gel and 3 filter papers, negative cathode side was added last. Transfers were run for 14 min at 25 V, 2.5 A. Once transferred the nitrocellulose membranes were blocked in PBS'a'/0.1% (v/v) Tween20 (Thermo Fisher Scientific) with 10% (w/v) skimmed milk (Marvel) for 1 h at room temperature while rocking. Blocking solution was replaced with primary antibody diluted in PBS'a'/0.1% (v/v) Tween20 with 1% (w/v) skimmed milk and incubated at 4 °C overnight while rocking. Next day, the membrane was washed with PBS'a'/0.1% (v/v) Tween20 thrice for 10 min. Secondary antibody was diluted in PBS'a'/0.1% (v/v) Tween20 with 1% (w/v) skimmed milk and incubated at room temperature for 1 h prior to three additional washes and scanning by the Odyssey CLX (LI-COR Biosciences).

6.2.3.7 ELISA

A) Protein detection in cell culture supernatants, allantoic fluid or serum samples

For protein detection in cell culture supernatants, allantoic fluid and serum samples ELISAs were performed. Briefly, Nunc MaxiSorp™ flat-bottom 96-well plates (Thermo Fisher Scientific) were used for coating with pure cell culture supernatants, allantoic fluid or serum samples diluted 2-fold across the plate.

Coated plates were incubated at 4 °C overnight prior to washing with PBS'a'/0.1% (v/v) Tween20 and blocking in 5% BSA (Thermo Fisher Scientific) for 1 h at room temperature. The protein present in supernatant samples was captured via CaptureSelect™ Biotin Anti-C-tag Conjugate (Thermo Fisher Scientific) diluted to 500 ng mL^{-1} in 5% BSA which was detected by streptavidin – HRP conjugate (Thermo Fisher Scientific) diluted to 500 ng mL^{-1} in 5% BSA. Four washes with washing buffer were performed between each step. All incubations were done for 1 h at room temperature. HRP was detected using 3,3′,5,5′-tetramethylbenzidine (TMB) substrate (BD Biosciences) and reactions stopped after 10 min with 2 M H_2SO_4. Plates were read at dual wavelength at 450 nm with 630 nm reference in an ELx808 Absorbance Microplate Reader (BioTek). Positive controls of purified antibody were included into each plate.

B) Antibody and antibody fragment binding to virus

To determine the antibody and antibody fragment ability to bind to respective antigens the procedure was identical as above apart from differences in coating conditions and subsequent capture steps. 64 HA units of live virus were used for initial coating step. Primary capture was done using purified antibodies diluted to a final concentration of 1 µg mL^{-1}. Full length antibodies containing mouse Fc region were probed via polyclonal rabbit anti-mouse immunoglobulins HRP (Agilent) diluted to 500 ng mL^{-1}. Antibody fragments were detected as in section 6.2.3.7. A).

C) Anti- antibody response detection in serum samples

To detect anti-antibody response plates were coated with antibody diluted to 200 ng mL^{-1} in coating buffer and serum diluted 1 in 1000 in 5% BSA. Anti-chicken IgY (IgG) (whole molecule) − peroxidase antibody produced in rabbit (Sigma Aldrich) diluted to 1 in 10.000 $^{-1}$ in 5% BSA was used for detection.

6.2.4 Virus rescue, growth and titration techniques

6.2.4.1 Virus rescue

A) Recombinant HVT virus rescue

Homology directed repair (HDR) – CRISPR/Cas9 mediated gene insertion was used for recombinant HVT virus generation. Briefly, CEF cells were pre-seeded were pre-seeded to 12-well plate. Once cells reached 70-80% confluency medium was changed to Opti-MEM reduced serum medium (Thermo Fisher Scientific) with 10% FCS and transfection complexes containing 1 µg donor plasmid, 1 µg gRNA plasmid and 6 µL of *Trans*IT-X2® Dynamic Delivery System (MirusBio) were prepared in a total volume of 200 µL diluted in Opti-MEM reduced serum media. Complexes were left for 25 min at room temperature and added into two wells of 12-well plate. Cells were incubated at 37 °C for 12 h prior to media change into CEF growth medium and infection with HVT-GFP at MOI 0.01 (HVT-GFP virus was kindly provided by Pengxiang Chang from Avian Influenza Virus group at The Pirbright Institute). 72 h post-infection cells and cell-associated virus were harvested and used for limiting dilution onto the freshly seeded CEF cells. Plaques were allowed to form for the next 72 h when 24 GFP negative plaques under fluorescence microscope were picked and used to infect 24-well plate of pre-seeded CEF cells. 3 days later HVT virus was harvested from each well and DNA extracted. DNA samples were used for gene - and site - specific PCRs to confirm genome editing. Double positive clones were transferred to 96-well plates and the process repeated twice to ensure purity of the plaques.

B) Influenza virus rescue

All viruses were rescued by previous lab members following bidirectional reverse genetics system described elsewhere (509). All viruses were rescued in PR8 backbone changing surface proteins (HA and NA) only.

6.2.4.2 Virus propagation

A) Recombinant HVT virus propagation in primary cells

Genome edited and wildtype HVT virus was propagated in primary CEF cells. T25 flasks were used for virus passaging and propagation every 5 days until P20 was reached. P5, P10, P15 and P20 stocks were grown in T150 flasks to obtain higher virus titers.

B) Recombinant HVT virus propagation in eggs

To propagate HVT virus in eggs 10 day old embryonated hens' eggs were used. The shell was sterilised with 70% (v/v) ethanol and a small hole was introduced into the eggshell just below the air sac. 100 µL of 20, 000 PFU of P5 viruses, were inoculated into allantoic cavity using 25G needle and 1 mL syringe. Eggs were incubated at 37 °C, 40-50% humidity, for 24 h or 72 h and candled every 24 h to ensure embryo viability. The top of the eggshell was removed using sterile forceps and embryo was decapitated using sterile scissors. Leg muscle tissues were collected for snap freezing and storage at -80 °C until further processing.

B) Influenza virus propagation in eggs

To propagate influenza virus stocks 10 day old embryonated chickens' eggs were used. The shell was sterilised with 70% (v/v) ethanol and a small hole was introduced into the eggshell just below the air sac. P0 viruses, rescued by previous lab members, were diluted 1 in 1000 and 100 µL were inoculated into allantoic cavity using 25G needle and 1 mL syringe (330). Eggs were incubated at 37 °C, 40-50% humidity, for 72 h and candled every 24 h to ensure embryo viability after virus inoculation. Embryos were culled by chilling at 4°C overnight prior to allantoic fluid harvest. The top of the eggshell was removed using sterile forceps and a Pasteur pipette was used for air sac rupture and the allantoic fluid harvested. The allantoic fluid was subjected to low-speed centrifugation (1000x g, 10 min) and stored at -80 °C in 1 mL aliquots until further analysis.

6.2.4.3 Virus stock titration by plaque assay

A) HVT virus stock titration in primary cells

CEF cells were used to titrate HVT virus. Briefly, cells were pre-seeded to 12-well plates to reach 90-95% confluency next day. Cell associated virus stocks were thawed in 37 °C and used for 10-fold serial dilutions in CEF growth medium. 200 µL of virus dilution was used per well, infected cells were left at 37 °C for 72 h to allow plaque formation. After 3 days media was removed, cells washed with PBS'a' and fixed with 500 µL of ice-cold methanol/acetone (50:50 v/v) for 15 min. Cells were washed twice with PBS'a' and stored at 4 °C for a maximum of 1 week until plaque staining.

B) Influenza virus stock titration in continuous cell lines

MDCK cells were used to titrate influenza virus. Briefly, on the day prior plaque assay cells were seeded in 12-well plates to reach 90-95% confluency. Virus samples were thawed at room temperature and serially diluted 10-fold in serum - free DMEM (Sigma Aldrich). Cells were washed with pre-warmed PBS'a' and infected with 200 µL of virus dilution. Cells were incubated at 37°C for 1 h prior to inoculum removal and cell wash with PBS'a'. 1 mL of overlay media containing 2 µg mL^{-1} of TPCK trypsin and 0.6% agar (Oxoid) as added onto the cells. Cells were incubated at 37 °C for 72 h, overlay was removed, and cells fixed/stained with crystal violet solution for 30 min and results read immediately.

6.2.4.4 Influenza virus stock titration by $TCID_{50}$

On the day prior to virus titrations MDCK cells were seeded into 96-well plates to reach 90-95% confluency. Virus samples were thawed and serially diluted 1-log in serum - free DMEM. Cells were washed with PBS'a' and virus dilutions used to infect cells in quadruplets. Cells were incubated at 37 °C for 1 h prior to inoculum removal and cell wash with PBS'a'. Cells were overlayed with serum free DMEM containing 2 µg mL^{-1} of TPCK trypsin and incubated at 37

°C for 72 h. Overlay was removed and cells fixed/stained with crystal violet solution for 30 min.

6.2.4.5 Influenza virus titration by hemagglutination (HA) assay

The HA assay was performed in V-bottom 96-well plates (Greiner Bio-One Ltd, cat no. #651101). Briefly, virus was thawed and used to prepare 2-fold dilutions in PBS'a' across the plate. A suspension of 1% (v/v) chicken red blood cells in PBS'a' was added into each well. Plates were incubated at room temperature for 45 min and results read. The last well containing virus dilution that allowed formation of lattice was considered as an end-point virus titre.

6.2.5 *In vitro* characterisation of viruses and antibodies

6.2.5.1 HVT growth curve

Virus was inoculated in 6-well plates of 90-95% confluent CEF cells at an MOI of 0.0001 (80 PFU/well) in triplicates. Cells and supernatant were harvested at 6, 24, 48, 72, 96, 120 and 144 h post infection.

6.2.5.2 HVT virus immunostaining

Infected, methanol: acetone fixed cells were washed with PBS'a' and blocked in 200 µL of PBS'a'/5% (v/v) FCS for 30 min at room temperature while shaking. Blocking buffer was removed and replaced with primary antibody (HVT serum diluted 1 in 500 or/and CaptureSelect™ Biotin Anti-C-tag Conjugate at 2 µg mL^{-1}) diluted in PBS'a'/5% (v/v) FCS. Primary antibody was incubated for 1 h at room temperature while shaking and cells were washed with PBS'a'/0.1% (v/v) Tween20 thrice for 10 min. Secondary antibody was diluted in PBS'a'/5% (v/v) FCS. If assay was performed to differentiate between wildtype and recombinant virus, secondary antibodies used were compatible with Odyssey CLX: IRDye® 680RD Donkey anti-Chicken IgG (H + L) (LI-COR Biosciences) diluted to 100 ng mL^{-1} or/and IRDye® 800CW Streptavidin at concentration of 500 ng mL^{-1}. Otherwise, anti-chicken IgY (IgG)

(whole molecule) − peroxidase antibody produced in rabbit was diluted to 1 in 10.000 $^{-1}$ in PBS'a'/5% (v/v) FCS. Plates were incubated at room temperature for 1 h following three washes with PBS'a'/0.1% (v/v) Tween20 for 10 min. Plates were either read with Odyssey CLX or 50 µL of DAB Chromogen and Substrate Buffer (Agilent) was added per well, incubated for 10 min, rinsed with water and brown - stained plaques counted.

6.2.5.3 DNA extraction from HVT infected cells

A) DNA extraction for PCR

Infected cells were harvested using 0.05% (v/v) Trypsin/Versene solution and centrifuged at 500x g, 5 min. Supernatants were removed, and the cell pellet subjected to 200 µL squishing buffer. Resuspended cells were incubated for 30 min at 65 °C.

B) DNA extraction for qPCR

Infected cells were harvested as in section A, centrifuged and pellets processed with DNeasy® Blood and Tissue Kit following the manufacturer's instructions. Briefly, cells were resuspended in 220 µL PBS'a' containing 9% (v/v) proteinase K and 200 µL of lysis buffer was added followed by 200 µL of 99-100% ethanol. Mixture was transferred to DNeasy mini columns which were washed twice with manufacturers' provided buffer diluted in ethanol (96-100%), DNA was eluted in elution buffer (10 mM Tris-Cl, 0.5 mM EDTA, pH 9.0) in 50 µL volume.

6.2.5.4 Influenza virus microneutralization (MNT) assay

Briefly, MDCK cells were pre-seeded into 96-well plates to reach 90–95% confluency. On the day of experiment, 60 µL of 150 TCID50 (50% tissue culture infective dose) of virus was added onto 2-fold serially diluted antibodies in 60 µL volume (starting at 1 mg mL-1) and incubated at 37 °C for 1 h. Cells were washed with PBS'a' and inoculated with 50 µL antibody – virus mixture in triplicates. Cells only, virus only and heat inactivated positive H9N2 serum

collected from birds challenged with UDL-1/08 at day 14 post-infection (animal experiment request number AR000562) controls were included into each plate. The cells were incubated at 37 °C for 1 h prior to inoculum removal and wash with PBS'a'. The cells were overlayed with serum free DMEM containing 2 µg mL-1 of TPCK trypsin. Fixation/staining with crystal violet for 30 min was done after 72 h incubation at 37 °C. The average dilution of antibody at which the cells were completely protected from cytopathic effect by the virus were noted.

6.2.6 *In vivo* techniques

6.2.6.1 Ethics statement

Animal studies and procedures were carried out in strict accordance with European and United Kingdom Home Office regulations and the Animals (Scientific Procedures) Act 1986 Amendment Regulations, 2012. These studies were carried out under the United Kingdom Home Office approved project license number P68D44CF. All work undergone ethical scrutiny before approval by The Pirbright Institute's Animal Welfare and Ethical Review Board (AWERB) under request numbers AR000992 and AR001131. All procedures on live birds were performed by trained staff who held a personal licence (Prof. Munir Iqbal, Dr. Holly Shelton, Dr. Jean-Remy Sadeyen, Dr. Pengxiang Chang, Dr. Sushant Bhat, Dr. Joshua Sealy, Deimante Lukosaityte, Angita Shrestha).

6.2.6.2 Influenza virus infectivity, transmission and pathogenicity study

Mixed sex, SPF eggs of Rhode Island Red chickens were sourced from the National Avian Research Facility (Roslin Institute) and hatched at The Pirbright Institute BSU by members of animal services team. Hatched birds were housed in floor pens for 1 day. On day 2 post-hatch all chickens were wing banded and randomly divided into five groups (n = 20/group): (group-1) non-treated and challenged with UDL-1/08; (group-2) scFv JF7 (200 µg/dose) treated and challenged with UDL-1/08; (group-3) scFv EC12 (300 µg/dose)

treated and challenged with UDL-1/08. Group-4 had 6 birds that were scFv EC12-treated and non-challenged and group-5 had 10 non-treated and non-challenged birds. Chickens from groups 1, 2 and 3 were transferred into three separate BioFlex B50 Rigid Body Poultry isolators (Bell Isolation Systems) maintaining negative pressure or left in the pen (groups 4 and 5). 19 days post hatch all chickens were swabbed from buccal and cloacal cavities and wing prick bled to obtain pre-infection samples. All birds that were placed in the isolators were further subdivided into directly inoculated group (n = 10) receiving 5×10^5 PFU of virus, diluted in PBS'a', delivered via intranasal route (50 µL in each nostril) and contact birds' group (n = 10) allowing to investigate virus transmission. scFv treatment was given intranasally using 50 µL per nostril. Birds from group-2 and group-3 that were to receive direct virus inoculum via the intransal route were given prophylaxis of the respective scFvs 24 h before the challenge (day 20 post-hatch) with the treatment continued daily until 7 days post-infection. Birds were challenged at 21 days of age (noted as day 0 of experiment) with no further procedures carried out on the same day. Birds that were considered as contacts started receiving scFv treatment at day 1 post infection. scFv treatment and sampling of the buccal and cloacal cavities with sterile polyester tipped swabs (on day 1-8, 10 and 14 post infection). Chickens were monitored for clinical signs and weight changes throughout the experiment by animal services staff. Four birds per group were sacrificed at day 4 post infection and the remaining birds were humanely killed at day 14 post virus inoculation when the experiment was terminated. All infected birds were culled by pentobarbital overdose while non- infected birds underwent cervical dislocation by animal services staff. Tissues were removed and snap frozen in dry ice or stored in RNAlater (Thermo Fisher Scientific) or 10% neutral buffered formalin, blood samples were used for serum preparation.

6.2.6.3 *HVT tolerability study*

Mixed sex, SPF eggs of Dekalb White leghorn chickens were obtained from VALO BioMedia and hatched at the Pirbright Institute BSU by members of animal services team. Hatched birds were housed in floor pens and wing banded by animal services staff randomly dividing chicks into two groups (n = 11/group): (group-1) received WT HVT; (group-2) received recombinant HVT carrying R1aB6 antibody (clone 2.2.4). HVT virus was inoculated at day 1 post hatch subcutaneously using the highest titre of virus obtained - 37600 PFU/dose of rHVT at P5 or 27200 PFU/dose of WT HVT at P5. 2 birds per group were removed at days 2, 3 and 4 post-hatch and culled by cervical dislocation by animal services staff prior to tissue harvesting and snap freezing in dry ice, spleens were collected and stored in Roswell Park Memorial Institute (RPMI) medium (Sigma Aldrich) at 4 °C until further processing. On day 6 post-hatch all remaining birds were bled and repeated HVT administration was done on day 7. Blood samples were collected at weekly intervals and the experiment terminated at day 42 when all birds were culled by cervical dislocation by animal services staff and tissues collected for further analysis as described previously.

6.2.6.4 Clinical scoring system

Throughout the challenge experiment birds were monitored twice daily for clinical signs. Mild disease signs expected were ruffled feathers, eye and nasal discharge, eye reddening, pale comb/wattles. Additional signs of ruffled feathers, swollen head and sporadic diarrhoea were treated as an indicative of moderate disease whilst severe symptoms were attributed to weight loss, persistent diarrhoea, and laboured breathing.

6.2.6.5 Swab sample processing

Swab samples were collected into 1 mL of virus transport medium (WHO, 2008) placed in 15 mL falcons. Swabs were vortexed for 10 sec, removed from media and centrifuged (1,600x g, 10 min). The resulting clarified medium was aliquoted into three 300 µL aliquots and stored in -80 °C until further processing. Viral titers in swabs were determined via plaque assay (section 6.2.4.2).

6.2.6.6 Tissue sample processing and virus isolation

A) Tissue processing from influenza virus study

20 mg of snap frozen tissues (nasal tissue, trachea, lung, spleen, caecal tonsils) were weighed and added to 1 mL of serum-free DMEM in a safe-lock Eppendorf tube. One sterile 5mm stainless steel bead was added per tube and tissues homogenised using TissueLyser LT (Qiagen) (20Hz, 4min). After one round of homogenisation, tissue disruption was checked and repeated if necessary, until the tissue was fully homogenised. Homogenates were centrifuged (16,000x g, 5 min, 4 °C) and the supernatants separated into two aliquots (each containing 500 µL), one aliquot was serially titrated by plaque assay (section 6.2.4.2). Another aliquot of clarified tissue homogenate was used for RNA extraction.

B) Tissue processing from HVT tolerability study

20 mg of snap frozen tissues (feather follicles, skin, lung) were weighed and processed using DNeasy® Blood and Tissue Kit following the manufacturer's instructions. Briefly, cut tissue was placed in 200 µL of lysis buffer containing proteinase K in a safe-lock Eppendorf tube and incubated for a minimum of 4 h at 56 °C with occasional vortexing. Lysed samples were applied to the provided columns, wash steps were performed as per instructions and bound DNA eluted in a total volume of 50 µL. Nucleic acid purity and concentration assessed by NanoPhotometer® NP80.

Spleens were used for B-cell isolation. Briefly, tissue was mashed using syringe plunger and cells passed through 40 µm nylon cell strainers prior to centrifugation at 200x g for 5 min at 4 °C. Palleted cells were resuspended in 10 mL of RPMI medium and underlaid with 5 mL of HistoPaque 1083 (Thermo Fisher Scientific). Samples were centrifuged at 390x g for 20 min with a low acceleration and deceleration rate. The 'interface' ('buffy coat') was removed into a new falcon tube, cells pelleted, washed with PBS'a' and counted prior to infection of pre-seeded CEF cells.

6.2.6.7 Blood processing for serum generation

Blood samples obtained were stored at 4 °C for 24 h to allow blood cell and blood clot separation. Samples were centrifuged (16,000x g, 30 min, 4 °C) and clarified serum aliquoted and stored at -20 °C until further processing. If serum samples were to be used in MNT assay (section 6.2.5.5.) heat inactivation at 56 °C for 30 min was performed to destroy complement activity.

6.2.6.8 Haemagglutinin inhibition (HI) assays

Briefly, HI assays were performed following WHO guidelines (510). The assay was done in V-bottom 96-well plates where 2-fold serum dilution in PBS'a' was prepared and 4 HA units of virus was added. The plate was incubated at 37 °C for 1 h prior to addition of 1% (v/v) of chicken red blood cells. The assay was read after 45 min incubation at room temperature. The first dilution of serum to result in red blood cell pellet in the presence of virus was recorded as an end-point dilution.

6.2.6.9 RNA isolation from swab samples and tissues

RNA extraction from swab samples was performed using BioRobot® Universal System (Qiagen) and QIAamp® One-For-All Nucleic Acid kit (Qiagen) following the manufacturer's instructions. Briefly, swab samples were thawed

and lysed in a microbiological safety cabinet with the rest of steps performed in the automated manner. Total RNA was eluted in 100 µL volume.

RNA isolation from tissue samples was carried out using an RNeasy kit (Qiagen) according to the manufacturer's instructions. Briefly, 500 µL tissue homogenates (section 6.2.6.6) were lysed in 1100 µL volume and all lysate and applied onto the columns. Subsequent washing steps were performed to remove any contaminants and the RNA was eluted in 20 µl of RNase free water. Nucleic acid purity and concentration assessed by NanoPhotometer® NP80.

6.2.6.10 *qPCR*

A) qRT-PCR for M gene and cytokine quantification

Single-step real-time reverse transcription PCR was used for determination of influenza virus M gene and specific cytokine mRNA levels. Superscript III Platinum One-Step qRT-PCR kit (Thermo Fisher Scientific) was used with either neat RNA extracted from swab samples or 150 ng of RNA extracted from tissue samples. Reactions were set up following the manufacturer's protocol in Optical FAST 96-well plates (Applied Biosystems) in 20 µL volume with primers and probes outlined in Table 6.12. qRT-PCR was run in a 7500 FAST ABI RT-PCR thermocycler (Applied Biosystems). Briefly, cycling conditions were as follows i) 5 min hold step at 50 °C, ii) 2 min hold step at 95 °C, and 40 cycles of iii) 3 sec at 95 °C, iv) 30 sec annealing and extension at 60 °C. Each sample was run in triplicate and each plate contained T7 RNA polymerase-transcribed RNA standard for M gene (for M gene quantification) or 28S rRNA serving as a constitutively expressed gene (for cytokine quantification) alongside negative controls for unspecific amplification.

B) qPCR for HVT genome quantification

Real-time quantitative PCR on DNA from cells and tissues derived from *in vitro, in ovo* and *in vivo* experiments was run using ABsolute Blue qPCR Low ROX mix (Thermo Fisher Scientific) in 7500 FAST ABI RT-PCR thermocycler. DNA

samples were diluted to 25 ng μL^{-1} with reactions prepared in 25 µL volume with primers and probes outlined in Table 6.12. using Optical FAST 96-well plates. Cycling conditions were as follows i) 2 min hold step at 50 °C, ii) 10 min hold step at 95 °C, and 40 cycles of iii) 15 sec at 94 °C, iv) 1 min annealing and extension at 60 °C. Each sample was run in triplicate and each plate contained pHVT-BAC3 and pGEMT-Ovo serially diluted plasmids as standards for HVT virus and for ovotransferrin gene, respectively, alongside negative controls for unspecific amplification.

6.2.6.11 HA sequencing from swabs

RNA from swab samples was used for HA sequence retrieval. Briefly, RNA conversion into cDNA was performed using universal primers and Superscript III one-step RT-PCR with Platinum™ *Taq* DNA polymerase (Thermo Fisher Scientific) in accordance with the manufacturer's instructions. Briefly, 50 µg mL^{-1} of RNA was used in 25 µL reaction volume with cycling conditions i) 30 min DNA synthesis at 95°C, ii) 2 min pre-denaturation at 94°C, iii) 15 sec denaturation at 94 °C, iv) 30 sec primer annealing at 55 °C, v) 2 min elongation at 68 °C, with steps iii) – v) performed for 40 cycles, and vi) a final 5 min elongation at 68 °C. Segment specific primers were used for nucleic acid amplification with PfuUltra II Hotstart 2x Master mix as described in section 6.2.1. PCR products were run on a gel and gel extracted prior to submission for Sanger sequencing.

6.2.7 Bioinformatic analysis

6.2.7.1 Analysis of antibody sequence and structure

Antibody variable domains were analysed using NCBI IgBLAST software and germline encoded genes extracted from IMGT database. scFv structure prediction was done using freely available abYsis tool.

6.2.7.2 Multiple sequence alignment and phylogenetics

HA gene segments and antibody variable domains were aligned using the MUSCLE algorithm in MEGA7 Software. All relevant HA sequences were downloaded from NCBI Influenza database and all antibody germline sequences were downloaded from IMGT database. The neighbour-joining algorithm with 1000 bootstrap replications were used for phylogenetic tree generation. The evolutionary distances were computed using the p-distance method.

6.2.7.3 Mapping of hemagglutinin structures

HA structure modelling and mutations of UDL-1/08 were generated using PDB ID 1JSD structure and rendered in PyMol v1.5.0. (www.pymol.org).

6.2.7.4 *Statistical analysis*

All statistical analyses were performed, and graphs generated using GraphPad Prism 8. p-values < 0.05 were considered significant. Nonsignificant (Ns) = p > 0.05; * = p ≤ 0.05; ** = p ≤ 0.01; *** = p ≤ 0.001; **** = p ≤ 0.0001. GraphPad Prism 8 was also used for curve fitting following nonlinear regression model.

Chapter 7 REFERENCES

1. von Behring E, Kitasato S. [The mechanism of diphtheria immunity and tetanus immunity in animals. 1890]. Mol Immunol. 1991;28(12):1317, 9-20.
2. Pauling L. A Theory of the Structure and Process of Formation of Antibodies*. Journal of the American Chemical Society. 1940;62(10):2643-57.
3. Burnet FM. A modification of Jerne's theory of antibody production using the concept of clonal selection (Reprinted from Australian Journal of Science, vol 20, 1957). Nat Immunol. 2007;8(10):1024-6.
4. van Oss CJ, Good RJ, Chaudhury MK. Nature of the antigen-antibody interaction. Primary and secondary bonds: optimal conditions for association and dissociation. J Chromatogr. 1986;376:111-9.
5. Braden BC, Dall'Acqua W, Eisenstein E, Fields BA, Goldbaum FA, Malchiodi EL, et al. Protein motion and lock and key complementarity in antigen-antibody reactions. Pharm Acta Helv. 1995;69(4):225-30.
6. Tizard I. The avian antibody response. Semin Avian Exot Pet. 2002;11(1):2-14.
7. Tiselius A, Kabat EA. An Electrophoretic Study of Immune Sera and Purified Antibody Preparations. J Exp Med. 1939;69(1):119-31.
8. Nomenclature of Human Immunoglobulins. B World Health Organ. 1973;48(3):373-.
9. Forthal DN. Functions of Antibodies. Microbiol Spectr. 2014;2(4):AID-0019-2014.
10. Bachmann MF, Kalinke U, Althage A, Freer G, Burkhart C, Roost H, et al. The role of antibody concentration and avidity in antiviral protection. Science. 1997;276(5321):2024-7.
11. Marrack JR, Hoch H, Johns RG. The valency of antibodies. Br J Exp Pathol. 1951;32(3):212-30.
12. Blank SE, Leslie GA, Clem LW. Antibody affinity and valence in viral neutralization. J Immunol. 1972;108(3):665-73.
13. Fujimori K, Covell DG, Fletcher JE, Weinstein JN. A Modeling Analysis of Monoclonal-Antibody Percolation through Tumors - a Binding-Site Barrier. J Nucl Med. 1990;31(7):1191-8.
14. Porter RR. The hydrolysis of rabbit y-globulin and antibodies with crystalline papain. Biochem J. 1959;73:119-26.
15. Adlersberg JB. The immunoglobulin hinge (interdomain) region. Ric Clin Lab. 1976;6(3):191-205.
16. Pritsch O, HudryClergeon G, Buckle M, Petillot Y, Bouvet JP, Gagnon J, et al. Can immunoglobulin C(H)1 constant region domain modulate antigen binding affinity of antibodies? Journal of Clinical Investigation. 1996;98(10):2235-43.
17. Dwek RA, Lellouch AC, Wormald MR. Glycobiology: 'the function of sugar in the IgG molecule'. J Anat. 1995;187 (Pt 2):279-92.
18. Sorensen V, Rasmussen IB, Norderhaug L, Natvig I, Michaelsen TE, Sandlie I. Effect of the IgM and IgA secretory tailpieces on polymerization and secretion of IgM and IgG. Journal of Immunology. 1996;156(8):2858-65.
19. Wiersma EJ, Chen F, Bazin R, Collins C, Painter RH, Lemieux R, et al. Analysis of IgM structures involved in J chain incorporation. J Immunol. 1997;158(4):1719-26.
20. Kabat EA, Wu TT. Attempts to locate complementarity-determining residues in the variable positions of light and heavy chains. Ann N Y Acad Sci. 1971;190:382-93.

21. Collis AVJ, Brouwer AP, Martin ACR. Analysis of the antigen combining site: Correlations between length and sequence composition of the hypervariable loops and the nature of the antigen. J Mol Biol. 2003;325(2):337-54.
22. North B, Lehmann A, Dunbrack RL. A New Clustering of Antibody CDR Loop Conformations. J Mol Biol. 2011;406(2):228-56.
23. Haakenson JK, Huang R, Smider VV. Diversity in the Cow Ultralong CDR H3 Antibody Repertoire. Front Immunol. 2018;9:1262.
24. Muyldermans S, Atarhouch T, Saldanha J, Barbosa JA, Hamers R. Sequence and structure of VH domain from naturally occurring camel heavy chain immunoglobulins lacking light chains. Protein Eng. 1994;7(9):1129-35.
25. Wu L, Oficjalska K, Lambert M, Fennell BJ, Darmanin-Sheehan A, Ni Shuilleabhain D, et al. Fundamental characteristics of the immunoglobulin VH repertoire of chickens in comparison with those of humans, mice, and camelids. J Immunol. 2012;188(1):322-33.
26. Feige MJ, Grawert MA, Marcinowski M, Hennig J, Behnke J, Auslander D, et al. The structural analysis of shark IgNAR antibodies reveals evolutionary principles of immunoglobulins. P Natl Acad Sci USA. 2014;111(22):8155-60.
27. Hamerscasterman C, Atarhouch T, Muyldermans S, Robinson G, Hamers C, Songa EB, et al. Naturally-Occurring Antibodies Devoid of Light-Chains. Nature. 1993;363(6428):446-8.
28. Harmsen MM, De Haard HJ. Properties, production, and applications of camelid single-domain antibody fragments. Appl Microbiol Biot. 2007;77(1):13-22.
29. Muyldermans S. Nanobodies: Natural Single-Domain Antibodies. Annual Review of Biochemistry, Vol 82. 2013;82:775-97.
30. Barthelemy PA, Raab H, Appleton BA, Bond CJ, Wu P, Wiesmann C, et al. Comprehensive analysis of the factors contributing to the stability and solubility of autonomous human VH domains. J Biol Chem. 2008;283(6):3639-54.
31. Mitchell LS, Colwell LJ. Comparative analysis of nanobody sequence and structure data. Proteins. 2018;86(7):697-706.
32. Corthesy B. Roundtrip ticket for secretory IgA: role in mucosal homeostasis? J Immunol. 2007;178(1):27-32.
33. Johansen FE, Braathen R, Brandtzaeg P. Role of J chain in secretory immunoglobulin formation. Scand J Immunol. 2000;52(3):240-8.
34. Woof JM, Kerr MA. IgA function--variations on a theme. Immunology. 2004;113(2):175-7.
35. Vidarsson G, Dekkers G, Rispens T. IgG subclasses and allotypes: from structure to effector functions. Front Immunol. 2014;5.
36. Boes M. Role of natural and immune IgM antibodies in immune responses. Molecular Immunology. 2000;37(18):1141-9.
37. Sutton BJ, Davies AM, Bax HJ, Karagiannis SN. IgE Antibodies: From Structure to Function and Clinical Translation. Antibodies. 2019;8(1).
38. Chen K, Cerutti A. The function and regulation of immunoglobulin D. Curr Opin Immunol. 2011;23(3):345-52.
39. Warr GW, Magor KE, Higgins DA. Igy - Clues to the Origins of Modern Antibodies. Immunol Today. 1995;16(8):392-8.
40. Hozumi N, Tonegawa S. Evidence for Somatic Rearrangement of Immunoglobulin Genes Coding for Variable and Constant Regions. P Natl Acad Sci USA. 1976;73(10):3628-32.
41. Leder P. The Genetics of Antibody Diversity. Sci Am. 1982;246(5):102-&.

42. Tonegawa S. Somatic Generation of Antibody Diversity. Nature. 1983;302(5909):575-81.
43. Papavasiliou F, Casellas R, Suh HY, Qin XF, Besmer E, Pelanda R, et al. V(D)J recombination in mature B cells: A mechanism for altering antibody responses. Science. 1997;278(5336):298-301.
44. Briney BS, Crowe JE. Secondary mechanisms of diversification in the human antibody repertoire. Front Immunol. 2013;4.
45. Kanyavuz A, Marey-Jarossay A, Lacroix-Desmazes S, Dimitrov JD. Breaking the law: unconventional strategies for antibody diversification. Nat Rev Immunol. 2019;19(6):355-68.
46. Sun Y, Liu ZC, Ren LM, Wei ZG, Wang P, Li N, et al. Immunoglobulin genes and diversity: what we have learned from domestic animals. J Anim Sci Biotechno. 2012;3.
47. McCormack WT, Tjoelker LW, Thompson CB. Avian B-cell development: generation of an immunoglobulin repertoire by gene conversion. Annu Rev Immunol. 1991;9:219-41.
48. Feige MJ, Hendershot LM, Buchner J. How antibodies fold. Trends Biochem Sci. 2010;35(4):189-98.
49. Sutton BJ, Phillips DC. The three-dimensional structure of the carbohydrate within the Fc fragment of immunoglobulin G. Biochem Soc Trans. 1983;11(2):130-2.
50. Mattu TS, Pleass RJ, Willis AC, Kilian M, Wormald MR, Lellouch AC, et al. The glycosylation and structure of human serum IgA1, Fab, and Fc regions and the role of N-glycosylation on Fcalpha receptor interactions. J Biol Chem. 1998;273(4):2260-72.
51. Maurer MA, Meyer L, Bianchi M, Turner HL, Le NPL, Steck M, et al. Glycosylation of Human IgA Directly Inhibits Influenza A and Other Sialic-Acid-Binding Viruses. Cell Rep. 2018;23(1):90-9.
52. Higel F, Seidl A, Sorgel F, Friess W. N-glycosylation heterogeneity and the influence on structure, function and pharmacokinetics of monoclonal antibodies and Fc fusion proteins. Eur J Pharm Biopharm. 2016;100:94-100.
53. Zagury D, Uhr JW, Jamieson JD, Palade GE. Immunoglobulin synthesis and secretion. II. Radioautographic studies of sites of addition of carbohydrate moieties and intracellular transport. J Cell Biol. 1970;46(1):52-63.
54. Kohler G, Milstein C. Continuous Cultures of Fused Cells Secreting Antibody of Predefined Specificity. Nature. 1975;256(5517):495-7.
55. Bradbury ARM, Trinklein ND, Thie H, Wilkinson IC, Tandon AK, Anderson S, et al. When monoclonal antibodies are not monospecific: Hybridomas frequently express additional functional variable regions. Mabs-Austin. 2018;10(4):539-46.
56. Ding GP, Chen XM, Zhu J, Cao B. Identification of two aberrant transcripts derived from a hybridoma with amplification of functional immunoglobulin variable genes. Cell Mol Immunol. 2010;7(5):349-54.
57. Carroll WL, Mendel E, Levy S. Hybridoma Fusion Cell-Lines Contain an Aberrant Kappa Transcript. Molecular Immunology. 1988;25(10):991-5.
58. Bradbury ARM, Sidhu S, Dubel S, McCafferty J. Beyond natural antibodies: the power of in vitro display technologies. Nat Biotechnol. 2011;29(3):245-54.
59. Smith GP. Filamentous Fusion Phage - Novel Expression Vectors That Display Cloned Antigens on the Virion Surface. Science. 1985;228(4705):1315-7.
60. Hammers CM, Stanley JR. Antibody phage display: technique and applications. J Invest Dermatol. 2014;134(2):1-5.

61. Feldhaus MJ, Siegel RW. Yeast display of antibody fragments: a discovery and characterization platform. J Immunol Methods. 2004;290(1-2):69-80.
62. Freudl R, Macintyre S, Degen M, Henning U. Cell-Surface Exposure of the Outer-Membrane Protein Ompa of Escherichia-Coli K-12. J Mol Biol. 1986;188(3):491-4.
63. Samuelson P, Gunneriusson E, Nygren PA, Stahl S. Display of proteins on bacteria. J Biotechnol. 2002;96(2):129-54.
64. Ho M, Pastan I. Mammalian cell display for antibody engineering. Methods Mol Biol. 2009;525:337-52, xiv.
65. Bowers PM, Horlick RA, Neben TY, Toobian RM, Tomlinson GL, Dalton JL, et al. Coupling mammalian cell surface display with somatic hypermutation for the discovery and maturation of human antibodies. Proc Natl Acad Sci U S A. 2011;108(51):20455-60.
66. Kastelic D, He M. Ribosome display and screening for protein therapeutics. Methods Mol Biol. 2012;899:61-72.
67. Valencia CA, Zou JW, Liu RH. In vitro selection of proteins with desired characteristics using mRNA-display. Methods. 2013;60(1):55-69.
68. Ramage W, Gaiotto T, Ball C, Risley P, Carnell GW, Temperton N, et al. Cross-Reactive and Lineage-Specific Single Domain Antibodies against Influenza B Hemagglutinin. Antibodies. 2019;8(1).
69. Ferrara F, D'Angelo S, Gaiotto T, Naranjo L, Tian HZ, Graslund S, et al. Recombinant renewable polyclonal antibodies. Mabs-Austin. 2015;7(1):32-41.
70. Nilsson K, Klein G, Henle W, Henle G. The establishment of lymphoblastoid lines from adult and fetal human lymphoid tissue and its dependence on EBV. Int J Cancer. 1971;8(3):443-50.
71. Simmons CP, Bernasconi NL, Suguitan AL, Mills K, Ward JM, Chau NVV, et al. Prophylactic and therapeutic efficacy of human monoclonal antibodies against H5N1 influenza. Plos Med. 2007;4(5):928-36.
72. Kozbor D, Roder JC, Chang TH, Steplewski Z, Koprowski H. Human Anti-Tetanus Toxoid Monoclonal-Antibody Secreted by Ebv-Transformed Human B-Cells Fused with Murine Myeloma. Hybridoma. 1982;1(3):323-8.
73. Shammah S, Mantovani TL, Dallafavera R, Casali P. Generation of Human Monoclonal-Antibodies by Transformation of Lymphoblastoid B-Cells with Ras Oncogene. J Immunol Methods. 1993;160(1):19-25.
74. Zubler RH, Erard F, Lees RK, Vanlaer M, Mingari C, Moretta L, et al. Mutant El-4 Thymoma Cells Polyclonally Activate Murine and Human B-Cells Via Direct Cell-Interaction. Journal of Immunology. 1985;134(6):3662-8.
75. Kwakkenbos MJ, Diehl SA, Yasuda E, Bakker AQ, van Geelen CMM, Lukens MV, et al. Generation of stable monoclonal antibody-producing B cell receptor-positive human memory B cells by genetic programming. Nat Med. 2010;16(1):123-U64.
76. Meijer PJ, Andersen PS, Hansen MH, Steinaa L, Jensen A, Lantto J, et al. Isolation of human antibody repertoires with preservation of the natural heavy and light chain pairing. J Mol Biol. 2006;358(3):764-72.
77. Kivi G, Teesalu K, Parik J, Kontkar E, Ustav M, Noodla L, et al. HybriFree: a robust and rapid method for the development of monoclonal antibodies from different host species. Bmc Biotechnol. 2016;16.
78. Nelson AL. Antibody fragments Hope and hype. Mabs-Austin. 2010;2(1):77-83.

79. Weisser NE, Hall JC. Applications of single-chain variable fragment antibodies in therapeutics and diagnostics. Biotechnol Adv. 2009;27(4):502-20.
80. Huston JS, Mudgetthunter M, Tai MS, Mccartney J, Warren F, Haber E, et al. Protein Engineering of Single-Chain Fv Analogs and Fusion Proteins. Method Enzymol. 1991;203:46-+.
81. Argos P. An Investigation of Oligopeptides Linking Domains in Protein Tertiary Structures and Possible Candidates for General Gene Fusion. J Mol Biol. 1990;211(4):943-58.
82. Huston JS, Levinson D, Mudgetthunter M, Tai MS, Novotny J, Margolies MN, et al. Protein Engineering of Antibody-Binding Sites - Recovery of Specific Activity in an Anti-Digoxin Single-Chain Fv Analog Produced in Escherichia-Coli. P Natl Acad Sci USA. 1988;85(16):5879-83.
83. Bird RE, Hardman KD, Jacobson JW, Johnson S, Kaufman BM, Lee SM, et al. Single-chain antigen-binding proteins. Science. 1988;242(4877):423-6.
84. Laursen NS, Friesen RHE, Zhu XY, Jongeneelen M, Blokland S, Vermond J, et al. Universal protection against influenza infection by a multidomain antibody to influenza hemagglutinin. Science. 2018;362(6414):598-+.
85. Gil D, Schrum AG. Strategies to stabilize compact folding and minimize aggregation of antibody-based fragments. Adv Biosci Biotechnol. 2013;4(4a):73-84.
86. Labrijn AF, Janmaat ML, Reichert JM, Parren P. Bispecific antibodies: a mechanistic review of the pipeline. Nat Rev Drug Discov. 2019;18(8):585-608.
87. Lu D, Jimenez X, Witte L, Zhu ZP. The effect of variable domain orientation and arrangement on the antigen-binding activity of a recombinant human bispecific diabody. Biochem Bioph Res Co. 2004;318(2):507-13.
88. Holliger P, Prospero T, Winter G. Diabodies - Small Bivalent and Bispecific Antibody Fragments. P Natl Acad Sci USA. 1993;90(14):6444-8.
89. Cai YX, Zhang JX, Lao XJ, Jiang HW, Yu YF, Deng YR, et al. Construction of a disulfide-stabilized diabody against fibroblast growth factor-2 and the inhibition activity in targeting breast cancer. Cancer Sci. 2016;107(8):1141-50.
90. Kim JH, Song DH, Youn SJ, Kim JW, Cho G, Kim SC, et al. Crystal structures of mono- and bi-specific diabodies and reduction of their structural flexibility by introduction of disulfide bridges at the Fv interface. Sci Rep-Uk. 2016;6.
91. Mack M, Riethmuller G, Kufer P. A Small Bispecific Antibody Construct Expressed as a Functional Single-Chain Molecule with High Tumor-Cell Cytotoxicity. P Natl Acad Sci USA. 1995;92(15):7021-5.
92. Wu JJ, Fu JP, Zhang MZ, Liu DL. Blinatumomab: a bispecific T cell engager (BiTE) antibody against CD19/CD3 for refractory acute lymphoid leukemia. J Hematol Oncol. 2015;8.
93. Coloma MJ, Morrison SL. Design and production of novel tetravalent bispecific antibodies. Nat Biotechnol. 1997;15(2):159-63.
94. Schoonjans R, Willems A, Schoonooghe S, Leoen J, Grooten J, Mertens N. A new model for intermediate molecular weight recombinant bispecific and trispecific antibodies by efficient heterodimerization of single chain variable domains through fusion to a Fab-chain. Biomol Eng. 2001;17(6):193-202.
95. Mayer K, Baumann AL, Grote M, Seeber S, Kettenberger H, Breuer S, et al. TriFabs-Trivalent IgG-Shaped Bispecific Antibody Derivatives: Design, Generation, Characterization and Application for Targeted Payload Delivery. Int J Mol Sci. 2015;16(11):27497-507.

96. Klein C, Schaefer W, Regula JT. The use of CrossMAb technology for the generation of bi- and multispecific antibodies. Mabs-Austin. 2016;8(6):1010-20.
97. Cao Y, Vinayagamoorthy T, Noujaim AA, Suresh MR. A rapid non-selective method to generate quadromas by microelectrofusion. J Immunol Methods. 1995;187(1):1-7.
98. Suresh MR, Cuello AC, Milstein C. Bispecific Monoclonal-Antibodies from Hybrid Hybridomas. Method Enzymol. 1986;121:210-28.
99. Ridgway JB, Presta LG, Carter P. 'Knobs-into-holes' engineering of antibody CH3 domains for heavy chain heterodimerization. Protein Eng. 1996;9(7):617-21.
100. Gunasekaran K, Pentony M, Shen M, Garrett L, Forte C, Woodward A, et al. Enhancing Antibody Fc Heterodimer Formation through Electrostatic Steering Effects APPLICATIONS TO BISPECIFIC MOLECULES AND MONOVALENT IgG. J Biol Chem. 2010;285(25):19637-46.
101. Labrijn AF, Meesters JI, de Goeij BECG, van den Bremer ETJ, Neijssen J, van Kampen MD, et al. Efficient generation of stable bispecific IgG1 by controlled Fab-arm exchange. P Natl Acad Sci USA. 2013;110(13):5145-50.
102. Davis JH, Aperlo C, Li Y, Kurosawa E, Lan Y, Lo KM, et al. SEEDbodies: fusion proteins based on strand-exchange engineered domain (SEED) C(H)3 heterodimers in an Fc analogue platform for asymmetric binders or immunofusions and bispecific antibodies. Protein Eng Des Sel. 2010;23(4):195-202.
103. Mouquet H, Warncke M, Scheid JF, Seaman MS, Nussenzweig MC. Enhanced HIV-1 neutralization by antibody heteroligation. Proc Natl Acad Sci U S A. 2012;109(3):875-80.
104. Xu L, Pegu A, Rao E, Doria-Rose N, Beninga J, McKee K, et al. Trispecific broadly neutralizing HIV antibodies mediate potent SHIV protection in macaques. Science. 2017;358(6359):85-90.
105. Bruggemann M, Winter G, Waldmann H, Neuberger MS. The Immunogenicity of Chimeric Antibodies. J Exp Med. 1989;170(6):2153-7.
106. Morrison SL. Transfectomas Provide Novel Chimeric Antibodies. Science. 1985;229(4719):1202-7.
107. Prabakaran M, Prabhu N, He F, Hongliang Q, Ho HT, Qiang J, et al. Combination Therapy Using Chimeric Monoclonal Antibodies Protects Mice from Lethal H5N1 Infection and Prevents Formation of Escape Mutants. Plos One. 2009;4(5).
108. Cheung NKV, Guo HF, Hu J, Tassev DV, Cheung IY. Humanizing murine IgG3 anti-GD2 antibody m3F8 substantially improves antibody-dependent cell-mediated cytotoxicity while retaining targeting in vivo. Oncoimmunology. 2012;1(4).
109. Hwang WYK, Almagro JC, Buss TN, Tan P, Foote J. Use of human germline genes in a CDR homology-based approach to antibody humanization. Methods. 2005;36(1):35-42.
110. Kim DS, Lee SH, Kim JS, Lee SC, Kwon MH, Kim YS. Generation of humanized anti-DNA hydrolyzing catalytic antibodies by complementarity determining region grafting. Biochem Bioph Res Co. 2009;379(2):314-8.
111. Rosok MJ, Yelton DE, Harris LJ, Bajorath J, Hellstrom KE, Hellstrom I, et al. A combinatorial library strategy for the rapid humanization of anticarcinoma BR96 Fab. J Biol Chem. 1996;271(37):22611-8.
112. Tan YR, Ng QY, Jia Q, Kwang J, He F. A Novel Humanized Antibody Neutralizes H5N1 Influenza Virus via Two Different Mechanisms. Journal of Virology. 2015;89(7):3712-22.
113. Roh J, Byun SJ, Seo Y, Kim M, Lee JH, Kim S, et al. Generation of a chickenized catalytic anti-nucleic acid antibody by complementarity-determining region grafting. Molecular Immunology. 2015;63(2):513-20.

114. Byun SJ, Yuk SS, Jang YJ, Choi H, Jeon MH, Erdene-Ochir T, et al. Transgenic Chickens Expressing the 3D8 Single Chain Variable Fragment Protein Suppress Avian Influenza Transmission. Sci Rep-Uk. 2017;7.
115. Lee G, Choi H, Sureshkumar S, Jung SK, Kim JS, Oh KB, et al. The 3D8 single chain variable fragment protein suppress infectious bronchitis virus transmission in the transgenic chickens. Res Vet Sci. 2019;123:293-7.
116. Lee EC, Liang Q, Ali H, Bayliss L, Beasley A, Bloomfield-Gerdes T, et al. Complete humanization of the mouse immunoglobulin loci enables efficient therapeutic antibody discovery. Nat Biotechnol. 2014;32(4):356-U219.
117. Murphy AJ, Macdonald LE, Stevens S, Karow M, Dore AT, Pobursky K, et al. Mice with megabase humanization of their immunoglobulin genes generate antibodies as efficiently as normal mice. P Natl Acad Sci USA. 2014;111(14):5153-8.
118. Jakobovits A, Amad RG, Yang X, RoskoS L, Schwab G. From XenoMouse technology to panitumumab, the first fully human antibody product from transgenic mice. Nat Biotechnol. 2007;25(10):1134-43.
119. Gardner CL, Sun CQ, Luke T, Raviprakash K, Wu H, Jiao JA, et al. Antibody Preparations from Human Transchromosomic Cows Exhibit Prophylactic and Therapeutic Efficacy against Venezuelan Equine Encephalitis Virus. Journal of Virology. 2017;91(14).
120. Luke T, Wu H, Zhao JC, Channappanavar R, Coleman CM, Jiao JA, et al. Human polyclonal immunoglobulin G from transchromosomic bovines inhibits MERS-CoV in vivo. Science Translational Medicine. 2016;8(326).
121. Dye JM, Wu H, Hooper JW, Khurana S, Kuehne AI, Coyle EM, et al. Production of Potent Fully Human Polyclonal Antibodies against Ebola Zaire Virus in Transchromosomal Cattle. Sci Rep-Uk. 2016;6.
122. Matsushita H, Sano A, Wu H, Jiao JA, Kasinathan P, Sullivan EJ, et al. Triple Immunoglobulin Gene Knockout Transchromosomic Cattle: Bovine Lambda Cluster Deletion and Its Effect on Fully Human Polyclonal Antibody Production. Plos One. 2014;9(3).
123. Winau F, Winau R. Emil von Behring and serum therapy. Microbes Infect. 2002;4(2):185-8.
124. Arabi YM, Hajeer AH, Luke T, Raviprakash K, Balkhy H, Johani S, et al. Feasibility of Using Convalescent Plasma Immunotherapy for MERS-CoV Infection, Saudi Arabia. Emerging Infectious Diseases. 2016;22(9):1554-61.
125. Winkler AM, Koepsell SA. The use of convalescent plasma to treat emerging infectious diseases: focus on Ebola virus disease. Curr Opin Hematol. 2015;22(6):521-6.
126. Duan K, Liu B, Li C, Zhang H, Yu T, Qu J, et al. Effectiveness of convalescent plasma therapy in severe COVID-19 patients. Proc Natl Acad Sci U S A. 2020;117(17):9490-6.
127. Nilsson P, Paavilainen L, Larsson K, Odling J, Sundberg M, Andersson AC, et al. Towards a human proteome atlas: High-throughput generation of mono-specific antibodies for tissue profiling. Proteomics. 2005;5(17):4327-37.
128. Blow N. Antibodies: The generation game. Nature. 2007;447(7145):741-+.
129. Wang XZ, Coljee VW, Maynard JA. Back to the future: recombinant polyclonal antibody therapeutics. Curr Opin Chem Eng. 2013;2(4):405-15.
130. Lipman NS, Jackson LR, Trudel LJ, Weis-Garcia F. Monoclonal versus polyclonal antibodies: distinguishing characteristics, applications, and information resources. ILAR J. 2005;46(3):258-68.

131. Leenaars M, Hendriksen CFM. Critical steps in the production of polyclonal and monoclonal antibodies evaluation and recommendations. Ilar Journal. 2005;46(3):269-79.
132. Farrugia A, Poulis P. Intravenous immunoglobulin: regulatory perspectives on use and supply. Transfusion Med. 2001;11(2):63-74.
133. Haurum JS. Recombinant polyclonal antibodies: the next generation of antibody therapeutics? Drug Discov Today. 2006;11(13-14):655-60.
134. Aizenshtein E, Yosipovich R, Kvint M, Shadmon R, Krispel S, Shuster E, et al. Practical aspects in the use of passive immunization as an alternative to attenuated viral vaccines. Vaccine. 2016;34(22):2513-8.
135. Oertel MD. RespiGam: an RSV immune globulin. Pediatr Nurs. 1996;22(6):525-8.
136. A joint statement with the Fetus and Newborn Committee. Palivizumab and respiratory syncytial virus immune globulin intravenous for the prophylaxis of respiratory syncytial virus infection in high risk infants. Paediatr Child Health. 1999;4(7):474-89.
137. Easdale S, Stasi R. Rozrolimupab, a first-in-class recombinant monoclonal antibody product for primary immune thrombocytopaenia. Expert Opin Biol Th. 2013;13(7):1085-92.
138. Robak T, Windyga J, Trelinski J, Prondzinski MV, Giagounidis A, Doyen C, et al. Rozrolimupab, a mixture of 25 recombinant human monoclonal RhD antibodies, in the treatment of primary immune thrombocytopenia. Blood. 2012;120(18):3670-6.
139. Hoa LNM, Mai LQ, Bryant JE, Thai PQ, Hang NLK, Yen NTT, et al. Association between Hemagglutinin Stem-Reactive Antibodies and Influenza A/H1N1 Virus Infection during the 2009 Pandemic. Journal of Virology. 2016;90(14):6549-56.
140. Jacobsen H, Rajendran M, Choi A, Sjursen H, Brokstad KA, Cox RJ, et al. Influenza Virus Hemagglutinin Stalk-Specific Antibodies in Human Serum are a Surrogate Marker for In Vivo Protection in a Serum Transfer Mouse Challenge Model. Mbio. 2017;8(5).
141. Krammer F, Palese P. Advances in the development of influenza virus vaccines. Nat Rev Drug Discov. 2015;14(3):167-82.
142. Ali SO, Takas T, Nyborg A, Shoemaker K, Kallewaard NL, Chiong R, et al. Evaluation of MEDI8852, an Anti-Influenza A Monoclonal Antibody, in Treating Acute Uncomplicated Influenza. Antimicrob Agents Ch. 2018;62(11).
143. Sui JH, Hwang WC, Perez S, Wei G, Aird D, Chen LM, et al. Structural and functional bases for broad-spectrum neutralization of avian and human influenza A viruses. Nat Struct Mol Biol. 2009;16(3):265-73.
144. Han T, Marasco WA. Structural basis of influenza virus neutralization. Year in Immunology. 2011;1217:178-90.
145. Xiao HX, Guo TL, Yang M, Qi JX, Huang CB, Hong YY, et al. Light chain modulates heavy chain conformation to change protection profile of monoclonal antibodies against influenza A viruses. Cell Discov. 2019;5.
146. Ekiert DC, Friesen RHE, Bhabha G, Kwaks T, Jongeneelen M, Yu WL, et al. A Highly Conserved Neutralizing Epitope on Group 2 Influenza A Viruses. Science. 2011;333(6044):843-50.
147. Lang S, Xie J, Zhu X, Wu NC, Lerner RA, Wilson IA. Antibody 27F3 Broadly Targets Influenza A Group 1 and 2 Hemagglutinins through a Further Variation in VH1-69 Antibody Orientation on the HA Stem. Cell Rep. 2017;20(12):2935-43.
148. Lerner RA. Rare antibodies from combinatorial libraries suggests an SOS component of the human immunological repertoire. Mol Biosyst. 2011;7(4):1004-12.

149. DiLillo DJ, Tan GS, Palese P, Ravetch JV. Broadly neutralizing hemagglutinin stalk-specific antibodies require Fc gamma R interactions for protection against influenza virus in vivo. Nat Med. 2014;20(2):143-51.
150. Morgan SB, Holzer B, Hemmink JD, Salguero FJ, Schwartz JC, Agatic G, et al. Therapeutic Administration of Broadly Neutralizing FI6 Antibody Reveals Lack of Interaction Between Human IgG1 and Pig Fc Receptors. Front Immunol. 2018;9.
151. Chen F, Tzarum N, Wilson IA, Law M. VH1-69 antiviral broadly neutralizing antibodies: genetics, structures, and relevance to rational vaccine design. Curr Opin Virol. 2019;34:149-59.
152. Lingwood D, McTamney PM, Yassine HM, Whittle JRR, Guo XT, Boyington JC, et al. Structural and genetic basis for development of broadly neutralizing influenza antibodies. Nature. 2012;489(7417):566-+.
153. Kallewaard NL, Corti D, Collins PJ, Neu U, McAuliffe JM, Benjamin E, et al. Structure and Function Analysis of an Antibody Recognizing All Influenza A Subtypes. Cell. 2016;166(3):596-608.
154. He WQ, Chen CJ, Mullarkey CE, Hamilton JR, Wong CK, Leon PE, et al. Alveolar macrophages are critical for broadly-reactive antibody-mediated protection against influenza A virus in mice. Nat Commun. 2017;8.
155. Dunand CJH, Leon PE, Huang M, Choi A, Chromikova V, Ho IY, et al. Both Neutralizing and Non-Neutralizing Human H7N9 Influenza Vaccine-Induced Monoclonal Antibodies Confer Protection. Cell Host Microbe. 2016;19(6):800-13.
156. Maamary J, Wang TT, Tan GS, Palese P, Ravetch JV. Increasing the breadth and potency of response to the seasonal influenza virus vaccine by immune complex immunization. P Natl Acad Sci USA. 2017;114(38):10172-7.
157. Lu Y, Welsh JP, Swartz JR. Production and stabilization of the trimeric influenza hemagglutinin stem domain for potentially broadly protective influenza vaccines. P Natl Acad Sci USA. 2014;111(1):125-30.
158. Chen CJ, Ermler ME, Tan GS, Krammer F, Palese P, Hai R. Influenza A Viruses Expressing Intra- or Intergroup Chimeric Hemagglutinins. Journal of Virology. 2016;90(7):3789-93.
159. Krammer F, Pica N, Hai R, Margine I, Palese P. Chimeric Hemagglutinin Influenza Virus Vaccine Constructs Elicit Broadly Protective Stalk-Specific Antibodies. Journal of Virology. 2013;87(12):6542-50.
160. Carter DM, Darby CA, Lefoley BC, Crevar CJ, Alefantis T, Oomen R, et al. Design and Characterization of a Computationally Optimized Broadly Reactive Hemagglutinin Vaccine for H1N1 Influenza Viruses. Journal of Virology. 2016;90(9):4720-34.
161. Guilleminault L, Azzopardi N, Arnoult C, Sobilo J, Herve V, Montharu J, et al. Fate of inhaled monoclonal antibodies after the deposition of aerosolized particles in the respiratory system. J Control Release. 2014;196:344-54.
162. Herve V, Rabbe N, Guilleminault L, Paul F, Schlick L, Azzopardi N, et al. VEGF neutralizing aerosol therapy in primary pulmonary adenocarcinoma with K-ras activating-mutations. Mabs-Austin. 2014;6(6):1638-48.
163. Ogura M, Deng SY, Preston-Hurlburt P, Ogura H, Shailubhai K, Kuhn C, et al. Oral treatment with foralumab, a fully human anti-CD3 monoclonal antibody, prevents skin xenograft rejection in humanized mice. Clin Immunol. 2017;183:240-6.

164. Kuhn C, Weiner HL. Therapeutic anti-CD3 monoclonal antibodies: from bench to bedside. Immunotherapy-Uk. 2016;8(8):889-906.
165. Weltzin R, Monath TP. Intranasal antibody prophylaxis for protection against viral disease. Clin Microbiol Rev. 1999;12(3):383-+.
166. Wilson JR, Belser JA, DaSilva J, Guo Z, Sun XJ, Gansebom S, et al. An influenza A virus (H7N9) anti-neuraminidase monoclonal antibody protects mice from morbidity without interfering with the development of protective immunity to subsequent homologous challenge. Virology. 2017;511:214-21.
167. El-Sherbiny IM, El-Baz NM, Yacoub MH. Inhaled nano- and microparticles for drug delivery. Glob Cardiol Sci Pract. 2015;2015:2.
168. Vermeulen B, De Backer P, Remon JP. Drug administration to poultry. Adv Drug Deliver Rev. 2002;54(6):795-803.
169. Joung YK, Son S, Jang JY, Kwon MH, Park KD. Sustained Cytoplasmic Delivery and Anti-viral Effect of PLGA Nanoparticles Carrying a Nucleic Acid-Hydrolyzing Monoclonal Antibody. Pharm Res-Dordr. 2012;29(4):932-42.
170. Calderon-Nieva D, Goonewardene KB, Gomis S, Foldvari M. Veterinary vaccine nanotechnology: pulmonary and nasal delivery in livestock animals. Drug Deliv Transl Re. 2017;7(4):558-70.
171. Zimmermann J, Saalbach I, Jahn D, Giersberg M, Haehnel S, Wedel J, et al. Antibody expressing pea seeds as fodder for prevention of gastrointestinal parasitic infections in chickens. Bmc Biotechnol. 2009;9.
172. Hollevoet K, Declerck PJ. State of play and clinical prospects of antibody gene transfer. J Transl Med. 2017;15.
173. Martinez-Navio JM, Fuchs SP, Pantry SN, Lauer WA, Duggan NN, Keele BF, et al. Adeno-Associated Virus Delivery of Anti-HIV Monoclonal Antibodies Can Drive Long-Term Virologic Suppression. Immunity. 2019;50(3):567-+.
174. van Lieshout LP, Soule G, Sorensen D, Frost KL, He SH, Tierney K, et al. Intramuscular Adeno-Associated Virus-Mediated Expression of Monoclonal Antibodies Provides 100% Protection Against Ebola Virus Infection in Mice. Journal of Infectious Diseases. 2018;217(6):916-25.
175. Balazs AB, Bloom JD, Hong CM, Rao DS, Baltimore D. Broad protection against influenza infection by vectored immunoprophylaxis in mice. Nat Biotechnol. 2013;31(7):647-U110.
176. Suarez DL, Pantin-Jackwood MJ. Recombinant viral-vectored vaccines for the control of avian influenza in poultry. Veterinary Microbiology. 2017;206:144-51.
177. Nakaya T, Cros J, Park MS, Nakaya Y, Zheng HY, Sagrera A, et al. Recombinant Newcastle disease virus as a vaccine vector. Journal of Virology. 2001;75(23):11868-73.
178. Li YQ, Reddy K, Reid SM, Cox WJ, Brown IH, Britton P, et al. Recombinant herpesvirus of turkeys as a vector-based vaccine against highly pathogenic H7N1 avian influenza and Marek's disease. Vaccine. 2011;29(46):8257-66.
179. Bublot M, Pritchard N, Swayne DE, Selleck P, Karaca K, Suarez DL, et al. Development and use of Fowlpox vectored Vaccines for avian influenza. Ann Ny Acad Sci. 2006;1081:193-201.
180. Pardi N, Parkhouse K, Kirkpatrick E, McMahon M, Zost SJ, Mui BL, et al. Nucleoside-modified mRNA immunization elicits influenza virus hemagglutinin stalk-specific antibodies. Nat Commun. 2018;9.

181. Kose N, Fox JM, Sapparapu G, Bombardi R, Tennekoon RN, de Silva AD, et al. A lipid-encapsulated mRNA encoding a potently neutralizing human monoclonal antibody protects against chikungunya infection. Sci Immunol. 2019;4(35).
182. Pardi N, Secreto AJ, Shan XC, Debonera F, Glover J, Yi YJ, et al. Administration of nucleoside-modified mRNA encoding broadly neutralizing antibody protects humanized mice from HIV-1 challenge. Nat Commun. 2017;8.
183. Esquivel RN, Patel A, Kudchodkar SB, Park DH, Stettler K, Beltramello M, et al. In Vivo Delivery of a DNA-Encoded Monoclonal Antibody Protects Non-human Primates against Zika Virus. Mol Ther. 2019;27(5):974-85.
184. Patel A, Park DH, Davis CW, Smith TRF, Leung A, Tierney K, et al. In Vivo Delivery of Synthetic Human DNA-Encoded Monoclonal Antibodies Protect against Ebolavirus Infection in a Mouse Model. Cell Rep. 2018;25(7):1982-+.
185. Andrews CD, Luo Y, Sun M, Yu J, Goff AJ, Glass PJ, et al. In Vivo Production of Monoclonal Antibodies by Gene Transfer via Electroporation Protects against Lethal Influenza and Ebola Infections. Mol Ther-Meth Clin D. 2017;7:74-82.
186. Taubenberger JK, Kash JC. Influenza virus evolution, host adaptation, and pandemic formation. Cell Host Microbe. 2010;7(6):440-51.
187. Yoon SW, Webby RJ, Webster RG. Evolution and Ecology of Influenza A Viruses. Curr Top Microbiol. 2014;385:359-75.
188. Wrigley NG. Electron microscopy of influenza virus. Br Med Bull. 1979;35(1):35-8.
189. Harris A, Cardone G, Winkler DC, Heymann JB, Brecher M, White JM, et al. Influenza virus pleiomorphy characterized by cryoelectron tomography. Proc Natl Acad Sci U S A. 2006;103(50):19123-7.
190. Webster RG, Bean WJ, Gorman OT, Chambers TM, Kawaoka Y. Evolution and ecology of influenza A viruses. Microbiol Rev. 1992;56(1):152-79.
191. Tong S, Li Y, Rivailler P, Conrardy C, Castillo DA, Chen LM, et al. A distinct lineage of influenza A virus from bats. Proc Natl Acad Sci U S A. 2012;109(11):4269-74.
192. Alexander DJ. A review of avian influenza in different bird species. Veterinary Microbiology. 2000;74(1-2):3-13.
193. Stienekegrober A, Vey M, Angliker H, Shaw E, Thomas G, Roberts C, et al. Influenza-Virus Hemagglutinin with Multibasic Cleavage Site Is Activated by Furin, a Subtilisin-Like Endoprotease. Embo Journal. 1992;11(7):2407-14.
194. Wood GW, Mccauley JW, Bashiruddin JB, Alexander DJ. Deduced Amino-Acid-Sequences at the Hemagglutinin Cleavage Site of Avian Influenza-a Viruses of H5 and H7 Subtypes. Archives of Virology. 1993;130(1-2):209-17.
195. Wong SS, Yoon SW, Zanin M, Song MS, Oshansky C, Zaraket H, et al. Characterization of an H4N2 influenza virus from Quails with a multibasic motif in the hemagglutinin cleavage site. Virology. 2014;468:72-80.
196. Mosley VM, Wyckoff RW. Electron micrography of the virus of influenza. Nature. 1946;157:263.
197. Cox JC, Hampson AW, Hamilton RC. An immunofluorescence study of influenza virus filament formation. Arch Virol. 1980;63(3-4):275-84.
198. Hutchinson EC, Charles PD, Hester SS, Thomas B, Trudgian D, Martinez-Alonso M, et al. Conserved and host-specific features of influenza virion architecture. Nat Commun. 2014;5.

199. McGeoch D, Fellner P, Newton C. Influenza virus genome consists of eight distinct RNA species. Proc Natl Acad Sci U S A. 1976;73(9):3045-9.
200. Lamb RA, Horvath CM. Diversity of coding strategies in influenza viruses. Trends Genet. 1991;7(8):261-6.
201. Hsu MT, Parvin JD, Gupta S, Krystal M, Palese P. Genomic Rnas of Influenza-Viruses Are Held in a Circular Conformation in Virions and in Infected-Cells by a Terminal Panhandle. P Natl Acad Sci USA. 1987;84(22):8140-4.
202. Gu W, Gallagher GR, Dai W, Liu P, Li R, Trombly MI, et al. Influenza A virus preferentially snatches noncoding RNA caps. Rna. 2015;21(12):2067-75.
203. Stevaert A, Naesens L. The Influenza Virus Polymerase Complex: An Update on Its Structure, Functions, and Significance for Antiviral Drug Design. Med Res Rev. 2016;36(6):1127-73.
204. Yamayoshi S, Watanabe M, Goto H, Kawaoka Y. Identification of a Novel Viral Protein Expressed from the PB2 Segment of Influenza A Virus. J Virol. 2016;90(1):444-56.
205. Zell R, Krumbholz A, Eitner A, Krieg R, Halbhuber KJ, Wutzler P. Prevalence of PB1-F2 of influenza A viruses. J Gen Virol. 2007;88(Pt 2):536-46.
206. Wise HM, Foeglein A, Sun J, Dalton RM, Patel S, Howard W, et al. A complicated message: Identification of a novel PB1-related protein translated from influenza A virus segment 2 mRNA. J Virol. 2009;83(16):8021-31.
207. Jagger BW, Wise HM, Kash JC, Walters KA, Wills NM, Xiao YL, et al. An overlapping protein-coding region in influenza A virus segment 3 modulates the host response. Science. 2012;337(6091):199-204.
208. Muramoto Y, Noda T, Kawakami E, Akkina R, Kawaoka Y. Identification of novel influenza A virus proteins translated from PA mRNA. J Virol. 2013;87(5):2455-62.
209. Skehel JJ, Wiley DC. Receptor binding and membrane fusion in virus entry: The influenza hemagglutinin. Annu Rev Biochem. 2000;69:531-69.
210. Air GM. Sequence Relationships among the Hemagglutinin Genes of 12 Subtypes of Influenza-a Virus. P Natl Acad Sci-Biol. 1981;78(12):7639-43.
211. Cianci C, Gerritz SW, Deminie C, Krystal M. Influenza nucleoprotein: promising target for antiviral chemotherapy. Antivir Chem Chemother. 2012;23(3):77-91.
212. Resa-Infante P, Jorba N, Coloma R, Ortin J. The influenza RNA synthesis machine Advances in its structure and function. Rna Biol. 2011;8(2):207-15.
213. Wanitchang A, Patarasirin P, Jengarn J, Jongkaewwattana A. Atypical characteristics of nucleoprotein of pandemic influenza virus H1N1 and their roles in reassortment restriction. Archives of Virology. 2011;156(6):1031-40.
214. Palese P, Tobita K, Ueda M, Compans RW. Characterization of temperature sensitive influenza virus mutants defective in neuraminidase. Virology. 1974;61(2):397-410.
215. Blumenkrantz D, Roberts KL, Shelton H, Lycett S, Barclay WS. The short stalk length of highly pathogenic avian influenza H5N1 virus neuraminidase limits transmission of pandemic H1N1 virus in ferrets. J Virol. 2013;87(19):10539-51.
216. Machkovech HM, Bloom JD, Subramaniam AR. Comprehensive profiling of translation initiation in influenza virus infected cells. Plos Pathogens. 2019;15(1).
217. Mould JA, Li HC, Dudlak CS, Lear JD, Pekosz A, Lamb RA, et al. Mechanism for proton conduction of the M(2) ion channel of influenza A virus. J Biol Chem. 2000;275(12):8592-9.

218. Wise HM, Hutchinson EC, Jagger BW, Stuart AD, Kang ZH, Robb N, et al. Identification of a novel splice variant form of the influenza A virus M2 ion channel with an antigenically distinct ectodomain. PLoS Pathog. 2012;8(11):e1002998.
219. Marc D. Influenza virus non-structural protein NS1: interferon antagonism and beyond. J Gen Virol. 2014;95(Pt 12):2594-611.
220. Paterson D, Fodor E. Emerging roles for the influenza A virus nuclear export protein (NEP). PLoS Pathog. 2012;8(12):e1003019.
221. Kuo RL, Li LH, Lin SJ, Li ZH, Chen GW, Chang CK, et al. Role of N Terminus-Truncated NS1 Proteins of Influenza A Virus in Inhibiting IRF3 Activation. Journal of Virology. 2016;90(9):4696-705.
222. Selman M, Dankar SK, Forbes NE, Jia JJ, Brown EG. Adaptive mutation in influenza A virus non-structural gene is linked to host switching and induces a novel protein by alternative splicing. Emerg Microbes Infec. 2012;1.
223. Connor RJ, Kawaoka Y, Webster RG, Paulson JC. Receptor Specificity in Human, Avian, and Equine H2 and H3 Influenza-Virus Isolates. Virology. 1994;205(1):17-23.
224. Xiong XL, McCauley JW, Steinhauer DA. Receptor Binding Properties of the Influenza Virus Hemagglutinin as a Determinant of Host Range. Curr Top Microbiol. 2014;385:63-91.
225. Matrosovich M, Tuzikov A, Bovin N, Gambaryan A, Klimov A, Castrucci MR, et al. Early alterations of the receptor-binding properties of H1, H2, and H3 avian influenza virus hemagglutinins after their introduction into mammals. Journal of Virology. 2000;74(18):8502-12.
226. Teng QY, Xu DW, Shen WX, Liu QF, Rong GY, Li XS, et al. A Single Mutation at Position 190 in Hemagglutinin Enhances Binding Affinity for Human Type Sialic Acid Receptor and Replication of H9N2 Avian Influenza Virus in Mice. Journal of Virology. 2016;90(21):9806-25.
227. Schrauwen EJA, Richard M, Burke DF, Rimmelzwaan GF, Herfst S, Fouchier RAM. Amino Acid Substitutions That Affect Receptor Binding and Stability of the Hemagglutinin of Influenza A/H7N9 Virus. Journal of Virology. 2016;90(7):3794-9.
228. Rogers GN, Paulson JC, Daniels RS, Skehel JJ, Wilson IA, Wiley DC. Single amino acid substitutions in influenza haemagglutinin change receptor binding specificity. Nature. 1983;304(5921):76-8.
229. DiLillo DJ, Palese P, Wilson PC, Ravetch JV. Broadly neutralizing anti-influenza antibodies require Fc receptor engagement for in vivo protection. J Clin Invest. 2016;126(2):605-10.
230. Zaraket H, Bridges OA, Russell CJ. The pH of Activation of the Hemagglutinin Protein Regulates H5N1 Influenza Virus Replication and Pathogenesis in Mice. Journal of Virology. 2013;87(9):4826-34.
231. Galloway SE, Reed ML, Russell CJ, Steinhauer DA. Influenza HA Subtypes Demonstrate Divergent Phenotypes for Cleavage Activation and pH of Fusion: Implications for Host Range and Adaptation. Plos Pathogens. 2013;9(2).
232. Russell CJ, Hu M, Okda FA. Influenza Hemagglutinin Protein Stability, Activation, and Pandemic Risk. Trends Microbiol. 2018;26(10):841-53.
233. Mair CM, Ludwig K, Herrmann A, Sieben C. Receptor binding and pH stability - How influenza A virus hemagglutinin affects host-specific virus infection. Bba-Biomembranes. 2014;1838(4):1153-68.
234. Gu WF, Gallagher GR, Dai WW, Liu P, Li RD, Trombly MI, et al. Influenza A virus preferentially snatches noncoding RNA caps. Rna. 2015;21(12):2067-75.

235. Li J, Yu M, Zheng WN, Liu WJ. Nucleocytoplasmic Shuttling of Influenza A Virus Proteins. Viruses-Basel. 2015;7(5):2668-82.
236. Perez JT, Varble A, Sachidanandam R, Zlatev I, Manoharan M, Garcia-Sastre A, et al. Influenza A virus-generated small RNAs regulate the switch from transcription to replication. P Natl Acad Sci USA. 2010;107(25):11525-30.
237. Deng T, Vreede FT, Brownlee GG. Different de novo initiation strategies are used by influenza virus RNA polymerase on its cRNA and viral RNA promoters during viral RNA replication. Journal of Virology. 2006;80(5):2337-48.
238. York A, Hengrung N, Vreede FT, Huiskonen JT, Fodor E. Isolation and characterization of the positive-sense replicative intermediate of a negative-strand RNA virus. P Natl Acad Sci USA. 2013;110(45):E4238-E45.
239. Elton D, Simpson-Holley M, Archer K, Medcalf L, Hallam R, McCauley J, et al. Interaction of the influenza virus nucleoprotein with the cellular CRM1-mediated nuclear export pathway. Journal of Virology. 2001;75(1):408-19.
240. Massin P, van der Werf S, Naffakh N. Residue 627 of PB2 is a determinant of cold sensitivity in RNA replication of avian influenza viruses. Journal of Virology. 2001;75(11):5398-404.
241. Bussey KA, Bousse TL, Desmet EA, Kim B, Takimoto T. PB2 Residue 271 Plays a Key Role in Enhanced Polymerase Activity of Influenza A Viruses in Mammalian Host Cells. Journal of Virology. 2010;84(9):4395-406.
242. Song WJ, Wang P, Mok BWY, Lau SY, Huang XF, Wu WL, et al. The K526R substitution in viral protein PB2 enhances the effects of E627K on influenza virus replication. Nat Commun. 2014;5.
243. Liu QF, Qiao CL, Marjuki H, Bawa B, Ma JQ, Guillossou S, et al. Combination of PB2 271A and SR Polymorphism at Positions 590/591 Is Critical for Viral Replication and Virulence of Swine Influenza Virus in Cultured Cells and In Vivo. Journal of Virology. 2012;86(2):1233-7.
244. Steel J, Lowen AC, Mubareka S, Palese P. Transmission of Influenza Virus in a Mammalian Host Is Increased by PB2 Amino Acids 627K or 627E/701N. Plos Pathogens. 2009;5(1).
245. Czudai-Matwich V, Otte A, Matrosovich M, Gabriel G, Klenka HD. PB2 Mutations D701N and S714R Promote Adaptation of an Influenza H5N1 Virus to a Mammalian Host. Journal of Virology. 2014;88(16):8735-42.
246. Long JS, Giotis ES, Moncorge O, Frise R, Mistry B, James J, et al. Species difference in ANP32A underlies influenza A virus polymerase host restriction. Nature. 2016;529(7584):101-4.
247. Long JS, Idoko-Akoh A, Mistry B, Goldhill D, Staller E, Schreyer J, et al. Species specific differences in use of ANP32 proteins by influenza A virus. Elife. 2019;8.
248. Bussey KA, Desmet EA, Mattiacio JL, Hamilton A, Bradel-Tretheway B, Bussey HE, et al. PA Residues in the 2009 H1N1 Pandemic Influenza Virus Enhance Avian Influenza Virus Polymerase Activity in Mammalian Cells. Journal of Virology. 2011;85(14):7020-8.
249. Mehle A, Dugan VG, Taubenberger JK, Doudna JA. Reassortment and Mutation of the Avian Influenza Virus Polymerase PA Subunit Overcome Species Barriers. Journal of Virology. 2012;86(3):1750-7.

250. Taubenberger JK, Reid AH, Lourens RM, Wang RX, Jin GZ, Fanning TG. Characterization of the 1918 influenza virus polymerase genes. Nature. 2005;437(7060):889-93.
251. Mondal A, Potts GK, Dawson AR, Coon JJ, Mehle A. Phosphorylation at the Homotypic Interface Regulates Nucleoprotein Oligomerization and Assembly of the Influenza Virus Replication Machinery. Plos Pathogens. 2015;11(4).
252. Linster M, Boheemen S, de Graaf M, Schrauwen EJA, Lexmond P, Manz B, et al. Identification, Characterization, and Natural Selection of Mutations Driving Airborne Transmission of A/H5N1 Virus. Cell. 2014;157(2).
253. Rossman JS, Lamb RA. Influenza virus assembly and budding. Virology. 2011;411(2):229-36.
254. Rossman JS, Jing XH, Leser GP, Lamb RA. Influenza Virus M2 Protein Mediates ESCRT-Independent Membrane Scission. Cell. 2010;142(6):902-13.
255. Schmidt NW, Mishra A, Wang J, DeGrado WF, Wong GCL. Influenza Virus A M2 Protein Generates Negative Gaussian Membrane Curvature Necessary for Budding and Scission. Journal of the American Chemical Society. 2013;135(37):13710-9.
256. Gaymard A, Le Briand N, Frobert E, Lina B, Escuret V. Functional balance between neuraminidase and haemagglutinin in influenza viruses. Clin Microbiol Infec. 2016;22(12):975-83.
257. Li JL, Dohna HZ, Cardona CJ, Miller J, Carpenter TE. Emergence and Genetic Variation of Neuraminidase Stalk Deletions in Avian Influenza Viruses. Plos One. 2011;6(2).
258. Li YF, Chen SJ, Zhang XJ, Fu Q, Zhang ZY, Shi SH, et al. A 20-Amino-Acid Deletion in the Neuraminidase Stalk and a Five-Amino-Acid Deletion in the NS1 Protein Both Contribute to the Pathogenicity of H5N1 Avian Influenza Viruses in Mallard Ducks. Plos One. 2014;9(4).
259. Munier S, Larcher T, Cormier-Aline F, Soubieux D, Su B, Guigand L, et al. A Genetically Engineered Waterfowl Influenza Virus with a Deletion in the Stalk of the Neuraminidase Has Increased Virulence for Chickens. Journal of Virology. 2010;84(2):940-52.
260. Banks J, Speidel ES, Moore E, Plowright L, Piccirillo A, Capua I, et al. Changes in the haemagglutinin and the neuraminidase genes prior to the emergence of highly pathogenic H7N1 avian influenza viruses in Italy. Archives of Virology. 2001;146(5):963-73.
261. Hossain MJ, Hickman D, Perez DR. Evidence of Expanded Host Range and Mammalian-Associated Genetic Changes in a Duck H9N2 Influenza Virus Following Adaptation in Quail and Chickens. Plos One. 2008;3(9).
262. Heaton NS, Sachs D, Chen CJ, Hai R, Palese P. Genome-wide mutagenesis of influenza virus reveals unique plasticity of the hemagglutinin and NS1 proteins. P Natl Acad Sci USA. 2013;110(50):20248-53.
263. Ferguson NM, Galvani AP, Bush RM. Ecological and immunological determinants of influenza evolution. Nature. 2003;422(6930):428-33.
264. Kobayashi Y, Suzuki Y. Compensatory Evolution of Net-Charge in Influenza A Virus Hemagglutinin. Plos One. 2012;7(7).
265. Yewdell JW, Caton AJ, Gerhard W. Selection of influenza A virus adsorptive mutants by growth in the presence of a mixture of monoclonal antihemagglutinin antibodies. J Virol. 1986;57(2):623-8.
266. Daniels RS, Jeffries S, Yates P, Schild GC, Rogers GN, Paulson JC, et al. The receptor-binding and membrane-fusion properties of influenza virus variants selected using anti-haemagglutinin monoclonal antibodies. EMBO J. 1987;6(5):1459-65.

267. Huang KYA, Rijal P, Schimanski L, Powell TJ, Lin TY, McCauley JW, et al. Focused antibody response to influenza linked to antigenic drift. Journal of Clinical Investigation. 2015;125(7):2631-45.
268. Steel J, Lowen AC. Influenza A Virus Reassortment. Curr Top Microbiol. 2014;385:377-401.
269. Garten RJ, Davis CT, Russell CA, Shu B, Lindstrom S, Balish A, et al. Antigenic and Genetic Characteristics of Swine-Origin 2009 A(H1N1) Influenza Viruses Circulating in Humans. Science. 2009;325(5937):197-201.
270. Trifonov V, Khiabanian H, Greenbaum B, Rabadan R. The Origin of the Recent Swine Influenza a(H1n1) Virus Infecting Humans. Eurosurveillance. 2009;14(17):6-.
271. Zhang R, Xu C, Duan Z. Novel antigenic shift in HA sequences of H1N1 viruses detected by big data analysis. Infect Genet Evol. 2017;51:138-42.
272. Tse LV, Hamilton AM, Friling T, Whittaker GR. A Novel Activation Mechanism of Avian Influenza Virus H9N2 by Furin. Journal of Virology. 2014;88(3):1673-83.
273. Seifi S, Asasi K, Mohammadi A. Natural co-infection caused by avian influenza H9 subtype and infectious bronchitis viruses in broiler chicken farms. Vet Arhiv. 2010;80(2):269-81.
274. Kishida N, Sakoda Y, Eto M, Sunaga Y, Kida H. Co-infection of Staphylococcus aureus or Haemophilus paragallinarum exacerbates H9N2 influenza A virus infection in chickens. Archives of Virology. 2004;149(11):2095-104.
275. Ma CN, Cui SJ, Sun Y, Zhao JC, Zhang DT, Zhang L, et al. Avian influenza A (H9N2) virus infections among poultry workers, swine workers, and the general population in Beijing, China, 2013-2016: A serological cohort study. Influenza Other Resp. 2019;13(4):415-25.
276. Heidari A, Mancin M, Nili H, Pourghanbari GH, Lankarani KB, Leardini S, et al. Serological evidence of H9N2 avian influenza virus exposure among poultry workers from Fars province of Iran. Virology Journal. 2016;13.
277. Li CJ, Yu KZ, Tian GB, Yu DD, Liu LL, Jing B, et al. Evolution of H9N2 influenza viruses from domestic poultry in Mainland China. Virology. 2005;340(1):70-83.
278. Guan Y, Shortridge KF, Krauss S, Webster RG. Molecular characterization of H9N2 influenza viruses: Were they the donors of the "internal" genes of H5N1 viruses in Hong Kong? P Natl Acad Sci USA. 1999;96(16):9363-7.
279. Guo YJ, Krauss S, Senne DA, Mo IP, Lo KS, Xiong XP, et al. Characterization of the pathogenicity of members of the newly established H9N2 influenza virus lineages in Asia. Virology. 2000;267(2):279-88.
280. Sun YP, Pu JA, Jiang ZL, Guan T, Xia YJ, Xu Q, et al. Genotypic evolution and antigenic drift of H9N2 influenza viruses in China from 1994 to 2008. Veterinary Microbiology. 2010;146(3-4):215-25.
281. Xu KM, Li KS, Smith GJD, Li JW, Tai H, Zhang JX, et al. Evolution and molecular epidemiology of H9N2 influenza A viruses from Quail in southern China, 2000 to 2005. Journal of Virology. 2007;81(6):2635-45.
282. Chang HP, Peng L, Chen L, Jiang LF, Zhang ZJ, Xiong CL, et al. Avian influenza viruses (AIVs) H9N2 are in the course of reassorting into novel AIVs. J Zhejiang Univ-Sc B. 2018;19(5):409-14.
283. Bahari P, Pourbakhsh SA, Shoushtari H, Bahmaninejad MA. Molecular characterization of H9N2 avian influenza viruses isolated from vaccinated broiler chickens in northeast Iran. Trop Anim Health Pro. 2015;47(6):1195-201.

284. Kilany WH, Ali A, Bazid AHI, El-Deeb AH, El-Abideen MAZ, El Sayed M, et al. A Dose-Response Study of Inactivated Low Pathogenic Avian Influenza H9N2 Virus in Specific-Pathogen-Free and Commercial Broiler Chickens. Avian Diseases. 2016;60(1):256-61.
285. Naeem K, Siddique N. Use of strategic vaccination for the control of avian influenza in Pakistan. Dev Biologicals. 2006;124:145-50.
286. Zhang P, Tang Y, Liu X, Peng D, Liu W, Liu H, et al. Characterization of H9N2 influenza viruses isolated from vaccinated flocks in an integrated broiler chicken operation in eastern China during a 5 year period (1998-2002). J Gen Virol. 2008;89(Pt 12):3102-12.
287. Banet-Noach C, Perk S, Simanov L, Grebenyuk N, Rozenblut E, Pokamunski S, et al. H9N2 influenza viruses from Israeli poultry: a five-year outbreak. Avian Dis. 2007;51(1 Suppl):290-6.
288. Rahn J, Hoffmann D, Harder TC, Beer M. Vaccines against influenza A viruses in poultry and swine: Status and future developments. Vaccine. 2015;33(21):2414-24.
289. Khurana S, Loving CL, Manischewitz J, King LR, Gauger PC, Henningson J, et al. Vaccine-induced anti-HA2 antibodies promote virus fusion and enhance influenza virus respiratory disease. Sci Transl Med. 2013;5(200):200ra114.
290. Mohan T, Berman Z, Luo Y, Wang C, Wang S, Compans RW, et al. Chimeric virus-like particles containing influenza HA antigen and GPI-CCL28 induce long-lasting mucosal immunity against H3N2 viruses. Sci Rep-Uk. 2017;7.
291. Garg AK, Desikan R, Dixit NM. Preferential Presentation of High-Affinity Immune Complexes in Germinal Centers Can Explain How Passive Immunization Improves the Humoral Response. Cell Rep. 2019;29(12):3946-+.
292. Cyranoski D. China's chicken farmers under fire for antiviral abuse. Nature. 2005;435(7045):1009-.
293. Dong G, Peng C, Luo J, Wang C, Han L, Wu B, et al. Adamantane-resistant influenza a viruses in the world (1902-2013): frequency and distribution of M2 gene mutations. Plos One. 2015;10(3):e0119115.
294. Takashita E, Meijer A, Lackenby A, Gubareva L, Rebelo-de-Andrade H, Besselaar T, et al. Global update on the susceptibility of human influenza viruses to neuraminidase inhibitors, 2013-2014. Antiviral Res. 2015;117:27-38.
295. Kiselev OI, Blinov VM, Kozeletskaia KN, Il'enko VI, Platonov VG, Chupakhin ON, et al. [The molecular mechanism of the action of antiviral preparations in the adamantane series]. Vestn Ross Akad Med Nauk. 1993(3):10-5.
296. Deyde VM, Xu XY, Bright RA, Shaw M, Smith CB, Zhang Y, et al. Surveillance of resistance to adamantanes among influenza A(H3N2) and A(H1N1) viruses isolated worldwide. Journal of Infectious Diseases. 2007;196(2):249-57.
297. Gubareva LV, Trujillo AA, Okomo-Adhiambo M, Mishin VP, Deyde VM, Sleeman K, et al. Comprehensive assessment of 2009 pandemic influenza A (H1N1) virus drug susceptibility in vitro. Antivir Ther. 2010;15(8):1151-9.
298. Kim CU, Lew W, Williams MA, Liu H, Zhang L, Swaminathan S, et al. Influenza neuraminidase inhibitors possessing a novel hydrophobic interaction in the enzyme active site: design, synthesis, and structural analysis of carbocyclic sialic acid analogues with potent anti-influenza activity. J Am Chem Soc. 1997;119(4):681-90.
299. Vonitzstein M, Wu WY, Kok GB, Pegg MS, Dyason JC, Jin B, et al. Rational Design of Potent Sialidase-Based Inhibitors of Influenza-Virus Replication. Nature. 1993;363(6428):418-23.

300. Vavricka CJ, Li Q, Wu Y, Qi J, Wang M, Liu Y, et al. Structural and functional analysis of laninamivir and its octanoate prodrug reveals group specific mechanisms for influenza NA inhibition. PLoS Pathog. 2011;7(10):e1002249.
301. Babu YS, Chand P, Bantia S, Kotian P, Dehghani A, El-Kattan Y, et al. BCX-1812 (RWJ-270201): Discovery of a novel, highly potent, orally active, and selective influenza neuraminidase inhibitor through structure-based drug design. J Med Chem. 2000;43(19):3482-6.
302. Byrn RA, Jones SM, Bennett HB, Bral C, Clark MP, Jacobs MD, et al. Preclinical Activity of VX-787, a First-in-Class, Orally Bioavailable Inhibitor of the Influenza Virus Polymerase PB2 Subunit. Antimicrob Agents Ch. 2015;59(3):1574-87.
303. Furuta Y, Takahashi K, Kuno-Maekawa M, Sangawa H, Uehara S, Kozaki K, et al. Mechanism of action of T-705 against influenza virus. Antimicrob Agents Ch. 2005;49(3):981-6.
304. Zenilman JM, Fuchs EJ, Hendrix CW, Radebaugh C, Jurao R, Nayak SU, et al. Phase 1 clinical trials of DAS181, an inhaled sialidase, in healthy adults. Antiviral Res. 2015;123:114-9.
305. Haffizulla J, Hartman A, Hoppers M, Resnick H, Samudrala S, Ginocchio C, et al. Effect of nitazoxanide in adults and adolescents with acute uncomplicated influenza: a double-blind, randomised, placebo-controlled, phase 2b/3 trial. Lancet Infect Dis. 2014;14(7):609-18.
306. Luo G, Danetz S, Krystal M. Inhibition of influenza viral polymerases by minimal viral RNA decoys. J Gen Virol. 1997;78 (Pt 9):2329-33.
307. Lyall J, Irvine RM, Sherman A, McKinley TJ, Nunez A, Purdie A, et al. Suppression of avian influenza transmission in genetically modified chickens. Science. 2011;331(6014):223-6.
308. Zhao H, To KKW, Chu H, Ding Q, Zhao X, Li C, et al. Dual-functional peptide with defective interfering genes effectively protects mice against avian and seasonal influenza. Nat Commun. 2018;9(1):2358.
309. He F, Kumar SR, Syed Khader SM, Tan Y, Prabakaran M, Kwang J. Effective intranasal therapeutics and prophylactics with monoclonal antibody against lethal infection of H7N7 influenza virus. Antiviral Res. 2013;100(1):207-14.
310. Bangaru S, Zhang H, Gilchuk IM, Voss TG, Irving RP, Gilchuk P, et al. A multifunctional human monoclonal neutralizing antibody that targets a unique conserved epitope on influenza HA. Nat Commun. 2018;9.
311. Benjamin E, Wang WJ, McAuliffe JM, Palmer-Hill FJ, Kallewaard NL, Chen ZY, et al. A Broadly Neutralizing Human Monoclonal Antibody Directed against a Novel Conserved Epitope on the Influenza Virus H3 Hemagglutinin Globular Head. Journal of Virology. 2014;88(12):6743-50.
312. Oh HL, Akerstrom S, Shen S, Bereczky S, Karlberg H, Klingstrom J, et al. An antibody against a novel and conserved epitope in the hemagglutinin 1 subunit neutralizes numerous H5N1 influenza viruses. J Virol. 2010;84(16):8275-86.
313. Wilson JR, Guo Z, Reber A, Kamal RP, Music N, Gansebom S, et al. An influenza A virus (H7N9) anti-neuraminidase monoclonal antibody with prophylactic and therapeutic activity in vivo. Antivir Res. 2016;135:48-55.

314. Stadlbauer D, Zhu XY, McMahon M, Turner JS, Wohlbold TJ, Schmitz AJ, et al. Broadly protective human antibodies that target the active site of influenza virus neuraminidase. Science. 2019;366(6464):499-+.
315. Kolpe A, Arista-Romero M, Schepens B, Pujals S, Saelens X, Albertazzi L. Super-resolution microscopy reveals significant impact of M2e-specific monoclonal antibodies on influenza A virus filament formation at the host cell surface. Sci Rep-Uk. 2019;9.
316. El Bakkouri K, Descamps F, De Filette M, Smet A, Festjens E, Birkett A, et al. Universal Vaccine Based on Ectodomain of Matrix Protein 2 of Influenza A: Fc Receptors and Alveolar Macrophages Mediate Protection. Journal of Immunology. 2011;186(2):1022-31.
317. Simhadri VR, Dimitrova M, Mariano JL, Zenarruzabeitia O, Zhong WM, Ozawa T, et al. A Human Anti-M2 Antibody Mediates Antibody-Dependent Cell-Mediated Cytotoxicity (ADCC) and Cytokine Secretion by Resting and Cytokine-Preactivated Natural Killer (NK) Cells. Plos One. 2015;10(4).
318. Ramos EL, Mitcham JL, Koller TD, Bonavia A, Usner DW, Balaratnam G, et al. Efficacy and Safety of Treatment With an Anti-M2e Monoclonal Antibody in Experimental Human Influenza. Journal of Infectious Diseases. 2015;211(7):1038-44.
319. Jegaskanda S, Co MDT, Cruz J, Subbarao K, Ennis FA, Terajima M. Induction of H7N9-Cross-Reactive Antibody-Dependent Cellular Cytotoxicity Antibodies by Human Seasonal Influenza A Viruses that are Directed Toward the Nucleoprotein. Journal of Infectious Diseases. 2017;215(5):818-23.
320. Vanderven HA, Ana-Sosa-Batiz F, Jegaskanda S, Rockman S, Laurie K, Barr I, et al. What Lies Beneath: Antibody Dependent Natural Killer Cell Activation by Antibodies to Internal Influenza Virus Proteins. Ebiomedicine. 2016;8:277-90.
321. June Byun S, Yuk SS, Jang YJ, Choi H, Jeon MH, Erdene-Ochir TO, et al. Transgenic Chickens Expressing the 3D8 Single Chain Variable Fragment Protein Suppress Avian Influenza Transmission. Sci Rep. 2017;7(1):5938.
322. Kim A, Lee JY, Byun SJ, Kwon MH, Kim YS. Viral genome RNA degradation by sequence-selective, nucleic-acid hydrolyzing antibody inhibits the replication of influenza H9N2 virus without significant cytotoxicity to host cells. Antivir Res. 2012;94(2):157-67.
323. Lee J, Park H, Kim M, Seo Y, Lee Y, Byun SJ, et al. Functional stability of 3D8 scFv, a nucleic acid-hydrolyzing single chain antibody, under different biochemical and physical conditions. Int J Pharm. 2015;496(2):561-70.
324. Pelegrin M, Naranjo-Gomez M, Piechaczyk M. Antiviral Monoclonal Antibodies: Can They Be More Than Simple Neutralizing Agents? Trends Microbiol. 2015;23(10):653-65.
325. Kwon S, Iba M, Kim C, Masliah E. Immunotherapies for Aging-Related Neurodegenerative Diseases-Emerging Perspectives and New Targets. Neurotherapeutics. 2020;17(3):935-54.
326. Mayes PA, Hance KW, Hoos A. The promise and challenges of immune agonist antibody development in cancer. Nat Rev Drug Discov. 2018;17(7):509-27.
327. Itoh Y, Yoshida R, Shichinohe S, Higuchi M, Ishigaki H, Nakayama M, et al. Protective efficacy of passive immunization with monoclonal antibodies in animal models of H5N1 highly pathogenic avian influenza virus infection. PLoS Pathog. 2014;10(6):e1004192.
328. Vigil A, Frias-Staheli N, Carabeo T, Wittekind M. Airway Delivery of Anti-influenza Monoclonal Antibodies Results in Enhanced Antiviral Activities and Enables Broad-Coverage Combination Therapies. J Virol. 2020;94(22).

329. Paules CI, Lakdawala S, McAuliffe JM, Paskel M, Vogel L, Kallewaard NL, et al. The Hemagglutinin A Stem Antibody MEDI8852 Prevents and Controls Disease and Limits Transmission of Pandemic Influenza Viruses. J Infect Dis. 2017;216(3):356-65.
330. Peacock T, Reddy K, James J, Adamiak B, Barclay W, Shelton H, et al. Antigenic mapping of an H9N2 avian influenza virus reveals two discrete antigenic sites and a novel mechanism of immune escape. Sci Rep. 2016;6:18745.
331. Gerhard W, Yewdell J, Frankel ME, Webster R. Antigenic structure of influenza virus haemagglutinin defined by hybridoma antibodies. Nature. 1981;290(5808):713-7.
332. Corti D, Voss J, Gamblin SJ, Codoni G, Macagno A, Jarrossay D, et al. A Neutralizing Antibody Selected from Plasma Cells That Binds to Group 1 and Group 2 Influenza A Hemagglutinins. Science. 2011;333(6044):850-6.
333. Bangaru S, Lang S, Schotsaert M, Vanderven HA, Zhu X, Kose N, et al. A Site of Vulnerability on the Influenza Virus Hemagglutinin Head Domain Trimer Interface. Cell. 2019;177(5):1136-52 e18.
334. Ekiert DC, Bhabha G, Elsliger MA, Friesen RH, Jongeneelen M, Throsby M, et al. Antibody recognition of a highly conserved influenza virus epitope. Science. 2009;324(5924):246-51.
335. Barbey-Martin C, Gigant B, Bizebard T, Calder LJ, Wharton SA, Skehel JJ, et al. An antibody that prevents the hemagglutinin low pH fusogenic transition. Virology. 2002;294(1):70-4.
336. Hong M, Lee PS, Hoffman RM, Zhu X, Krause JC, Laursen NS, et al. Antibody recognition of the pandemic H1N1 Influenza virus hemagglutinin receptor binding site. J Virol. 2013;87(22):12471-80.
337. Hershberger E, Sloan S, Narayan K, Hay CA, Smith P, Engler F, et al. Safety and efficacy of monoclonal antibody VIS410 in adults with uncomplicated influenza A infection: Results from a randomized, double-blind, phase-2, placebo-controlled study. Ebiomedicine. 2019;40:574-82.
338. Lee J, Paparoditis P, Horton AP, Fruhwirth A, McDaniel JR, Jung J, et al. Persistent Antibody Clonotypes Dominate the Serum Response to Influenza over Multiple Years and Repeated Vaccinations. Cell Host Microbe. 2019;25(3):367-76 e5.
339. Klein F, Diskin R, Scheid JF, Gaebler C, Mouquet H, Georgiev IS, et al. Somatic mutations of the immunoglobulin framework are generally required for broad and potent HIV-1 neutralization. Cell. 2013;153(1):126-38.
340. Rock EP, Sibbald PR, Davis MM, Chien YH. CDR3 length in antigen-specific immune receptors. J Exp Med. 1994;179(1):323-8.
341. Schroeder HW, Jr., Zemlin M, Khass M, Nguyen HH, Schelonka RL. Genetic control of DH reading frame and its effect on B-cell development and antigen-specifc antibody production. Crit Rev Immunol. 2010;30(4):327-44.
342. Lin SG, Ba Z, Du Z, Zhang Y, Hu J, Alt FW. Highly sensitive and unbiased approach for elucidating antibody repertoires. Proc Natl Acad Sci U S A. 2016;113(28):7846-51.
343. Wyrzucki A, Dreyfus C, Kohler I, Steck M, Wilson IA, Hangartner L. Alternative recognition of the conserved stem epitope in influenza A virus hemagglutinin by a VH3-30-encoded heterosubtypic antibody. J Virol. 2014;88(12):7083-92.
344. Hauge S, Madhun A, Cox RJ, Haaheim LR. Quality and kinetics of the antibody response in mice after three different low-dose influenza virus vaccination strategies. Clin Vaccine Immunol. 2007;14(8):978-83.

345. Nimmerjahn F, Ravetch JV. Divergent immunoglobulin g subclass activity through selective Fc receptor binding. Science. 2005;310(5753):1510-2.
346. Sealy R, Surman S, Hurwitz JL, Coleclough C. Antibody response to influenza infection of mice: different patterns for glycoprotein and nucleocapsid antigens. Immunology. 2003;108(4):431-9.
347. Coutelier JP, van der Logt JT, Heessen FW, Vink A, van Snick J. Virally induced modulation of murine IgG antibody subclasses. J Exp Med. 1988;168(6):2373-8.
348. Balkovic ES, Florack JA, Six HR. Immunoglobulin G subclass antibody responses of mice to influenza virus antigens given in different forms. Antiviral Res. 1987;8(3):151-60.
349. Nachbagauer R, Choi A, Izikson R, Cox MM, Palese P, Krammer F. Age Dependence and Isotype Specificity of Influenza Virus Hemagglutinin Stalk-Reactive Antibodies in Humans. Mbio. 2016;7(1):e01996-15.
350. NCBI IgBLAST tool National Center for Biotechnology Information, U.S. National Library of Medicine

8600 Rockville Pike, Bethesda MD, 20894 USA: National Center for Biotechnology Information; [Available from: https://www.ncbi.nlm.nih.gov/igblast/.
351. Saitou N, Nei M. The neighbor-joining method: a new method for reconstructing phylogenetic trees. Mol Biol Evol. 1987;4(4):406-25.
352. Felsenstein J. Confidence Limits on Phylogenies: An Approach Using the Bootstrap. Evolution. 1985;39(4):783-91.
353. Nei M, Kumar S. Molecular Evolution and Phylogenetics. New York: Oxford University Press; 2000.
354. Kumar S, Stecher G, Tamura K. MEGA7: Molecular Evolutionary Genetics Analysis Version 7.0 for Bigger Datasets. Mol Biol Evol. 2016;33(7):1870-4.
355. Martin ACR. abYmod University College London, London, England, United Kingdom2015-2020 [Available from: http://abymod.abysis.org/index.cgi.
356. Peacock THP, James J, Sealy JE, Iqbal M. A Global Perspective on H9N2 Avian Influenza Virus. Viruses. 2019;11(7).
357. Bruhns P. Properties of mouse and human IgG receptors and their contribution to disease models. Blood. 2012;119(24):5640-9.
358. Pommie C, Levadoux S, Sabatier R, Lefranc G, Lefranc MP. IMGT standardized criteria for statistical analysis of immunoglobulin V-REGION amino acid properties. J Mol Recognit. 2004;17(1):17-32.
359. Dondelinger M, Filee P, Sauvage E, Quinting B, Muyldermans S, Galleni M, et al. Understanding the Significance and Implications of Antibody Numbering and Antigen-Binding Surface/Residue Definition. Front Immunol. 2018;9:2278.
360. Chothia C, Lesk AM. Canonical structures for the hypervariable regions of immunoglobulins. J Mol Biol. 1987;196(4):901-17.
361. Birtalan S, Zhang Y, Fellouse FA, Shao L, Schaefer G, Sidhu SS. The intrinsic contributions of tyrosine, serine, glycine and arginine to the affinity and specificity of antibodies. J Mol Biol. 2008;377(5):1518-28.
362. Fellouse FA, Wiesmann C, Sidhu SS. Synthetic antibodies from a four-amino-acid code: a dominant role for tyrosine in antigen recognition. Proc Natl Acad Sci U S A. 2004;101(34):12467-72.
363. Mian IS, Bradwell AR, Olson AJ. Structure, function and properties of antibody binding sites. J Mol Biol. 1991;217(1):133-51.

364. Ramaraj T, Angel T, Dratz EA, Jesaitis AJ, Mumey B. Antigen-antibody interface properties: composition, residue interactions, and features of 53 non-redundant structures. Biochim Biophys Acta. 2012;1824(3):520-32.
365. Xu R, Krause JC, McBride R, Paulson JC, Crowe JE, Jr., Wilson IA. A recurring motif for antibody recognition of the receptor-binding site of influenza hemagglutinin. Nat Struct Mol Biol. 2013;20(3):363-70.
366. Whittle JR, Zhang R, Khurana S, King LR, Manischewitz J, Golding H, et al. Broadly neutralizing human antibody that recognizes the receptor-binding pocket of influenza virus hemagglutinin. Proc Natl Acad Sci U S A. 2011;108(34):14216-21.
367. Betz AG, Rada C, Pannell R, Milstein C, Neuberger MS. Passenger transgenes reveal intrinsic specificity of the antibody hypermutation mechanism: clustering, polarity, and specific hot spots. Proc Natl Acad Sci U S A. 1993;90(6):2385-8.
368. Rogozin IB, Diaz M. Cutting edge: DGYW/WRCH is a better predictor of mutability at G:C bases in Ig hypermutation than the widely accepted RGYW/WRCY motif and probably reflects a two-step activation-induced cytidine deaminase-triggered process. J Immunol. 2004;172(6):3382-4.
369. Shi B, Ma L, He X, Wang X, Wang P, Zhou L, et al. Comparative analysis of human and mouse immunoglobulin variable heavy regions from IMGT/LIGM-DB with IMGT/HighV-QUEST. Theor Biol Med Model. 2014;11:30.
370. Koenig P, Lee CV, Walters BT, Janakiraman V, Stinson J, Patapoff TW, et al. Mutational landscape of antibody variable domains reveals a switch modulating the interdomain conformational dynamics and antigen binding. Proc Natl Acad Sci U S A. 2017;114(4):E486-E95.
371. Wilson PC, de Bouteiller O, Liu YJ, Potter K, Banchereau J, Capra JD, et al. Somatic hypermutation introduces insertions and deletions into immunoglobulin V genes. J Exp Med. 1998;187(1):59-70.
372. Lantto J, Ohlin M. Uneven distribution of repetitive trinucleotide motifs in human immunoglobulin heavy variable genes. J Mol Evol. 2002;54(3):346-53.
373. Weitzner BD, Dunbrack RL, Jr., Gray JJ. The origin of CDR H3 structural diversity. Structure. 2015;23(2):302-11.
374. Luo D, Mah N, Krantz M, Wilde K, Wishart D, Zhang Y, et al. Vl-linker-Vh orientation-dependent expression of single chain Fv-containing an engineered disulfide-stabilized bond in the framework regions. J Biochem. 1995;118(4):825-31.
375. Desplancq D, King DJ, Lawson AD, Mountain A. Multimerization behaviour of single chain Fv variants for the tumour-binding antibody B72.3. Protein Eng. 1994;7(8):1027-33.
376. Albrecht H, Denardo GL, Denardo SJ. Monospecific bivalent scFv-SH: effects of linker length and location of an engineered cysteine on production, antigen binding activity and free SH accessibility. J Immunol Methods. 2006;310(1-2):100-16.
377. Rajagopal V, Pastan I, Kreitman RJ. A form of anti-Tac(Fv) which is both single-chain and disulfide stabilized: comparison with its single-chain and disulfide-stabilized homologs. Protein Eng. 1997;10(12):1453-9.
378. Kato K, Matsunaga C, Odaka A, Yamato S, Takaha W, Shimada I, et al. Carbon-13 NMR study of switch variant anti-dansyl antibodies: antigen binding and domain-domain interactions. Biochemistry. 1991;30(26):6604-10.

379. Torosantucci A, Chiani P, Bromuro C, De Bernardis F, Palma AS, Liu Y, et al. Protection by anti-beta-glucan antibodies is associated with restricted beta-1,3 glucan binding specificity and inhibition of fungal growth and adherence. Plos One. 2009;4(4):e5392.
380. Jegerlehner A, Schmitz N, Storni T, Bachmann MF. Influenza A vaccine based on the extracellular domain of M2: weak protection mediated via antibody-dependent NK cell activity. J Immunol. 2004;172(9):5598-605.
381. Lukosaityte D, Sadeyen JR, Shrestha A, Sealy JE, Bhat S, Chang P, et al. Engineered Recombinant Single Chain Variable Fragment of Monoclonal Antibody Provides Protection to Chickens Infected with H9N2 Avian Influenza. Vaccines (Basel). 2020;8(1).
382. Hermans D, Pasmans F, Messens W, Martel A, Van Immerseel F, Rasschaert G, et al. Poultry as a host for the zoonotic pathogen Campylobacter jejuni. Vector Borne Zoonotic Dis. 2012;12(2):89-98.
383. Stevens MP, Humphrey TJ, Maskell DJ. Molecular insights into farm animal and zoonotic Salmonella infections. Philos Trans R Soc Lond B Biol Sci. 2009;364(1530):2709-23.
384. Goebel SJ, Taylor J, Barr BC, Kiehn TE, Castro-Malaspina HR, Hedvat CV, et al. Isolation of avian paramyxovirus 1 from a patient with a lethal case of pneumonia. J Virol. 2007;81(22):12709-14.
385. Claas EC, Osterhaus AD, van Beek R, De Jong JC, Rimmelzwaan GF, Senne DA, et al. Human influenza A H5N1 virus related to a highly pathogenic avian influenza virus. Lancet. 1998;351(9101):472-7.
386. Gao R, Cao B, Hu Y, Feng Z, Wang D, Hu W, et al. Human infection with a novel avian-origin influenza A (H7N9) virus. N Engl J Med. 2013;368(20):1888-97.
387. Cook JK, Jackwood M, Jones RC. The long view: 40 years of infectious bronchitis research. Avian Pathol. 2012;41(3):239-50.
388. Berg TP. Acute infectious bursal disease in poultry: a review. Avian Pathol. 2000;29(3):175-94.
389. Tian H, Zhou S, Dong L, Van Boeckel TP, Cui Y, Newman SH, et al. Avian influenza H5N1 viral and bird migration networks in Asia. Proc Natl Acad Sci U S A. 2015;112(1):172-7.
390. Fourment M, Darling AE, Holmes EC. The impact of migratory flyways on the spread of avian influenza virus in North America. BMC Evol Biol. 2017;17(1):118.
391. Sun Y, Pu J, Jiang Z, Guan T, Xia Y, Xu Q, et al. Genotypic evolution and antigenic drift of H9N2 influenza viruses in China from 1994 to 2008. Vet Microbiol. 2010;146(3-4):215-25.
392. Smietanka K, Minta Z, Swieton E, Olszewska M, Jozwiak M, Domanska-Blicharz K, et al. Avian influenza H9N2 subtype in Poland--characterization of the isolates and evidence of concomitant infections. Avian Pathol. 2014;43(5):427-36.
393. Lindh E, Ek-Kommonen C, Vaananen VM, Vaheri A, Vapalahti O, Huovilainen A. Molecular epidemiology of H9N2 influenza viruses in Northern Europe. Vet Microbiol. 2014;172(3-4):548-54.
394. Song W, Qin K. Human-infecting influenza A (H9N2) virus: A forgotten potential pandemic strain? Zoonoses Public Health. 2020;67(3):203-12.
395. FAO. H7N9 situation update Food and Agriculture Organization, Rome, Italy2018 [Available from: http://www.fao.org/ag/againfo/programmes/en/empres/H7N9/Situation_update.html.
396. FAO. Global AIV with Zoonotic Potential situation update Food and Agriculture Organization, Rome, Italy2021

397. Shi W, Gao GF. Emerging H5N8 avian influenza viruses. Science. 2021;372(6544):784-6.
398. Li H, Li Q, Li B, Guo Y, Xing J, Xu Q, et al. Continuous Reassortment of Clade 2.3.4.4 H5N6 Highly Pathogenetic Avian Influenza Viruses Demonstrating High Risk to Public Health. Pathogens. 2020;9(8).
399. Ellis TM, Sims LD, Wong HK, Wong CW, Dyrting KC, Chow KW, et al. Use of avian influenza vaccination in Hong Kong. Dev Biol (Basel). 2006;124:133-43.
400. Ohmit SE, Victor JC, Rotthoff JR, Teich ER, Truscon RK, Baum LL, et al. Prevention of antigenically drifted influenza by inactivated and live attenuated vaccines. N Engl J Med. 2006;355(24):2513-22.
401. WHO. Global Influenza Surveillance and Response System (GISRS) [Available from: https://www.who.int/influenza/gisrs_laboratory/en/.
402. Nachbagauer R, Feser J, Naficy A, Bernstein DI, Guptill J, Walter EB, et al. A chimeric hemagglutinin-based universal influenza virus vaccine approach induces broad and long-lasting immunity in a randomized, placebo-controlled phase I trial. Nat Med. 2021;27(1):106-14.
403. Abdel-Motal UM, Guay HM, Wigglesworth K, Welsh RM, Galili U. Immunogenicity of influenza virus vaccine is increased by anti-gal-mediated targeting to antigen-presenting cells. J Virol. 2007;81(17):9131-41.
404. Deliyannis G, Boyle JS, Brady JL, Brown LE, Lew AM. A fusion DNA vaccine that targets antigen-presenting cells increases protection from viral challenge. Proc Natl Acad Sci U S A. 2000;97(12):6676-80.
405. Capua I, Cattoli G, Marangon S. DIVA--a vaccination strategy enabling the detection of field exposure to avian influenza. Dev Biol (Basel). 2004;119:229-33.
406. Kapczynski DR, Tumpey TM, Hidajat R, Zsak A, Chrzastek K, Tretyakova I, et al. Vaccination with virus-like particles containing H5 antigens from three H5N1 clades protects chickens from H5N1 and H5N8 influenza viruses. Vaccine. 2016;34(13):1575-81.
407. Kanekiyo M, Wei CJ, Yassine HM, McTamney PM, Boyington JC, Whittle JR, et al. Self-assembling influenza nanoparticle vaccines elicit broadly neutralizing H1N1 antibodies. Nature. 2013;499(7456):102-6.
408. Tang N, Zhang Y, Sadigh Y, Moffat K, Shen Z, Nair V, et al. Generation of A Triple Insert Live Avian Herpesvirus Vectored Vaccine Using CRISPR/Cas9-Based Gene Editing. Vaccines (Basel). 2020;8(1).
409. Ochiai H, Kurokawa M, Matsui S, Yamamoto T, Kuroki Y, Kishimoto C, et al. Infection enhancement of influenza A NWS virus in primary murine macrophages by anti-hemagglutinin monoclonal antibody. J Med Virol. 1992;36(3):217-21.
410. Winarski KL, Tang J, Klenow L, Lee J, Coyle EM, Manischewitz J, et al. Antibody-dependent enhancement of influenza disease promoted by increase in hemagglutinin stem flexibility and virus fusion kinetics. Proc Natl Acad Sci U S A. 2019;116(30):15194-9.
411. Skowronski DM, De Serres G, Crowcroft NS, Janjua NZ, Boulianne N, Hottes TS, et al. Association between the 2008-09 seasonal influenza vaccine and pandemic H1N1 illness during Spring-Summer 2009: four observational studies from Canada. Plos Med. 2010;7(4):e1000258.
412. Kimball JA, Norman DJ, Shield CF, Schroeder TJ, Lisi P, Garovoy M, et al. OKT3 antibody response study (OARS): a multicenter comparative study. Transplant Proc. 1993;25(1 Pt 1):558-60.

413. Nagy ZA, Horvath E, Urban Z. Antigen capture in chicken spleen during the primary immune response and relationship to phagocytic activity. Nat New Biol. 1973;242(121):241-4.
414. Lone NA, Spackman E, Kapczynski D. Immunologic evaluation of 10 different adjuvants for use in vaccines for chickens against highly pathogenic avian influenza virus. Vaccine. 2017;35(26):3401-8.
415. Kapczynski DR, Pantin-Jackwood MJ, Spackman E, Chrzastek K, Suarez DL, Swayne DE. Homologous and heterologous antigenic matched vaccines containing different H5 hemagglutinins provide variable protection of chickens from the 2014 U.S. H5N8 and H5N2 clade 2.3.4.4 highly pathogenic avian influenza viruses. Vaccine. 2017;35(46):6345-53.
416. Yang J, Cui H, Teng Q, Ma W, Li X, Wang B, et al. Ducks induce rapid and robust antibody responses than chickens at early time after intravenous infection with H9N2 avian influenza virus. Virol J. 2019;16(1):46.
417. Wilson JR, Belser JA, DaSilva J, Guo Z, Sun X, Gansebom S, et al. An influenza A virus (H7N9) anti-neuraminidase monoclonal antibody protects mice from morbidity without interfering with the development of protective immunity to subsequent homologous challenge. Virology. 2017;511:214-21.
418. Kolpe A, Schepens B, Ye L, Staeheli P, Saelens X. Passively transferred M2e-specific monoclonal antibody reduces influenza A virus transmission in mice. Antiviral Res. 2018;158:244-54.
419. Fujimoto Y, Tomioka Y, Takakuwa H, Uechi GI, Yabuta T, Ozaki K, et al. Cross-protective potential of anti-nucleoprotein human monoclonal antibodies against lethal influenza A virus infection. J Gen Virol. 2016;97(9):2104-16.
420. Yewdell JW, Webster RG, Gerhard WU. Antigenic variation in three distinct determinants of an influenza type A haemagglutinin molecule. Nature. 1979;279(5710):246-8.
421. Pendzialek J, Roose K, Smet A, Schepens B, Kufer P, Raum T, et al. Bispecific T cell engaging antibody constructs targeting a universally conserved part of the viral M2 ectodomain cure and prevent influenza A virus infection. Antiviral Res. 2017;141:155-64.
422. Laursen NS, Friesen RHE, Zhu X, Jongeneelen M, Blokland S, Vermond J, et al. Universal protection against influenza infection by a multidomain antibody to influenza hemagglutinin. Science. 2018;362(6414):598-602.
423. Unverdorben F, Richter F, Hutt M, Seifert O, Malinge P, Fischer N, et al. Pharmacokinetic properties of IgG and various Fc fusion proteins in mice. Mabs-Austin. 2016;8(1):120-8.
424. Leyva-Grado VH, Tan GS, Leon PE, Yondola M, Palese P. Direct administration in the respiratory tract improves efficacy of broadly neutralizing anti-influenza virus monoclonal antibodies. Antimicrob Agents Chemother. 2015;59(7):4162-72.
425. Stevens NE, Hatjopolous A, Fraser CK, Alsharifi M, Diener KR, Hayball JD. Preserved antiviral adaptive immunity following polyclonal antibody immunotherapy for severe murine influenza infection. Sci Rep. 2016;6:29154.
426. Corbanie EA, Matthijs MG, van Eck JH, Remon JP, Landman WJ, Vervaet C. Deposition of differently sized airborne microspheres in the respiratory tract of chickens. Avian Pathol. 2006;35(6):475-85.

427. Post J, Burt DW, Cornelissen JB, Broks V, van Zoelen D, Peeters B, et al. Systemic virus distribution and host responses in brain and intestine of chickens infected with low pathogenic or high pathogenic avian influenza virus. Virol J. 2012;9:61.
428. Iqbal M, Yaqub T, Mukhtar N, Shabbir MZ, McCauley JW. Infectivity and transmissibility of H9N2 avian influenza virus in chickens and wild terrestrial birds. Vet Res. 2013;44:100.
429. McNee A, Smith TRF, Holzer B, Clark B, Bessell E, Guibinga G, et al. Establishment of a Pig Influenza Challenge Model for Evaluation of Monoclonal Antibody Delivery Platforms. J Immunol. 2020;205(3):648-60.
430. Greenall SA, Tyack SG, Johnson MA, Sapats SI. Antibody fragments, expressed by a fowl adenovirus vector, are able to neutralize infectious bursal disease virus. Avian Pathol. 2010;39(5):339-48.
431. Gao H, Cui H, Cui X, Shi X, Zhao Y, Zhao X, et al. Expression of HA of HPAI H5N1 virus at US2 gene insertion site of turkey herpesvirus induced better protection than that at US10 gene insertion site. Plos One. 2011;6(7):e22549.
432. Huang ZY, Fang D, Lv P, Bian XB, Ruan XZ, Yan Y, et al. Differential cellular immune responses between chickens and ducks to H9N2 avian influenza virus infection. Vet Immunol Immunop. 2012;150(3-4):169-80.
433. Dai M, Li S, Keyi S, Sun H, Zhao L, Deshui Y, et al. Comparative analysis of key immune protection factors in H9N2 avian influenza viruses infected and immunized specific pathogen-free chicken. Poult Sci. 2021;100(1):39-46.
434. Kaverin NV, Rudneva IA, Ilyushina NA, Lipatov AS, Krauss S, Webster RG. Structural differences among hemagglutinins of influenza A virus subtypes are reflected in their antigenic architecture: analysis of H9 escape mutants. J Virol. 2004;78(1):240-9.
435. Okamatsu M, Sakoda Y, Kishida N, Isoda N, Kida H. Antigenic structure of the hemagglutinin of H9N2 influenza viruses. Arch Virol. 2008;153(12):2189-95.
436. Stevens J, Blixt O, Tumpey TM, Taubenberger JK, Paulson JC, Wilson IA. Structure and receptor specificity of the hemagglutinin from an H5N1 influenza virus. Science. 2006;312(5772):404-10.
437. Sang X, Wang A, Ding J, Kong H, Gao X, Li L, et al. Adaptation of H9N2 AIV in guinea pigs enables efficient transmission by direct contact and inefficient transmission by respiratory droplets. Sci Rep. 2015;5:15928.
438. Shirley JL, de Jong YP, Terhorst C, Herzog RW. Immune Responses to Viral Gene Therapy Vectors. Mol Ther. 2020;28(3):709-22.
439. Gaudet D, Methot J, Dery S, Brisson D, Essiembre C, Tremblay G, et al. Efficacy and long-term safety of alipogene tiparvovec (AAV1-LPLS447X) gene therapy for lipoprotein lipase deficiency: an open-label trial. Gene Ther. 2013;20(4):361-9.
440. Suhy DA, Kao SC, Mao T, Whiteley L, Denise H, Souberbielle B, et al. Safe, long-term hepatic expression of anti-HCV shRNA in a nonhuman primate model. Mol Ther. 2012;20(9):1737-49.
441. Elmer BM, Swanson KA, Bangari DS, Piepenhagen PA, Roberts E, Taksir T, et al. Gene delivery of a modified antibody to Abeta reduces progression of murine Alzheimer's disease. Plos One. 2019;14(12):e0226245.
442. Del Rosario JMM, Smith M, Zaki K, Risley P, Temperton N, Engelhardt OG, et al. Protection From Influenza by Intramuscular Gene Vector Delivery of a Broadly Neutralizing

Nanobody Does Not Depend on Antibody Dependent Cellular Cytotoxicity. Front Immunol. 2020;11:627.
443. Martinez-Navio JM, Fuchs SP, Mendes DE, Rakasz EG, Gao G, Lifson JD, et al. Long-Term Delivery of an Anti-SIV Monoclonal Antibody With AAV. Front Immunol. 2020;11:449.
444. Swayne DE, Garcia M, Beck JR, Kinney N, Suarez DL. Protection against diverse highly pathogenic H5 avian influenza viruses in chickens immunized with a recombinant fowlpox vaccine containing an H5 avian influenza hemagglutinin gene insert. Vaccine. 2000;18(11-12):1088-95.
445. Pavlova SP, Veits J, Mettenleiter TC, Fuchs W. Live vaccination with an H5-hemagglutinin-expressing infectious laryngotracheitis virus recombinant protects chickens against different highly pathogenic avian influenza viruses of the H5 subtype. Vaccine. 2009;27(37):5085-90.
446. Chang P, Yao Y, Tang N, Sadeyen JR, Sealy J, Clements A, et al. The Application of NHEJ-CRISPR/Cas9 and Cre-Lox System in the Generation of Bivalent Duck Enteritis Virus Vaccine against Avian Influenza Virus. Viruses. 2018;10(2).
447. Gardin Y, Palya V, Dorsey KM, El-Attrache J, Bonfante F, Wit S, et al. Experimental and Field Results Regarding Immunity Induced by a Recombinant Turkey Herpesvirus H5 Vector Vaccine Against H5N1 and Other H5 Highly Pathogenic Avian Influenza Virus Challenges. Avian Dis. 2016;60(1 Suppl):232-7.
448. Rautenschlein S, Lemiere S, Prandini F. Evaluation of the effects of an HVT-IBD vector vaccine on the immune system of layer pullets in comparison with two commercial live IBD vaccines. XVIIIth WVPA Congress Nantes, August 19th-23rd; France2013.
449. Turner-Alston K, Bosserd M, Taylor L, Dickson J, Embrey J, Rong S. Onset of Immunity of A Recombinant HVT-ND against of a Velogenic NDV Challenge in SPF Birds. AAAP 20192019.
450. Afonso CL, Tulman ER, Lu Z, Zsak L, Rock DL, Kutish GF. The genome of turkey herpesvirus. J Virol. 2001;75(2):971-8.
451. Andoh K, Yamazaki K, Honda Y, Honda T. Turkey herpesvirus with an insertion in the UL3-4 region displays an appropriate balance between growth activity and antibody-eliciting capacity and is suitable for the establishment of a recombinant vaccine. Arch Virol. 2017;162(4):931-41.
452. Baigent SJ, Petherbridge LJ, Smith LP, Zhao Y, Chesters PM, Nair VK. Herpesvirus of turkey reconstituted from bacterial artificial chromosome clones induces protection against Marek's disease. J Gen Virol. 2006;87(Pt 4):769-76.
453. Li K, Liu Y, Liu C, Gao L, Zhang Y, Cui H, et al. Recombinant Marek's disease virus type 1 provides full protection against very virulent Marek's and infectious bursal disease viruses in chickens. Sci Rep. 2016;6:39263.
454. Tang N, Zhang Y, Pedrera M, Chang P, Baigent S, Moffat K, et al. A simple and rapid approach to develop recombinant avian herpesvirus vectored vaccines using CRISPR/Cas9 system. Vaccine. 2018;36(5):716-22.
455. Brouns SJ, Jore MM, Lundgren M, Westra ER, Slijkhuis RJ, Snijders AP, et al. Small CRISPR RNAs guide antiviral defense in prokaryotes. Science. 2008;321(5891):960-4.
456. van der Oost J, Jore MM, Westra ER, Lundgren M, Brouns SJ. CRISPR-based adaptive and heritable immunity in prokaryotes. Trends Biochem Sci. 2009;34(8):401-7.
457. Jansen R, Embden JD, Gaastra W, Schouls LM. Identification of genes that are associated with DNA repeats in prokaryotes. Mol Microbiol. 2002;43(6):1565-75.

458. Nouspikel T. DNA repair in mammalian cells: So DNA repair really is that important? Cell Mol Life Sci. 2009;66(6):965-7.
459. Su T, Liu F, Gu P, Jin H, Chang Y, Wang Q, et al. A CRISPR-Cas9 Assisted Non-Homologous End-Joining Strategy for One-step Engineering of Bacterial Genome. Sci Rep. 2016;6:37895.
460. Branzei D, Foiani M. Regulation of DNA repair throughout the cell cycle. Nat Rev Mol Cell Biol. 2008;9(4):297-308.
461. Hufton SE, Risley P, Ball CR, Major D, Engelhardt OG, Poole S. The breadth of cross sub-type neutralisation activity of a single domain antibody to influenza hemagglutinin can be increased by antibody valency. Plos One. 2014;9(8):e103294.
462. Kapczynski DR, Esaki M, Dorsey KM, Jiang H, Jackwood M, Moraes M, et al. Vaccine protection of chickens against antigenically diverse H5 highly pathogenic avian influenza isolates with a live HVT vector vaccine expressing the influenza hemagglutinin gene derived from a clade 2.2 avian influenza virus. Vaccine. 2015;33(9):1197-205.
463. Bublot M, Pritchard N, Le Gros FX, Goutebroze S. Use of a vectored vaccine against infectious bursal disease of chickens in the face of high-titred maternally derived antibody. J Comp Pathol. 2007;137 Suppl 1:S81-4.
464. Witter RL, Burmester BR. Differential effect of maternal antibodies on efficacy of cellular and cell-free Marek's disease vaccines. Avian Pathol. 1979;8(2):145-56.
465. Chang P, Ameen F, Sealy JE, Sadeyen JR, Bhat S, Li Y, et al. Application of HDR-CRISPR/Cas9 and Erythrocyte Binding for Rapid Generation of Recombinant Turkey Herpesvirus-Vectored Avian Influenza Virus Vaccines. Vaccines (Basel). 2019;7(4).
466. Tsukamoto K, Saito S, Saeki S, Sato T, Tanimura N, Isobe T, et al. Complete, long-lasting protection against lethal infectious bursal disease virus challenge by a single vaccination with an avian herpesvirus vector expressing VP2 antigens. J Virol. 2002;76(11):5637-45.
467. Gimeno IM, Faiz NM, Cortes AL, Barbosa T, Villalobos T, Pandiri AR. In Ovo Vaccination with Turkey Herpesvirus Hastens Maturation of Chicken Embryo Immune Responses in Specific-Pathogen-Free Chickens. Avian Dis. 2015;59(3):375-83.
468. Bavananthasivam J, Read L, Astill J, Yitbarek A, Alkie TN, Abdul-Careem MF, et al. The effects of in ovo administration of encapsulated Toll-like receptor 21 ligand as an adjuvant with Marek's disease vaccine. Sci Rep. 2018;8(1):16370.
469. Gimeno IM, Cortes AL, Guy JS, Turpin E, Williams C. Replication of recombinant herpesvirus of turkey expressing genes of infectious laryngotracheitis virus in specific pathogen free and broiler chickens following in ovo and subcutaneous vaccination. Avian Pathol. 2011;40(4):395-403.
470. Longenecker BM, Pazderka F, Stone HS, Gavora JS, Ruth RF. In ovo assay for Marek's disease virus and turkey herpesvirus. Infect Immun. 1975;11(5):922-31.
471. Sharma JM. Delayed replication of Marek's disease virus following in ovo inoculation during late stages of embryonal development. Avian Dis. 1987;31(3):570-6.
472. Sharma JM. Embryo vaccination of specific-pathogen-free chickens with infectious bursal disease virus: tissue distribution of the vaccine virus and protection of hatched chickens against disease. Avian Dis. 1986;30(4):776-80.
473. Remy S, Le Pape G, Gourichon D, Gardin Y, Denesvre C. Chickens can durably clear herpesvirus vaccine infection in feathers while still carrying vaccine-induced antibodies. Vet Res. 2020;51(1):24.

474. De Vlieger D, Ballegeer M, Rossey I, Schepens B, Saelens X. Single-Domain Antibodies and Their Formatting to Combat Viral Infections. Antibodies (Basel). 2018;8(1).
475. Baker JH, Lindquist KE, Huxham LA, Kyle AH, Sy JT, Minchinton AI. Direct visualization of heterogeneous extravascular distribution of trastuzumab in human epidermal growth factor receptor type 2 overexpressing xenografts. Clin Cancer Res. 2008;14(7):2171-9.
476. Vanderven HA, Kent SJ. The protective potential of Fc-mediated antibody functions against influenza virus and other viral pathogens. Immunol Cell Biol. 2020;98(4):253-63.
477. de Vries RD, Nieuwkoop NJ, Pronk M, de Bruin E, Leroux-Roels G, Huijskens EGW, et al. Influenza virus-specific antibody dependent cellular cytoxicity induced by vaccination or natural infection. Vaccine. 2017;35(2):238-47.
478. Mullarkey CE, Bailey MJ, Golubeva DA, Tan GS, Nachbagauer R, He W, et al. Broadly Neutralizing Hemagglutinin Stalk-Specific Antibodies Induce Potent Phagocytosis of Immune Complexes by Neutrophils in an Fc-Dependent Manner. Mbio. 2016;7(5).
479. Terajima M, Cruz J, Co MD, Lee JH, Kaur K, Wrammert J, et al. Complement-dependent lysis of influenza a virus-infected cells by broadly cross-reactive human monoclonal antibodies. J Virol. 2011;85(24):13463-7.
480. van den Berg FT, Makoah NA, Ali SA, Scott TA, Mapengo RE, Mutsvunguma LZ, et al. AAV-Mediated Expression of Broadly Neutralizing and Vaccine-like Antibodies Targeting the HIV-1 Envelope V2 Region. Mol Ther Methods Clin Dev. 2019;14:100-12.
481. Sack BK, Merchant S, Markusic DM, Nathwani AC, Davidoff AM, Byrne BJ, et al. Transient B cell depletion or improved transgene expression by codon optimization promote tolerance to factor VIII in gene therapy. Plos One. 2012;7(5):e37671.
482. Faust SM, Bell P, Cutler BJ, Ashley SN, Zhu Y, Rabinowitz JE, et al. CpG-depleted adeno-associated virus vectors evade immune detection. J Clin Invest. 2013;123(7):2994-3001.
483. Samelson-Jones BJ, Finn JD, Favaro P, Wright JF, Arruda VR. Timing of Intensive Immunosuppression Impacts Risk of Transgene Antibodies after AAV Gene Therapy in Nonhuman Primates. Mol Ther Methods Clin Dev. 2020;17:1129-38.
484. Chan YK, Wang SK, Chu CJ, Copland DA, Letizia AJ, Costa Verdera H, et al. Engineering adeno-associated viral vectors to evade innate immune and inflammatory responses. Sci Transl Med. 2021;13(580).
485. Tutykhina IL, Sedova ES, Gribova IY, Ivanova TI, Vasilev LA, Rutovskaya MV, et al. Passive immunization with a recombinant adenovirus expressing an HA (H5)-specific single-domain antibody protects mice from lethal influenza infection. Antiviral Res. 2013;97(3):318-28.
486. Limberis MP, Adam VS, Wong G, Gren J, Kobasa D, Ross TM, et al. Intranasal antibody gene transfer in mice and ferrets elicits broad protection against pandemic influenza. Sci Transl Med. 2013;5(187):187ra72.
487. Matsui R, Tanabe Y, Watanabe D. Avian adeno-associated virus vector efficiently transduces neurons in the embryonic and post-embryonic chicken brain. Plos One. 2012;7(11):e48730.
488. Adam M, Oualikene W, Le Cocq H, Guittet M, Eloit M. Replication-defective adenovirus type 5 as an in vitro and in vivo gene transfer vector in chickens. J Gen Virol. 1995;76 (Pt 12):3153-7.
489. Jahiel RI, Kilbourne ED. Reduction in plaque size and reduction in plaque number as differing indices of influenza virus-antibody reactions. J Bacteriol. 1966;92(5):1521-34.

490. Zebedee SL, Lamb RA. Influenza A virus M2 protein: monoclonal antibody restriction of virus growth and detection of M2 in virions. J Virol. 1988;62(8):2762-72.
491. Wohlbold TJ, Podolsky KA, Chromikova V, Kirkpatrick E, Falconieri V, Meade P, et al. Broadly protective murine monoclonal antibodies against influenza B virus target highly conserved neuraminidase epitopes. Nat Microbiol. 2017;2(10):1415-24.
492. Okuya K, Yoshida R, Manzoor R, Saito S, Suzuki T, Sasaki M, et al. Potential Role of Nonneutralizing IgA Antibodies in Cross-Protective Immunity against Influenza A Viruses of Multiple Hemagglutinin Subtypes. J Virol. 2020;94(12).
493. Ekiert DC, Kashyap AK, Steel J, Rubrum A, Bhabha G, Khayat R, et al. Cross-neutralization of influenza A viruses mediated by a single antibody loop. Nature. 2012;489(7417):526-32.
494. Chai N, Swem LR, Reichelt M, Chen-Harris H, Luis E, Park S, et al. Two Escape Mechanisms of Influenza A Virus to a Broadly Neutralizing Stalk-Binding Antibody. PLoS Pathog. 2016;12(6):e1005702.
495. Wu NC, Thompson AJ, Lee JM, Su W, Arlian BM, Xie J, et al. Different genetic barriers for resistance to HA stem antibodies in influenza H3 and H1 viruses. Science. 2020;368(6497):1335-40.
496. Yumura K, Akiba H, Nagatoishi S, Kusano-Arai O, Iwanari H, Hamakubo T, et al. Use of SpyTag/SpyCatcher to construct bispecific antibodies that target two epitopes of a single antigen. J Biochem. 2017;162(3):203-10.
497. Alam MK, Brabant M, Viswas RS, Barreto K, Fonge H, Ronald Geyer C. A novel synthetic trivalent single chain variable fragment (tri-scFv) construction platform based on the SpyTag/SpyCatcher protein ligase system. Bmc Biotechnol. 2018;18(1):55.
498. Wichgers Schreur PJ, van de Water S, Harmsen M, Bermudez-Mendez E, Drabek D, Grosveld F, et al. Multimeric single-domain antibody complexes protect against bunyavirus infections. Elife. 2020;9.
499. Ma W, Saccardo A, Roccatano D, Aboagye-Mensah D, Alkaseem M, Jewkes M, et al. Modular assembly of proteins on nanoparticles. Nat Commun. 2018;9(1):1489.
500. Spackman E, Pantin-Jackwood M, Swayne DE, Suarez DL, Kapczynski DR. Impact of route of exposure and challenge dose on the pathogenesis of H7N9 low pathogenicity avian influenza virus in chickens. Virology. 2015;477:72-81.
501. Talat S, Abouelmaatti RR, Almeer R, Abdel-Daim MM, Elfeil WK. Comparison of the Effectiveness of Two Different Vaccination Regimes for Avian Influenza H9N2 in Broiler Chicken. Animals (Basel). 2020;10(10).
502. Clements AL, Sealy JE, Peacock TP, Sadeyen JR, Hussain S, Lycett SJ, et al. Contribution of Segment 3 to the Acquisition of Virulence in Contemporary H9N2 Avian Influenza Viruses. J Virol. 2020;94(20).
503. Ruiz-Hernandez R, Mwangi W, Peroval M, Sadeyen JR, Ascough S, Balkissoon D, et al. Host genetics determine susceptibility to avian influenza infection and transmission dynamics. Sci Rep. 2016;6:26787.
504. Chtarto A, Bender HU, Hanemann CO, Kemp T, Lehtonen E, Levivier M, et al. Tetracycline-inducible transgene expression mediated by a single AAV vector. Gene Ther. 2003;10(1):84-94.
505. Brown BD, Venneri MA, Zingale A, Sergi Sergi L, Naldini L. Endogenous microRNA regulation suppresses transgene expression in hematopoietic lineages and enables stable gene transfer. Nat Med. 2006;12(5):585-91.

506. Roscilli G, Rinaudo CD, Cimino M, Sporeno E, Lamartina S, Ciliberto G, et al. Long-term and tight control of gene expression in mouse skeletal muscle by a new hybrid human transcription factor. Mol Ther. 2002;6(5):653-63.
507. Van Hoecke L, Verbeke R, De Vlieger D, Dewitte H, Roose K, Van Nevel S, et al. mRNA Encoding a Bispecific Single Domain Antibody Construct Protects against Influenza A Virus Infection in Mice. Mol Ther Nucleic Acids. 2020;20:777-87.
508. Buchman A, Gamez S, Li M, Antoshechkin I, Li HH, Wang HW, et al. Broad dengue neutralization in mosquitoes expressing an engineered antibody. PLoS Pathog. 2020;16(1):e1008103.
509. Hoffmann E, Neumann G, Kawaoka Y, Hobom G, Webster RG. A DNA transfection system for generation of influenza A virus from eight plasmids. Proc Natl Acad Sci U S A. 2000;97(11):6108-13.
510. Webster R, Cox N, Stöhr K. WHO Manual on Animal Influenza Diagnosis and Surveillance. WHO Global Influenza Programme. 2002;WHO/CDS/CSR/NCS/2002.5 Rev. 1 https://www.who.int/csr/resources/publications/influenza/whocdscsrncs20025rev.pdf.